The University Of Sheffield.

The role of VEGFA isoform expression in response to Anti-VEGFA therapy in ovarian cancer

Brenda Lourdes Agüero Burgos

A thesis submitted in partial fulfilment of the requirements for the degree of Doctor of Philosophy

The University of Sheffield
Faculty of Medicine, Dentistry & Health
The Medical School

September 2020

Acknowledgments

Firstly, I would like to express my gratitude for the funding received towards my PhD from CONACyT, FIDERH and the Weston Park Hospital Cancer Charity. Without their support, the completion of my PhD and development of this project would not have been possible.

Secondly, I would like to express my gratitude to my supervisor Dr. Will English for his continuous support during my PhD, for his patience, motivation and immense knowledge. I also thank the rest of the members of the English' lab for their help and for keeping me company in the lab over the last two years. My sincere thanks also goes to Dr. Dennis Wang and Dr. Manoj Valluru for their guidance on my bioinformatics training required to develop this project.

Finally, I am indebt to my family, my loving boyfriend Seb and my friends for supporting me through this journey and for constantly reminding me that there was a life outside the lab. I would never be able to express with words all the emotional and moral support that you represent in my life.

Abstract

High Grade Serous Ovarian Cancer (HGSOC) is one of the most aggressive gynaecological malignancies in women. Anti-VEGFA therapy in combination with chemotherapy has shown promise for the treatment of HGSOC. However, as not all women benefit and side effects can be severe, predictive biomarkers are urgently needed to improve treatment outcome. As high plasma levels of the VEGFA isoform VEGFA121 had shown promise as a prognostic and predictive biomarker in breast, gastrointestinal and pancreatic cancer, this project aimed to investigate the potential of VEGFA isoform measurement as a biomarker in HGSOC.

Analysis of RNAseq data from The Cancer Genome Atlas Ovarian (TCGA OV) dataset was used to investigate associations between VEGFA mRNA isoform expression and clinical outcome. Different methods were explored for the development of novel ovarian cancer cell lines expressing increased VEGFA121. These were characterised *in vitro* and then in *in vivo* pre-clinical models of advanced disease.

Analysis of RNAseq data showed different patterns of VEGFA mRNA isoform expression exists between HGSOC patient's tumours. Segregation based on VEGFA165 expression had the strongest correlation with prognosis, with low levels of VEGFA165 associated with significantly decreased overall survival (HR 2.0, 95% CI 1.24-3.23, p-value 0.005). HGSOC tumours with low VEGFA165 also had increased expression of VEGFA121 mRNA. The VEGFA165-high group, with low expression of VEGFA121, had increased expression of genes associated with improved response to bevacizumab, hypoxia (e.g. *MTOR*, *PDK1*, *ANGPLT4* and *CA9*) and angiogenesis (e.g. *FLT1*, *KDR*, *DLL4* and *NOTCH4*) (FDR < 0.05). *In vitro,* ID8 mouse ovarian cancer cells overexpressing VEGFA120 (ID8 120) had decreased proliferation and migration. Mice injected with ID8 120 cells took longer to reach clinical end points and had a reduced response to anti-VEGFA antibodies compared to mice injected with ID8 cells. However, neither was statistically significant.

In conclusion, although measurement of VEGFA mRNA isoform expression may have use as a prognostic and predictive biomarker after further characterisation, further efforts are needed to develop pre-clinical models to improve understanding of underlying mechanisms.

Declaration

I, the author, confirm that the Thesis is my own work. I am aware of the University's Guidance on the Use of Unfair Means (www.sheffield.ac.uk/ssid/unfair-means). This work has not been previously been presented for an award at this, or any other, university.

Table of contents

List of figures

List of tables

List of abbreviations

AQRT-PCR	Absolute Quantitative Real Time-PCR
BCA	Bicinchoninic acid
BSA	Bovine serum albumin
CA-125	Cancer antigen 125
CA9	Carbonic anhydrase 9
cDNA	Complementary DNA
CI	Confidence interval
CMV	Cytomegalovirus
CPM	Counts per million reads mapped
Ct	Cycle threshold
DEG	Differentially expressed genes
DMEM	Dulbecco's Modified Eagle Medium
DMSO	Dimethyl sulfoxide
DNA	Deoxyribonucleic acid
DTT	Dithiothreitol
ECL	Enhanced chemiluminescence
ECM	Extracellular matrix
EDTA	Ethylenediaminetetraacetic acid
ELISA	Enzyme-linked immunosorbent assay
EMT	Epithelial–mesenchymal transition
FBS	Fetal bovine serum
FC	Fold change
FDR	False discovery rate
FFPE	Formalin-fixed Paraffin-embedded
FIGO	International Federation of Gynecology and Obstetrics
GFP	Green fluorescent protein
GSEA	Gene set enrichment analysis
GTEX	The Genotype-Tissue Expression
H&E	Haemotoxylin and Eosin
HGSOC	High-grade serous ovarian cancer
HIF	Hypoxia-inducible factor
HR	Hazard ratio
HRD	Homologous recombination deficiency
HRE	Hypoxia response element
HRP	Horseradish peroxidase
HUVEC	Human umbilical vein endothelial cells
IFN-γ	Interferon gamma
IHC	Immunohistochemistry
IP	Intraperitoneal
IVIS	In Vivo Imaging System
LD50	Lethal dose 50%
miRNA	MicroRNA
MMP	Metalloproteinase
mRNA	Messenger RNA

mTOR	Mammalian target of rapamycin
MTT	3-(4,5-Dimethylthiazol-2-yl)-2,5-Diphenyltetrazolium Bromide
MVD	Micro-vascular density
NRP	Neuropilin
NSG	NOD scid gamma
O2	Oxygen
OCT	Optimal cutting temperature compound
OS	Overall survival
PARP	Poly (ADP-ribose) polymerase
PBS	Phosphate buffered saline
PCR	Polymerase chain reaction
PD1	Programmed cell death-1 receptor
PDK1	Pyruvate dehydrogenase kinase 1
PDX	Patient derived xenografts
PFS	Progression-free survival
PGF	Placental growth factor
PPI	Protein-protein interaction
pVEGFA	Plasma VEGFA
RIPA	Radioimmunoprecipitation assay buffer
RNA	Ribonucleic acid
SC	Subcutaneous
SCID	Severe combined immunodeficiency
SNP	Single nucleotide polymorphism
SOC	Super optimal broth with catabolite repression
TBE	Tris-borate-EDTA
TBS	Tris-buffered saline
TCGA	The Cancer Genome Atlas
TEMED	Tetramethylethylenediamine
TIL	Tumour Infiltrating Lymphocytes
TKI	Tyrosine kinase inhibitor
TMB	3,3′,5,5′-Tetramethylbenzidine
TPM	Transcripts per million
UTR	Untranslated region
VDGs	VEGF-dependent gene signature
VEGF	Vascular endothelial growth factor
VEGFR	Vascular endothelial growth factor receptor
VHL	Von Hippel Lindau
VPF	Vascular permeability factor
WT	Wild type
ZFN	Zinc finger nucleases

Chapter 1

1. Introduction

1.1 Introduction to Ovarian cancer

Epithelial ovarian cancer is considered a heterogeneous disease, consisting of four different histological subtypes: Endometrioid, mucinous, clear cell and serous ovarian cancer (Vaughan et al., 2011). These four subtypes are mainly differentiated by their morphology and tissue architecture. The most abundant, the serous subtype, resembles tissue architecture of the inner layer of the fallopian tube. The endometrioid subtype presents a glandular architecture similar to the inner layer of the uterus. The mucinous subtype has features of cells from the endocervical or intestinal epithelium while the clear cell subtype includes clear and hobnail cells (Chen, V.W. et al., 2003). Each subtype is associated with different clinical characteristics and treatment response, however for at least three decades it has been treated as a single disease. Current ovarian cancer treatment primarily involves surgical intervention in combination with platinum-based chemotherapy (Banerjee and Kaye, 2013). At early stages and wherever possible, debulking surgery is used to remove the primary tumour. This is subsequently followed by chemotherapy in order to target any residual disease. Such treatment is effective for FIGO stage I/II (Fig.1) and a favourable prognosis is described for localised cancer with approximately 90% of women surviving beyond 5 years (Jayson et al., 2014).

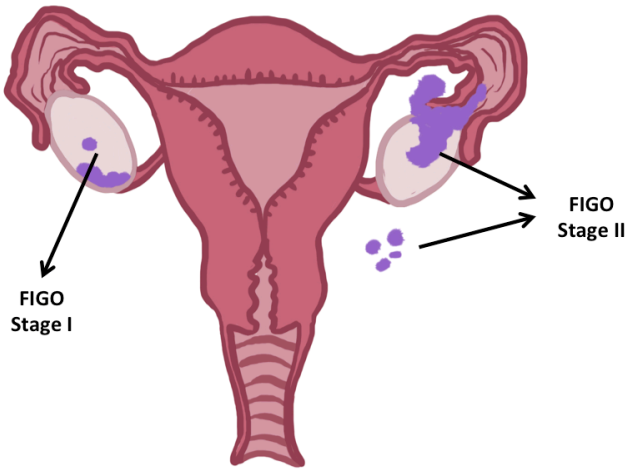

Figure 1. Early stage ovarian cancer.

FIGO stage I indicates that ovarian cancer is inside the ovaries, while stage II indicates that the cancer has grown outside the ovaries and is growing into other tissue in the pelvis and cancer cells can be found in abdominal fluid.

Although standard treatment can be curative for most patients at early stages, most ovarian cancer cases present at an advanced disease stage; FIGO III/IV (Fig.2). At advanced stages where the cancer has spread within the peritoneal cavity and beyond, chemotherapy is commonly administered in order to reduce tumour volume prior to surgical intervention (Coleman, R. et al., 2013). Although these cases typically respond initially to first line therapy, around 90% of patients experience recurrent disease and develop resistance to platinum-based therapy, ultimately impacting on patient survival (Miow et al., 2014). Ovarian cancer patients with a relapse usually receive a second line of chemotherapy, which typically involves different regimens of carboplatin or a combination of different cytotoxic drugs such as doxorubicin or topotecan (Jayson et al., 2014).

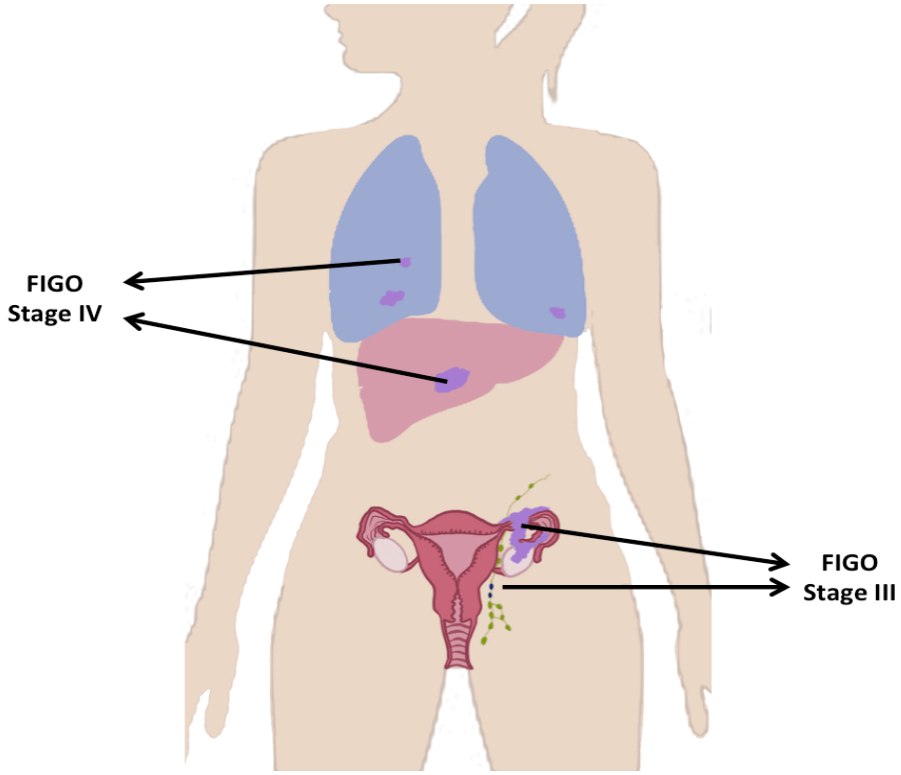

Figure 2. Advanced stage ovarian cancer.

FIGO stage III indicates that ovarian cancer has spread outside the pelvic region into the peritoneal cavity or lymph nodes around the abdomen or womb. Stage IV indicates the cancer has spread to other distant organs such as liver or lungs.

1.1.1 High-grade serous ovarian cancer and mechanisms of metastasis

The epithelial serous ovarian cancer subtype is stratified into low-grade and high-grade tumours based on the degree of cell differentiation. Although these two groups share similar histological characteristics, recently, specific mechanisms of tumourigenesis, genetic and molecular features have been associated with each group (Lisio et al., 2019). This work will focus solely on studying the high-grade subtype. High-grade serous ovarian cancer (HGSOC) represents the majority of ovarian cancer cases (70-80%) and has the highest rate of mortality of cancers exclusive to women (Bowtell et al., 2015). HGSOC is difficult to diagnose at early stages due to the lack of disease specific associated symptoms, therefore the majority of HGSOC patients present with advanced disease (FIGO stage III or IV) (Kumaran et al., 2008) (Fig. 2). HGSOC is characterised by the production of large volumes of ascites, which leads to serious clinical difficulties such as altered bowel habit, difficulties with breathing and a distended abdomen (Ahmed and Stenvers, 2013). Tumours induce ascites by overexpressing Vascular Endothelial Growth Factor A (VEGFA), which increases vascular leakage leading to the abnormal accumulation of ascites fluid and also increases dissemination of cancer cells throughout the peritoneum (Ahmed and Stenvers, 2013). HGSOC mortality commonly arises when the cancer has metastasised beyond the pelvic region to the gastrointestinal tract and the diaphragm causing abnormal physiological functions (Jayson et al., 2014). Additionally, metabolic changes leading to loss of muscle mass and adipose tissue are considered as important factors that contribute approximately to 20% of cancer deaths (Aust et al., 2015).

The metastatic pattern in ovarian cancer is different from other cancer types and its underlying mechanisms are still unclear. Ovarian cancer cells mainly spread through the peritoneal fluids after losing cell-cell adhesion from tumours and disseminate into the peritoneal cavity (Mitra, A., 2016). Cells from the primary tumour can spread not only as single cells but also as cell aggregates or spheroids within the peritoneal fluid and then invade the mesothelium covering the basement membrane of the peritoneal organs (Lengyel, 2010). One of the reasons for the highly metastatic profile of ovarian cancer is the lack of an anatomical barrier, which allows the cancer cells to disseminate earlier than other cancers without the common processes of invasion, intravasation and extravasation through surrounding extracellular matrix and into the vascular or lymphatic systems (Mitra, A., 2016). However, more recently it has been described that ascites within the peritoneum are drained through the lymphatic vessels, which allow ovarian cancer cells to disseminate through the

lymph nodes and enter into the blood circulation (Mitra, A., 2016; Honami and Denise, 2005).

1.1.2 Genetic and molecular characteristics of HGSOC

Genetically, HGSOC is commonly characterised by frequent mutations in *TP53* followed by *BRCA1* and *BRCA2* mutations, defective homologous recombination DNA repair mechanisms and alterations in signalling pathways such as PI3K, NOTCH, RAS and FOXM1 (Jayson et al., 2014). It has been proposed that HGSOC shares more genomic characteristics with basal breast cancer than it has with other ovarian cancer subtypes (Vaughan et al., 2011). Additionally, it has been suggested that HGSOC arises from secretory cells in the fallopian tube rather than the ovary (Lee, Y. et al., 2007). In genetically engineered mouse models, it has been shown that HGSOC can emerge from the fallopian tube and spread throughout the peritoneum showing similar metastatic pattern and genomic characteristics of the human disease (Perets et al., 2013). However, there are some HGSOC cases that do not show fallopian tube lesions and the precursor cells for this number of cases remains unclear (Bowtell et al., 2015).

Gene expression profiles in HGSOC have identified different molecular subtypes that have been associated with patient prognosis and treatment response (Bowtell et al., 2015). The four main molecular subtypes described and their associated gene expression are: Immunoreactive (*CXCL11*, *CXCL10* and *CXCR3*), differentiated (*MUC16*, *MUC1* and *SLPI*), proliferative (*HMGA2*, *SOX11*, *MCM2* and *PCNA*) and mesenchymal (*HOX*, *FAP*, *ANGPTL2* and *ANGPTL1*) (Cancer Genome Atlas Research, 2011). The latter group has shown worse survival outcomes when compared with the other groups in different patient cohorts (Konecny et al., 2014; Chen, G.M. et al., 2018). Additionally, the mesenchymal and proliferative subtypes have also been linked to better response to anti-VEGFA treatment with bevacizumab, showing improved PFS (Kommoss et al., 2017). Based on this, it is essential to take into consideration recent histological and molecular findings when exploring new strategies for understanding and treating HGSOC.

1.2 Targeted therapies in ovarian cancer

Targeted therapies represent a novel approach for improving clinical outcome in ovarian cancer and are considered a more selective strategy than chemotherapy to kill cancer cells and overcome chemoresistance. Targeted therapies include low molecular weight inhibitors, such as olaparib that targets PARP, hormone receptor inhibitors and biological targeted therapies, such as anti-VEGF/VEGFR therapy. Currently, the most promising approaches include PARP and anti-VEGF/VEGFR agents, which only show a small improvement in progression-free survival when used as single agents (Banerjee and Kaye, 2013). Therefore, these therapies are commonly evaluated in combination with platinum compounds either in sensitive or recurrent tumours. Additionally, the success of PARP inhibitors such as olaparib has been biomarker driven, as it has widely been associated with use in patients with BRCA mutated tumours, which exhibit defective DNA, repair pathways and show higher sensitivity to this inhibition (Papa et al., 2016). However, despite improvements in therapeutic strategies for the treatment of ovarian cancer through the use of targeted therapy, the most important advancement required for an impact on treatment response remains improving our understanding of mechanisms of resistance and finding strategies for prospective patient selection to improve the probability of an improved response to therapy.

1.2.1 Discovery of VEGFA and the development of anti-VEGF and VEGFR therapies

In 1971, Judah Folkman stated that tumours require a blood supply in order to survive and grow, and introduced the hypothesis that angiogenesis, the *de novo* formation of blood vessels, regulates tumour development (Ribatti, 2008a). It was the first suggestion that the inhibition of angiogenesis could be therapeutic by inhibiting the blood supply to the tumour. To date, angiogenesis remains one of the most important hallmarks for tumour development (Hanahan and Weinberg, 2011). Further research by Harold Dvorak and colleagues showed that different cancer cells produced a vascular permeability factor (VPF) and suggested that VPF stimulates angiogenesis in tumours (Ribatti, 2007). Later, VPF was renamed vascular endothelial growth factor (VEGF) when the gene was cloned by Napolene Ferarra and this then led to the development of the first monoclonal antibody (bevacizumab, Avastin^{TM,} Genentech Inc) to block angiogenesis induced by VEGF (Ribatti, 2008b). Later, other tyrosine kinase inhibitor (TKI) molecules such as Sorafenib, Sunitinib and Pazopanib were developed with the aim of targeting VEGF receptors (Clarke and Hurwitz, 2013). The first clinical trials evaluating their effect on anti-angiogenic therapy in cancer showed poor results and suggested that tumour growth can be independent of angiogenesis and mechanisms of resistance can occur (Medina et al., 2007). These observations suggested that VEGF and VEGFR inhibition was more complex than initial assumptions indicated, which led to an increased interest in the biology and signalling of VEGF.

VEGF signalling is a central pathway that controls tumour growth and metastatic spread (Schmid and Oehler, 2014; Goel, H. and Mercurio, 2013). Inhibition of VEGF signalling has been considered a potential strategy for treating cancer by blocking angiogenesis and inhibiting the vascular blood supply to the tumour, a fundamental process of tumour growth and dissemination (Mabuchi et al., 2008). VEGFA inhibitors e.g. bevacizumab and VEGFR inhibitors e.g. cediranib are an example of therapies that inhibit angiogenesis (Burger, R., 2011). Targeted anti-VEGFA therapy has shown activity as a single agent in ovarian cancer (Kumaran et al., 2008), however, therapeutic efficacy is more beneficial when cytotoxic therapy is administered (Monk et al., 2013) (Table 1). It is not clear why anti-VEGFA therapy is clinically more effective in combination with standard chemotherapy. Although the effects of vascular normalisation and increased delivery of chemotherapy to tumours have been explored, the potential contribution of VEGFA-VEGFR signalling to chemotherapy response within HGSOC cells themselves is not understood. These mechanisms of action are discussed in more detail in section 1.4.

Table 1. Summary of clinical trials of bevacizumab in combination with chemotherapy in ovarian cancer.

Clinical Trial	Clinical setting	Treatment	Primary Outcome Measure	Reference
ICON7	First line therapy	Chemotherapy (n=764) Chemotherapy + Avastin (n=764)	PFS increased 2.4 months (5.5 months in Stage III/IV)	(Perren et al., 2011)
GOG-0218	First line therapy	Chemotherapy (n=625) Avastin + chemotherapy (n=625) Avastin + chemotherapy followed by Avastin (n=623)	PFS increased 3.8 months	(Burger, R.A. et al., 2011)
OCEANS	Platinum sensitive (recurrent OC)	Chemotherapy (n=242) Avastin + chemotherapy (n=242)	PFS increased 4 months	(Aghajanian et al., 2012)
GOG-0213	Platinum sensitive (recurrent OC)	Chemotherapy (n=337) Avastin + chemotherapy (n=337)	OS increased 4.9 months	(Coleman, R.L. et al., 2017)
AURELIA	Platinum resistant (recurrent OC)	Chemotherapy (n=182) Avastin + chemotherapy (n=179)	PFS increased 3.3 months	(Pujade-Lauraine et al., 2014)

1.2.2 Biomarkers for bevacizumab in ovarian cancer

Different studies have evaluated potential biomarkers to predict treatment response to bevacizumab. Initial studies following the ICON7 clinical trial evaluated the potential of circulating biomarkers in serum and plasma, these included mesothelin, VEGFR3, AGP, cancer antigen 125 (CA-125), ANG1 and TIE2 (Collinson et al., 2013; Backen et al., 2014; Zhou et al., 2016). Recently, retrospective analysis of advanced ovarian cancer patients from the GOG-0218 study evaluated potential biomarkers for predictive response to bevacizumab using immunohistochemistry (IHC) analyses on tumour samples and ELISA in plasma (Bais et al., 2017; Alvarez Secord et al., 2020). Five potential markers were evaluated using IHC including VEGFA, VEGFR2, NRP1, MET and CD31. Results from this study showed that high micro-vascular density (MVD) measured by CD31 was associated with increased PFI and OS as a result of bevacizumab treatment (Bais et al., 2017). Additionally, ELISA from blood samples evaluated the potential biomarker value of different angiogenic and inflammatory markers including IL6, ANG2, OPN, SDF1, VEGFD, IL6R and GP130. Results from this study showed that high levels of IL6 were associated with an increased response to bevacizumab (Alvarez Secord et al., 2020). Other predictive biomarkers suggested for bevacizumab in ovarian cancer include adiposity levels, inflammatory indexes, molecular subtypes and miRNAs (Slaughter et al., 2014; Farolfi et al., 2018; Kommoss et al., 2017; Halvorsen et al., 2017).

1.3 The VEGF and VEGF receptor families– an overview

There are several different ligands and receptors that compose the vascular endothelial growth factor (VEGF) family. In first instance, VEGF ligands include VEGFA (originally called VPF and VEGF), B, C, D and placental growth factor (PGF) (Vempati et al., 2014). Additionally, variants of these members can be found due to different mechanisms including alternative ribosomal start sites, mRNA splicing and proteolytic processing. This is described for VEGFA in more detail in section 1.5.

The VEGF receptor family includes VEGFR1, 2 and 3, which are type-I transmembrane proteins composed of a ligand binding site and an intracellular tyrosine kinase domain (Koch et al., 2011). Similarly to the VEGF ligands, splicing mechanisms and proteolytic processes can generate VEGFR variants including soluble VEGF receptors, which have different ligand affinity and can compete for ligand binding with the membrane anchored receptors (Koch et al., 2011). VEGF receptors can form homodimers or heterodimers between VEGF receptors (e.g. VEGFR1/VEGFR2 and VEGFR2/VEGFR3) resulting in differences in activation of intracellular signalling. In order to explore VEGFA regulation in ovarian cancer cells it is essential to understand VEGFA-VEGFR signalling, which will be described in more detail in the following sections.

1.3.1 VEGF-VEGF receptor signalling

Tyrosine kinase VEGF receptors play an important role in the biology of cancer development by directly contributing to the regulation of different intracellular signalling pathways (Fig. 3). Although VEGF receptor function is not well characterised in cancer cells it has been studied in more detail in endothelial cells. VEGF receptors are proteins that consist of an extracellular domain comprised of seven immunoglobulin-like domains, a transmembrane domain and an intracellular tyrosine kinase domain containing different tyrosine residues, which are involved in the activation of downstream signalling pathways (Shibuya, 2011). These downstream signalling pathways are also dependent on VEGFR cellular localisation. For example, activation of VEGFR2 in endosomes after ubiquitination and internalisation is dependent on its binding with NRP1. In a similar way, VEGFR3's endosomal internalisation induces activation of downstream signalling involving AKT, MAPK1 and RAC1 by regulation of the Ephrin B2 transmembrane protein (Koch et al., 2011).

Different proteins bind the VEGFR intracellular tyrosine kinase domains and mediate specific downstream signalling activation. These signalling proteins have specific domains that mediate the interaction between the tyrosine kinase receptor and other proteins involved in a variety of signalling pathways. Signalling proteins, such as GRB, SOS, and P85 bind to specific phosphorylated tyrosine residues and recruit proteins associated with downstream signalling transduction (Schlessinger, 2000). Some of these proteins are considered adaptor proteins. For example, GRB2 links tyrosine kinase receptor activation with the MAPK1 signalling pathway (Schlessinger, 2000). Another example involves the binding of the P85 PI3K subunit, a regulatory subunit that binds a specific phosphorylated tyrosine on activated receptors and induces the activation of the PI3K signalling pathway (Schlessinger, 2000).

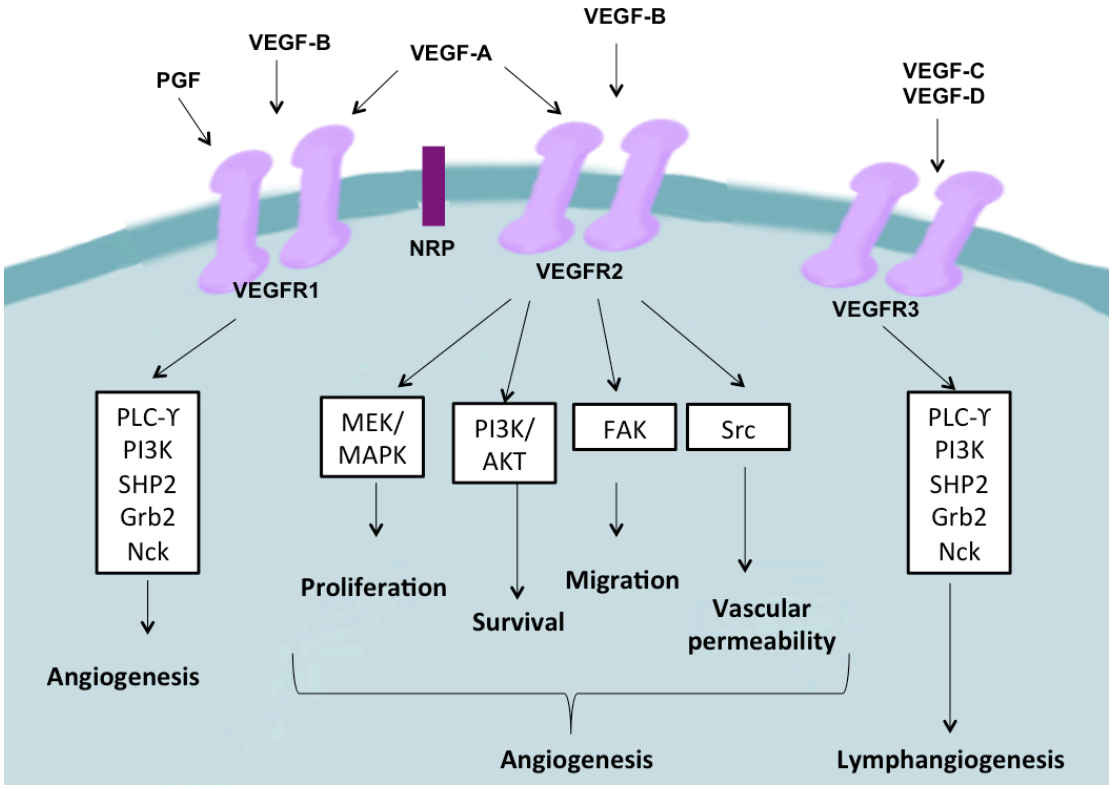

Figure 3. VEGF-VEGFR signalling.

VEGF receptors mediate diverse biological processes through the activation of different signalling pathways. VEGFA, B and PGF bind to VEGFR1 and activate downstream signalling pathways that are involved in angiogenesis. VEGFA and B principally activate VEGFR2 and consequently not only angiogenesis but also proliferation, survival, migration and vascular permeability through MAPK1, PI3K, FAK and SRC signalling pathways. Finally, VEGFC and –D mainly activate VEGFR3, which is associated with the development with lymphangiogenesis.

VEGFR signalling is commonly mediated through the interaction between dimers of both VEGF ligands and receptors. It has been shown that VEGF signalling is different between activation of homodimeric or heterodimeric receptors and it has been suggested that the phosphorylation pattern might be specific for each complex formed. Heterodimer formation between VEGFR1 and VEGFR2 has been observed to be activated by VEGFA, however the downstream activation of biological processes differs from the ones induced by VEGFR2 homodimer signalling (Domigan et al., 2015). Complexes between VEGFR2 and VEGFR3 can be activated by VEGFC in lymphatic endothelial cells, however downstream signalling is not well understood (Domigan et al., 2015). Although there is no evidence that VEGFA activates VEGFR3, VEGFR3 blockade induces a decrease in VEGFA dependent capillary sprout formation by endothelial cells, which suggests that VEGFR3 might have an effect on the response to VEGFA through complex formation with VEGFR2 (Domigan et al., 2015). Based on this, it is important to consider that VEGF-VEGFR signalling will be differentially regulated by homodimeric or heterodimeric complexes and these might explain alternative signalling and different cell responses.

VEGFRs can also interact with other transmembrane proteins that can further regulate signalling. Co-receptors such as neuropilins (NRPs) can also bind VEGF ligands, but lack tyrosine kinase activity themselves, and modulate ligand-receptor affinity and selectivity (Koch et al., 2011). VEGFRs can also interact with other tyrosine kinases including MET and PDGFR as well as integrins and MMP14. Ultimately the complexity of ligand – receptor – co-receptor interactions leads to cell type and context specific signalling that is tightly regulated.

1.4 VEGFA and the tumour microenvironment

1.4.1 VEGFA, angiogenesis and vascular normalisation

Angiogenesis is an essential process for supporting tumour growth by generating new blood vessels and allowing the delivery of oxygen and nutrients to the tumour, but this new vessel formation is physiologically abnormal in tumours (Goel, H. and Mercurio, 2013). However, it has been shown that tumours can have alternative mechanisms to obtain blood supply, such as vascular co-option, which is a process where some tumours grow on the top of existing vessels and anti-angiogenic therapy will not affect tumour blood supply in this instance (Leenders et al., 2002). Activation of angiogenesis is primarily regulated by the activation of endothelial cells through growth factors that are present in the tumour microenvironment such as the vascular endothelial growth factor A (VEGFA) (Biselli-Chicote et al., 2012). In cancer, the major producers of angiogenesis are the cancer cells themselves, as these express the majority of VEGFA, which is induced by hypoxia (Verheul and Pinedo, 2000).

VEGFA induces angiogenesis by stimulating endothelial cell proliferation and migration through signalling mechanisms such as MAPK1 and PI3K-AKT pathway. Subsequently, expression of metalloproteinases, such as MMP2, MMP9 and MMP14 allow the degradation of the basement membrane and ECM components which allows endothelial cell invasion and consequently the formation of lumen structures that develop into new vascular structures (Claesson-Welsh and Welsh, 2013). All these vascular changes result in new blood vessels with decreased endothelial cell-cell and basement membrane interactions that contribute to increased vascular permeability within the tumours (Claesson-Welsh and Welsh, 2013).

Anti-VEGFA agents mainly normalise blood vessel structures by increasing pericyte coverage and restoring endothelial function leading to recovery of natural vascular structure and function (Fig. 4). This decreases permeability and leakiness, thus improving blood flow rates. This also decreases interstitial fluid pressure as the balance of tissue fluid drainage from the vasculature to the lymphatic system is restored. The normalised tumour vasculature enhances cytotoxic drug uptake within the tumour, leading to an improvement in response to chemotherapy (Goel, S. et al., 2012).

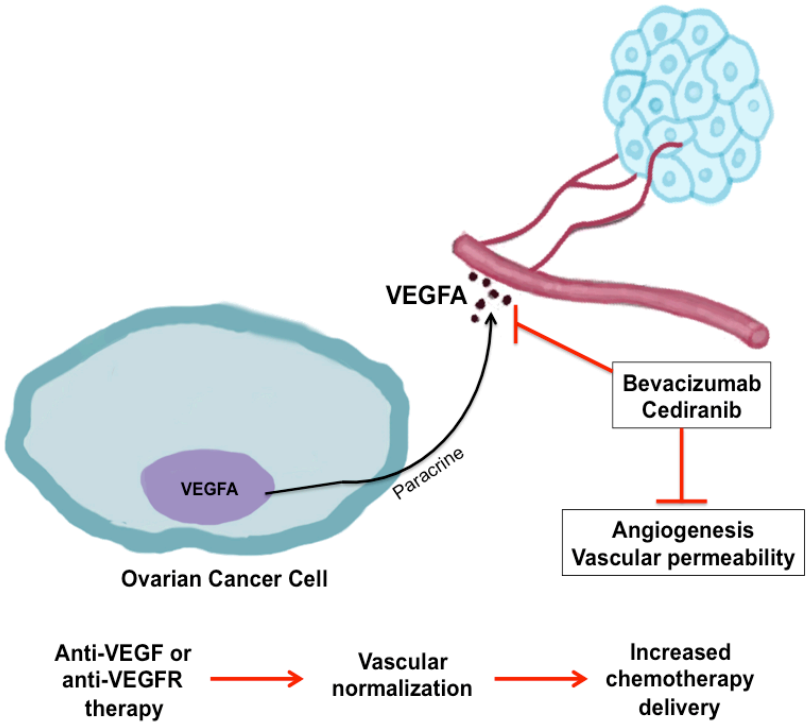

Figure 4. The effect of anti-VEGFA therapy on endothelial cells.

Anti-VEGFA therapy normalises blood vessel structure by increasing pericyte coverage and restoring endothelial function leading to recovery of natural vascular structure and function. The normalised tumour vasculature enhances drug delivery leading to an improvement in response to chemotherapy.

However, the function of VEGFA can be independent of angiogenesis and not restricted to endothelial cells (Goel, H. and Mercurio, 2013). Cancer cells themselves express various VEGF receptors, which can mediate different cellular functions such as proliferation, survival and migration (Goel, H. and Mercurio, 2013). Therefore, it is important to take into consideration the role of VEGFA not only between tumour and vascular stromal cells but also the role of VEGF-VEGFR signalling within ovarian cancer cells and its effect on therapeutic response.

1.4.2 VEGF and cancer cell biology

VEGF receptors can activate proliferation, survival and migration signalling pathways within some cancer cells via autocrine signalling where VEGF ligands bind the VEGFR after secretion or via intracrine signalling where VEGF ligands bind the receptor within the cell before secretion (Fig. 5). Therefore, anti-VEGF/VEGFR agents have an effect on cancer cells and the mechanism of response or resistance is dependent on cell type (Simon et al., 2017). It has been shown that bevacizumab has an effect on different myeloma cell lines by decreasing survival and proliferation (Simon et al., 2017). Additionally, VEGFR tyrosine kinase inhibitors such as sunitinib induce apoptosis and decrease cell viability in adrenocortical carcinoma cell lines. However, the same anti-VEGF/VEGFR effect has not been observed in *in vitro* studies performed in other cancer cells (Simon et al., 2017).

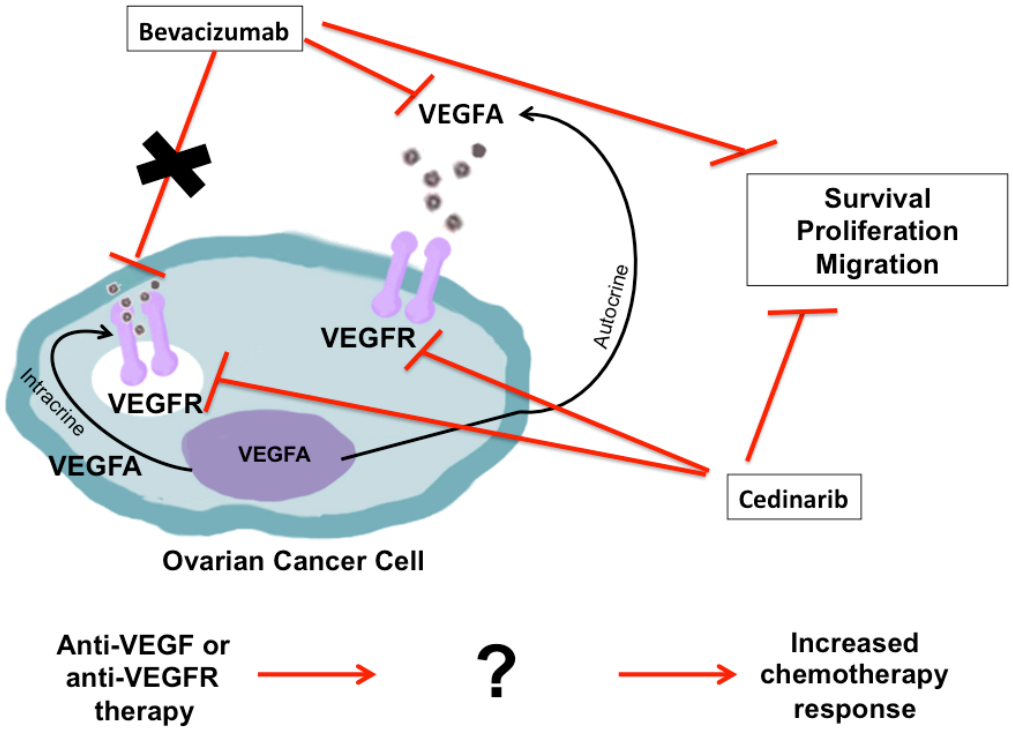

Figure 5. Effects of VEGF on cancer cells.

VEGFRs can activate survival signalling pathways within some cancer cells via autocrine signalling where VEGFA binds the VEGFR after secretion or via intracrine signalling where VEGFA binds the receptor within the cell before secretion. This could also be a mechanism by which VEGF-VEGFR therapy enhances chemotherapy in HGSOC.

Anti-VEGFA agents such as bevacizumab, a monoclonal antibody blocking VEGFA, do not completely block VEGFA-VEGFR signalling in some cancers, leading to the enhancement of tumour aggressiveness by using alternative activation of the VEGFR signalling pathway. *In vitro* studies in osteosarcoma cell lines showed that autocrine VEGFA-VEGFR1 signalling induced proliferation and survival leading to more aggressive tumour progression when tested *in vivo* (Ohba et al., 2014). Additionally, studies in melanoma and glioblastoma cells showed that blocking of VEGFA with bevacizumab increased proliferation while sunitinib, a VEGFR tyrosine kinase inhibitor decreased it (Simon et al., 2017). However, it is important to take into consideration that tyrosine kinase inhibitors, such as sunitinib, might block the activation of multiple signalling pathways through targeting different tyrosine kinase receptors (e.g. PDGFRB, KIT) while bevacizumab acts only by targeting VEGFA and therefore fewer signalling pathways. The effect of anti-VEGFA therapy in HGSOC cells has not been fully explored and in order to provide new insights into the mechanisms of response or resistance to these therapeutic approaches, an improved understanding of VEGF-VEGFR signalling in HGSOC cells is essential.

In cancer cells, activation of autocrine VEGF signalling pathways has been associated with invasion and migration. Specifically, activation of VEGFR1 by exogenous VEGFA, VEGFB and VEGFC was correlated with the activation of intracellular signalling pathways such as AKT and MAPK1 in hepatocellular cancer cells (Morelli et al., 2009). The activation of these downstream kinases was also associated with the activation of VEGFR3, however VEGFR3 phosphorylation levels were saturated as they could not be increased by the addition of further exogenous VEGF ligands (Morelli et al., 2009). Blocking of VEGFR1/VEGFR3 signalling by using pharmacological inhibition with cediranib showed a decrease in phosphorylated AKT and MAPK1 levels and migration (Morelli et al., 2009). Additionally, autocrine PGF-VEGFR1 signalling was shown to induce cell invasion in glioblastoma cells by activating AKT and MAPK1 signalling pathways after bevacizumab treatment, which indicates it might be a mechanism of resistance to this type of therapy (Simon et al., 2017). Activation of VEGFR1 by PGF has also been observed in breast and pancreatic cells (Ning et al., 2013; Yang et al., 2006). Additionally, ovarian cancer cells can induce invasiveness and migration through autocrine VEGFR3 activation by VEGFC (Decio et al., 2014). Another study in ovarian cancer cells showed that phosphorylation of VEGFR3 by VEGFC induced activation of the downstream MAPK1 signalling pathway while inhibition of VEGR3 by

treatment with the VEGFR3 selective tyrosine kinase inhibitor MAZ51 decreased it and improved response to treatment with cisplatin (Lim et al., 2014).

Initial evidence of an intracrine VEGF signalling pathway has been described in melanoma, colorectal and breast cancer cells (Adamcic et al., 2012; Bhattacharya et al., 2016; Lee, T. et al., 2007). Intracrine signalling has also been detected between VEGFA and VEGFR1 in colorectal cancer cells and this mechanism mediates cell survival, possibly through the AKT pathway (Bhattacharya et al., 2016). A different study suggested that loss of VEGFA intracrine signalling in colorectal cancer cells has an impact not only on cell survival but also in sensitivity to cytotoxic compounds such as 5-fluorouracil (Samuel et al., 2010). These could be important mechanisms by which anti-VEGF/VEGFR therapy enhances the response to chemotherapy. However, autocrine and/or intracrine VEGF-VEGFR signalling in HGSOC has not been described in detail. In order to understand if VEGF signalling can influence response and resistance to both anti-VEGF/VEGFR therapy and platinum based chemotherapy, it is essential to understand how VEGF-VEGFR signalling is regulated in HGSOC cells.

1.4.3 VEGFA and immune cell function

The role of VEGFA on immune cell function has been extensively described (Li, Y.L. et al., 2016). In ovarian cancer, VEGFA can induce immune suppression by decreasing the activation of T-cells through VEGFR2 (Gavalas et al., 2012). It has also been described that VEGFA expression is associated with increased abundance of myeloid-derived suppressor cells (MDSC) and inhibition of T-cell activation, which is associated with immune evasion in mouse models (Horikawa et al., 2017). Additionally, VEGFA can increase the expression of immune checkpoint modulators such as the programmed cell death-1 receptor (PD1) and VEGF/VEGFR inhibition is associated with decreased expression of PD1 on T-cells in *in vitro* and *in vivo* colorectal cancer models (Voron et al., 2015). More recently, the impact of VEGFA on the immune system has created particular interest in the combination of anti-angiogenic therapy with immune checkpoint inhibition (Ciciola et al., 2020).

Additionally, changes in the immune system in ovarian cancer patients have been associated with clinical outcome. One of these immune characteristics includes the presence of tumour infiltrating lymphocytes (TIL). In HGSOC, abundance of TIL has been associated with

improved survival in different studies (Webb et al., 2016; Pinto et al., 2018). In particular, hypoxia can modulate the infiltration of immune cells and impact treatment response. Townsend et. al described that highly vascularised HGSOC tumours expressing CD31 and VEGFA showed survival advantage when compared with poor vascularised tumours. This study also determined that the presence of TIL was higher in patients with highly vascularised tumours, specifically high vascular density was associated with the presence of CD8, CD4 and FOXP3 positive cells (Townsend et al., 2013). Interestingly, TIL prognostic relevance in HGSOC patients can depend on tumour vasculature as presence of TIL in tumours with low vascular density showed decreased survival outcome (Townsend et al., 2013). It is important to understand the role of immune cells within the HGSOC microenvironment in order to develop and improve treatment for this disease.

1.5 *VEGFA* – Gene structure and transcriptional regulation

The genomic location of the human *VEGFA* gene is on chromosome 6 at locus 6p21.1 (Arcondeguy et al., 2013). The *VEGFA* gene consists of 7 introns and 8 exons that encodes 206 amino acids. The 5' UTR region of the gene includes a promoter sequence that allows the binding of transcriptional regulator molecules (Arcondeguy et al., 2013). The *VEGFA* gene is regulated by hypoxia through transcriptional activators such as the Hypoxia Inducible Factor (HIF) (Arcondeguy et al., 2013). In normoxia HIF1 levels are regulated mainly by post transcriptional modification by prolyl hydroxylases that induce its recognition by the von Hippel Lindau (VHL) protein and subsequently proteasome degradation (Ramakrishnan et al., 2014). However, under hypoxic conditions HIF1 translocates into the nucleus where it then binds to the hypoxic response elements (HRE) within the 5' UTR region of the *VEGFA* gene inducing its up-regulation (Ramakrishnan et al., 2014).

Single nucleotide polymorphisms (SNPs) in the *VEGFA* gene have been associated with human diseases such as diabetes, cardiovascular disease and cancer (Buroker, 2015; Liu, D. et al., 2016). In ovarian cancer, Janardhan et al. studied six different SNPs associated with tumour progression and clinical outcomes in 300 patients. In this study, SNP rs3025039 was described as potential marker for poor prognosis as it showed significant association with advanced FIGO stage, presence of ascites, tumour recurrence and increased post-operative levels of CA-125 (Janardhan et al., 2015). Additionally, Steffensen et al. described that *VEGFA* SNPs can be closely related to the levels of VEGFA in serum in patients with

epithelial ovarian cancer, suggesting that these SNPs can potentially regulate gene function (Steffensen et al., 2010).

1.5.1 Post-transcriptional regulation of VEGFA – pre-mRNA splicing, miRNA targeting and proteolysis

Alternative splicing is the main post-transcriptional mechanism of regulation of VEGFA. VEGFA isoforms are created by the retention or removal of specific exons which result in protein variants with different numbers of amino acids (Arcondeguy et al., 2013). The *VEGFA* gene consists of 8 exons and the site of recognition for VEGFR binding is encoded by exons 1 to 5. These specific exons are therefore present in all VEGFA isoforms. The distinctions between isoforms resides in the presence or absence of exons 6 to 7 (Stimpfl et al., 2002). These exons regulate association with the extracellular matrix (ECM), and therefore diffusion of VEGFA isoforms, as well as association with co-receptors including the neuropilins that regulate downstream signalling (Vempati et al., 2014). The most common VEGFA isoforms generated include VEGFA121, VEGFA145, VEGFA165, VEGFA183 and VEGFA189. The *Vegfa* mouse gene encodes VEGFA isoforms that are virtually identical to the human equivalent, but with one amino acid less, for example VEGFA120, VEGFA164 and VEGFA188 (Arcondeguy et al., 2013).

Alternative splicing within exon 8 of *VEGFA* can generate isoforms of similar length to the previously described isoforms, only with a different amino acid sequence within the C-terminal region of the protein (Ladomery et al., 2007). These specific variants are defined as VEGFAxxxb isoforms, such as VEGFA121b, VEGFA165b and VEGFA189b, and have been associated with anti-angiogenic regulation in different tumours (Bates et al., 2002). Recently, the existence of these VEGFAxxxb isoforms has been widely discussed. Bridgett et al. showed that VEGFAxxxb mRNA expression was not detected by RNA sequencing in human tissue, suggesting that these isoforms might be non-existent or their abundance extremely low (Stephen et al., 2017). Additionally, it has been suggested that these VEGFAxxxb isoforms are a consequence of artefactual generation of PCR products (Harris et al., 2012; Dardente et al., 2020).

The presence of an alternative initiation codon (CUG) within the 5'UTR region of the *VEGFA* gene has shown to be involved in the synthesis of longer isoforms (L-VEGFA) (Arcondeguy et al., 2013). It has been suggested that these L-VEGFA proteins may represent the storage or inactive form that will later generate the classical VEGFA isoforms (Tee and Jaffe, 2001; Huez et al., 2001). Additionally, the presence of this 5' UTR extension might be important in the regulation of VEGFA isoform stability in hypoxia (Rosenbaum-Dekel et al., 2005).

Another mechanism associated with post-transcriptional regulation of *VEGFA* is miRNA targeting and different miRNA binding sites have been identified within the *VEGFA* 3' UTR region (Arcondeguy et al., 2013). These miRNAs can alter the activity of the alternative CUG initiation codon and consequently regulate VEGFA isoform expression (Karaa et al., 2009). In ovarian cancer, miR-6086 has been associated with downregulation of VEGFA. Additionally, *in vitro* inhibition of this miRNA has been demonstrated to enhance VEGFA expression in Caov3 and COV362 ovarian cancer cells (Wu et al., 2020).

Finally, VEGFA isoforms can also be generated by proteolytic cleavage. Plasmin proteolysis of VEGFA165 generates cleavage products that differ in their biological activity (Roth et al., 2006). Specifically, proteolytic cleavage of VEGFA165 by plasmin results in a VEGFA fragment with 110 amino acids defined as VEGFA110 (Roth et al., 2006). Additionally, cleavage of VEGFA188 and VEGFA164 by metalloproteinases can generate VEGFA fragments with 113 amino acids (VEGFA113), which display similar biological effects to VEGFA120 in *in vivo* models (Lee et al., 2005). VEGFA can also be regulated by association with CCN2, which binds and inactivates VEGFA, and in common with other growth factor binding proteins, proteolytic cleavage by matrix metalloproteinases releases VEGFA from CCN2 (Nishida et al., 2009).

1.5.2 VEGFA isoforms - biology and signalling

Differences in isoform expression patterns mediate the activation of specific signalling pathways and expression of different genes, which consequently influences biological processes in development and pathology (Biselli-Chicote et al., 2012). For example, VEGFA164 expression leads to normal embryonic vascular development in mouse models (Küsters et al., 2003). In contrast, expression of VEGFA121 led to lethal abnormalities in vascular development (Küsters et al., 2003). VEGFA isoforms vary in their interaction with VEGFRs, their co-receptors and the ECM, resulting in differences in proliferation, apoptosis and migration (Vempati et al., 2014). Zhang et al. described that VEGFA165 induces cell proliferation by activation of the MAPK1 pathway while VEGFA121 increases permeability by activation of the SRC pathway on HUVEC cells *in vitro* (Zhang, Y. et al., 2008).

VEGFA isoforms activate the migration of endothelial cells at different levels. VEGFA165 activates phosphorylation of VEGFR2, then a further interaction with PLCG1 induces nuclear translocation of NFATC2 and consequently regulation of endothelial cell migration. Although this signalling mechanism is also observed with VEGFA121 stimulation, a reduced effect is observed (Fearnley, G.W. et al., 2015). VEGFA isoform signalling has also been associated with endothelial cell-cell interactions. Specifically, VEGFA165 stimulates phosphorylation of VEGFR2 that induces activation of the MAPK1 kinase and ATF2. This mechanism regulates VCAM1 expression, which in consequence modulates interactions between endothelial cells and leukocytes. Unlike VEGFA121, which does not induce significant phosphorylation of VEGFR2 at Y1175, VEGFA165 activates this phosphorylation site rapidly leading to an increased impact on signalling via this specific site. These isoforms can have different effects not only on activation and synthesis of VEGFR2 but also other receptors such as VCAM1 (Fearnley, G.W. et al., 2014). VEGFA isoforms can also regulate endocytosis of VEGFRs differently, which as described in previous sections, influences downstream signalling. While VEGFA121 appears to have a minor effect in promoting endocytosis via VEGFR2 signalling, VEGFA165 shows increased activation of this process through the VEGFR2-AKT-MAPK1 pathway (Fearnley, G. et al., 2016). The regulation of VEGFR signalling by VEGFA isoforms is poorly understood and the effect of this on HGSOC response to therapy has not yet been explored.

1.6 Clinical relevance of VEGFA isoform expression

High expression levels of different VEGFA isoforms in cancer patients have not only been associated with poor prognosis but also with an improved response to VEGFA therapy. To date, there are no predictive biomarkers validated for clinical use to identify cancer patients that are more likely to respond positively to anti-VEGFA therapy. Retrospective analysis of phase III trials of bevacizumab in gastric, breast and pancreatic cancer has identified improved progression-free survival in patients with high plasma levels of VEGFA121 when measured using a VEGFA121 selective ELISA (Miles et al., 2013; Van Cutsem et al., 2011; Van Cutsem et al., 2012).

Although measurement of short VEGFA isoforms in plasma had emerged as a promising biomarker for anti-VEGFA therapy after retrospective analyses, recent prospective studies did not validate these findings. MERiDiAN, a prospective study in breast cancer, does not support the use of plasma VEGFA (pVEGFA) as a predictive biomarker for response to anti-VEGFA therapy (Miles et al., 2017). The failure of MERiDiAN to prospectively validate the retrospective hypothesis generated of the AVADO studies was ultimately identified in part due to poor initial characterisation of the IMPACT ELISA developed by ROCHE GmbH and also a failure to identify that pVEGFA can vary significantly in patients day-to-day. This may have led to MERiDiAN being under-powered and pVEGFA cut-offs for decision to treat or not to treat with bevacizumab incorrectly being set (Bais et al., 2014). Published details of the IMPACT assay describe that different VEGFA isoforms were used as a standard reference protein for the assay during its development, and included VEGFA189 and VEGFA165 at different times, but not VEGFA121, despite the ELISA's original development to be highly selective for VEGFA121/110 (Miles et al., 2017). It has also been suggested that the ELISA method for VEGFA isoform detection in the circulation has important fundamental limitations. The ELISA assays used in different studies have difficulty in measuring multiple VEGFA isoforms and might not be representative of the tumour and also related to other type of cells (Rana et al., 2017).

Improvements in ELISA assays have been made in order to overcome these limitations but it might be possible that the detection strategy has to be changed in order to be able to measure VEGFA isoform levels accurately within tumours. The retrospective analysis of AVADO also measured cell free circulating VEGF121 mRNA and VEGFA isoform mRNA has been measured in renal and colorectal tumours by QRT-PCR, suggesting PCR rather than ELISA

may be more appropriate. Further work is needed to determine whether tumour cell expression of VEGF121 or related markers could be used as predictive biomarkers.

1.7 Background data

Pilot data obtained within the English lab had suggested alteration of VEGFA mRNA isoform expression may lead to differences in sensitivity to bevacizumab *in vitro* and *in vivo*. Zinc Finger Nuclease (ZFN) gene-editing technology was used to produce human ovarian COV362 cancer cells expressing different levels of VEGFA121 by using homology repair within a cut in exon 4 to introduce spliced exons 4 – 8, similar to the approach used to generate the $Vegfa^{120/120}$ mice (Vieira et al., 2007; Tozer et al., 2008). This preliminary data showed that cells heterozygous for $VEGFA^{121/WT}$ have increased proliferation *in vitro* that is inhibited by bevacizumab compared to $VEGFA^{WT/WT}$ cells. These also showed increased responsiveness to bevacizumab in pre-clinical models of metastatic disease (Valluru M and English WR unpublished). Although these results were promising, this was from only one clone and analysis of additional clones is required to confirm this result was not a clonal artefact. Isolation of correctly edited clones was also highly inefficient as sequence analysis showed the majority had edits in the inserted region and were effectively $VEGFA^{KO/WT}$ cells, meaning further development of the gene editing method is needed.

1.8 Hypothesis and aims

Based on evidence from the literature and unpublished data from studies preceding this thesis, we hypothesised that changes in VEGFA isoform expression may regulate HGSOC disease progression and tumours expressing increased levels of VEGFA121 could be particularly sensitive to anti-VEGFA therapy.

Objectives:

1. To identify if there is a correlation between *VEGFA* mRNA isoform expression and clinical outcome in HGSOC patients.
2. To create new ovarian cancer cell lines expressing increased VEGFA121.
3. To determine if increased VEGFA121 expression regulates response to chemotherapy and bevacizumab in ovarian cancer cells *in vitro* and *in vivo*.

Chapter 2

2. Materials and Methods

Description and suppliers of consumables, reagents and kits are described in tables 2 and 3.

Table 2. List of consumables and reagents.

Reagent / Consumable	**Company**	**Cat. No.**
Agar	Alfa Aesar	A10752
Agarose	Geneflow	A4-0698
Amersham ECL Reagents	GE Healthcare	RPN2209
Ammonium Persulphate (APS)	Sigma-Aldrich	A3678
Ampicillin	Sigma-Aldrich	A9518
B20-4.1.1	Genentech	-
BlueStar Plus Prestained Protein Marker	NIPPON Genetics	MWP04
Carboplatin	LKT Laboratories	C0171
Culture-Insert 2 Well	Ibidi	80209
CutSmart® Buffer	New England BioLabs	B7204S
Deoxyribonuclease I Amplification grade kit	Invitrogen	18068-015
Deparaffinization Solution	Qiagen	19093
Dimethyl Sulfoxide (DMSO)	Sigma-Aldrich	D8418
Dithiothreitol (DTT)	Sigma-Aldrich	D9163
Dual-chamber slides	Bio-Rad	1450015
Dulbecco's Modified Eagle Medium (DMEM)	Sigma-Aldrich	D6429
Subcloning Efficiency DH5α Competent Cells	Invitrogen	18265017

Electoporation cuvettes	Geneflow	E6-0062
Ethylenediaminetetraacetic acid (EDTA)	Sigma-Aldrich	3690
ELISA STOP solution	CellSignaling	7002S
Fast SYBR® GreenMaster Mix	Applied Biosystems	4385612
Fetal Bovine Serum (FBS)	Sigma-Aldrich	F9665
FseI	New England BioLabs	R0588S
Gel Loading Dye (6x)	New England BioLabs	B7025S
HindIII-HF	New England BioLabs	R3104S
Ingenio® Electroporation Solution	Mirus	MIR50111
Isofluorane	Zoetis	-
L-glutamine Solution (200 mM)	Lonza	3MB042
Laemmli buffer (4x)	Bio-Rad	1610747
LB-Lennox broth	Alfa Aesar	H26760
MicroAmp Optical 384-well plate	Invitrogen	4309849
MicroAmp Optical adhesive Film	Invitrogen	4374966
MluI-HF	New England BioLabs	R3198S
Nitrocellulose membrane	Bio-Rad	1620112
NuPAGE® transfer buffer	Thermo Fisher Scientific	NP0006
OCT Mounting Medium	Thermo Fisher Scientific	LAMB-OCT
Penicillin-Streptomycin	Sigma-Aldrich	P4333
Phosphatase inhibitors	Merck Millipore	524625
Phosphate-Buffered Saline	Lonza	17-516F
Protease inhibitors (Complete-Mini EDTA-free)	Merck Millipore	5892791001

Protogel (30%)	National Diagnostics	A2-0072
Protogel Resolving Buffer	National Diagnostics	B9-0012
ProtoGel Stacking Buffer	National Diagnostics	B9-0014
Puromycin	Sigma-Aldrich	P8833
Quick-Load DNA ladder	New England BioLabs	N0551S
RIPA buffer	Thermo Fisher Scientific	89900
SOC medium	Invitrogen	15544-034
Stripping buffer	Thermo Fisher Scientific	46430
SYBR safe	Invitrogen	S33102
T4 DNA ligase	New England BioLabs	M0202S
T4 DNA ligase buffer	New England BioLabs	B0202S
Tris-Borate-EDTA (TBE) buffer	National Diagnostics	B9-0020
Tetramethylethylenediamine (TEMED)	Sigma-Aldrich	T9281
TMB Substrate Solution	Thermo Fisher Scientific	34028
TransIT-2X	Mirus	MIR6000
Tris-Buffered Saline (TBS) buffer	Chem Cruz	sc-362305
Tris-Glycine SDS-PAGE buffer	National Diagnostics	EC-870
Trypan Blue Dye (0.4%)	Bio-Rad	1450021
Trypsin-EDTA	Sigma	T3924
Tween-20	Sigma	P9416
UltraPure™ DNase/RNase-Free Distilled Water	Thermo Fisher Scientific	10977035
Vinblastin	Sigma-Aldrich	V1377

Table 3. List of Kits.

KIT	Company	Cat. No.
GenElute™ Mammalian Genomic DNA Miniprep Kit	Sigma-Aldrich	G1N70
GenElute™ Total RNA Purification Kit	Sigma-Aldrich	RTN70
High Capacity cDNA Reverse Transcription Kit	Invitrogen	4374966
Human VEGF DuoSet ELISA	R&D	DY293B
Monarch® DNA Gel Extraction Kit	New England BioLabs	T1020S
Mouse VEGFA DuoSet ELISA	R&D	DY493
MTT Vybrant® Cell Proliferation Assay	Thermo Fisher Scientific	V-13154
Pierce™ BCA Protein Assay	Thermo Fisher Scientific	23227
Q5® Site-Directed Mutagenesis Kit	New England BioLabs	E0554S
QIAprep® HiSpeed® Plasmid Maxi Kit	Qiagen	12643
QIAprep® Spin Miniprep Kit	Qiagen	27104
RNeasy FFPE Kit	Qiagen	73504

2.1 Pre-clinical models

2.1.1 Licences and ethical approval

Ethical approval for work presented in this thesis, conducted under the Home Office Personal Project Licence (PPL) PDA78C678, was granted by the Animal Welfare & Ethical Review Body Project Applications and Amendments Sub-committee (PAAC), the University's Ethical Review Process constituted under the Animals (Scientific Procedures) Act 1986 (ASPA) Ethical Review Process. All experiments were conducted in accordance with the ASPA as well as guidance provided by the Home Office, the Laboratory Animal Science Association (LASA), the National Centre for the 3Rs (NC3R), the Nominated Vetinary Surgeon (NVS) and the Nominated Animal Welfare Care Officers (NACWO) at the University of Sheffield facilities (Section 2C Establishment Licence (PEL) X57506C3D). Work conducted on the PPL PDA78C678 was subject to review by the Universities Animal Welfare & Ethical Review Body (ASPA Ethical Review Process) 3Rs sub-committee. All protocols were submitted for review by the NVS and NACWO before their start.

2.1.2 Animals

6-8 week-old female NSG, SCID and C57BL6J mice were obtained from Charles River and were allowed ten days to acclimatise in the Sheffield facility before the start of protocols. Mice were pathogen free and maintained in individually ventilated cages. Pathogen status was periodically monitored through the use of sentinel mice in the same IVC raking system also exposed to bedding from mice in the same rack.

2.1.3 Subcutaneous tumour growth

Subcutaneous tumours were established by injection of 3 x 10^6 ID8 WT or ID8 VEGFA120 cells in 50 μl of PBS. Tumour volume was measured weekly with a digital calliper. As this was a pilot experiment, four mice per group were chosen to provide initial estimates of growth and variance that could be used for subsequent power calculations needed to estimate sample size for larger studies.

2.1.4 Intraperitoneal tumour growth

Based on previous small pilot studies conducted by Dr Will English prior to the start of this PhD, intraperitoneal tumours were established by injection of 5 x 10^6 ID8 WT or ID8 VEGFA120 cells in 100 μl of PBS. Although these initial studies established the number cells to be injected, they were not suitable for power calculations needed to estimate group size for treatment. To this end, pilot experiments using a group size of six were used for ID8 and ID8 cell lines expressing VEGFA120. Based on this data power calculations showed it would be possible to detect a 20% difference in weight change (primary end point for ascites/tumours) with alpha 0.05 and 80%power with a group size of eight mice and more than 90% power with a group size of ten. A group size of ten was selected >80% power would be maintained even if two mice were lost prior to the end of the protocol, e.g. through lack of tumour take or other adverse events (poor recovery from anaesthesia etc.).

Weight change was monitored weekly and mice were treated upon a weight increase of 30% being reached. For treatment with control IgG or anti-VEGFA (BE5 or B20-4.1.1 respectively, kindly provided by Genentech Inc) (Liang et al., 2006), mice were injected twice a week with 5 mg/kg antibody in 50 μl PBS for 6-7 weeks or up to either a maximum of 50% weight increase or if showing more than a moderate level of suffering, which was

defined as an easily detectable clinical changes including physical discomfort, abnormal behaviour or significant weight loss. Mice were randomised for treatment between groups and cages to avoid cage effects.

Non-invasive ultrasound imaging was used for monitoring tumour progression and ascites accumulation. Mice were anesthetised using 2-3% isofluorane and hair was removed with removal cream from the abdominal site to enable imaging. For each selected mouse, abdominal ultrasound was performed weekly using Vevo3100 system. This was performed in collaboration with Professor Allan Lawrie's group with the help of Nadine Arnold.

2.1.5 Sample collection

Mice were placed under terminal anaesthesia (using 2-3% isofluorane in O_2) for plasma collection via cardiac bleeding. Specifically, blood was collected in tubes containing 50 µl cold EDTA and centrifuged at 10,000 x g for 10 minutes at 4 °C to remove cells and platelets. The supernatant (plasma) was transferred to a new tube and stored at -80 °C. Additionally, ascitic fluid was removed with a needle through a small dermal incision to the side of the abdomen. Cells were recovered from the ascitic fluid by centrifuging at 1,200 x g for 10 minutes at 4 °C and frozen as described in Methods section 2.3.3. The ascitic fluid was stored at -80 °C. Finally tumours were removed and frozen in optimal cutting temperature mounting medium (OCT) and stored at -80 °C for further sectioning and protein and RNA analysis.

2.2 Cell culture

The human ovarian cancer cell line COV362 was purchased from ECACC. Mouse ID8 cells were obtained from Kansas University, KU Center for Technology Commercialization, USA. All cell lines were maintained using Dulbecco's Modified Eagle's Medium (DMEM) supplemented with 10% v/v heat inactivated fetal bovine serum (FBS), 2 mM L-glutamine, 1% penicillin-streptomycin (100 units and 100 μg/ml, respectively). Cells were incubated at 37 °C and 5% CO_2 until passage 30 after receipt from the culture collection.

2.2.1 Cell thawing

For cell thawing, cryotubes containing cells were placed at 37 °C in a water bath and samples were then transferred into 15 ml tubes containing pre-warmed cell culture medium. Cells were centrifuged at 400 x g for 5 minutes, the supernatant was discarded and the cell pellet was resuspended in fresh cell culture medium and transferred into T25 flasks containing 5 ml of pre-warmed medium.

2.2.2 Cell passage

For cell maintenance, cell cultured medium was changed every two days until 80-90% cell confluence was reached. For cell passaging, the cell culture medium was discarded and 2 ml of trypsin-EDTA (0.5 g/l trypsin and 0.2 g/l EDTA) was added to detach the adherent cells. The flasks were incubated at 37 °C for 5 minutes or until cells detached. 2 ml of pre-warmed medium was used to wash the detached cells and the cell suspension was collected in 15 ml tubes. Subsequently, cells were centrifuged at 400 x g for 5 minutes, the supernatant was discarded and the cell pellet was resuspended in fresh cell culture medium. Cells were then transferred into a new flask at the required cell density.

2.2.3 Cell freezing

For cell freezing, cells were trypsinised as previously described in the cell passaging protocol and resuspended in freezing medium containing 90% FBS v/v and 10% DMSO v/v. Cell aliquots containing approximately 1 x 10^6 cells were transferred into cryotubes and

frozen in a freezing container at -80 °C and transferred to liquid nitrogen for long term storage.

2.2.4 Cell counting

Cell counting was performed using a BioRad automated cell counter (TC20). The cell suspension was mixed with 1:1 trypan blue reagent, and 10 µl of the mixed suspension was loaded into a counting slide and viable cells were counted.

2.2.5 Cell transfection

2.2.5.1 Reagent based transfection

ID8 cells were transfected using TransIT-X2 transfection reagent. 5 x 10^4 cells were seeded in 6-well plates and incubated overnight. 1 µg of plasmid DNA (Piggy Bac Transposon system is described in section 2.5.2) was added to 250 µl of warmed serum-free cell culture medium. Subsequently, 7.5 µl of warm Transit-X2 was added to the DNA mixture and incubated for 15 minutes at room temperature. Later, the DNA-Transit-X2 mixture was added to the wells and incubated for 24 hours. Finally, transfected ID8 cells were selected in fresh cell culture medium containing 4 µg/ml of puromycin for 3 to 5 days.

2.2.5.2 Electroporation

For electroporation, COV362 cells were trypsinised as previously described and 2 x 10^6 cells were used per transfection. Cells were resuspended in 100 µl of electroporation solution and 1 µg of plasmid DNA was added (ZFN system described in section 2.5.1). The cell suspension was then transferred to an electroporation cuvette and electroporated with an Amaxa® Nucleofector using V-020 program. Immediately after electroporation, samples were transferred to a 6-well plate containing pre-warmed cell culture medium and incubated. After 24 hours, cells were treated with 0.2 µM of Vinblastin for 6 hours.

2.2.6 Single cell cloning

Isolation of cell colonies was performed by single cell dilution as follows. Transfected cells were trypsinised as previously described and diluted to a concentration of 5 cells/ml. Then, 100 µl of the cell suspension was transferred into each well of a 96-well plate allowing for an average cell density of 0.5 cells per well. Wells containing single cells were incubated for 3-4 weeks and the plate was monitored for cell growth by microscopy. Once wells were confluent, colonies were expanded for further analysis.

2.2.7 Cell viability assays

Cell viability was measured using the MTT assay, an assay for measuring metabolic activity, which is presumed to be directly proportional to the number of viable cells. Specifically, viable cells convert soluble MTT to a purple formazan that accumulates within the cells as an insoluble precipitate, while dead cells cannot convert the MTT to formazan (Assay guidance manual). However, this assay might be a measure of mitochondrial activity rather than cell proliferation (Berridge et al., 1996). Therefore, MTT results were validated using trypan blue assay.

Dose response curves to carboplatin and B20-4.1.1 were performed on the ovarian cancer cell lines. ID8 cells were plated in 96 well plates at 5 x 10^3 cells per well and allowed to attach for 24 hours. Subsequently, cell culture medium was supplemented with 0-4000 µM of carboplatin or 0-100 nM of B20-4.1.1 for 48 hours at 21% O_2. Cell viability was investigated using the MTT Vybrant® Cell Proliferation Assay. Cells were labelled with 10 µl of 12 mM MTT in 100 µl of fresh maintenance medium and incubated at 37 ºC for 4 hours. After labelling, 100 µl of dimethyl sulfoxide (DMSO) was used as a solubilising agent. Finally, the plate was read on a microtitre plate reader at an absorbance of 450 nm. The Lethal dose 50% (LD50) was calculated using a four-parameter dose-response curve in GraphPad Prism 7.

2.2.8 Migration assay

Migration studies were performed using the wound-healing assay with the Ibidi 2 well culture-inserts. Ibidi inserts were placed on 12-well plates, 5 x 10^4 cells were seeded into each well of the culture-insert in 50 µl of cell culture medium and incubated overnight at 37 °C and 5% CO_2. Subsequently, cell culture-insert was removed using sterile forceps and cells

were washed twice with PBS to remove non-attached cells. Wells were filled with 2 ml of fresh cell culture medium and the gap between the two groups of cells was monitored by microscopy using a 4x objective with the Nikon Eclipse TS100 system. The size of the scratch wound was measured for each time point using the Wound Healing Tool in ImageJ.

2.3 Western blotting

2.3.1 Cell lysates

ID8 cells were seeded in T25 flasks and then cultured to 80-90% confluence. The cell culture medium was then removed and the cells washed with cold PBS while the flasks were kept on ice. The cells were scraped using 500 µl of cold lysis buffer supplemented with EDTA (5 mM), phosphatase and protease inhibitors (2x). Lysates were prepared by passing the cells in lysis buffer through a 23-gauge needle 3 times, centrifuged at 10,000 g x 10 minutes at 4 °C and stored at -20 °C for further analysis.

2.3.2 Protein quantification

Protein concentration was determined by the Pierce™ BCA protein assay according to the manufacturer's protocol. Briefly, 2 mg/ml BSA in doubling serial dilutions was used as reference protein for standard concentrations and protein samples were diluted 1:100 in PBS. 150 µl of standard or lysate samples were loaded into 96 well plates in triplicate and subsequently labelled with 1:1 BCA assay reagent. Finally, the plate was incubated for 30 minutes at 37 °C and then absorbance was measured at 560 nm using a SpectraMax M5e plate reader. Absorbance readings were converted to protein concentration using the BSA standard curve assuming a linear relationship between protein concentration and absorbance.

2.3.3 SDS-PAGE gel electrophoresis and protein transfer

Lysates were diluted with 4 x Laemmli sample buffer and a protein ladder was used as reference to estimate the molecular weight of the proteins of interest. Samples containing 0.1 M DTT were resolved on an 8% w/v SDS polyacrylamide gel (SDS-PAGE). The gel was run in Tris-Glycine SDS-PAGE buffer for 90 minutes at 120 volts. Proteins were transferred onto

a nitrocellulose membrane using a semi-dry system (BioRad) with NuPAGE® transfer buffer for 60 minutes at 15 volts. Subsequently, the nitrocellulose membranes were blocked with 5% w/v fat free dried milk in tris-buffered saline (TBS) containing 0.1% v/v Tween-20 (TBS-T) for 30 minutes.

2.3.4 Antibody staining and detection

After the blocking step, membranes were incubated with the primary antibody diluted in TBS-T buffer containing the blocking agent (5% w/v dried milk) and incubated on a shaker overnight at 4ºC (Table 4). The membranes were rinsed three times with TBS-T for 15 minutes after primary antibody incubation. The membranes were then incubated with the appropriate HRP-conjugated secondary antibody diluted in TBS-T containing 2.5% w/v dried milk and incubated on a shaker for 60 minutes. The membranes were rinsed three times with TBS-T for 15 minutes after secondary antibody incubation. All incubations were performed at room temperature unless otherwise specified. Finally, protein detection was performed using chemiluminescent detection with ECL reagents and the BioRad ChemiDoc system.

Table 4. Primary and Secondary antibodies**.**

Antibody	**Origin**	**Supplier**	**Dilution**	**MW** (kDa)
β-catenin	Mouse	BD Bioscience (610153)	1:1000	~ 92
E-cadherin	Mouse	BD Bioscience (610182)	1:1000	~ 120
N-cadherin	Rabbit	Abcam (ab18203)	1:1000	~ 100
GAPDH	Mouse	Abcam (Ab8245)	1:10000	~ 36
Vimentin	Mouse	Abcam (ab8978)	1:1000	~ 57
Anti-rabbit HRP	Donkey	Jackson Immunoresearch (715035152)	1:10000	
Anti-mouse HRP	Donkey	Jackson Immunoresearch (715035150)	1:10000	

2.3.5 Membrane stripping

In order to reprobe the membrane for the housekeeping protein GAPDH to confirm equal loading of total protein, the membranes were briefly rinsed in TBS-T and incubated in 10 ml stripping buffer for 10 minutes at room temperature. Membranes were then washed 3 times with TBS-T for 15 minutes and blocked as before with 5% w/v dried milk in TBS-T and incubated for 30 minutes at room temperature. The GAPDH antibody was diluted as described in table 4 in TBS-T buffer containing 5% w/v dried milk and incubated for 1 hour at room temperature. Membranes were rinsed three times with TBS-T for 15 minutes and incubated with the appropriate HRP-conjugated secondary antibodies diluted in TBS-T containing 2.5% w/v dried milk, after which they were incubated on a shaker for 60 minutes. The membranes were rinsed three times with TBS-T for 15 minutes after secondary antibody incubation phase. Detection processes was performed through chemiluminescent detection as described in section 2.4.4.

2.4 ELISA assay

Mouse and human VEGFA secreted into cell culture supernatants and plasma samples collected from the *in vivo* studies were measured using specific DuoSet ELISAs (R&D Systems). Ovarian cancer cells were plated in T25 flasks at a density of 2.5 x 10^5 cells per flask in standard growth conditions for 24 hours before medium was aspirated and replaced with 2 ml fresh growth medium. 24 hours later, supernatants were collected and centrifuged for 5 minutes at 400 x g. Analysis of concentrations of secreted VEGFA was performed according to the manufacturer's protocols.

2.5 Molecular biology

2.5.1 ZFN system – Mutagenesis of the donor plasmid used for homologous recombination.

Zinc Finger Nucleases (ZFNs) allow the integration of a gene of interest into the genome. Firstly, Zinc Finger Nucleases target a specific nucleotide sequence and cut the double stranded DNA. Secondly, a plasmid donor, which includes the gene of interest and homology sequences to the integration site, stimulates an homology-repair mechanism that integrates the gene of interest into the genome (Hansen et al., 2012). Directed mutagenesis was used to make translationally silent point mutations in the donor plasmid encoding VEGFA121 (pVEGFA121) used for homology repair during genome editing with Zinc Finger Nucleases. This was to reduce the re-targeting of the inserted homology repair DNA in the donor plasmid by the ZFNs after insertion in the genome and to enable detection of the VEGFA121 mRNA expressed by the edited gene via RNA sequencing and SNP detection. Sets of primers were designed with 5' ends annealing back-to-back to include the desired substitutions without affecting the translated protein sequence (Fig. 6 and Table 5). Mutagenesis was performed using the Q5® Site-Directed Mutagenesis Kit according to the manufacturer's protocol using specific thermocycling conditions (Table 6). For isolation of clones, the *E. coli* DH5α strain was transformed and selected as described in section Methods 2.6.4. Single colonies were grown in 5 ml of LB-Lennox broth containing 100 μg/ml ampicillin overnight at 4ºC at 225 rpm. Plasmids were isolated using the QIAprep® miniprep system (Qiagen) according to the manufacturer's protocol. Finally, inserted mutations in the plasmid were validated using DNA sequencing (Table 7). A ZFN pair targeting exon 4 of the human *VEGFA* gene was produced and validated by the design service provided by Sigma (Fig. S1). All primers were purchased from Sigma-Aldrich and all denovo gene synthesis was performed by Genewiz.

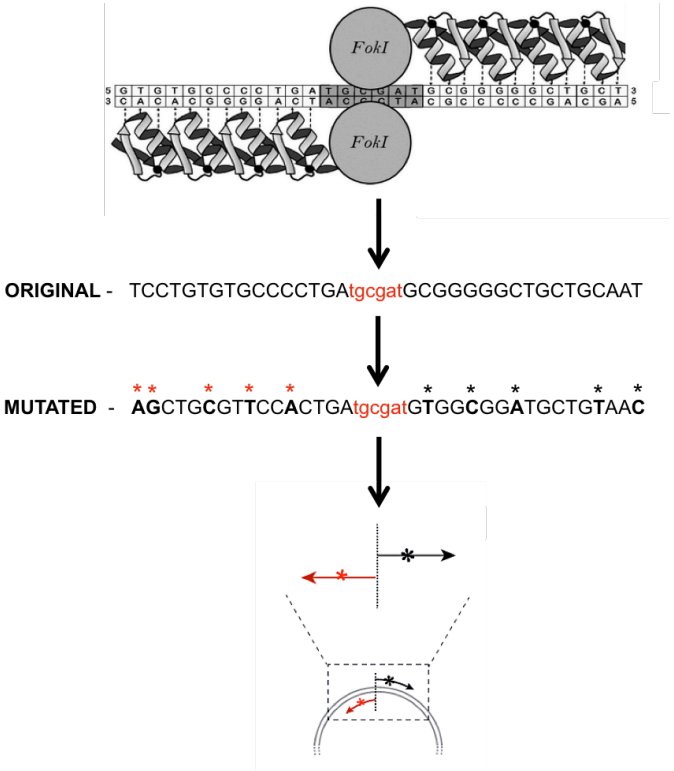

Figure 6. Directed mutagenesis strategy.

Q5® Site-Directed Mutagenesis Kit was used to make 10 silent point mutations in the donor plasmid encoding VEGFA121 by using primers designed with 5' ends annealing back-to-back to include the desired substitutions.

Table 5. Mutagenesis primers.

Forward primer (5'-3')	Reverse Primer (5'-3')
GATGTGGCGGATGCTGTAACGACGAGGG CCTGGAGTGTGTGCCCACTGAGGAGTCC	GCATCAGTGGAACGCAGCTTGGCTTGA AGATGTACTCGATCTCATCAGGGTACT CC
CGAGTACATCTTCAAGCCAAGCTGCGTTC CACTGATGCGATGTGGCGGATGCTGTAA CGACGAGGGCCTGGAGTGTGTGC	ATCTCATCAGGGTACTCCTGGAAGATG TCCACCAGGGTCTCGATTGGATGGCAG TAGCTGCGCTGATAGACATCC
CGAGTACATCTTCAAGCCATCCTGTGTGC CCCTGATGCGATGCGGGGGC	ATCTCATCAGGGTACTCCTGGAAGATG TCCACCAGGGTCTCGATTGGATGG

Table 6. Thermocycling conditions for PCR amplification.

Step	Temperature	Time
Initial Denaturation	98 ºC	30 seconds
26 Cycles	98ºC	10 seconds
	67 ºC	20 seconds
	72 ºC	105 seconds
Final Extension	72 ºC	2 minutes
Hold	4 ºC	-

Table 7. Sequencing primers.

Sequencing primers (5'-3')
ATGCAGTGGTGAAGTTCATGG
TAGTTGCCAGCCATCTGTTG
GTATGGTGGGGTCTTGCCTT
ATGTTGGACTCCTCAGTGGG

2.5.2 pCLIIP-[HRE]x5-minCMV-VEGFA construct

All denovo gene synthesis was performed by Genewiz. For the construction of the [HRE]x5-minCMV-VEGFA system, which enables regulation of VEGFA expression by HIF1 binding to hypoxia response elements (HRE) and providing a mechanism of regulation comparable to the endogenous *VEGFA* gene, cloning into the pCLIIP plasmid (English et al., 2017) was performed by removing the Luciferase2-E2A-mStrawberry fragment and then introducing the [HRE]x5-minCMV-VEGFA element as follows.

2.5.2.1 DNA digestion

A double digestion with FseI and MluI digestion enzymes was used. 1 μg of plasmid DNA was mixed with 1x of CutSmart® Buffer, 2 units of each digestion enzyme and up to 50 μl of nuclease-free water. DNA mixture was incubated for 15 minutes at room temperature.

2.5.2.2 DNA gel extraction

DNA digested product was separated using agarose gel as described in Methods 2.6.3 Monarch® DNA Gel Extraction Kit was used according to the manufacturer's protocol.

2.5.2.3 DNA ligation

50 ng of DNA plasmid were mixed with the DNA insert at a 1:3 molar ratio (vector: insert) in 1x T4 DNA ligase buffer containing 1 unit of T4 DNA ligase and up to 20 μl of nuclease-free water. The mixture was incubated at room temperature for 10 minutes and heat inactivated at 65 ºC for 10 minutes.

2.5.3 Agarose gel electrophoresis

DNA samples were separated by electrophoresis using agarose gels. 1-2% w/v agarose was prepared using TBE buffer with SYBR® Safe DNA gel stain. Samples were mixed with 6 x loading gel buffer and a DNA ladder was used as a molecular weight size reference. Gels were run at 100 volts for approximately 60 minutes.

2.5.4 Transformation of competent cells

DNA plasmid propagation was performed in *E. coli* DH5α by heat shock transformation. A 50 μl vial of DH5α competent cells were thawed on ice and 1-10 ng of plasmid DNA were added to the cells. DH5α were incubated on ice for 30 minutes, heat shocked for 20 seconds in a hot block at 42 ºC following which the tubes were place on ice for 2 minutes. Following transformation, 950 μl of pre-warmed SOC medium were added to the tubes and these were incubated for 1 hour at 37 ºC at 225 rpm. Finally, DH5α were plated

onto agar plates containing 100 μg/ml of ampicillin and incubated overnight at 37 ºC for colony selection.

2.5.5 Plasmid DNA purification

Single bacterial colonies were grown in LB-Lennox broth containing 100 μg/ml ampicillin overnight at 37 ºC and shaken at 225 rpm. The plasmids were isolated using either Qiagen QIAprep® Mini or HiSpeed® Plasmid Maxi kits according to the manufacturer's protocol.

2.5.6 DNA isolation and quantification

DNA was isolated using GenElute™ Mammalian Genomic DNA Miniprep kit according to the manufacturer's protocol. DNA concentration was quantified using the Nanodrop 1000 UV-Vis system at a wavelength of 260 nm.

2.5.7 RNA isolation and quantification

RNA was isolated using the GenElute™ Total RNA Purification kit according to the manufacturer's protocol. RNA concentration was quantified using the Nanodrop 1000 UV-Vis system at a wavelength of 260 nm.

2.5.8 Absolute Quantitative Real Time-PCR

2.5.8.1 Preparing a standard curve with plasmids containing each VEGFA isoform

It has previously been reported that linear plasmids are a valid and reliable tool to be used as the standard for gene quantification in AQRT-PCR (Hou et al., 2010). [HRE]x5-minCMV-VEGFA plasmids were designed for each mouse VEGFA isoform (120, 164 and 188). All denovo gene synthesis was performed by Genewiz. Linearised plasmids were used for creating a standard curve for Real-Time PCR. Specifically, plasmids were linearised using HindIII digestion enzyme as described in Methods section 2.6.2.1. 10-fold serial dilutions of each linearised standard were used from of 2.5 copies to 250,000 copies. Standard curves for each isoform were included in each AQRT-PCR run and isoform quantification of each sample was calculated from plots of C_T versus copy number of standard plasmid for each isoform assuming a linear relationship between both.

2.5.8.2 Reverse Transcription

cDNA synthesis was performed using a High Capacity cDNA Reverse Transcription Kit. Briefly, 1 µg of RNA was diluted in 10 µl of nuclease-free water. 2 µl of 10 x RT buffer, 0.8 µl of 25 x dNTP mix, 2 µl of 10 x RT random primers, 1 µl MultiScribe™ reverse transcriptase and 1 µl of RNase inhibitor were added to the DNA mixture. Samples were heated in a thermocycler at 25 ºC for 10 minutes, followed by incubation at 37 ºC for 120 minutes and finally 5 minutes incubation at 85 ºC. cDNA samples were stored at -20 ºC.

2.5.8.3 SYBR® Green Real-Time PCR

cDNA samples obtained by reverse transcription were amplified by SYBR® Green Real-Time PCR. 10 µl total reaction containing 15 ng of RNA converted to cDNA or plasmid standards, 200 nM of forward and reverse primers (Table 8) and 5 µl SYBR® Green PCR Master Mix were used in 384-well plates. The PCR reaction was performed using the Applied Biosystems 7900HT Fast Real-Time PCR System as indicated in table 9. All experiments were performed in triplicate and a melting curve was performed at the end of every run. All primers were purchased from Sigma-Aldrich.

Table 8. Real-Time PCR Primers.

	Forward primer (5'-3')	**Reverse primer (5'-3')**	**Product length (bp)**	**Reference**
Mouse VEGFA120	GCCAGCACATAGGAGAGATGAGC	GGCTTGTCACATTTTTCTGG	94	(Darland et al., 2011)
Mouse VEGFA164	GCCAGCACATAGGAGAGATGAGC	CAAGGCTCACAGTGATTTTCTGG	97	(Darland et al., 2011)
Mouse VEGFA188	GCCAGCACATAGGAGAGATGAGC	AACAAGGCTCACAGTGAACGCT	171	(Darland et al., 2011)
Mouse Total VEGFA	CACGACAGAAGGAGAGCAGAAG	CTCAATCGGACGGCAGTAGC	82	(Brennan et al., 2009)
Mouse GAPDH	ATGGTGAAGGTCGGTGTGAACG	CGCTCCTGGAAGATGGTGATGG	233	(Brennan et al., 2009)

Table 9. SYBR® Green Real-Time PCR Parameters.

Step	Temperature	Time
Enzyme activation	95 ºC	20 seconds
40 Cycles	95ºC	1 seconds
	60 ºC	20 seconds

2.6 Statistical Analysis

All statistical analyses were performed using the GraphPad Prism 7.0 software. Differences between two groups were determined by using an unpaired Welch t-test or Mann-Whitney test for parametric and non-paramedic data respectively. For grouped data, multiple comparisons were made using an ANOVA test followed by the Tukey test or Dunnett's test for parametric and non-paramedic data respectively. All numerical values shown are the means ± standard error. Statistical significance was defined as $P < 0.05$ (*), $P < 0.01$ (**), $P < 0.001$ (***) and $P < 0.0001$ (****).

2.7 *In silico* methods

2.7.1 The Genotype-Tissue Expression (GTEx) Project

The GTEx consortium is a collection of tissue-specific gene expression and genetic variations across multiple normal human tissues (GTEx Consortium, 2013). The dataset for ovary tissue includes 133 RNAseq samples (Release V7) of which 88 cases include transcript quantification and are available in the UCSC Xena compendium.

2.7.2 The Cancer Genome Atlas (TCGA) project

The TCGA is a collection of data from a wide variety of cancer patients, and aims to improve our understanding about cancer development, prevention, diagnosis and treatment. Specifically, the TCGA Pan-Cancer Atlas (PanCanAtlas) project is a comprehensive cross-cancer analysis, which identified genomic and cellular pattern in 33 tumour types, including ovarian. The PanCanAtlas catalogues genomic alterations, epigenetics and gene expression across tumour types. The ovarian cancer project within the TCGA Pan-Cancer study (TCGA OV) has 604 patient cases, of which 70.7% includes transcript quantification data and are available in the UCSC Xena compendium.

2.7.3 Data acquisition

GTEx and TCGA data for normal ovary tissue and ovarian cancer samples were acquired and analysed. Available RNAseq transcript-level data sets were downloaded from the GTEx and TCGA Pan-Cancer cohort from the UCSC RNAseq recomputed compendium version 2016-09-02 (Goldman et al., 2020). Ensembl id transcript annotations were used to define VEGFA isoforms and Transcripts Per Million (TPM) and isoform percentage values were obtained for VEGFA121 (ENST00000372077.8), VEGFA165 (ENST00000372067.7) and VEGF189 (ENST00000520948.5) for each tissue donor. Gene expression RNA-seqV2_RSEM_Genes raw count matrix for ovarian cancer was obtained from the BROAD GDAC Firehose version 2016_01_28.

2.7.4 Data Filtering

TCGA OV dataset includes 604 cases, however only 70.7% have transcript quantification available and only 50.3% have publically available access to RSEM raw counts. Isoform expression data available (TPM and isoform percentage) was therefore filtered for cases with primary tumour with high histologic grade (G2 or G3) and IIIC clinical stage (Fig. 7). Due to the diversity of HGSOC and based on the characteristics of the disease at diagnosis, this analysis is focused on stage IIIC that represents the degree of dissemination with a sufficient number of cases for further analysis.

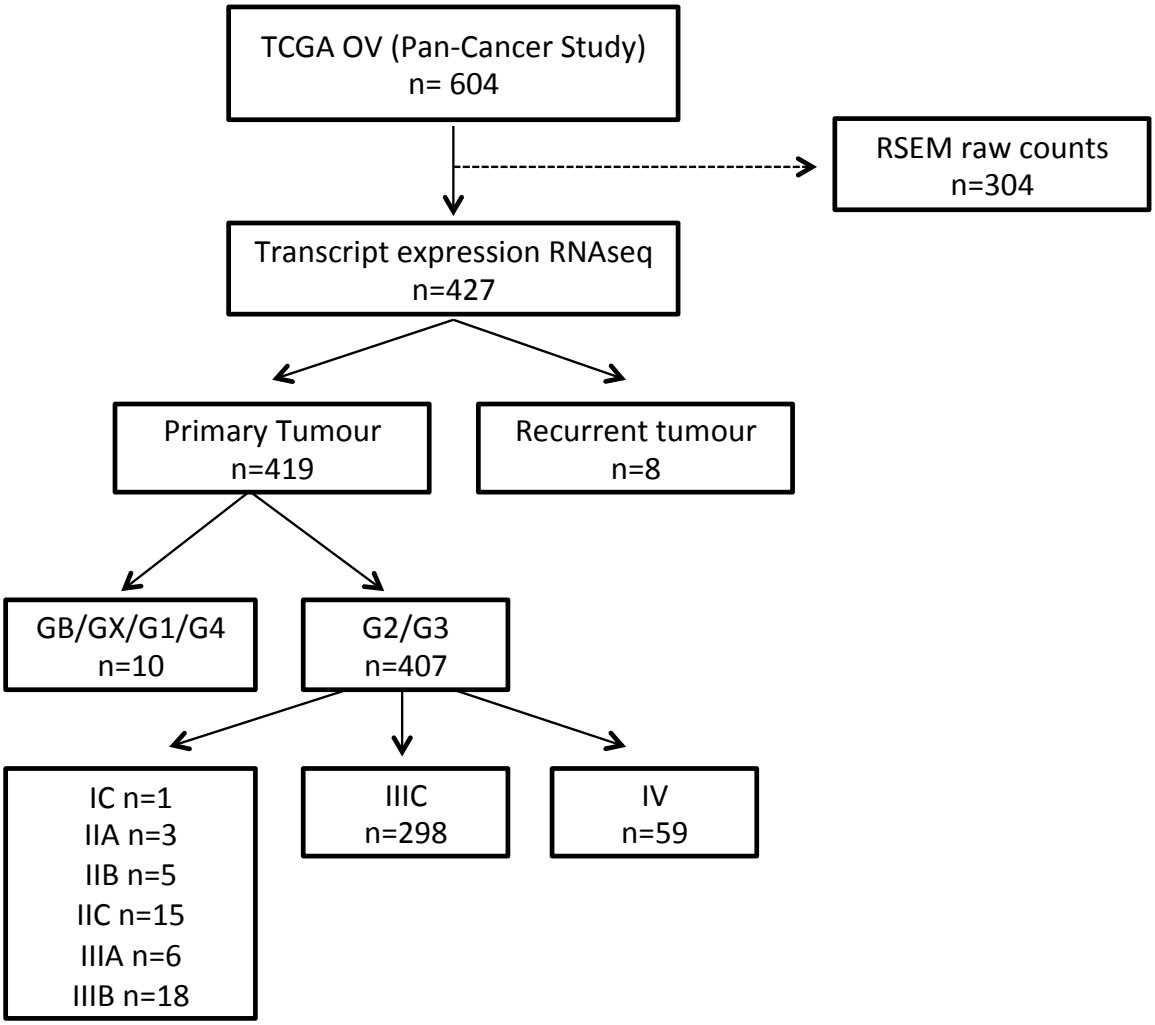

Figure 7. Data filtering process.

TCGA OV samples were filtered for cases that met the following established criteria: had transcript expression data available, the data corresponded to primary tumour samples, and the tumours presented as high histological grade (G2/G3) and IIIC FIGO staging.

2.7.5 Analysis of VEGFA isoform expression in HGSOC patients

For each patient, only VEGFA121, VEGFA165 and VEGFA189 transcripts were considered based on ovary transcript abundance described in section 3.2.1. Two different methods were developed to identify VEGFA isoform expression levels in HGSOC patients. For the purpose of this work we have defined the first approach as the 'Individual segregation model', which consists of grouping the data according to a quartile cut-off point for each individual isoform's expression and analysing each separately from the other isoforms (Fig.8A). For each isoform, the expression level was considered low or high following 25^{th} - and 75^{th} TPM-quartile cut-offs respectively.

The second approach is defined as the 'Clustered segregation model' and consists of identifying the switch between the three isoforms together (Fig.8B). Differential isoform expression was analysed using the Morpheus software. Specifically, isoform percentage values were Z-score transformed and a hierarchical clustering approach was used for grouping patients with isoform expression similarities. Cluster associations were performed using the one minus Pearson correlation and the complete linkage method (LaTulippe et al., 2002).

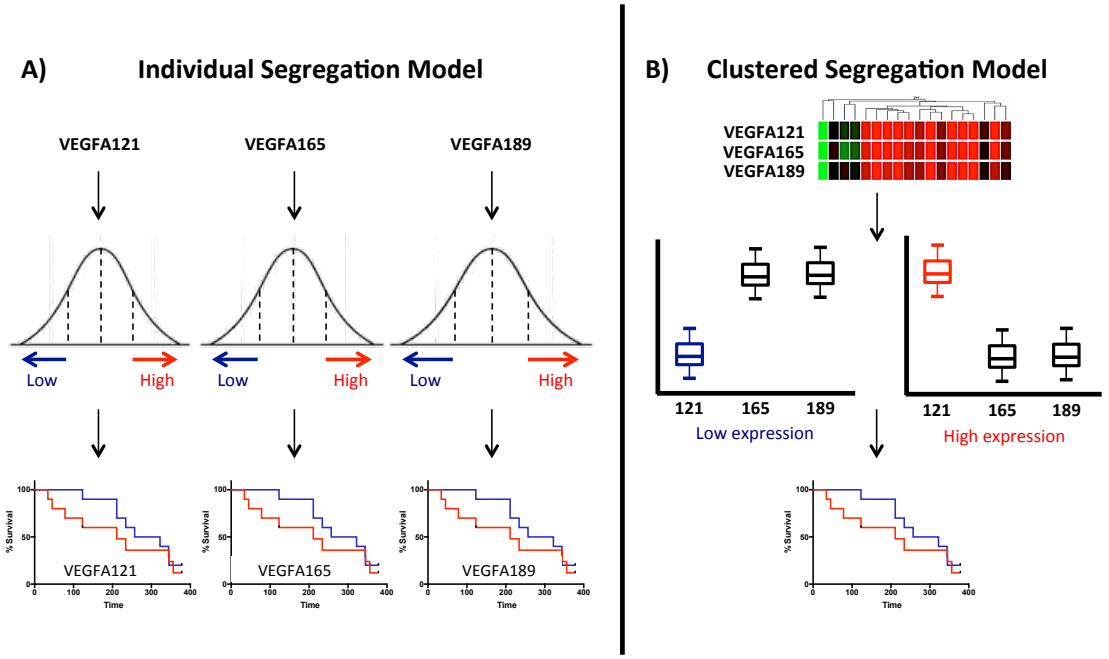

Figure 8. Methods for HGSOC patient segregation.

Illustrative diagram of the proposed methods for patient segregation based on VEGFA isoform expression. **A)** For the 'Individual segregation model', groups were divided based on quartile of one isoform's expression. **B)** For the 'Clustered segregation model' groups were divided based on the isoform expression pattern between all three of the isoforms.

2.7.6 Survival analysis

Survival analyses were performed using survminer version 0.4.8 through RStudio version 1.1.463. To determine clinical relevance of VEGFA isoform expression, clinical attributes such as age, histological grade, clinical stage, molecular subtype, vital status, progression-free (PFS) and overall survival (OS) were obtained for each patient. Information regarding performance status, residual tumour and patient treatment was not fully described within the TCGA clinical data, therefore these characteristics were not considered for survival analysis in this work.

Associations between isoform expression levels and survival were investigated using the multiple linear regression model, in order to identify clinical factors associated with overall and progression-free survival. Hazard ratios with their corresponding 95% confidence intervals were determined. Survival rates were calculated using the Kaplan-Meier method and the comparisons between the groups were analysed by the log-rank test. P-values below 0.05 were considered statistically significant.

2.7.7 DEG

Differentially expressed genes (DEG) were detected using edgeR package through RStudio version 1.1.463. A two-group comparison was performed using the RNA-seqV2_RSEM_Genes raw count matrix. Unpaired DEG analysis was performed to assess changes within VEGFA isoform expression groups. Filtering for read counts was set to a threshold of 0.5 CPM. Raw count normalisation was specified as the default normalisation method provided by the EdgeR package. Cut-off criterion for DEG was false discovery rate (FDR) ≤ 0.05.

2.7.8 Gene set enrichment analyses

Gene set enrichment analysis (GSEA) was performed with software version 3.0. Pre-ranked analysis was performed using the default settings with the exception of "collapse dataset to gene symbols" which was set to False. Prior to analysis, a ranked list was calculated with each gene assigned a score base on the p-value and the direction of the fold change (FC) (rank = sign (FC)*-log10 (p-value)). The hallmark gene sets (h.all.V7.1

MSigDB) were applied to evaluate whether genes were assigned to a specific biological process. Gene sets were identified as significant if FDR q-val < 0.05.

A VEGFA-dependent gene signature developed by Yin et al. (2016) was used for predicting patient response for VEGFA targeted therapy. This gene set was applied to the ranked list created from the DEG analysis through the GSEA software following the settings specified above.

2.7.9 Immune cell analysis

Immune population subsets were studied using xCell method (Aran et al., 2017) which is a gene signature-based approach that allows the identification of approximately 64 immune cell types. Access to pre-calculated TCGA data by xCell was retrieved and filtered for ovarian cancer samples to match our HGSOC cases. For each patient, the xCell score for different immune subsets were taken and used to compare their abundances across patient groups. Comparisons between the groups were analysed by the Wilcoxon t-test. P-values below 0.05 were considered statistically significant.

2.7.10 Protein network analysis

The protein network analysis was constructed via the STRINGApp version 1.4.0 available for Cytoscape version 3.8.0. Genes with FDR < 0.05 from the DEG analysis were imported into Cytoscape using the STRING public database (protein query) for Homo sapiens. The parameters for the protein-protein interaction (PPI) network included a confidence score ≥ 0.4 and no additional number of interactions. STRING enrichment data was used to retrieve functional information about the network.

Chapter 3

3. Associations between expression of VEGFA mRNA isoforms, disease progression and molecular features

RNAseq open-access data collections have allowed us to explore gene expression, genetic alterations and their associations with clinical outcomes in common human diseases. These resources are the result of large analyses across various tissues that aim to provide tools to better understand the molecular mechanisms underlying different diseases. This chapter aims to investigate the associations between VEGFA mRNA isoform expression, disease progression and molecular signatures in patients with High-Grade Serous Ovarian Cancer using data from The Cancer Genome Atlas (TCGA). In the first part, differences in VEGFA isoform expression between normal and cancerous ovarian tissue are investigated across two different studies.

In order to categorise patients based on differences in VEGFA mRNA isoform expression, different approaches for patient segregation were created based on individual or clustered VEGFA isoform expression levels. Next, associations between expression of VEGFA mRNA isoforms with survival were investigated. Finally, we explored different methods of analysis to identify novel differentially expressed genes (DEGs) that could provide mechanistic insights into the links between VEGFA isoform signalling, disease progression and response and resistance to therapy in HGSOC.

3.1 Introduction

Alternative VEGFA transcripts or isoforms refer to species that are the product of alternatively spliced pre-mRNA or posttranscriptional proteolytic cleavage. The most common VEGFA mRNA isoforms are VEGFA121, VEGFA165 and VEGFA189, named after the number of amino acids in the mature, secreted peptide. These isoforms differ in their exon regions and by consequence in their biological function and bioavailability. The shorter isoform VEGFA121 is highly soluble while the longer isoforms VEGFA165 and VEGFA189 are highly basic and are bound to the extracellular matrix as previously described in section 1.5.1. Different technologies to measure transcripts have been developed mainly based on hybridisation (such as microarrays), or sequencing (such as tag-based methods). The former relies on existing knowledge about the genome sequence and commonly shows low sensitivity and limited detection ranges followed by difficult signal comparison across different experiments. The latter methods are based on Sanger sequencing and provide gene expression levels. However, not all tag probes are exclusively mapped to one region of the genome and only a small proportion of transcripts can be analysed, which makes it difficult to fully distinguish between isoforms (Wang, Z. et al., 2009).

RNA sequencing (RNAseq) refers to the use of high-throughput sequencing technologies that allows us to discover and quantify transcripts and thereby identify isoform changes in development and disease. RNAseq includes several steps; firstly RNA is converted into cDNA fragments to which sequencing adaptors are added. This is followed by an amplification step on a chip to produce clonal copies of all the fragments. Next, short cDNA fragments are sequenced using a modified version of the Sanger method, and imaged in real-time to provide sequence information of each clonal copy (Wang, Z. et al., 2009). The resulting reads are aligned to a reference genome and classified as exonic reads, junction reads or poly(A) end-reads. This system provides transcriptome structure and expression levels for each gene. RNAseq allows a more accurate measurement of isoform levels and offers additional advantages over previous methods. RNAseq analysis of transcripts is not limited to existing transcript knowledge and reveals more information about exon boundaries and sequence variations or polymorphisms. Furthermore, this technology offers the measurement of a dynamic range of expression levels and more reproducibility between technical and biological replicates (Wang, Z. et al., 2009).

RNAseq is still a new technology and as such certain challenges will need to be overcome before its full potential can be achieved. Bioinformatic challenges include the standardisation of methods to store, retrieve and process RNAseq data to reduce errors in analysis. One of the main challenges of using RNAseq open-access collections is the inability to compare across data sets, mainly due to a difference in data processing such as alignment and quantification. Recently, novel RNAseq pipelines have been published in an effort to unify data from different sources and these strategies allow for comparisons between studies. The UCSC Toil RNAseq pipeline, one example of these strategies, aims to process RNAseq samples across different datasets and create a single large compendium (Wang, Q. et al., 2018). The Cancer Genome Atlas (TCGA) and The Genotype-Tissue Expression (GTEx) RNAseq data are uniformly re-aligned to the hg38 genome, and re-processed using RSEM methods with gencode v23 annotations to generate expression estimates. UCSC Xena hosts and displays gene and transcript expression results of this analysis (Wang, Q. et al., 2018).

3.2 Expression of all VEGFA isoforms is up-regulated in HGSOC

Differential usage of isoforms in different conditions, often referred to as isoform switching, can have substantial biological impact, caused by the difference in each of their functional potential (Vitting-Seerup and Sandelin, 2017). Data from the TCGA and the GTEx consortium was used to analyse VEGFA isoform expression across normal ovarian and ovarian cancer tissues corresponding to 88 and 419 human samples respectively. As previously reported, it is possible to identify different transcripts for the *VEGFA* gene, however not all of them code for functional proteins as annotated in the UniProt consortium, as some have intronic retention for example (UniProt, 2019). Additionally, their quantification showed that not all annotated transcripts are abundant and the VEGFAxxxb 'anti-angiogenic' isoforms are not expressed in ovary tissue, consistent with recent observations in other tissues (Dardente et al., 2020) (Fig. 9). VEGFA121, VEGFA165 and VEGF189 were identified as the predominant protein coding isoforms in both normal ovarian tissue and ovarian cancer samples. It was observed that the VEGFA165 transcript has an extended 5' UTR encoding a longer signal peptide, which is not present in the other two isoforms. This has been reported to be relevant in regulating transcript stability during hypoxia (Rosenbaum-Dekel et al., 2005). Increased expression of these three isoforms was observed in HGSOC when compared to normal ovarian tissue (Fig. 10). Across the three isoforms, VEGFA121 was expressed at lower levels in normal ovarian tissue, however this transcript showed not only increased expression in HGSOC but also higher expression levels when compared with the other two isoforms.

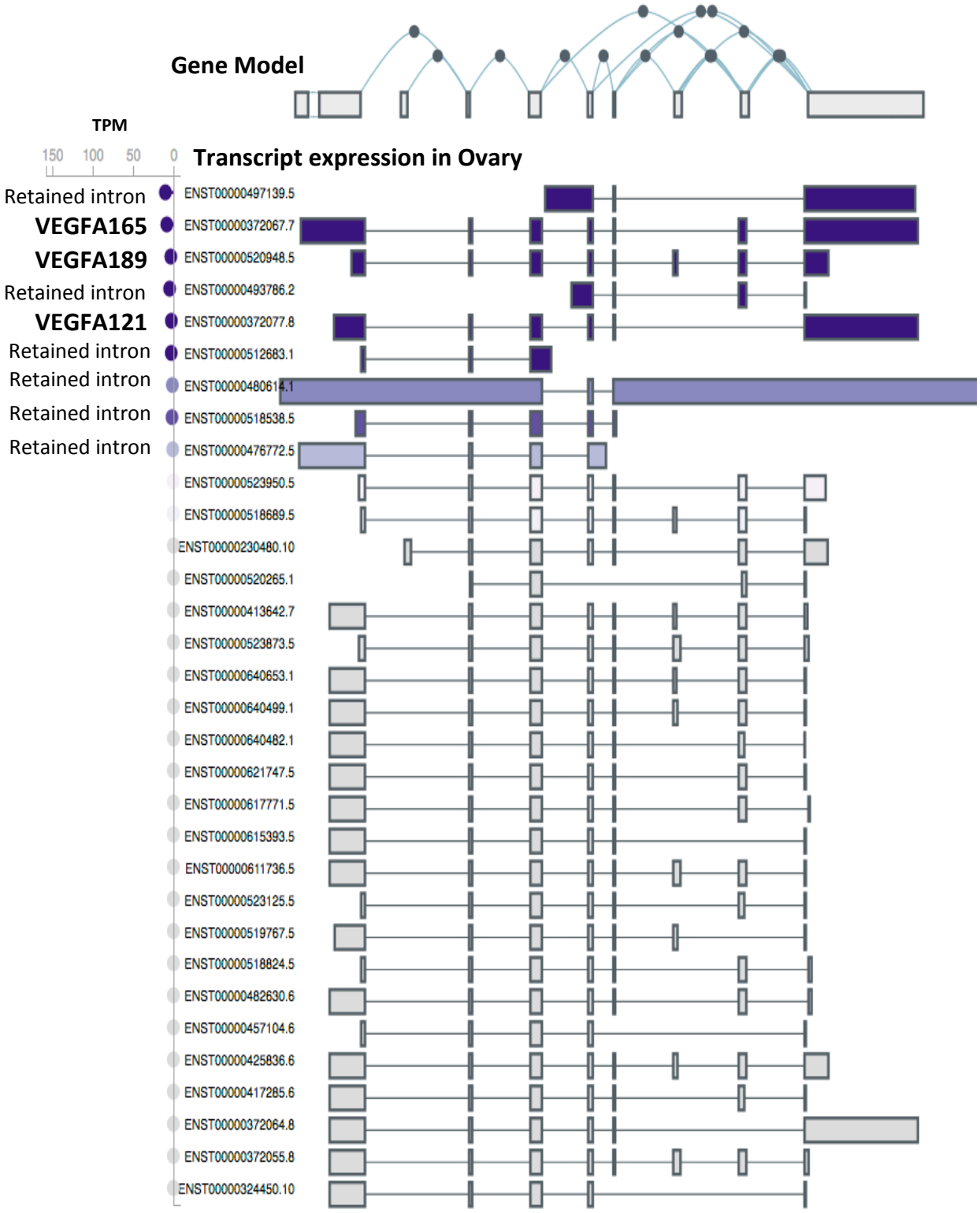

Figure 9. VEGFA transcript expression in the normal ovary.

These results correspond to the GTEx data for normal ovary samples. GTEx samples were obtained post-mortem using tissue from most normal regions of the left ovary (and right if necessary to obtain sufficient aliquots). TPM expression is shown for each VEGFA transcript and ranked based on their relative abundance. Dominant functional transcripts correspond to VEGFA121 (ENST00000372077.8), VEGFA165 (ENST00000372067.7) and VEGFA189 (ENST00000520948.5). Plot created using the GTEx Portal.

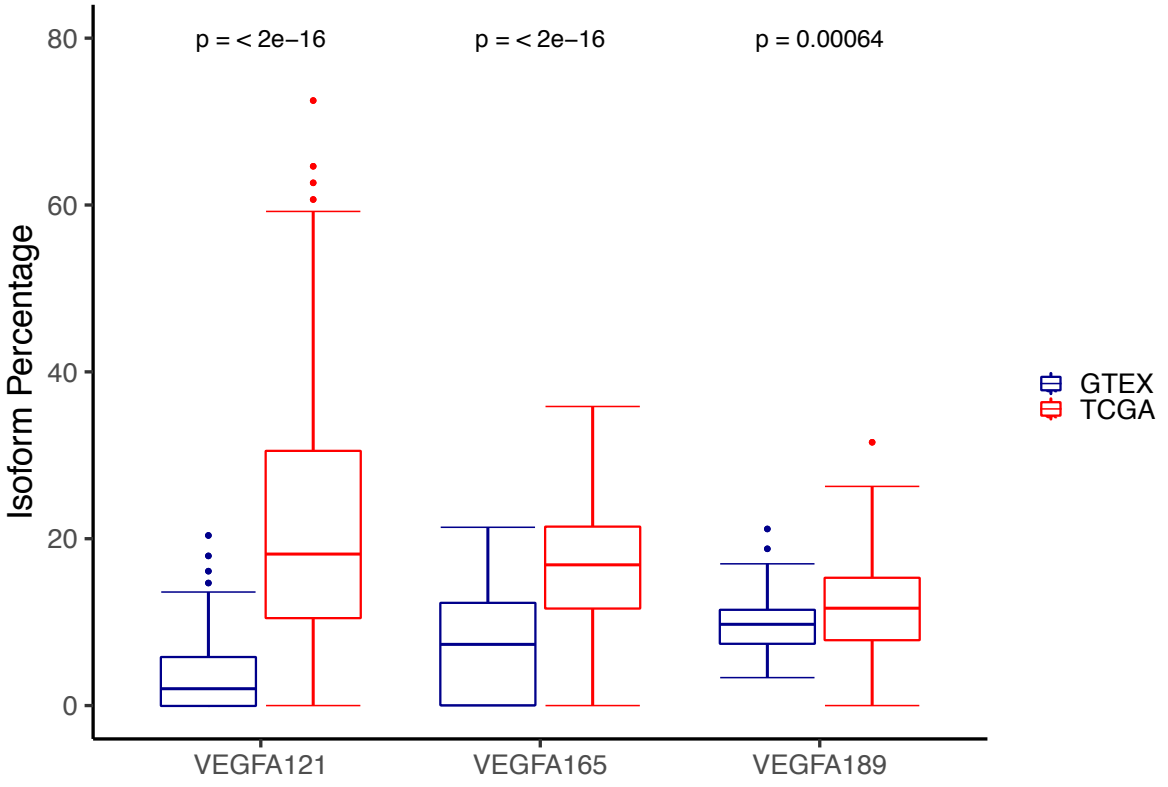

Figure 10. VEGFA isoform mRNA expression in HGSOC and normal tissue.

Alterations of expression levels of mRNA VEGFA isoforms are shown between HGSOC patients and normal ovary tissue. GTEx samples were obtained post-mortem using tissue from most normal regions of the left ovary (and right if necessary to obtain sufficient aliquots). Data for normal ovary tissue (n=88) and HGSOC (n=419) are shown as box plots. Differences between groups were assessed using the Wilcoxon test and P-values below 0.05 were considered statistically significant.

3.3 VEGFA isoform expression levels and their effect on HGSOC patient survival

3.3.1 Individual Isoform Segregation Model

Due to the complexity of VEGFA isoform expression, it is important to study the effect that each individual isoform generates in the progression of HGSOC. The first method included the segregation of patients based on the expression levels of each isoform individually while omitting the others. After filtering, our dataset contained isoform expression values from 298 HGSOC cases with stage IIIC disease. To identify isoform expression levels in patients, only the predominant VEGFA isoforms VEGFA121, 165 and 189 were analysed, as described in the previous section. For each isoform, the expression level was considered low or high following 25th - and 75th percentile cut-offs respectively (Table 10). Based on this segregation model, patient cases that met the cut-off criteria were grouped in low and high expression for each isoform (Fig. 11).

Table 10. Cut-off values for VEGFA isoform expression levels.

Cut-off	**VEGFA121** Log2(TPM*+0.001)	**VEGFA165** Log2(TPM*+0.001)	**VEGFA189** Log2(TPM*+0.001)
Low expression	3.0130	2.5730	2.0290
High expression	4.2825	4.3525	4.0250
* TPM = Transcripts Per Million			

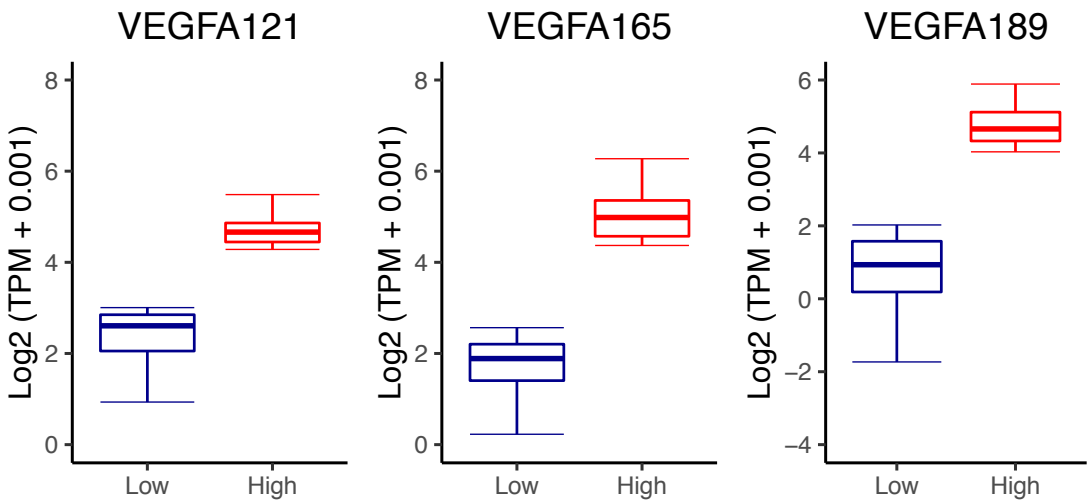

Figure 11. Individual isoform segregation of HGSOC patients.

For each isoform, low and high expression groups using Log2 TPM values were segregated based on 25th - and 75th -percentile cut-off respectively. TPM = Transcripts Per Million

The individual effect of each isoform's expression on survival was also explored. Kaplan-Meier analysis between high and low groups for each isoform showed that low levels of VEGFA121, VEGFA165 and VEGFA189 are individually associated with worse overall survival, while those with high individual levels of expression showed a better survival outcome (Fig. 12). No differences in progression-free survival were observed between any of the groups (Fig. 12). Additionally, no association between total VEGFA mRNA expression and overall or progression-free survival was observed (Fig. S2-S3).

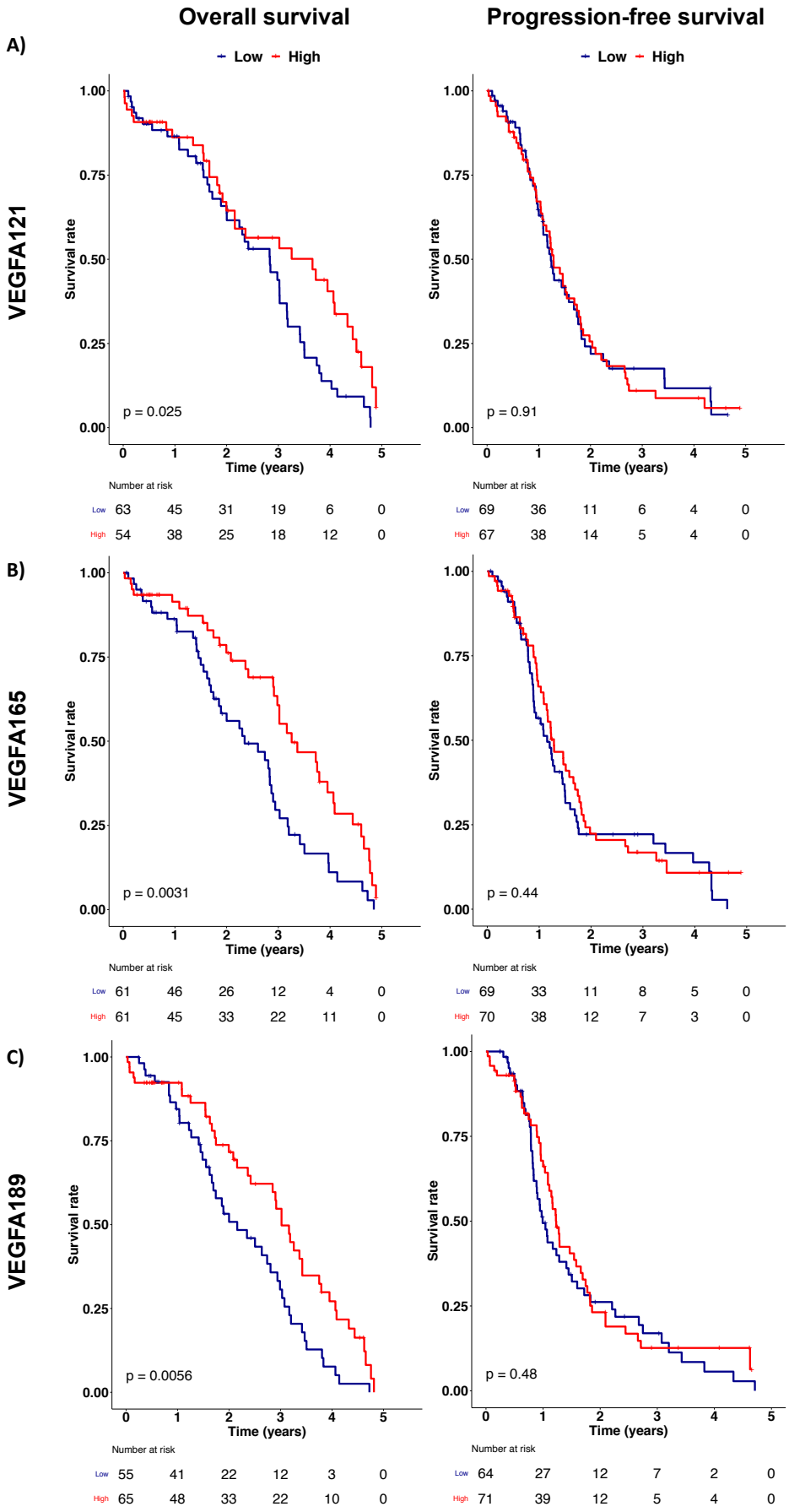
Overall survival
Progression-free survival
A)
B)
C)
VEGFA121
VEGFA165
VEGFA189
Low
High
Survival rate
Time (years)
p = 0.025
p = 0.91
p = 0.0031
p = 0.44
p = 0.0056
p = 0.48
Number at risk
Low 63 45 31 19 6 0
High 54 38 25 18 12 0
Low 69 36 11 6 4 0
High 67 38 14 5 4 0
Low 61 46 26 12 4 0
High 61 45 33 22 11 0
Low 69 33 11 8 5 0
High 70 38 12 7 3 0
Low 55 41 22 12 3 0
High 65 48 33 22 10 0
Low 64 27 12 7 2 0
High 71 39 12 5 4 0

Figure 12. Kaplan-Meier analysis for individual isoform segregation groups.

Kaplan-Meier analysis for overall and progression-free survival is shown for patients with low and high VEGFA isoform expression based on the individual isoform segregation method. **A)** VEGFA121 (p = 0.025 OS, p = 0.91 PFS), **B)** VEGFA165 (p = 0.0031 OS, p = 0.44 PFS), **C)** VEGFA189 (p = 0.0056 OS, p = 0.48 PFS). Differences between groups were assessed using a log-rank test and P-values below 0.05 were considered statistically significant. OS = Overall survival, PFS = Progression-free survival.

3.3.2 Clustered Segregation Model

Most of the methods used in studies evaluating VEGFA as a potential biomarker do not differentiate between circulating or tumour expressed VEGFA isoforms. Its prognostic and predictive associations are therefore merely describing the use of total VEGFA expression rather than that of individual isoforms. Additionally, VEGFA isoform mRNA patterns have already been described in other cancers and associated with different clinical outcomes. In colorectal cancer patients, three different VEGFA isoform patterns have been identified using RT-PCR: VEGFA121 (type 1), VEGFA121 + VEGFA165 (type 2) and VEGFA121 + VEGFA165 + VEGFA189 (type 3). In this specific cancer, the type 3 pattern was associated with increased metastasis and worse prognosis (Tokunaga et al., 1998). This suggests that the differential expression of all VEGFA isoforms is important when evaluating their potential value as biomarkers.

Given that the proportion of VEGFA isoforms and the shift in their ratios may be important for tumour progression and treatment success in HGSOC, their grouped expression pattern was also analysed. In order to explore the full spectrum of VEGFA isoform expression, for each patient, isoform percentages were compared and grouped with cases with a similar isoform switch. VEGFA isoform expression patterns were found to vary across HGSOC patients. Four main isoform switches were identified and defined as Switch 1 to 4 (Fig. 13).

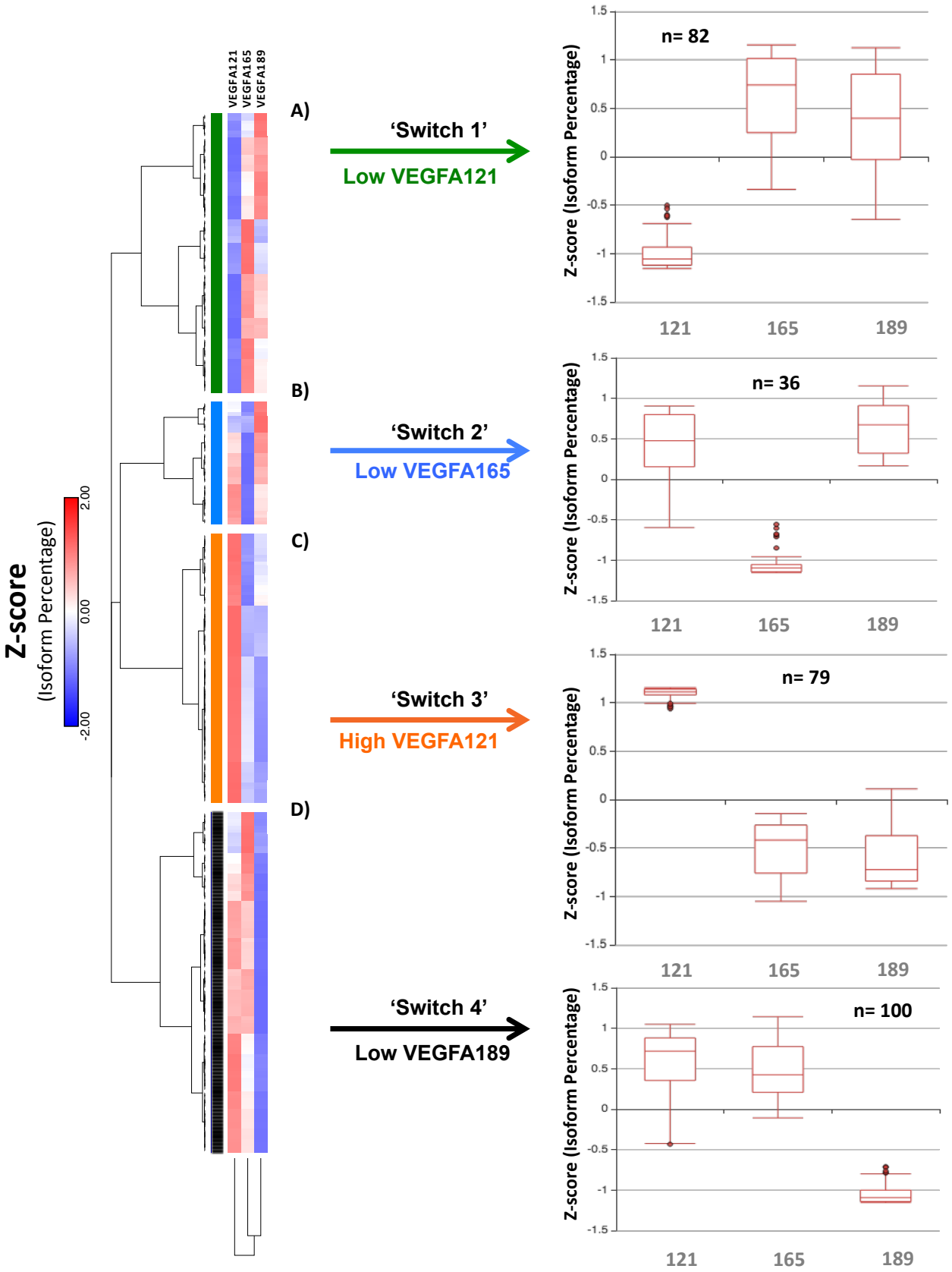

Figure 13. Differential isoform segregation of HGSOC patients.

HGSOC patients were grouped into four main VEGFA isoform expression patterns. A) Switch 1: Low VEGFA121 (n=82), B) Switch 2: Low VEGFA165 (n=36), C) Switch 3: High VEGFA121 (n=79), D) Switch 4: Low VEGFA189 (n=100). Hierarchical clustering was performed using the one minus Pearson correlation with complete linkage method.

Overall survival was analysed for the four defined isoform switches (Fig.14). Median overall survival was 3.16 years (95% CI, 2.90-3.79) in the low VEGFA121 group (Switch 1), 2.83 years (95% CI, 1.85-3.95) in the low VEGFA165 (Switch 2), 2.74 years (95% CI, 1.82-2.94) in the high VEGFA121 group and 3.08 years (95% CI, 2.64-3.66) in the low VEGFA189 group (Switch 4). Pairwise comparisons between the groups showed that there is a significant overall survival difference between low VEGFA189 and high VEGFA121 groups (p-value 0.031), in addition to, low and high VEGFA121 (p-value 0.024). Specifically, the survival curves show a decreased overall survival for the high VEGFA121 group when compared with either low VEGFA189 or low VEGFA121 (Fig. 14). No significant differences were observed for overall survival between the remaining group comparisons. Compared to patients within the low VEGFA121 group, the hazard ratio of mortality of patients with high VEGFA121 expression was 1.53 fold (p-value 0.05) (Table 11).

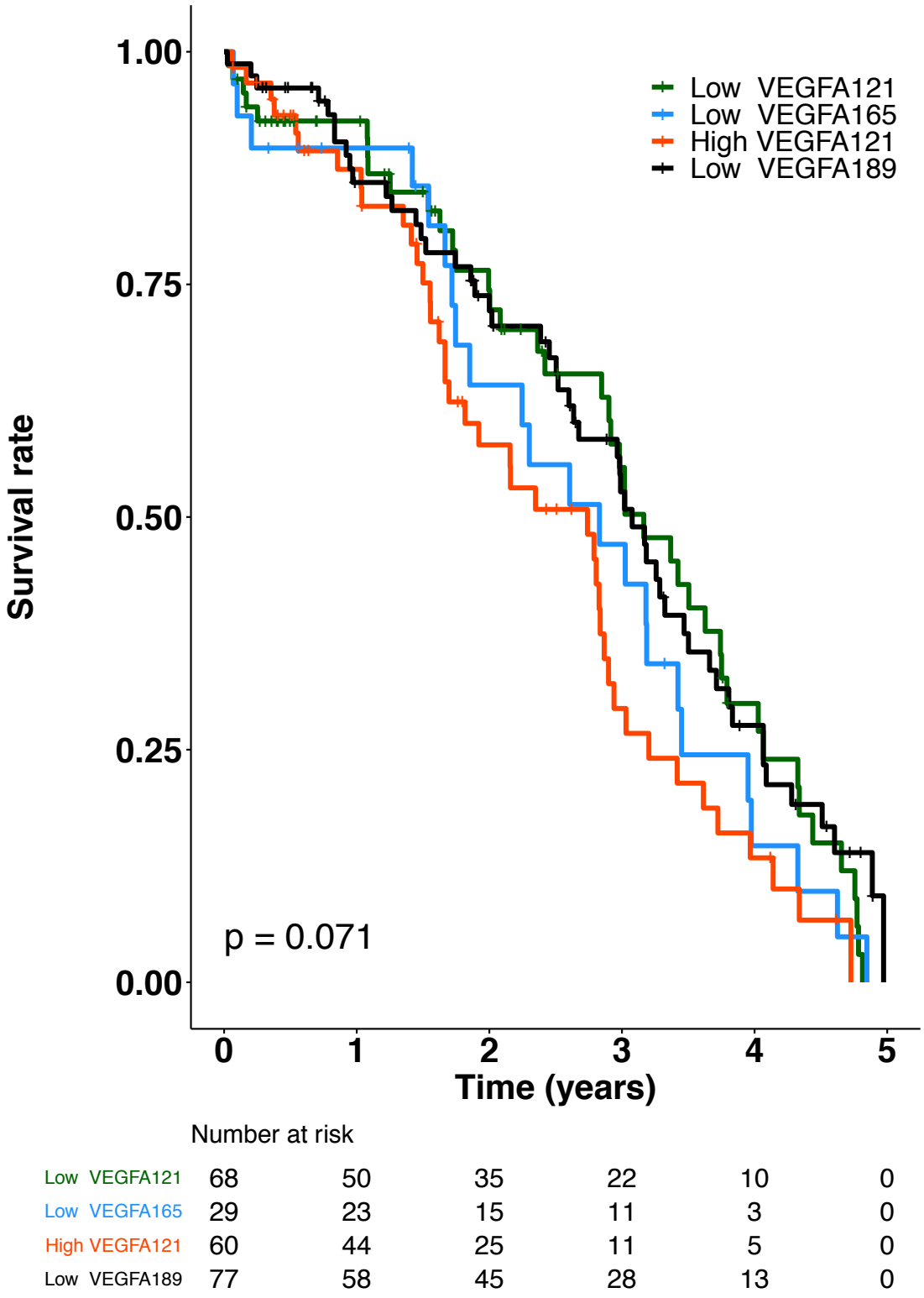

Figure 14. Overall survival analysis for differential isoform segregation groups.

Kaplan-Meier analysis for overall survival in patients with differential VEGFA isoform expression. Differences between groups were assessed using a long rank test and P-values below 0.05 were considered statistically significant.

Table 11. Hazard ratio analysis for overall survival

Hazard ratios with 95% confidence interval for overall survival in different VEGFA isoform expression groups. Groups were compared with the low VEGFA121 group, which is defined as the reference category for this analysis.

Group	HR*	95% CI*	p-value
Low VEGFA121	_	_	
Low VEGFA165	1.25	0.75, 2.08	0.4
High VEGFA121	1.53	0.99, 2.36	0.05
Low VEGFA189	0.90	0.60, 1.37	0.6

*** HR = Hazard Ratio, CI = Confidence Interval**

Additionally, progression-free survival was analysed for the four defined isoform switches (Fig.15). Median progression-free survival was 1.51 years (95% CI, 1.23-1.82) in the low VEGFA121 group (Switch 1), 1.20 years (95% CI, 1.08-1.75) in the low VEGFA165 (Switch 2), 1.23 years (95% CI, 0.94-1.50) in the high VEGFA121 group (Switch 3) and 1.26 years (95% CI, 1.04-1.60) in the low VEGFA189 group (Switch 4). Pairwise comparisons between the groups showed that there are no significant differences in progression-free survival between the groups. Compared to patients within the low VEGFA121 group, no evidence of a greater progression-free risk was found for the rest of the patient groups (Table 12).

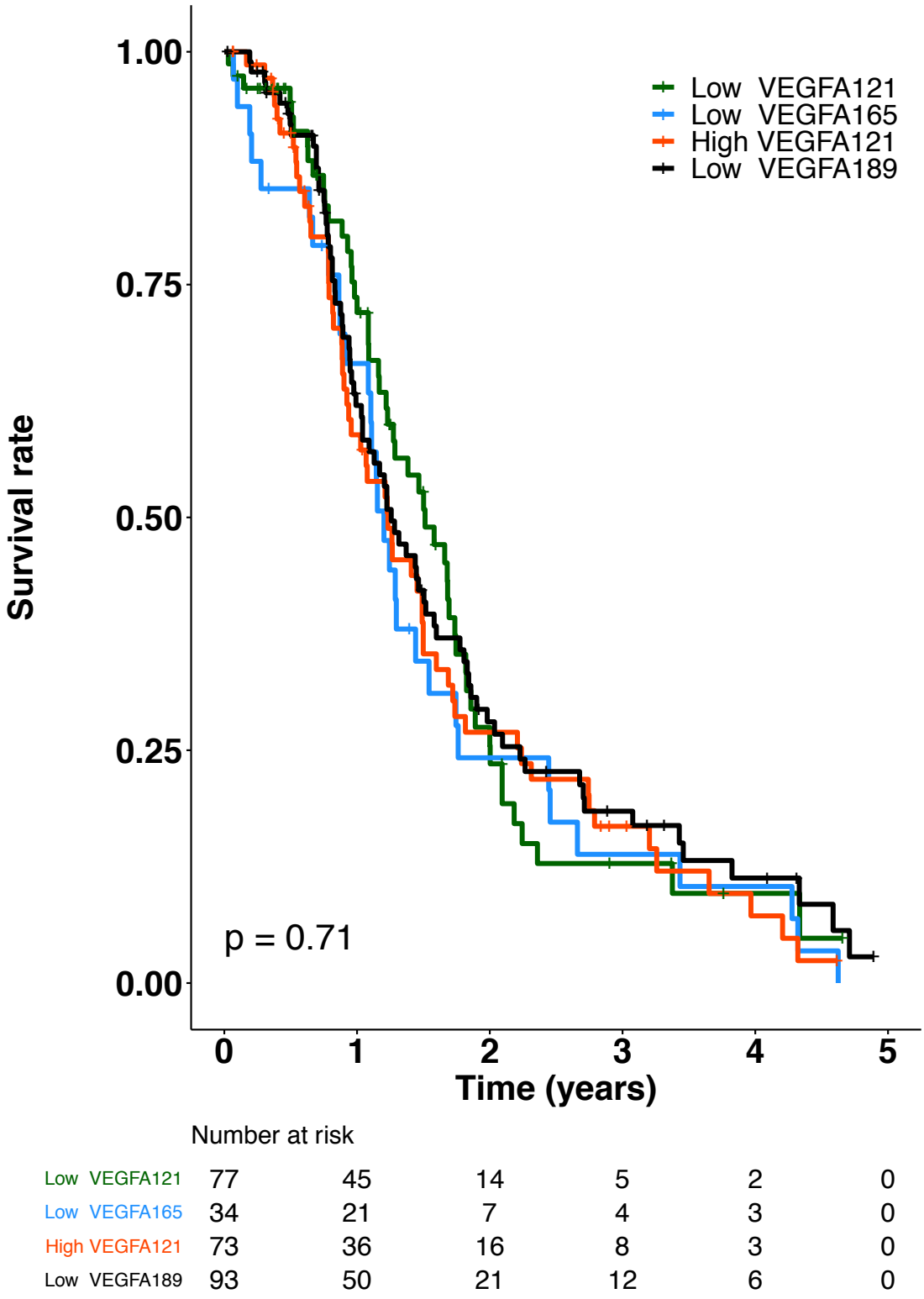

Figure 15. Progression-free survival analysis for differential isoform segregation groups**.**

Kaplan-Meier analysis for progression-free survival in patients with differential VEGFA isoform expression. Differences between groups were assessed using a long rank test and P-values below 0.05 were considered statistically significant.

Table 12. Hazard ratio analysis for progression-free survival

Hazard ratios with 95% confidence interval for progression-free survival in different VEGFA isoform expression groups. Groups were compared with the low VEGFA121 group, which is defined as the reference category for this analysis.

Group	HR*	95% CI*	p-value
Low VEGFA121	_	_	
Low VEGFA165	1.23	0.78, 1.92	0.4
High VEGFA121	1.16	0.79, 1.70	0.4
Low VEGFA189	1.01	0.71, 1.45	> 0.9
*** HR = Hazard Ratio, CI = Confidence Interval**			

3.3.3 Comparison of individual and clustered analysis of VEGFA isoform expression in HGSOC

Results from the two different methods (individual and clustered model) for HGSOC patient segregation raise an interesting question regarding the effect of VEGFA isoform expression on patient survival outcome: are they due to an individual isoform effect or the result of a grouped pattern effect? In order to investigate this further, differential isoform expression patterns were analysed within the low and high expression groups for each individual isoform.

The clustered pattern within the high VEGFA121 individual group indicates higher levels of VEGFA121 than VEGFA165 and VEGFA189, which is consistent with our 'Switch 4 – Low VEGFA189' cluster. On the other hand, the isoform pattern for the low VEGFA121 individual group is not fully comparable with any of our previous differential cluster analysis, with lower levels of VEGFA121 than VEGFA165 and VEGFA189, most similar to the 'Switch 1 – Low VEGFA121' cluster, but no statistical difference between the levels of VEGFA165 and VEGFA189 were detected in this group (Fig. 16).

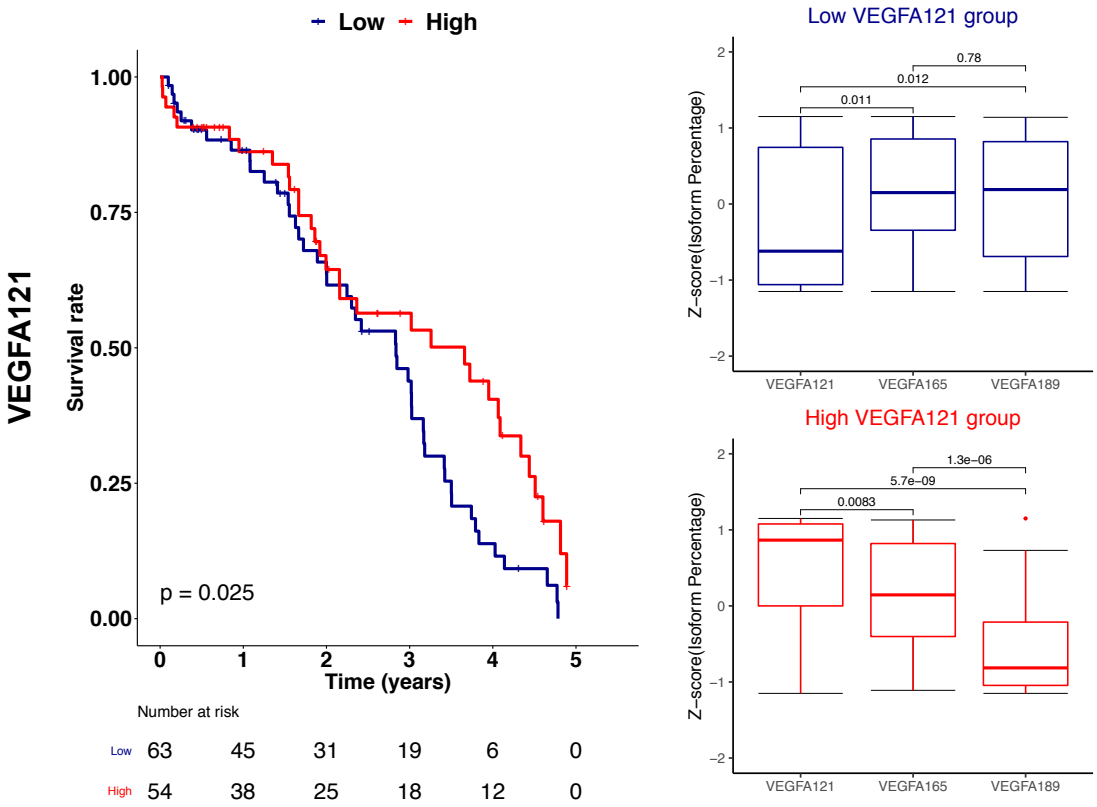

Figure 16. Differential VEGFA isoform analysis in the VEGFA121 individual groups.

Distribution of VEGFA isoform expression was evaluated for low and high VEGFA121 quartile groups. Pairwise comparisons between groups were assessed using the Wilcoxon test and P-values below 0.05 were considered statistically significant.

In the low VEGFA165 individual group, we found a similar isoform pattern to the 'Switch 3 – High VEGFA121' cluster. In the high VEGFA165 individual group, we found a similar pattern to the 'Switch 1 – Low VEGFA121' cluster (Fig. 17). In both methods, 'Switch 3' showed a decreased overall survival compared to 'Switch 1'.

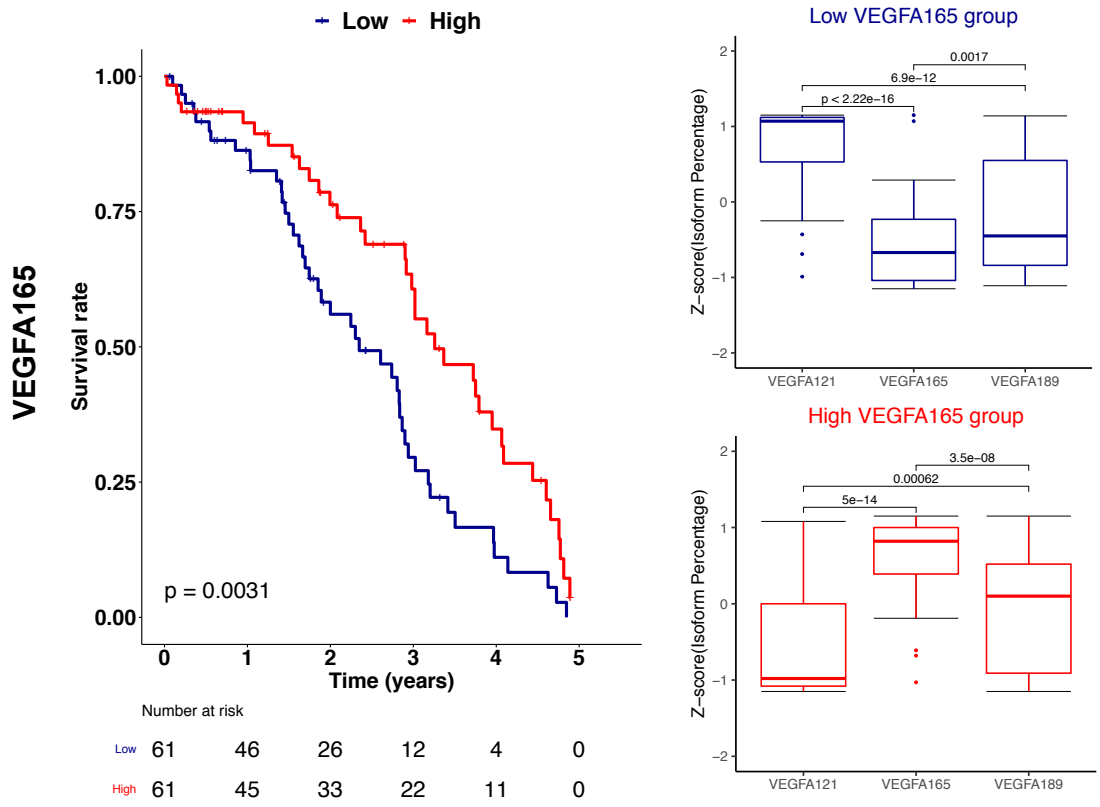

Figure 17. Differential VEGFA isoform analysis in the VEGFA165 individual groups.

Distribution of VEGFA isoform expression was evaluated for low and high VEGFA165 quartile groups. Pairwise comparisons between groups were assessed using the Wilcoxon test and P-values below 0.05 were considered statistically significant.

In the low VEGFA189 individual group, we found a similar isoform pattern to the 'Switch 4 – Low VEGFA189' cluster. On the other hand, the isoform pattern for the high VEGFA189 individual group is similar to the 'Switch 1 – Low VEGFA121' cluster, but no statistical difference between the relative levels of VEGFA165 and VEGFA189 were detected in this group (Fig. 18).

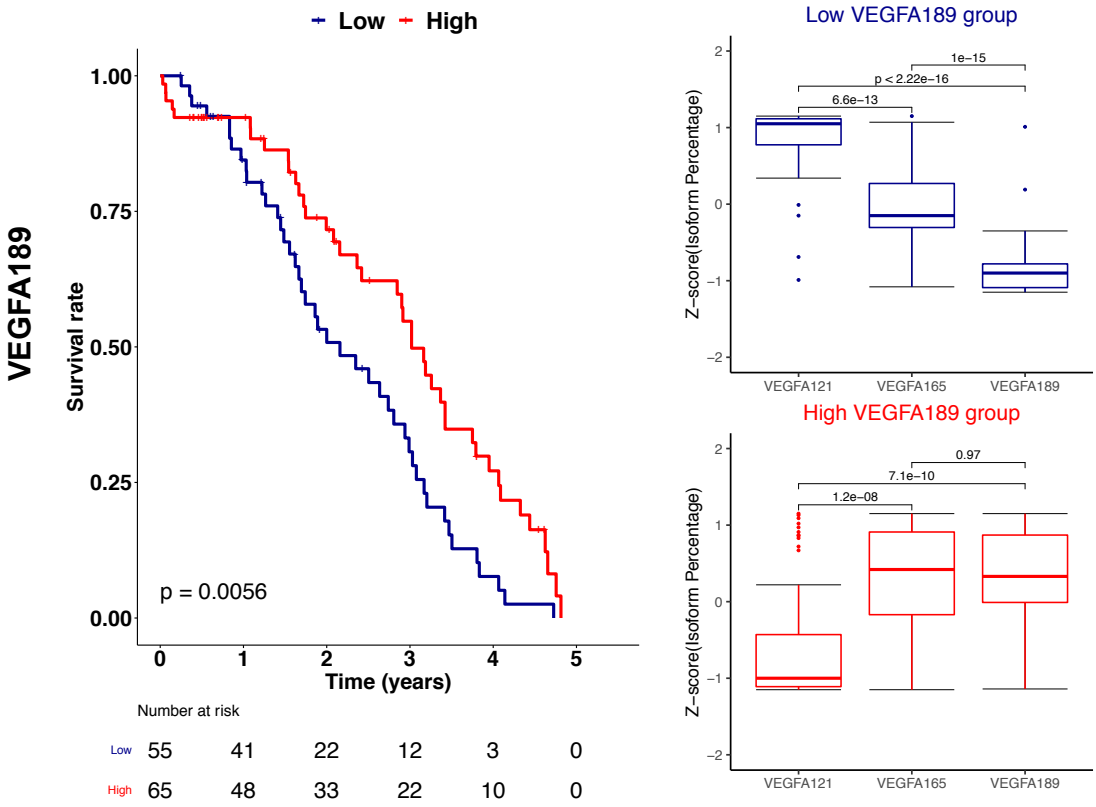

Figure 18. Differential VEGFA isoform analysis in the VEGFA189 individual groups.

Distribution of VEGFA isoform expression was evaluated for low and high VEGFA189 quartile groups. Pairwise comparisons between groups were assessed using the Wilcoxon test and P-values below 0.05 were considered statistically significant.

With this in mind, the activity of VEGFA signalling regulating survival might be affected not only by changes in individual isoform expression, but also by changes in the ratio of expression, especially considering there is no correlation between overall survival and total VEGFA mRNA expression (Fig. S2). Although the individual segregation approach shows survival differences between upper and lower quartile expression of VEGFA121, VEGFA165 and VEGFA189 independently, the isoform patterns identified through hierarchical clustering are also present within these individual groups when all the isoforms are considered (Fig. 16-18). An overlap between the alternative methods can be observed, showing a poor overall survival for groups with higher levels of VEGFA121 than the longer heparin/ECM binding isoforms 165 and 189. However this does not hold true for measurement of VEGFA121 in isolation.

We hypothesised that VEGFA121 expression levels could be used as a prognostic marker to predict patient survival in HGSOC. The different segregation models of VEGFA isoform expression in HGSOC patients in this section allowed us to identify patients that have higher VEGFA121 levels compared with VEGFA165 and VEGFA189 as well as those with lower VEGFA121 levels compared with the other two isoforms, as being of interest. The hazard ratio in relation to overall survival was assessed for each model through independent univariate analysis (Fig.19). The aim of this was to describe the risk of death for groups with higher levels of VEGFA121 than VEGFA165 and VEGFA189 when compared with the low VEGFA121 group in each patient segregation model. For most of the models with the exception of the VEGFA121 quartile groups, OS was significantly worse for those groups with higher levels of VEGFA121 compared to those with the longer isoforms. Based on this analysis, VEGFA165 quartile segregation model was selected for further bioinformatics study.

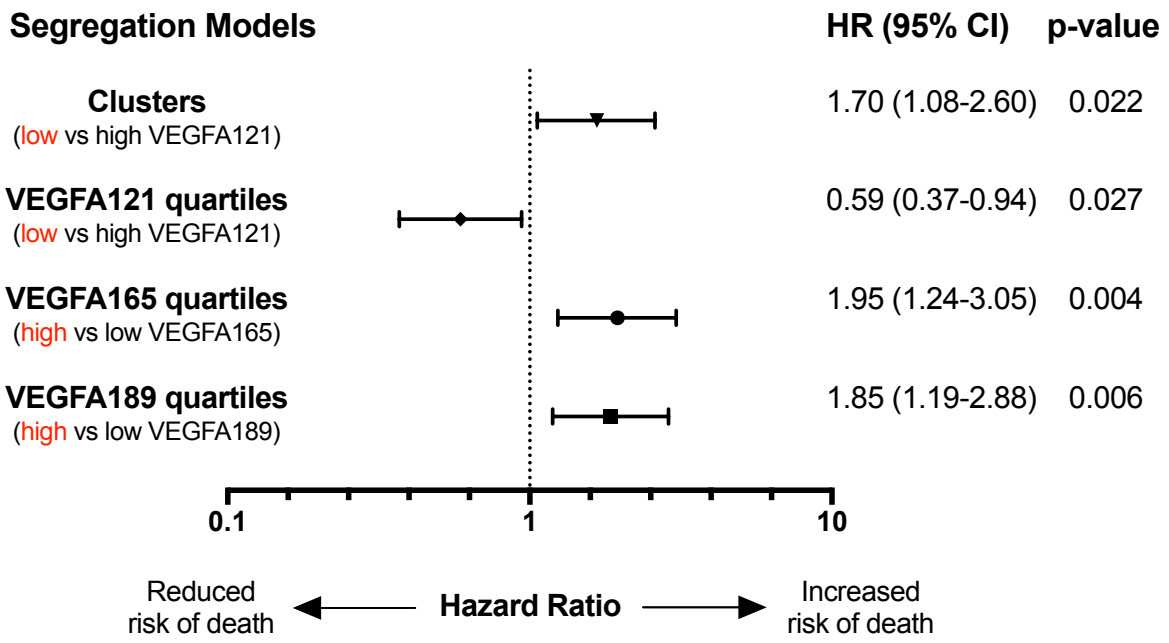

Figure 19. Hazard ratio analysis for the different segregation models.

Univariate analysis for overall survival in patients with low and high VEGFA121 expression based on the different VEGFA isoform segregation models. Group names marked in red indicate the reference group used for comparison in each model. Symbols within the bars represent the hazard ratio value and the horizontal bars extend from the lower limit to the upper limit of the 95% confidence interval. P-values below 0.05 were considered statistically significant.

Although a significant difference in overall survival was observed between patient groups with high and low VEGFA165 expression, the impact of other clinical factors on survival was also explored. To achieve this, multivariate analysis was used to study the effect of age, grade and molecular subtype together with VEGFA165 quartile segregation. The multi regression model showed that within these variables only VEGFA165 expression levels (HR 2.00, 95% CI, 1.24 to 3.23, p-value = 0.005) added statistical significance to the prediction (Table 13). This indicates that there is a link between VEGFA165 expression levels and overall survival regardless of the effect of other clinical features.

Table 13. Multivariate analysis for VEGFA165 expression level groups, grade, age and molecular subtype in HGSOC.

VEGFA165 expression, grade, age and molecular subtype categories were incorporated into the multivariate models to describe how these factors impact in overall survival. Hazard ratio, 95% confidence intervals and statistical significance are shown for each of these factors in relation to overall survival.

Characteristic	HR*	95% CI*	p-value
VEGFA165			
High	_	_	
Low	2.00	1.24, 3.23	0.005
GRADE			
G2	_	_	
G3	1.82	0.71, 4.67	0.2
AGE			
<61	_	_	
>=61	1.34	0.81, 2.21	0.2
SUBTYPE			
Differentiated	_	_	
Immunoreactive	1.63	0.78, 3.40	0.2
Mesenchymal	0.91	0.50, 1.65	0.8
Proliferative	0.90	0.49, 1.64	0.7

*** HR = Hazard Ratio, CI = Confidence Interval**

3.4 High VEGFA165 is associated with increases in gene expression linked to hypoxia, angiogenesis and EMT

In order to understand the regulation of VEGFA isoform signalling and the effect of this on HGSOC, differentially expressed genes and pathway analysis across patient groups were explored. When comparing women with high (good OS) versus low VEGFA165 expression (poor OS), 657 genes were differentially expressed (DEGs), of which 252 were down-regulated and 405 up-regulated in the high VEGFA165 group relative to low VEGFA165 (Fig. 20). These DEGs were associated with several hallmark gene sets. Hallmark processes with a high percentage of DEGs up-regulated in the high VEGFA165 group were related to biological processes, such as hypoxia, angiogenesis, epithelial-mesenchymal transition (EMT) and glycolysis. On the other hand, hallmark processes enriched in the low VEGFA165 group were associated with metabolic processes such as oxidative phosphorylation, fatty acid metabolism and adipogenesis. (Fig. 21) (Table S1).

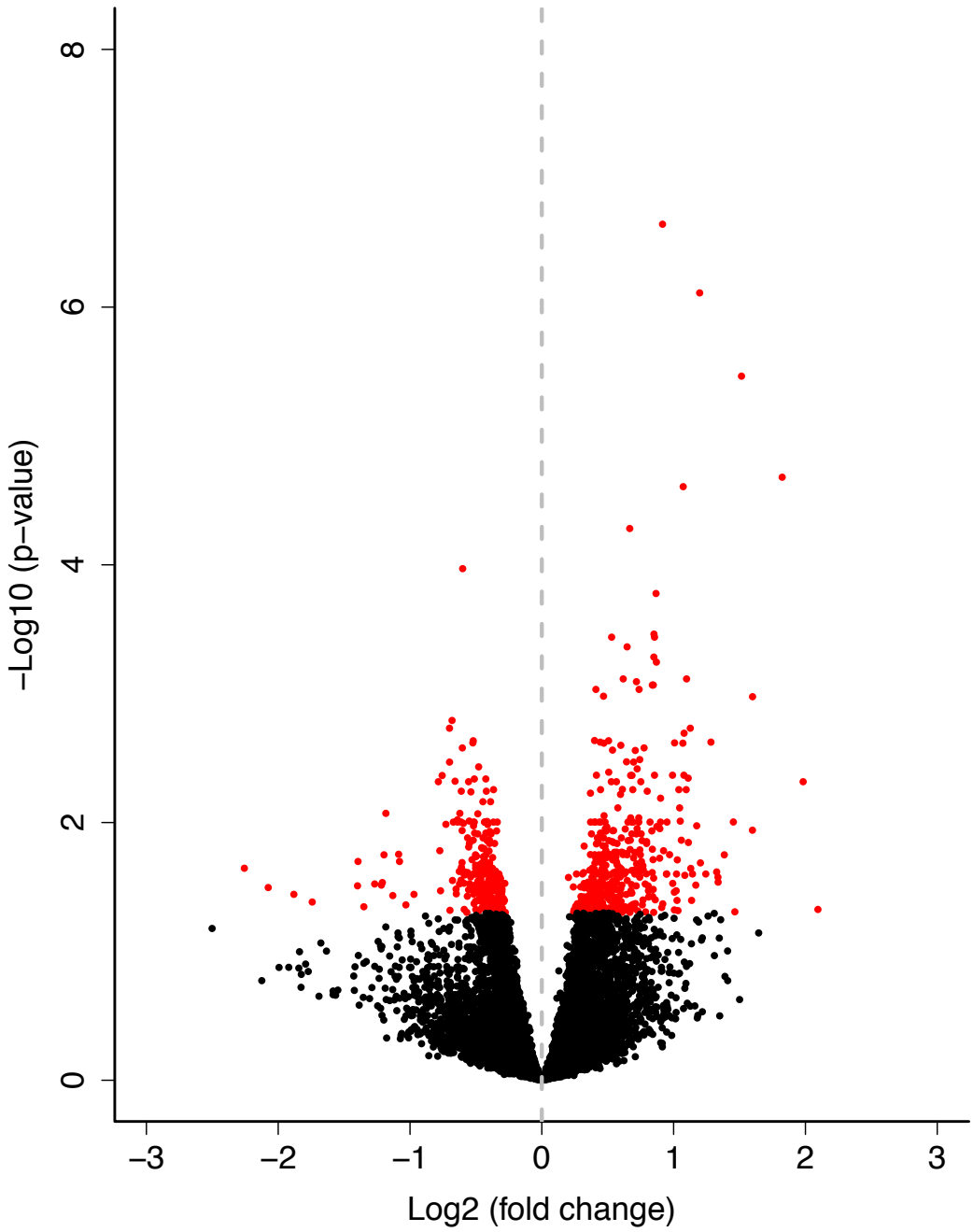

Figure 20. Volcano plot for differentially expressed genes between VEGFA165 expression groups.

Down- and up-regulated expressed genes in VEGFA165 expression level groups. The Cut-off criterion for DEG significance was FDR ≤ 0.05. The y-axis displays the –log10 p value, while the x-axis displays the log2 fold change for each gene.

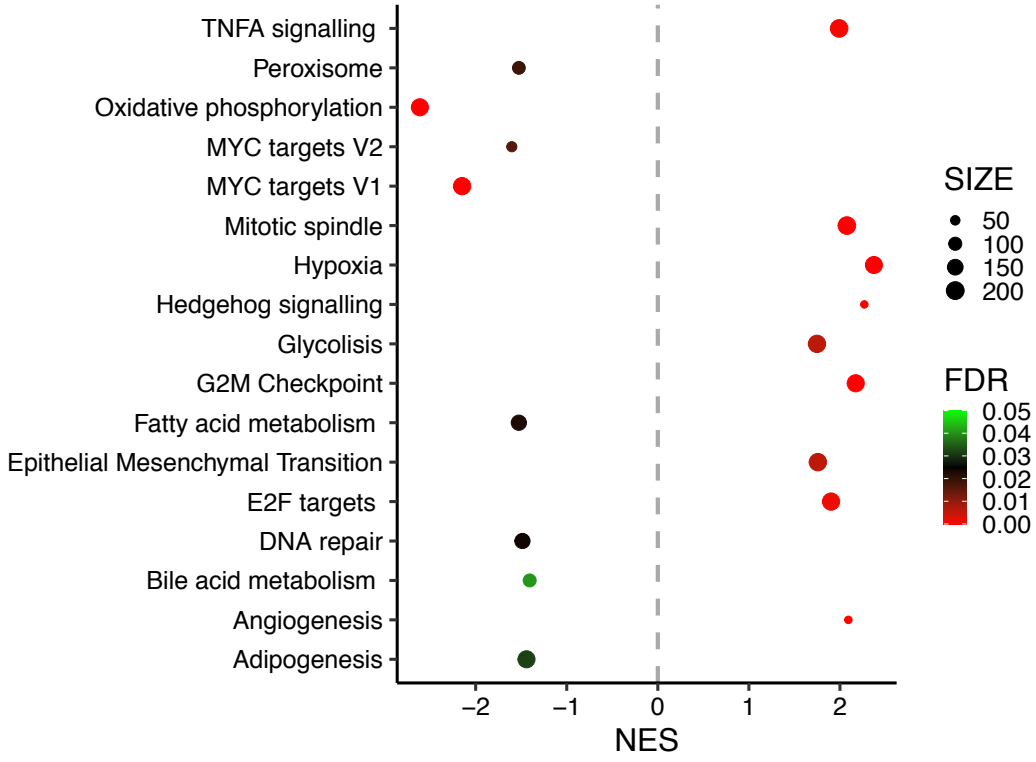

Figure 21. Biological processes enriched in VEGFA165 expression groups.

The hallmark gene sets (h.all.V7.1 MSigDB) shown above were significantly up-regulated in patients with high VEGFA165 expression if NES > 0 or with low VEGFA165 if NES < 0. The cut-off criterion for significance was FDR q-value ≤ 0.05. NES = Normalised Enrichment Score.

GSEA analyses using the gene sets hosted by the molecular signatures database (MsigDB) allow us to generate new hypotheses and drive further research. However, in order to identify if more specific pathways are involved in the resulting biological processes, predicted protein - protein interactions were analysed to identify functional networks among DEGs. Based on the GSEA results between low and high VEGFA165, hypoxia is associated with high VEGFA165 expression. The hypoxia scores, based on the Buffa gene signature (Buffa et al., 2010), were obtained for each patient through the cBioPortal and these were compared between VEGFA165 expression groups (Fig. 22A). Tumours with high levels of VEGFA165 showed an increased hypoxic score as suggested by our GSEA results. Subsequently, we analysed the DEGs related to hypoxic response and generated a protein-protein interaction network (Fig. 22B). Within the up-regulated genes linked to hypoxia were *MTOR* (FDR = 0.03, FC = 1.3), *PDK1* (FDR = 0.01, FC = 1.4), *ANGPTL4* (FDR = .002, FC = 2.4) and *CA9* (FDR = 0.004, FC = 4). Additionally, GSEA results show that angiogenesis gene signature is enriched in the high VEGFA165 expression group. Within the up-regulated genes linked to angiogenesis were VEGFR1 (*FLT1*, FDR = < 0.0005, FC = 1.89) and VEGFR2 (*KDR*, FDR = 0.003, FC = 1.56). Other implicated genes include basement membrane genes such as collagens and other blood vessel morphogenesis components such as *DLL4* and *NOTCH4* (Table S2).

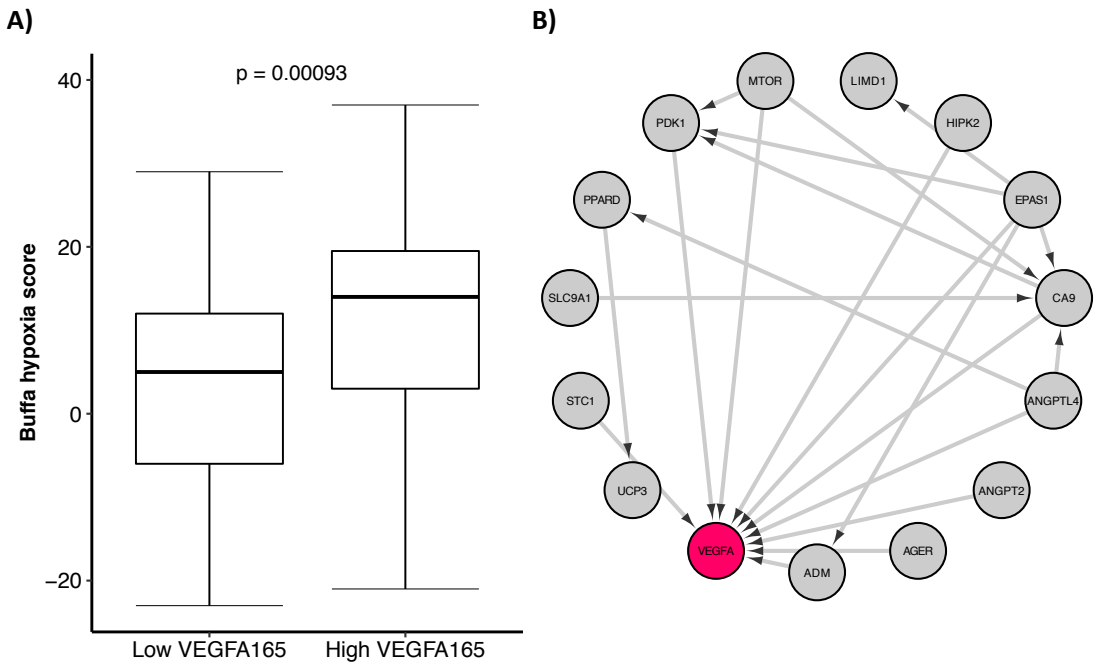

Figure 22. Associations between hypoxia and VEGFA165 expression levels.

A) Hypoxia scores were obtained from the cBioPortal and values were compared between low (n=47) and high (n=60) VEGFA165 expression groups. Differences between groups were assessed using a Wilcoxon test and p-value below 0.05 was considered statistically significant. **B)** Protein-Protein interaction network for hypoxia response constructed using StringApp and Cytoscape.

3.5 Immune cell populations

Previous published data has identified six different immune subtypes across different cancers using the TCGA data (Thorsson et al., 2018). In order to explore the distribution of immune subtypes between our VEGFA165 groups, the predicted immune signatures were obtained for each patient and percentages were calculated for each immune model within each group (Table 14). These results suggest similar immune characteristics between low and high VEGFA165 expression groups with the IFN-γ dominant subtype in more than 50% of the cases, followed by wound healing and lymphocyte depleted subtypes.

Table 14. Immune subtypes in VEGFA165 expression groups.

This table shows the proportion of samples belonging to each immune subtype within the VEGFA165 expression groups. Parentheses show the number of samples per subtype from the total cases within each patient group.

Immune Subtype	Low VEGFA165	High VEGFA165
Wound healing	19.5 % (8/41)	21.1% (11/52)
IFN-γ dominant	51.2% (21/41)	55.8% (29/52)
Inflammatory	0% (0/41)	1.9 % (1/52)
Lymphocyte depleted	29.3 % (12/41)	21.2% (11/52)

The GSEA analysis of hallmark gene signatures does not suggest an association between immune processes and expression levels of VEGFA165, however these results do not allow comparisons between cell types within the tumour. For this we collected data from the xCell study and compared the abundance of different cell types in our TCGA OV samples. In general, this approach was able to recover a signal from several major cell types, including, pericytes, fibroblasts, microvascular endothelial cells, macrophages, CD4+, CD8+, natural killer and regulatory T-cells (Fig. 23-24). The xCell scores for most of the cell types showed a similar abundance between low and high VEGFA165 expression groups, however there is a significant decrease in pericyte and natural killer cells in the low VEGFA165 expression group (Fig. 23-24), while macrophage abundance, predominantly M1 macrophages, is higher when compared to the high VEGFA165 group (Fig. 24).

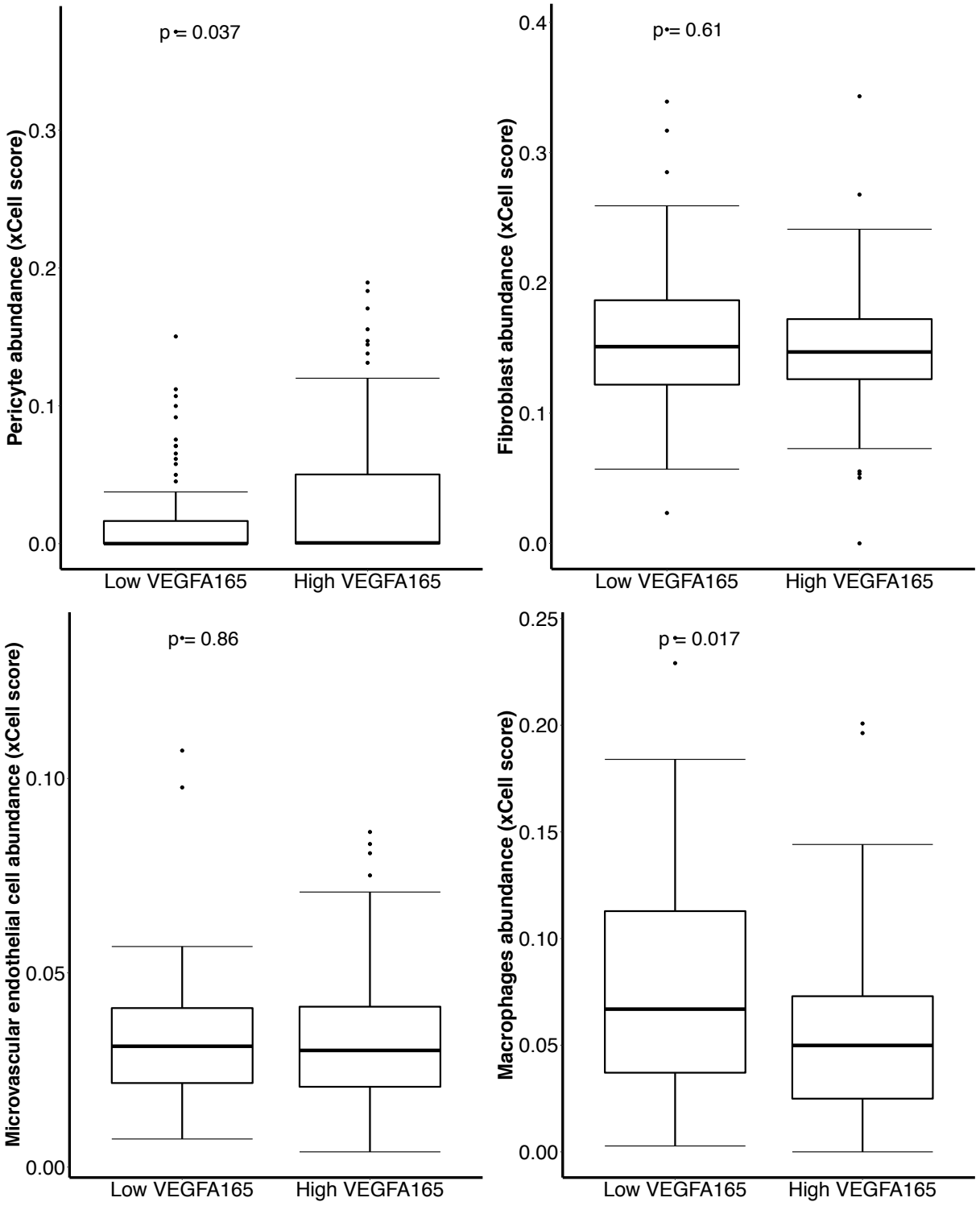

Figure 23. Cell type abundance in HGSOC tumours.

XCell scores from different immune populations were obtained for each patient sample. For each cell type, abundance values were compared between low (n=74) and high (n=74) VEGFA165 expression groups. Differences between groups were assessed using a Wilcoxon test and p-value below 0.05 was considered statistically significant.

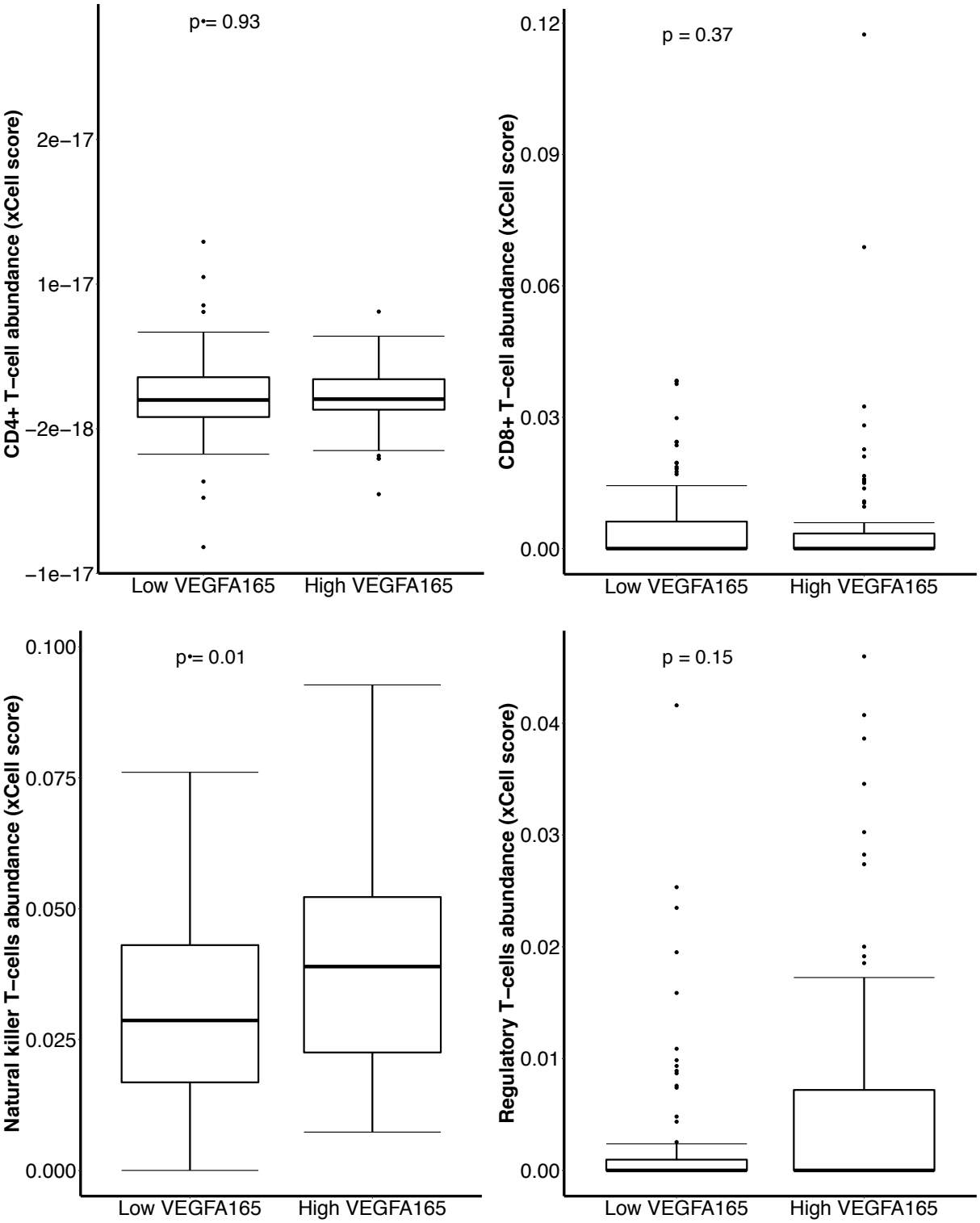

Figure 24. Cell type abundance in HGSOC tumours continued.

XCell scores from different immune populations were obtained for each patient sample. For each cell type, abundance values were compared between low (n=74) and high (n=74) VEGFA165 expression groups. Differences between groups were assessed using a Wilcoxon test and p-value below 0.05 was considered statistically significant.

3.6 High VEGFA165 is associated with a predictive response to anti-VEGF therapy

A VEGFA-dependent gene signature (VDGs) associated with response to anti-VEGFA therapy was developed by Yin et al. (2016). Specifically, enrichment of VDGs in ovarian cancer has been suggested to be predictive for bevacizumab therapy. This gene list includes approximately 139 human genes, which contains vascular and basement membrane genes (Yin et al., 2016). The evaluation of the VDGs in our HGSOC groups through GSEA analysis showed that this signature is highly enriched in patients with high VEGFA165 (FDR q-val < 0.001), which suggest a potential benefit from bevacizumab for patients in this group (Fig. 25).

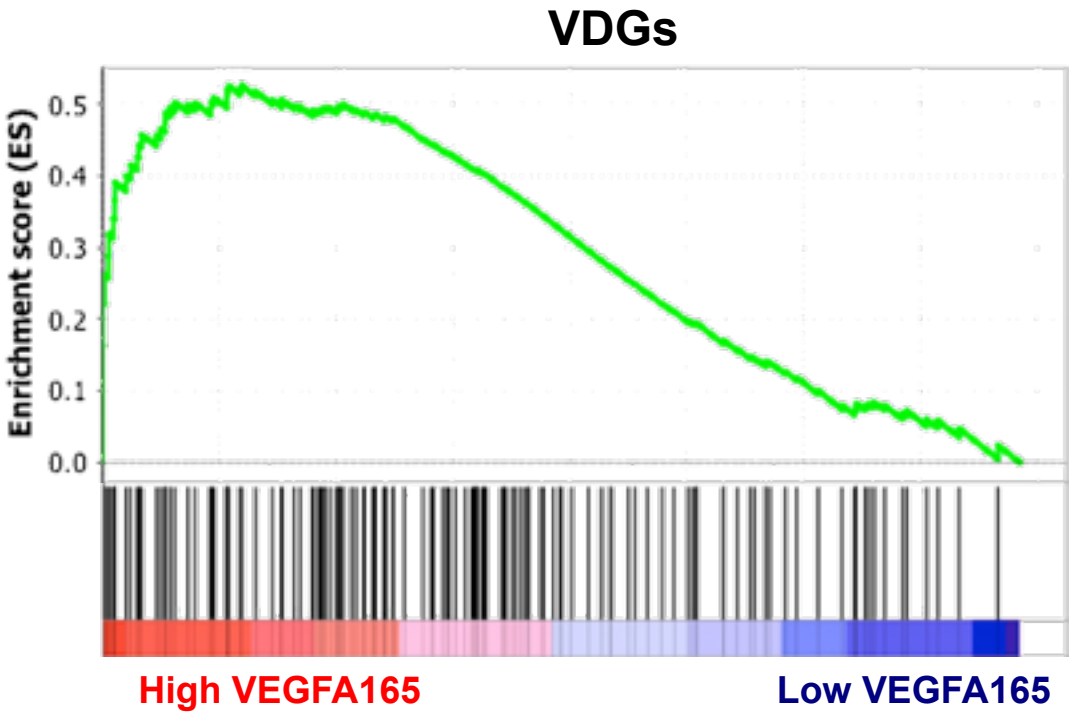

Figure 25. GSEA analysis of the VEGFA-dependent gene signature.

Enrichment score plot for the VEGFA-dependent gene signature. Positive enrichment is observed for the high VEGFA165 (FDR q-val <0.001). This association indicates that the group with enriched VEGFA-dependent genes might respond better to treatment with bevacizumab.

3.7 Associations between VEGFA165 expression levels and genomic instability

HGSOC is characterised by frequent mutations in the *TP53* gene, which have been found in more than 96% of the cases (Lisio et al., 2019). Less frequent mutations involve oncogenic changes in *BRCA1*, *BRCA2* and others such as *CSMD3*, *NF1*, *CDK12*, *GABRA6* and *RB1* (Lisio et al., 2019). Additionally, genes like *CCNE1*, *MYC* and *MECOM* have shown frequent copy number variation, which results in gene amplification (Lisio et al., 2019). In order to analyse the genomic landscape between VEGFA165 expression groups, mutation frequency values were compared between the groups for the genes with the highest frequency (Fig. 26A). *TP53* showed the highest mutation frequency in both groups with 63.64 % and 63.61% for low and high VEGFA165 groups respectively. However, no significant difference was observed between the groups for *TP53* or any other mutated genes typical of ovarian cancer shown in this analysis. In a similar way, genes with the highest copy number alteration frequency were compared between our groups (Fig. 26B). Although no significant difference was found, a smaller percentage of genomic alterations was observed for the low VEGFA165 expression group for these genes when compared to the high VEGFA165 group.

Homologous recombination deficiency (HRD) has been recently associated with HGSOC progression, survival and response to platinum chemotherapy or targeted therapy, such as PARP inhibitors (Takaya et al., 2020). GSEA analysis showed that the DNA repair gene signature is enriched in the low VEGFA165 group; therefore in order to investigate this further we compared total mutation count and HRD score between VEGFA165 groups. Our results did not show significant difference between low and high VEGFA165 neither for mutation count nor HRD score (Fig. 27).

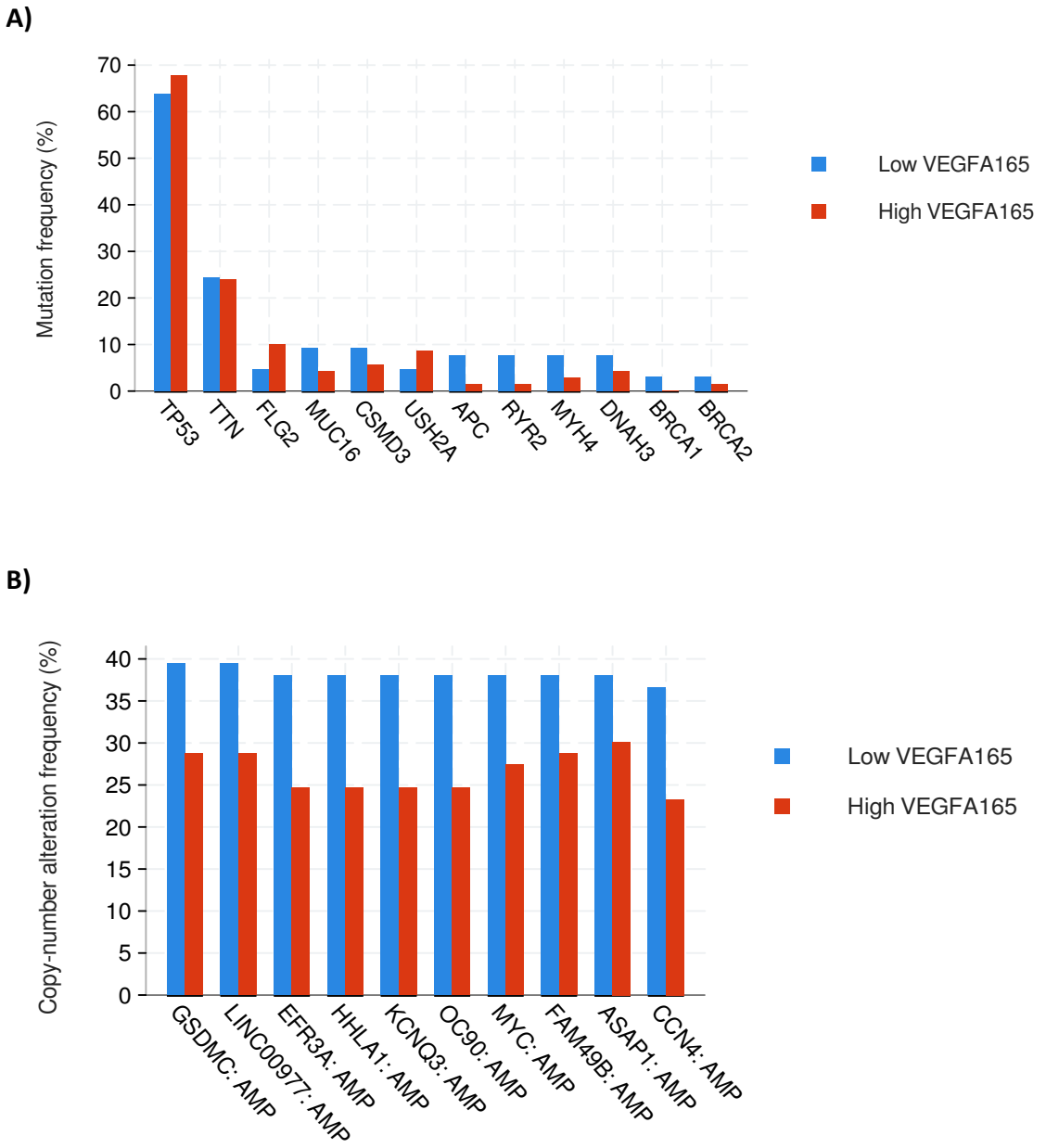

Figure 26. Genes with the highest genomic alterations in VEGFA165 expression groups.

A) Mutation frequency and **B)** Copy number alteration frequency between low (n=72) and high (73) VEGFA165. Plots and group comparisons were performed through the cBioPortal platform (Gao et al., 2013).

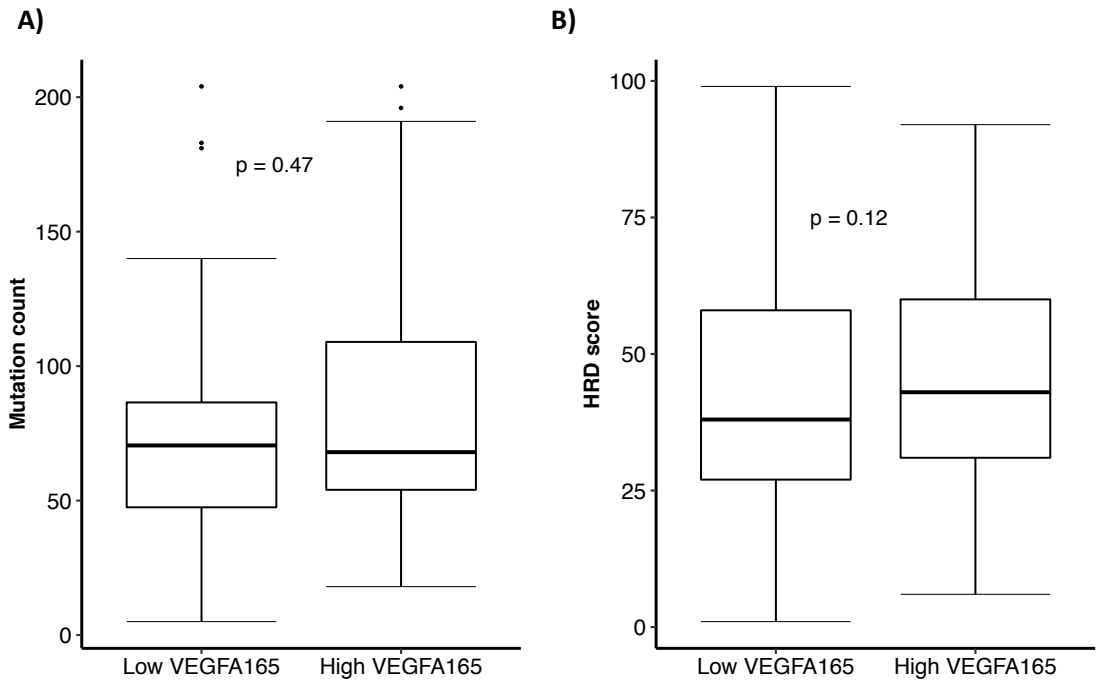

Figure 27. Association between VEGFA165 expression, mutation count and HRD.

A) Total mutation count comparison between low (n=44) and high (n=51) VEGFA165. **B)** HRD score comparison between low (n=73) and high VEGFA165 (n=73). Differences between groups were assessed using a Wilcoxon test and p-value below 0.05 was considered statistically significant.

3.8 Summary

Results from these studies show that the VEGFA isoforms predominantly expressed in ovarian tissue are VEGFA121, VEGFA165 and VEGFA189. Expression of other VEGFA isoforms such as VEGFA145 or VEGFAxxxb variants was not detected in this analysis. These predominant isoforms are increased in human tumour samples when compared with normal ovarian tissue. It is important to mention that ovary samples within the GTEx database were obtained post-mortem using 10 mm x 10 mm x 4 mm sections from most normal regions of the ovary (GTEx Consortium, 2013). It is not clear if this sampling collection procedure can have an effect on transcript expression or if other characteristics such as menopausal status or presence of hypoxia during follicular development can impact VEGFA isoform expression. Previous work within the English' lab has shown that the use of different tissue preservation methods such as freezing, warming at 37 °C followed by freezing and FFPE does not affect mRNA VEGFA isoform quantification in pre-clinical models (Magon, 2018). It will be important to further evaluate if other sample characteristics can be factors to consider when measuring mRNA expression in ovarian tissue.

This work evaluated different methods to segregate HGSOC patients based on VEGFA isoform expression levels. The first method, defined as the "Individual Segregation model" showed that low levels of VEGFA121, VEGFA165 and VEGFA189 are individually associated with worse overall survival, while those with high individual levels of expression showed a better survival outcome. For this first method, patient group segregation was defined based on upper and lower quartiles for each isoform expression. This approach provides sufficient data for comparison and allows for study of the cases that are the most detached from the rest of the distribution. This data can also be divided at the middle 50% or by tertiles, which will increase the number of observed cases in each group. However, for this individual segregation model only the quartile cut-off was studied. Future work can look at the effect of establishing different cut-offs within the presented model and therefore determine if a different approach could be more clinically relevant.

The second method, defined as the "Clustered Segregation model" showed a decreased overall survival for the high VEGFA121 group when compared with either low VEGFA189 or low VEGFA121. No significant differences were observed for PFS between the groups regardless of the method of segregation that was applied. Additionally, no association between total VEGFA mRNA expression and overall or progression-free survival was

observed. As previously mentioned in section 2.7.6, information regarding patient treatment is not fully described within the TCGA clinical data, therefore these variables could not be considered for survival analysis in this work. Although early TCGA reports described that most patients were treated with platinum and taxane chemotherapy (Cancer Genome Atlas Research, 2011), access to this information might explain why a significant difference can be observed for overall survival but not for progression-free survival between the studied groups.

Comparison between the different segregation models identified that HGSOC patients with relative higher levels of VEGFA121 than VEGFA165 and VEGFA189 tend to show worse overall survival when compared with those patients showing lower levels of VEGFA121 compared to the rest of the isoforms. VEGFA165 segregation based on upper and lower quartiles showed the best survival segregation across the different models; therefore patient groups segregated using this approach were used for further analysis. A multivariate analysis including VEGFA165 expression levels, age, grade and molecular subtype characteristics indicated that there is a link between VEGFA165 expression levels and overall survival independent of other clinical features. One of the main disadvantages of this analysis is the lack of access to information regarding treatment strategies and other important prognostic factors such as patient performance status and residual disease.

Gene expression analyses showed that the high VEGFA165 group was associated with increases in biological processes such as hypoxia, angiogenesis, epithelial-mesenchymal transition and glycolysis. Additionally, this group of patients presented an increased abundance of pericytes and immune cells such as NK cells but also a decrease in M1 macrophages. Results from the GSEA analysis suggests that patients with high VEGFA165 may show potential benefit from bevacizumab treatment. Finally, no difference in genomic alterations such as mutation or copy-number alteration frequency was observed between the VEGFA165 expression groups. Although the expression of VEGFRs was not studied directly in these bioinformatics analyses, differential gene expression showed that mRNA levels of VEGFR1 (*FLT1*) and VEGFR2 (*KDR*) are up-regulated in tumours with high levels of VEGFA165. Future work should evaluate if the expression of VEGFRs correlates with VEGFA isoforms and clinical outcome in HGSOC patients. Looking at VEGFRs and other components of this signalling could potentially explain the survival discrepancies observed between the models proposed within this project.

Chapter 4

4. Functional characterisation of ovarian cancer cells overexpressing the VEGFA120 isoform

A hindrance in the study of HGSOC is the need for cell lines that better represent human HGSOC disease. This has led to an increased effort into replicating HGSOC histological and molecular characteristics in cell lines. VEGFA signalling has been widely studied in ovarian cancer, however *in vitro* models designed to study VEGFA isoform effects in HGSOC are still limited. Generally, there is a lack of characterisation of VEGFA isoform expression in cancer cell lines and it is essential to overcome this limitation in order to select appropriate models to explore VEGFA isoform signalling that will efficiently translate into pre-clinical and clinical research.

Previous efforts to achieve this within the English lab attempted to use ZFN technology to create human ovarian cancer cell lines that overexpress VEGFA121 through introducing spliced exons in the *VEGFA* gene via homologous recombination in COV362 and COV318 HGSOC cells (Valluru MK and English WR, unpublished). Unfortunately, although a single clone expressing increased VEGFA121 underwent initial characterisation, these initial attempts using a ZFN based approach were on the whole unsuccessful due to low genomic integration efficiency, re-editing of the inserted DNA and a lack of appropriate screening tools for the transfected clones. This chapter will describe strategies to overcome these limitations.

A backup plan was needed in the eventuality that the ZFN editing still prove unsuccessful. A PiggyBac transposon based system was developed to make stable cell lines over-expressing VEGFA isoforms from control of the HRE, allowing some replication of transcriptional control of the endogenous gene. As the initial bioinformatics analysis showed patients with high and low VEGFA121 may also have significant differences in adaptive immune cell signalling, mouse ID8 cells were used with the objective of having an appropriate model to study the role of VEGFA120 in an immune competent pre-clinical model.

To address the need for improved assays for clone selection and characterisation, an absolute quantitative real-time PCR (AQRT-PCR) assay was developed to characterise VEGFA mRNA isoform expression. The role of VEGFA120 signalling *in vitro* was explored by measuring cell viability, migration and response to carboplatin. Additionally, EMT expression markers were characterised using western blot. Sadly, experiments set up to study the effect of anti-VEGFA antibodies on these parameters had to be abandoned due to restrictions on laboratory working due to the COVID pandemic.

In the next sections I will review the previous studies characterising ovarian cancer cell lines in terms of their suitability as models of HGSOC as well as cellular models used to study VEGFA isoform expression. I will then present and discuss results from my own *in vitro* studies examining VEGFA isoform expression in ovarian cancer cells.

4.1 Introduction

It is important to consider the genetic and molecular features of commonly used HGSOC cell lines as models of disease. In many previous studies, ovarian cancer cell lines have been used as such models, however these have more recently been shown not to be appropriate for modelling HGSOC due to their lack of genetic and molecular similarity to HGSOC cells from clinical tumour samples (Domcke et al., 2013). Two different studies have characterised panels of ovarian cancer cell lines to find suitable representative models for studying HGSOC (Domcke et al., 2013; Beaufort et al., 2014). Specifically, it has been observed that some of the most common used cell lines such as IGROV-1 have high rates of genomic alterations not present in the clinical genomic HGSOC profile. Conversely, less popular cell lines such as COV318 and COV362 have genetic alterations more specific to HGSOC, such as *TP53* and *BRCA* mutations (Beaufort et al., 2014; Domcke et al., 2013), which make these human cell lines a better avenue to study HGSOC in *in vitro* and *in vivo* models.

Different *in vitro* models have been created with the objective to overexpress VEGFA isoforms. Commonly, VEGFA isoform cDNA is cloned into an expression vector containing a specific antibiotic resistance as a selection marker. In human breast cancer cells (MDA-MB-231), VEGFA165 and VEGFA189 overexpression was generated using an expression vector, pRCEN, which contains the cytomegalovirus promoter and the neomycin resistance gene (Di Benedetto et al., 2015; Herve et al., 2008). Additionally, VEGFA121 and

VEGFA165 overexpression has been described in MCF-7 cells. cDNA inserts for each isoform were cloned into a pCEP4 expression vector and stably transfected cells were selected using hygromycin resistance (Guo, P. et al., 2003; Fenton et al., 2004). Similar systems have been used in human lung cancer cells (CL1-0), human melanoma cells (WM1341B) and murine mammary carcinoma cells (EMT-6). (Yuan et al., 2011; Bayko et al., 1998; Zhang, H. et al., 2015).

Recombinant retroviral vectors have also been used to overexpress VEGFA isoforms. Retroviral particles containing VEGFA121 or VEGFA165 cDNAs have been used to overexpress these isoforms in human astrocytes (Sonoda et al., 2003). A GFP co-expressing lentiviral system has also been used in order to generate VEGFA165 stably transduced 293T cells (Sun et al., 2011). In mouse ovarian cancer cells, a retroviral vector, MigR1, containing GFP has been used to overexpress VEGFA164 (Zhang, L. et al., 2002b).

However, in all these systems VEGFA isoforms are expressed from strong promoters that lack endogenous mechanisms of regulation contained in the human (*VEGFA*) or mouse (*Vegfa*) promoter. Mouse fibrosarcoma cells overexpressing VEGFA120 or VEGFA188 have been developed from embryonic fibroblasts derived from mice genetically engineered to express a single VEGFA isoform through introduction of a new region into the *Vegfa* gene containing different spliced exons between exon 3 and 8, thus retaining the endogenous transcriptional control (Vieira et al., 2007; Tozer et al., 2008). These models have helped to study the role of individual VEGFA isoforms in morphological and functional characteristics in tumours and their response to anti-angiogenic therapy (Tozer et al., 2008; Akerman et al., 2013; Kanthou et al., 2014; English et al., 2017).

One way of altering VEGFA isoform expression in cell lines, while retaining the endogenous regulatory elements of the human (*VEGFA*) or mouse (*Vegfa*) gene, is to use gene-editing technology to replicate the approach used in the genetically engineered mice. Zinc Finger Nuclease (ZFN) technology is a genome-editing tool that allows the deletion, modification or integration of a gene of interest into new cell lines (Hansen et al., 2012). Firstly, Zinc Finger Nucleases target a specific nucleotide sequence and cut the double stranded DNA. Secondly, a plasmid donor, which includes both the gene of interest and homology sequences to the integration site, stimulates an homology-repair mechanism that integrates the gene of interest into the genome (Hansen et al., 2012). Advantages of this system include targeting specific genomic loci and the generation of stable gene modifications. Disadvantages include gene

editing in only 1-20% of transfected cells and a lack of selectable marker for screening and isolation (Hansen et al., 2012).

An alternative to using gene editing would be to replace the strong promoters used by others with one that can replicate the endogenous promoter, particularly its regulation by hypoxia. The Hypoxia Response Element (HRE) is a recognition site for binding of the hypoxia-inducible Factor 1 (HIF1) that allows the regulation of the *VEGFA* gene (Ramakrishnan et al., 2014). This mechanism has allowed the use of HRE as a based promoter system to enhance the expression of specific genes under hypoxic conditions. The construction of the [HRE]x5-minCMV promoter has been previously described (Shibata et al., 1998). It contains five copies of a 35-bp fragment from the HRE element of the human *VEGFA* gene linked by 5 nucleotides and followed by a minimal human cytomegalovirus promoter (minCMV). This system has successfully induced VEGFA expression in tumour cells during hypoxia while providing lower levels of expression in atmospheric oxygen levels compared to strong promoters like CMV and EF-1α (Shibata et al., 2000).

Additionally, the piggyBac transposon system is a gene-editing tool that allows the deletion or integration of a specific gene into a genome by transposing DNA sequences between expression vectors and chromosomes via a "cut-and-paste" mechanism (Zhao et al., 2016). The main advantages of this system are the high integration efficiency and generation of stable cell lines in multiple mammalian cells at greater efficiency than previous inefficient methods used to generate cell lines through random integration into the genome (Zhao et al., 2016).

As described earlier, it is essential to develop a quantification method that allows us to characterise mRNA expression of VEGFA isoforms in cell models and ultimately clinical samples. The ELISA assay is commonly used to characterise VEGFA expression, however this approach quantifies total VEGFA rather than specific VEGFA isoforms. ELISA assays are commercially available for VEGFA121, however there is limited information about the specificity of this test to make this a reliable method. QRT-PCR may be a more appropriate technique to measure VEGFA isoform mRNA expression accurately within cancer cells or tumour samples. An adaptation of this method that includes a 'cDNA standard' for each cDNA derived from mRNA reverse transcription allows accurate quantification in terms of copy number rather than the ΔΔCt method that can be influenced by differences in amplification rate in the QRT-PCR reaction between different amplicons.

4.2 Development of ovarian cancer cells expressing increased levels of VEGFA isoforms

4.2.1 Gene editing to generate human ovarian cancer cells expressing increased VEGFA121

As the initial attempts to use ZFN based gene editing to insert donor DNA containing spliced exons 4-8 into the *VEGFA* gene was inefficient a revised strategy was developed. Site directed mutagenesis was used to make translationally silent-point mutations in the donor plasmid encoding VEGFA121 (pVEGFA121), which is used for homology repair during genome editing with Zinc Finger Nucleases (ZFNs). The aim was to reduce the re-targeting of the inserted homology repair DNA after insertion in the genome, and to enable detection of the VEGF121 mRNA expressed by the edited gene via RNA sequencing and SNP detection. However, site-directed mutagenesis in pVEGFA121 vector resulted in sequence deletions due to a high degree of sequence similarity within the plasmid (Fig. S4). Although the desired silent point mutations were inserted after mutagenesis, a deletion in the sequence was observed. To solve this issue, the desired mutations within the donor pVEGFA121 were incorporated by chemical synthesis using Genewiz gene synthesis services.

ZFN plasmids were then transfected together with the synthesised donor pVEGFA121 into COV362 cells by electroporation. Following this, cell viability was very low and cells showed poor attachment on the cell culture surface. Four to six weeks were required for cells to recover from transfection and reach 70-80% confluency for further characterisation. Single cell isolation from the electroporated cells was also challenging as COV362 cells have very poor rates of proliferation at such low cell densities, which also had an impact on the time required to achieve clone isolation. Despite these issues it was possible to isolate some COV362 clones transfected with the ZFN system, however the limited number clones showing successful integration of VEGFA121 donor DNA using PCR assays (Fig. 28) did not show an increase in secreted VEGFA when measured by ELISA (Fig. 29). In fact, some clones expressed virtually no VEGFA, suggesting the inserts may have resulted in a functional knock out. Due to all these technical complications there was a critical need to re-design a more suitable approach to overcome these limitations and achieve the objective of overexpression of VEGFA121 in ovarian cancer cells within the time limit available for the PhD.

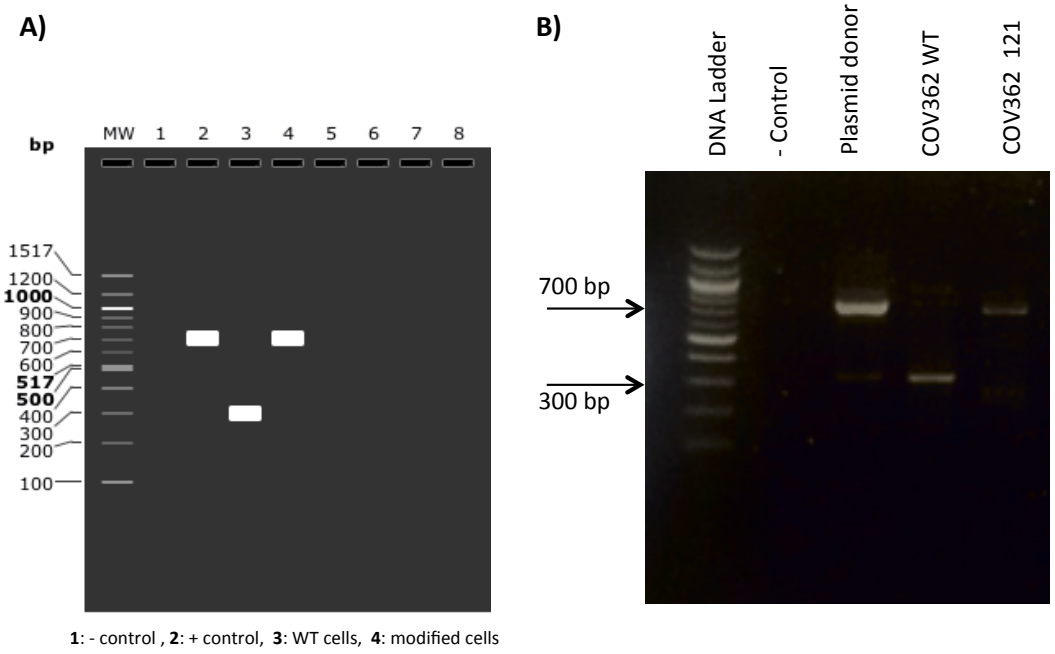

Figure 28. VEGFA121 integration in COV362 cells by Zinc Finger Nuclease Technology.

A) Simulated agarose gel for genomic integration of VEGFA121 using the ZFN system. **B)** 1% agarose gel of VEGFA121 integration using PCR assays in COV362 WT and COV362 121 cells.

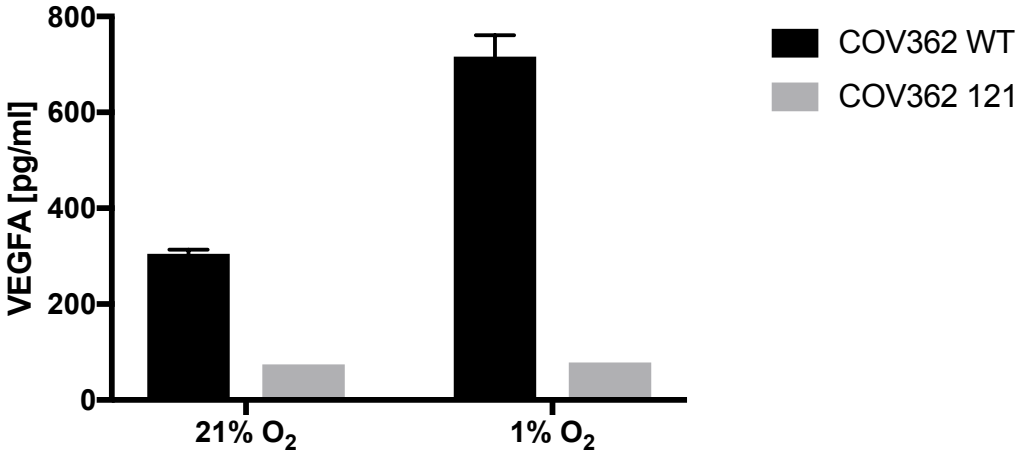

Figure 29. VEGFA expression levels in electroporated COV362 cell lines.

COV362 WT and COV362 VEGFA121 cells were cultured in T25 flasks in 2 ml of fresh medium and incubated for 12 hours at 21% and 1% O_2. Human VEGFA levels were quantified using ELISA. All data values are expressed as mean ± standard error of two replicates.

4.2.2 [HRE]x5-minCMV-VEGFA plasmid design

As described in the introduction to this chapter, transposases can be used to rapidly generate stable cell lines with high efficiency and artificial promoters can be used to replicate endogenous VEGFA expression levels and control. To this end, the PiggyBac transposon for the generation of stable cell lines was created using pCLIIP-C-LS vector (English et al., 2017) by removing the Luciferase2-E2A-mStrawberry fragment and then introducing the [HRE]x5-minCMV-VEGFA121 or 120 element into the MluI and FseI sites (Fig. 30). The insertion of the VEGFA121 or VEGFA120 fragment following the minCMV promoter allowed the generation of a human and mouse version of this vector respectively (Fig. 31). The final construct was verified by sequencing (Fig. S5-S8).

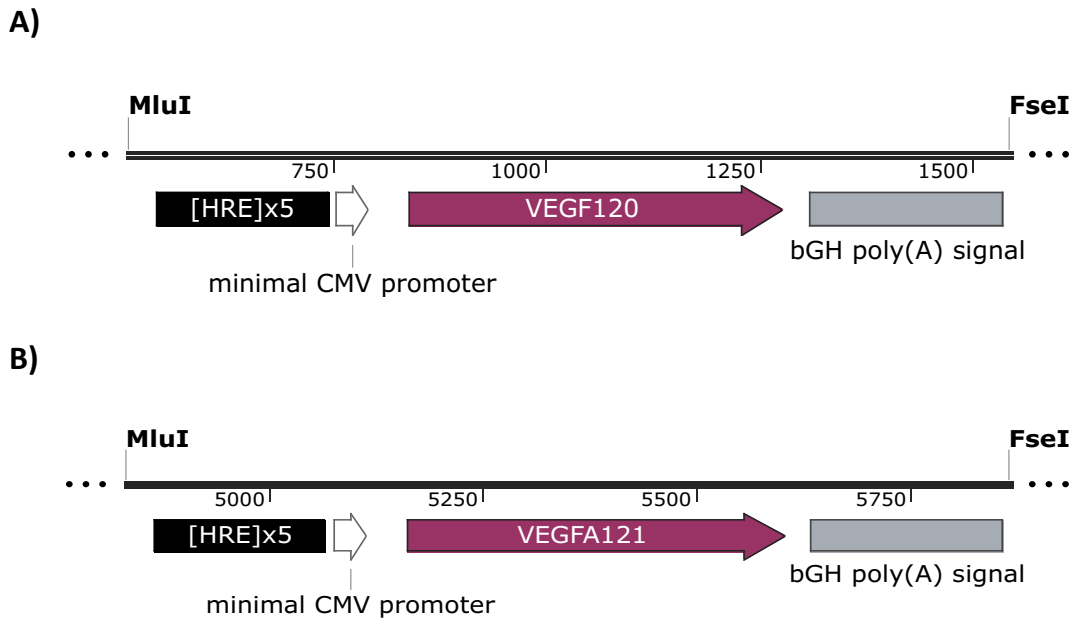

Figure 30. [HRE]x5-minCMV-VEGFA120/121 design.

In this construct **A)** VEGFA120 or **B)** VEGFA121 is under the control of the hypoxia-responsive element and a minimal cytomegalovirus promoter. The VEGFA120 and 121 gene (Red) is inserted downstream of the HRE (black) and minCMV promoter (white).

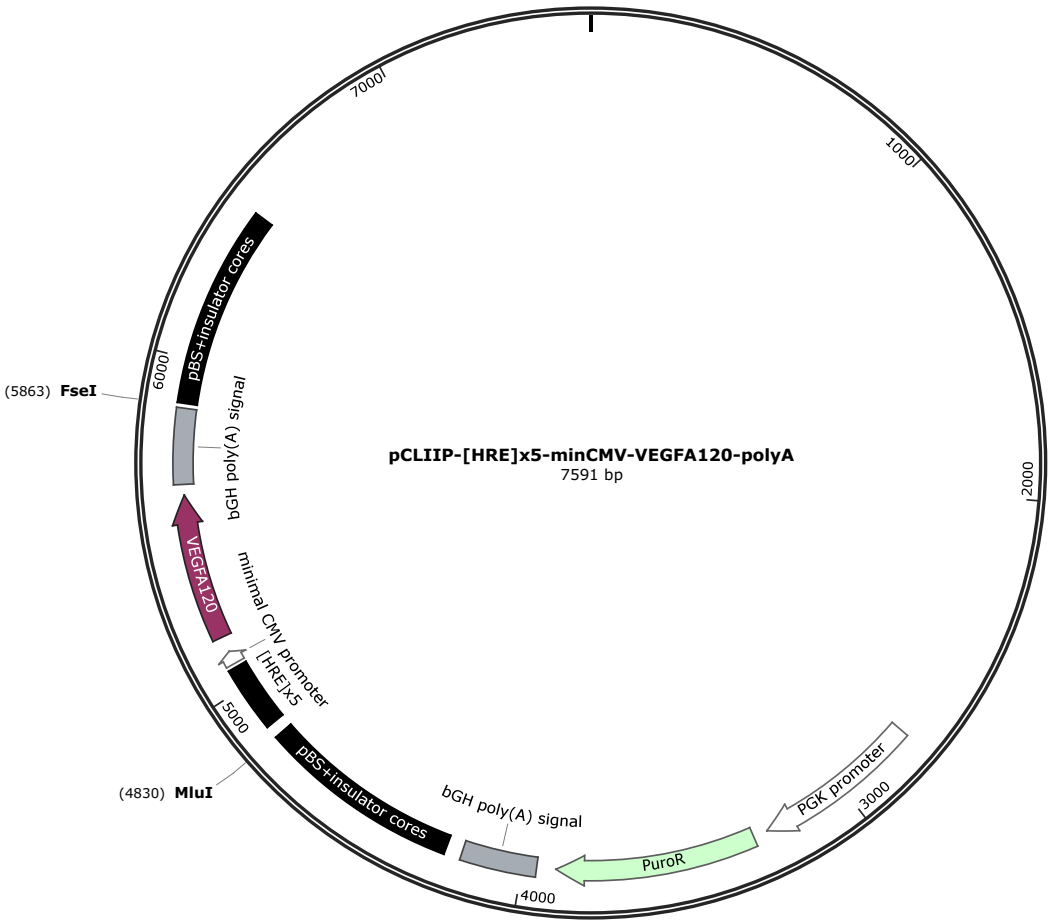

Figure 31. pCLIIP-[HRE]x5-minCMV-VEGFA120 construct.

The [HRE]x5-minCMV-VEGFA120 DNA fragment was prepared by restriction enzyme digestion and ligated into the linearised pCLIIP vector. The constructed plasmid was recovered from transformed *E.coli* cells and selected by ampicillin resistance. The final plasmid was validated by DNA sequencing.

Expression from the vectors was then tested by transient transfection of human or mouse cells with the vector encoding VEGFA120 or VEGFA121 respectively and using a species specific ELISA. Human VEGFA expression was found to be increased in ID8 mouse cells transfected with [HRE]x5-minCMV-VEGFA121 or pCLIIP-[HRE]x5-minCMV-VEGFA121 vectors, although this was not significant (Fig. 32). Additionally, mouse VEGFA expression increased in HCT116 human cells transfected with [HRE]x5-minCMV-VEGFA120 or pCLIIP-[HRE]x5-minCMV-VEGFA120 vectors (Fig. 33).

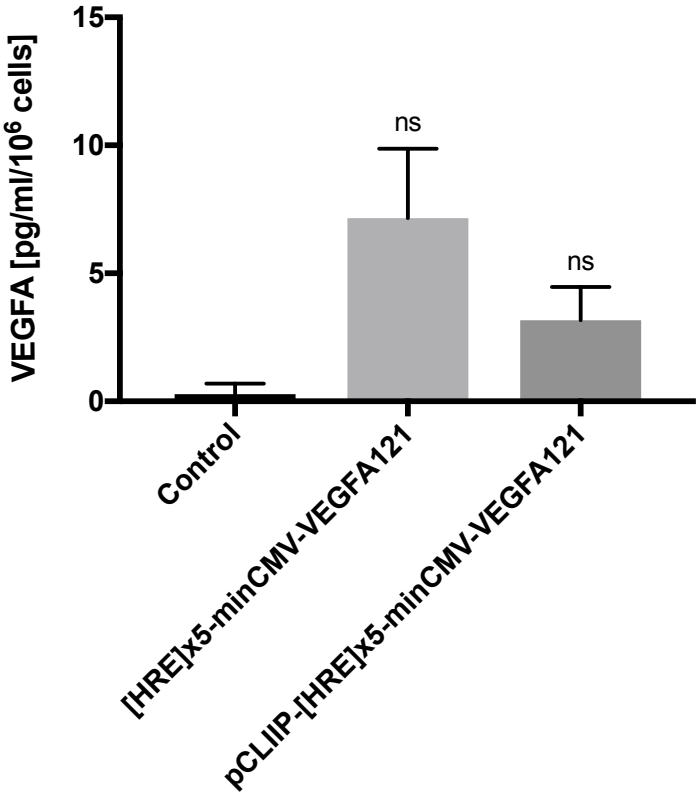

Figure 32. Human VEGFA transient expression in the ID8 mouse cell line.

ID8 cells were transiently transfected with either [HRE]x5-minCMV-VEGFA121 or pCLIIP-[HRE]x5-minCMV-VEGFA121 vectors. Cells were cultured in 6 well-plates in 1 ml of fresh medium and incubated for 24 hours in 21% O_2. Human VEGFA levels were quantified using ELISA. All data values are expressed as mean ± standard error of three independent experiments. One-way ANOVA test was performed. ns not significant

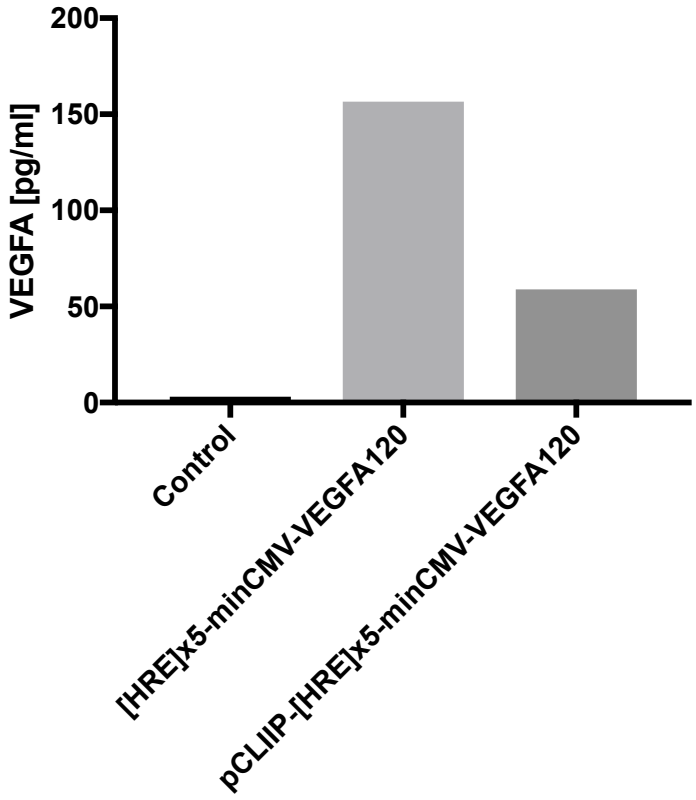

Figure 33. Mouse VEGFA transient expression in the HCT116 human cell line.

HCT116 cells were transiently transfected with either [HRE]x5-minCMV-VEGFA120 or pCLIIP-[HRE]x5-minCMV-VEGFA120 vectors. Cells were cultured in 6 well-plates in 1 ml of fresh medium and incubated for 24 hours in 21% O_2. Mouse VEGFA levels were quantified using ELISA. Data from one experiment performed by Claudia Madrigal.

4.2.3 Stable cell line development with the piggyBac transposon system

As the preliminary bioinformatics results indicated HGSOC patients with high VEGFA121 had increased expression of growth factors and cytokines that suggested a prominent role for the adaptive immune system, more emphasis was placed on developing the mouse ID8 cell line model as this can be grown in mice with a full immune system. Furthermore, isolation of single COV362 clones expressing VEGFA121 was still proving technically difficult. After transfection and puromycin selection, a mouse specific VEGFA ELISA was used to evaluate secreted VEGFA levels in the stably transfected ID8 cell lines. Firstly, the pool of puromycin selected cells showed higher levels of VEGFA when compared with the ID8 WT cells (Fig. 34). Additionally, after clonal selection, the VEGFA ELISA results showed that approximately 60 % of the clones created were secreting higher levels of VEGFA when compared with the ID8 WT cells (Fig. 35).

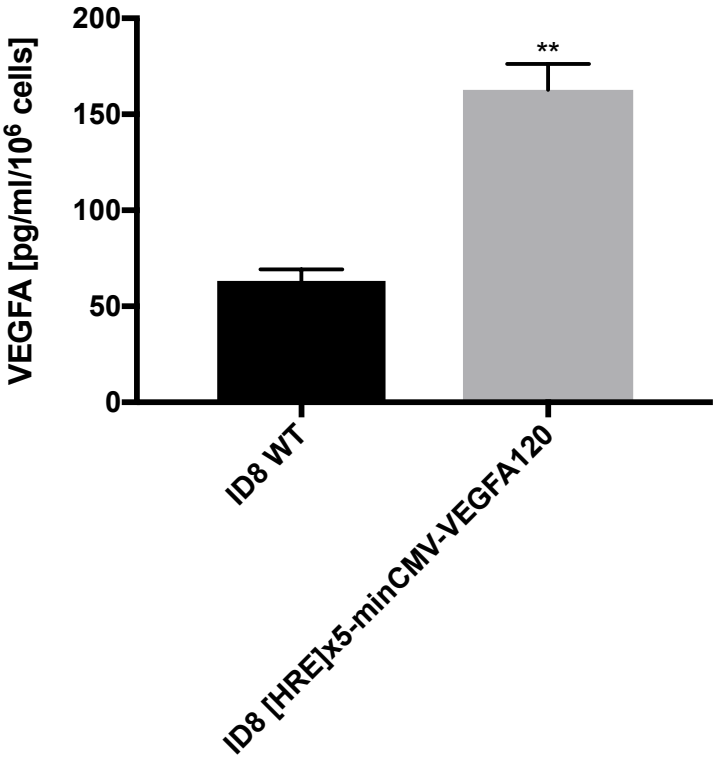

Figure 34. VEGFA expression levels in transfected ID8 cell lines.

ID8 WT and ID8 VEGFA120 cells were cultured in T25 flasks in 2 ml of fresh medium and incubated for 24 hours at 21% O_2. Mouse VEGFA levels were quantified using ELISA. All data values are expressed as mean ± standard error of three independent experiments. A t-test was performed to determine statistical significance. ** p-value < 0.01.

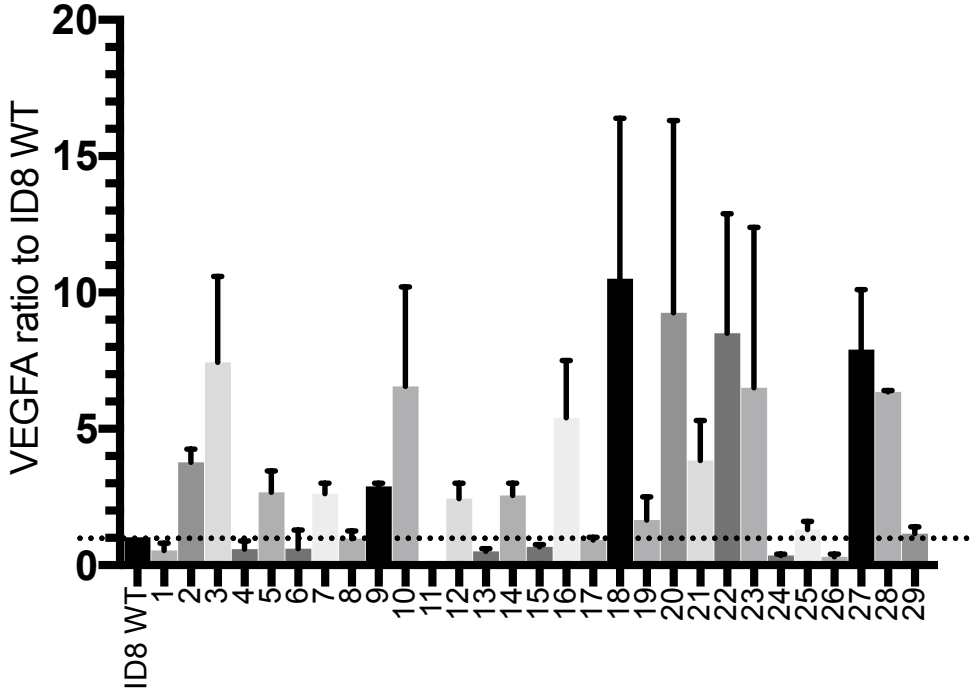

Figure 35. VEGFA expression levels in ID8 VEGFA120 clones.

ID8 WT and ID8 VEGFA120 clones were cultured in T25 flasks in 2 ml of fresh medium and incubated for 24 hours at 21% O_2. Mouse VEGFA levels were quantified using ELISA. All data values are expressed as mean ± standard error of two independent experiments.

From the transfected clones (Fig. 35), some were chosen for further study based on their VEGFA expression levels. Two different clones (120.5 and 120.14) had a 3-4 fold increase in VEGFA expression when compared to the ID8 WT cells (p-value < 0.05), while clones 120.18 and 120.20 had a 7-9 fold increase in expression when compared with the control cells (p-value < 0.0001) (Fig. 36). ID8 cells expressing luciferase were previously created within the English' lab using the pCLIIP piggyBac transposon system. These ID8 L/S cells were also used in further experiments as control for cells that had undergone puromycin selection and genomic integration of a transposable element.

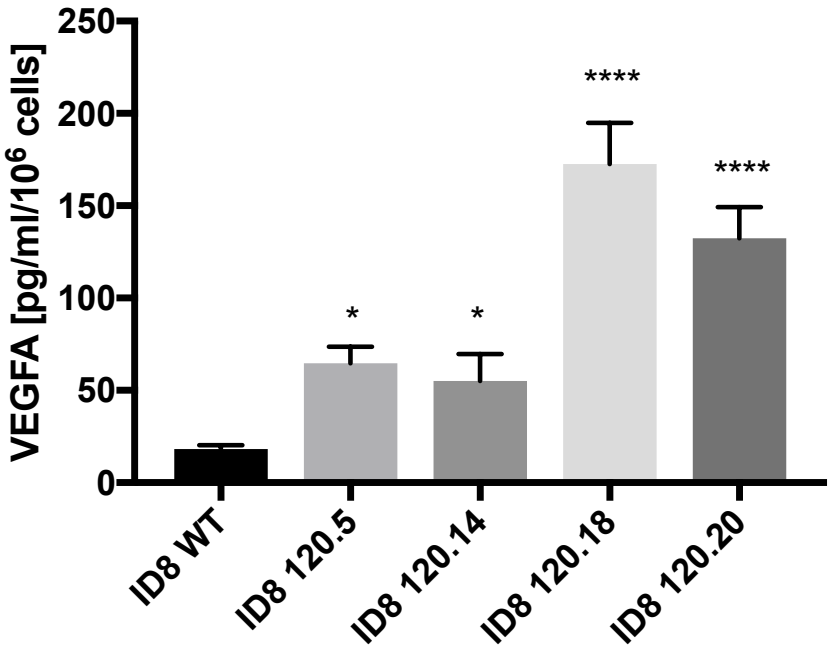

Figure 36. VEGFA expression levels in selected ID8-VEGFA120 clones.

ID8 WT and selected ID8 VEGFA120 clones were cultured in T25 flasks in 2 ml of fresh medium and incubated for 24 hours at 21% O_2. Mouse VEGFA levels were quantified using ELISA. All data values are expressed as mean ± standard error of three independent experiments. One-way ANOVA test was performed followed by multiple comparisons using the Dunnett's test. * p-value <0.05, **** p-value < 0.0001.

4.2.4 Total VEGFA protein expression in atmospheric O_2 (21%) and hypoxia (1% O_2)

To test whether the amount of secreted VEGFA is increased by hypoxia (1% O_2), as expected if the HRE is functioning correctly, VEGFA levels were measured from conditioned medium from cells incubated overnight at 1% O_2 and compared with those at normal atmospheric conditions (21% O_2). As previously described, VEGFA levels are increased in ID8 120 clones when compared with ID8 WT cells in 21% O_2. Additionally, VEGFA expression levels were higher in cells exposed to hypoxia when compared with atmospheric conditions across all the cell lines (Fig. 37). However no significant increase was observed between the VEGFA120 clones and the WT cells in 1% O_2. On the contrary, clone ID8 120.14 showed a significantly decreased VEGFA expression in hypoxic conditions (p-value < 0.01).

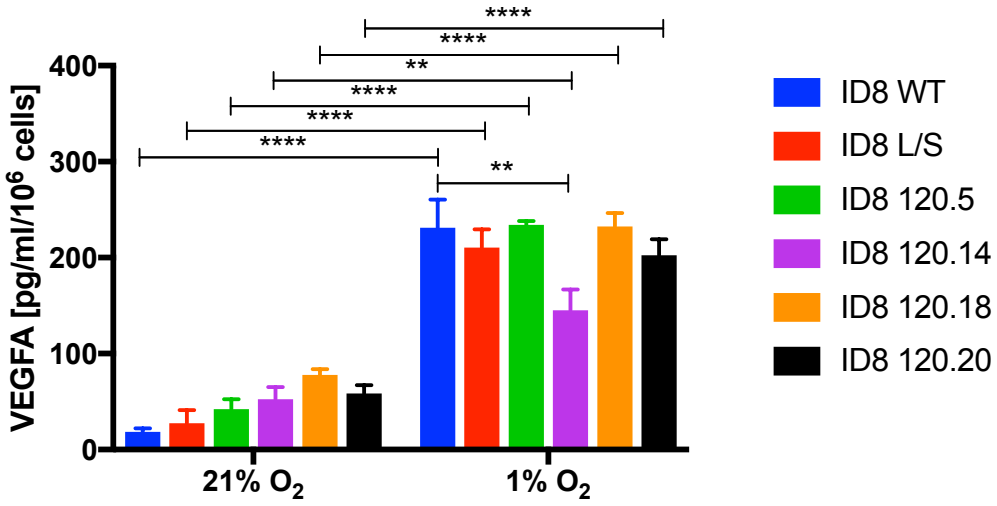

Figure 37. VEGFA expression levels in 21% and 1% O_2 in selected ID8-VEGFA120 clones.

ID8 WT and ID8 VEGFA120 clones were cultured in T25 flasks in 2 ml of fresh medium and incubated for 12 hours at 21% or 1% O_2. Mouse VEGFA levels were quantified using ELISA. All data values are expressed as mean ± standard error of two independent experiments. Two-way ANOVA test was performed followed by multiple comparisons using the Dunnett's test. * p-value <0.05, ** p-value < 0.01, **** p value < 0.0001.

4.2.5 VEGFA isoform mRNA expression by AQRT-PCR

As the ELISA measures total VEGFA expression rather than the levels of each individual isoform, an AQRT-PCR assay was designed to measure mouse VEGFA mRNA isoform expression. Firstly, exon-exon junction primer specificity was validated for each target by sequencing the resulting cDNA products from each isoform primer pair after reverse transcription. For the mouse probes, RNA samples from ID8 WT cells were used (Fig. S9-S11). Secondly, linearity range was evaluated by the construction of a standard curve for each isoform using different concentrations from the linear plasmids. The efficiency of the AQRT-PCR was determined as follows: ~ 97% for VEGFA120, ~ 94% for VEGFA164 and ~ 93% for VEGFA188. Standard curves using linearised plasmid were included in each assay making sure that the coefficient of determination (R^2) was above 0.99 (Fig. S12). Thirdly, AQRT-PCR specificity was evaluated using a melt curve analysis in order to validate that a single PCR product was detected within each analysed sample (Fig. S13-S15).

In order to determine the individual VEGFA isoform expression in each cell line, AQRT-PCR was used. RNA samples from each cell line were extracted and VEGFA isoforms were compared between ID8 clones when incubated at 21% and 1% O_2. At 21% O_2, clones ID8 120.5 and 120.18 showed a significant increase in VEGFA120 expression when compared with the ID8 WT cells. No significant differences were observed in the expression of VEGFA164 and VEGFA188 (Fig. 38A). Although no significant difference is observed for VEGFA164, there is a small increase of this isoform in clone ID8 120.18 in both 21% and 1% O2 conditions when compared to the WT cells.

At 1% O_2, clone ID8 120.5 showed a significant increase in VEGFA120 when compared with the ID8 WT cells. No significant differences were observed in the expression of VEGFA164 and VEGFA188 (Fig. 38B). These results indicate that clone ID8 120.5 is expressing the highest levels of VEGFA120 across all the created clones and the ID8 WT cells in both atmospheric and hypoxic conditions. An additional analysis was performed to quantify VEGFA isoforms in ID8 WT cells at 21% and 1% O_2 (Fig. 39). All three isoforms showed an increased expression in hypoxia when compared to 21% O_2, however a significant difference was observed only for VEGFA120, suggesting the hypoxic response element in the vector is functioning.

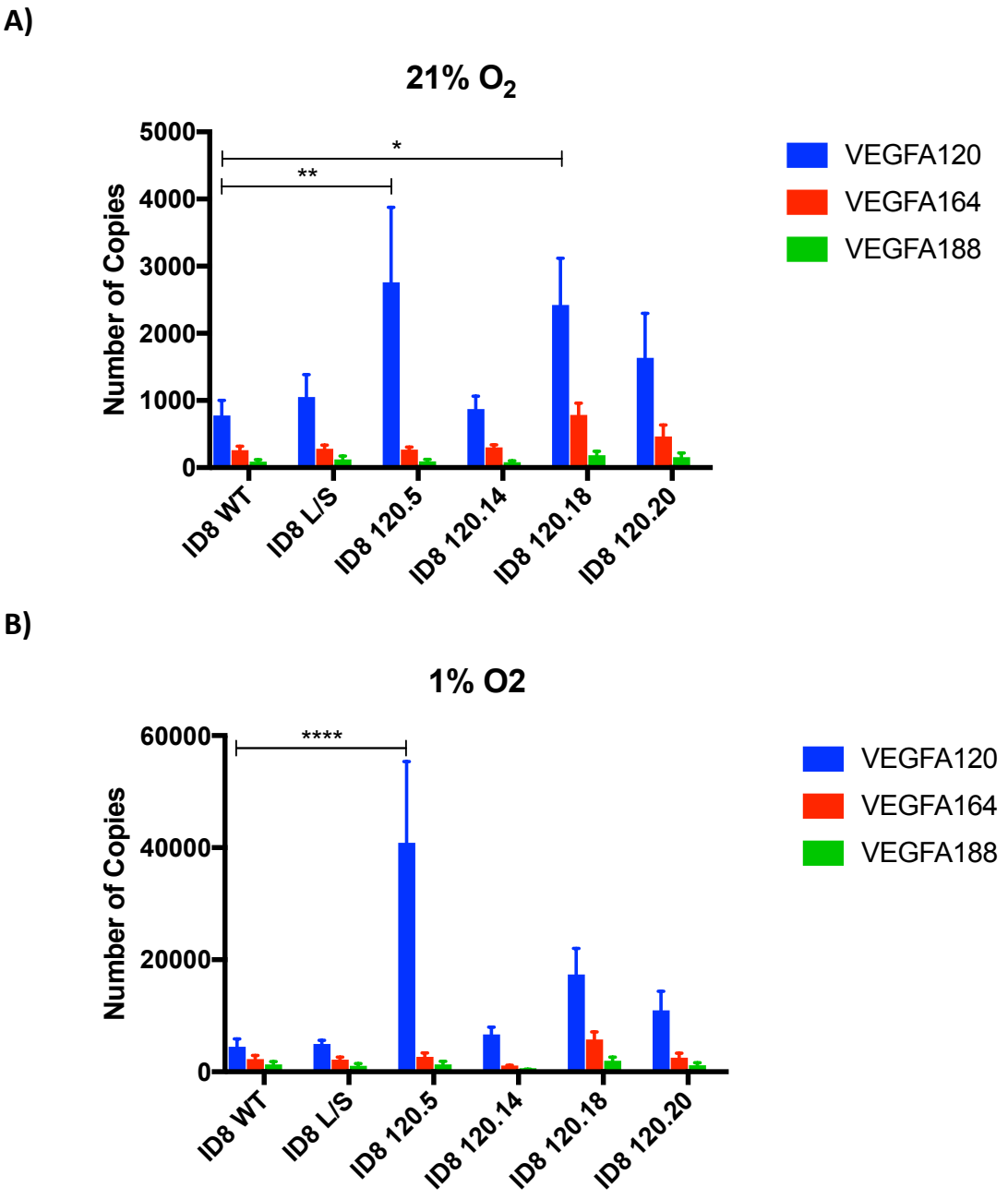

Figure 38. VEGFA isoform expression levels in 21% and 1% O_2.

VEGFA120, VEGFA164, VEGFA188 and total VEGFA expression was quantified by AQRT-PCR for each ID8 cell lines at **A)** 21% and **B)** 1% O_2. Number of copies per isoform was normalised to the mRNA levels of GAPDH gene. All data values are expressed as mean ± standard error of three independent experiments. Two-way ANOVA test was performed followed by multiple comparisons using the Dunnett's test. *$p < 0.05$, **$p < 0.01$, ****$p < 0.0001$

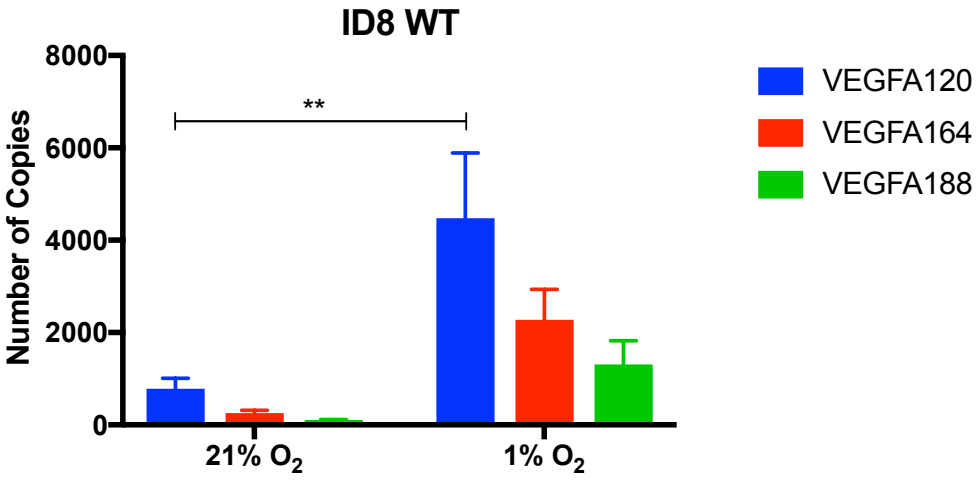

Figure 39. VEGFA isoform expression for ID8 WT cells in 21% and 1% O_2.

VEGFA120, VEGFA164 and VEGFA188 expression was quantified by AQRT-PCR for ID8 WT cells at 21% and 1% O_2. Number of copies per isoform was normalised to the mRNA levels of GAPDH gene. All data values are expressed as mean ± standard error of three independent experiments. Two-way ANOVA test was performed followed by multiple comparisons using the Sidak's test. ** $p < 0.01$.

4.3 Functional characterisation of ID8 cells overexpressing VEGFA120

4.3.1 ID8 120 cell proliferation *in vitro*

In order to characterise the effects of increased VEGFA120 expression in the clones selected different functional assays were used. Cell proliferation was evaluated by using the MTT assay and trypan blue staining. Overexpression of VEGFA120 in ID8 cells resulted in a variable effect on proliferation. ID8 WT cells and most of the clones showed a similar growth pattern, however proliferation of clone 120.5 and 120.20 was reduced at 72 hours in both MTT assay (Fig. 40) and trypan blue staining (Fig. 41). No significant differences were observed between the clones and the WT cells at 24 or 48 hours.

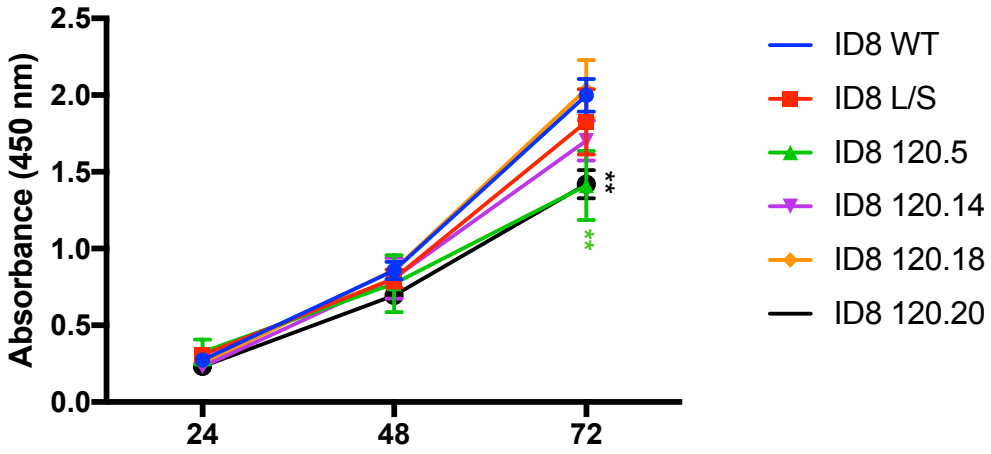

Figure 40. ID8 cell proliferation by MTT assay.

Cell survival was assessed by MTT assay at 24, 48 and 72 hours at 21% O_2. All data values are expressed as mean ± standard error of three independent experiments. Two-way ANOVA test was performed followed by a multiple comparisons using Dunnett's test. **$p < 0.01$

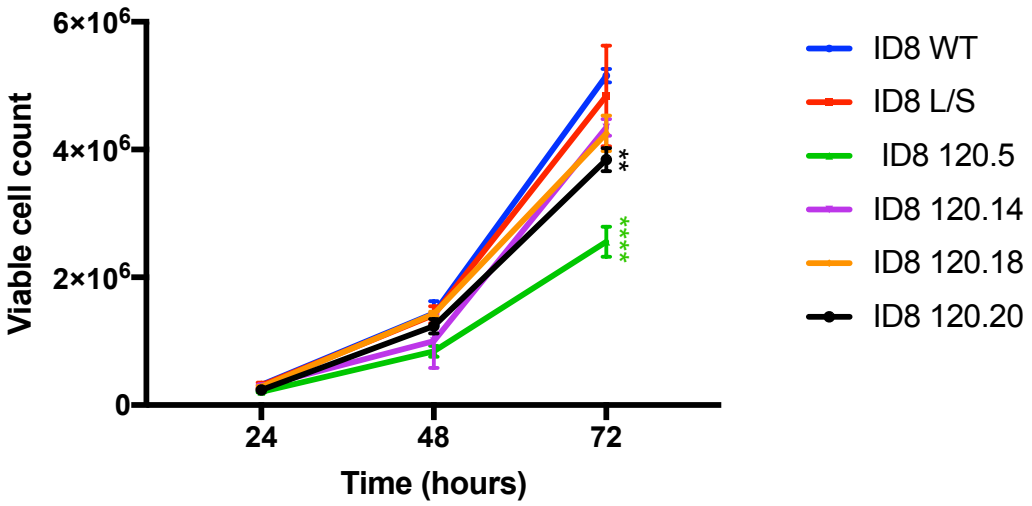

Figure 41. ID8 cell proliferation by Trypan blue assay.

Cell survival was assessed by trypan blue assay at 24, 48 and 72 hours at 21% O_2. All data values are expressed as mean ± standard error of three independent experiments. Two-way ANOVA test was performed followed by a multiple comparisons using Dunnett's test. **p < 0.01, **** p<0.0001

4.3.2 The ability of the ID8 120 cells to migrate and invade *in vitro*

As changes in VEGFA isoform expression have also been shown to influence cell migration (Kanthou et al., 2014), we also examined the role of VEGFA120 overexpression on cell migration. ID8 WT and LS cells had a faster migration rate when compared to the ID8 120 clones using a wound healing assay (Fig. 42). More specifically, clones ID8 120.5 and 120.20 showed significantly decreased migration at 6 hours.

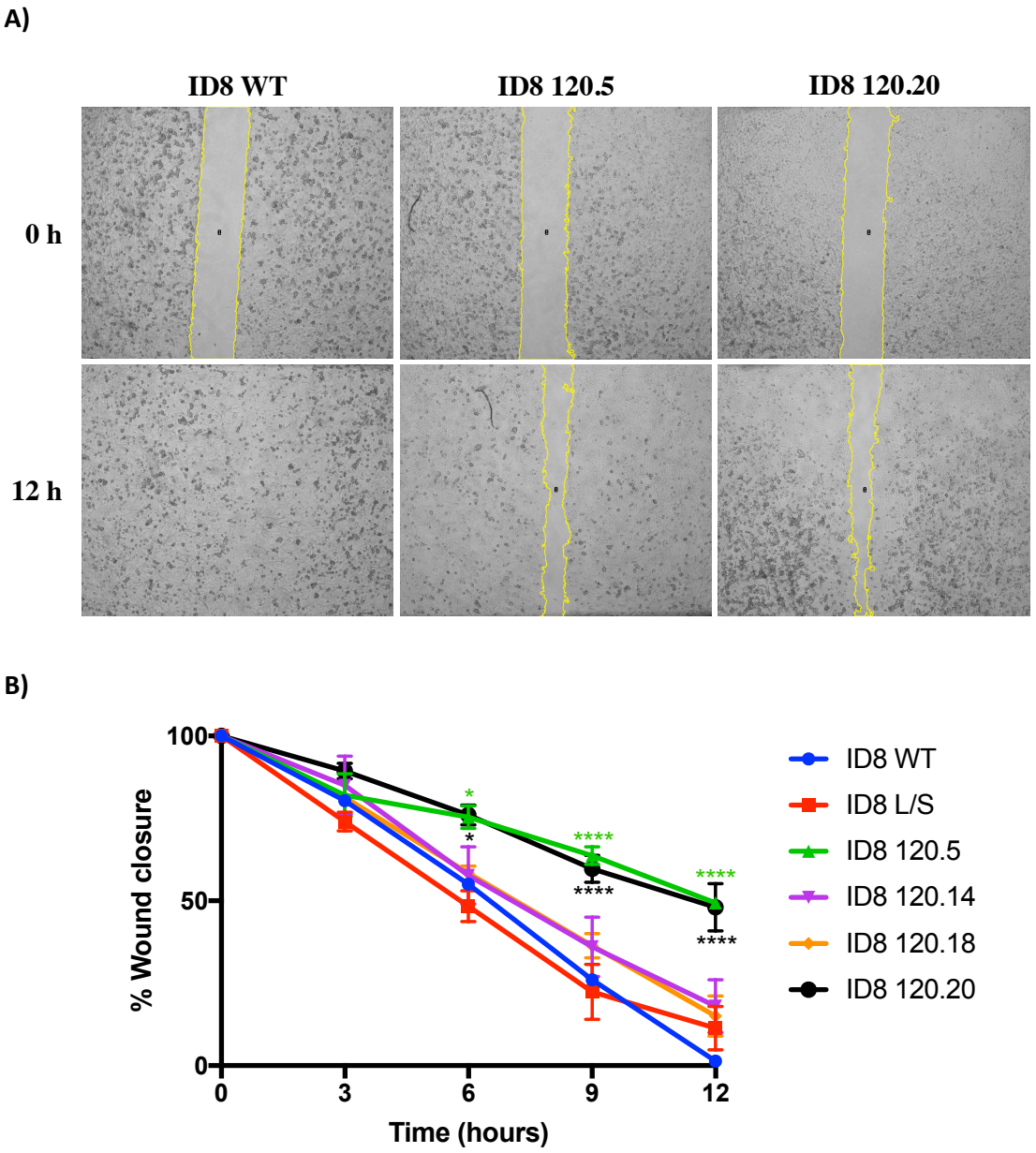

Figure 42. Wound healing assay with ID8 cells expressing VEGFA120.

A) Example images. Cells were scratched and imaged every 3 hours for a total of 12 hours at 21% O_2. **B)** Wound closure was quantified using MRI Wound Healing tool of ImageJ. All data values are expressed as mean ± standard error of three independent experiments. Two-way ANOVA test was performed followed by multiple comparisons using the Dunnett's test. * $p < 0.05$, **** $p < 0.0001$

4.3.3 Expression of epithelial-mesenchymal transition markers

EMT has been described as an important process in the progression of HGSOC, metastasis and resistance to chemotherapy (Loret et al., 2019). EMT has an impact in cell morphology and cell migratory capacity. During this process, morphological changes are accompanied by changes in the expression of important cell adhesion components. For example, the loss of cell adhesion molecules such as E-cadherin, Epcam and claudins is commonly observed when epithelial cells with limited migratory capacity lose their polygonal structure and cell-cell adhesion. Simultaneously, these cells acquire a mesenchymal phenotype showing a spindle shape and increased migratory capacity. When the cells assume this mesenchymal phenotype, an increase in mesenchymal protein expression such as vimentin, fibronectin and N-cadherin is observed (Loret et al., 2019).

Cell morphology changes were observed between our selected ID8 120 clones and ID8 WT cells that suggested EMT might have occurred (Fig. 43). When compared with the ID8 WT cells, it is possible to observe that ID8 120.5 and ID8 120.14 cells showed a more epithelial-like morphology, while ID8 120.18 and ID8 120.20 display a more mesenchymal-like phenotype. The expression of EMT markers was analysed in order to investigate these morphological observations and explore if changes in the expression of cell adhesion components followed the common characteristics described during an EMT process. The protein expression of β-catenin, E-cadherin, N-cadherin and vimentin was detected by western blot analysis (Fig. 44 and S16). This analysis demonstrated that ID8 WT cells expressed both epithelial and mesenchymal markers. The protein expression of β-catenin, E-cadherin and N-cadherin in ID8 120 clones was predominantly reduced when compared with the ID8 WT cells (Fig. 45). A change in vimentin expression was not observed between clones ID8 120.14 and 120.20 and the ID8 WT cells, however a slight increase in expression of this marker was observed in clones ID8 120.5 and ID8 120.18 (Fig. 45D). These observations indicate that changes in these EMT markers do not follow the typical EMT characteristics expected for the observed morphologies and migration capacity of these cells, however it might be possible that an intermediate or partial EMT is occurring as features of both epithelial and mesenchymal cells are present within the cells. It is not possible at this stage to conclude if the overexpression of VEGFA120 or changes in the other isoforms play a role in these observations and it is important to include the effect of hypoxia, endogenous VEGFA isoforms and their inhibitions in further experiments.

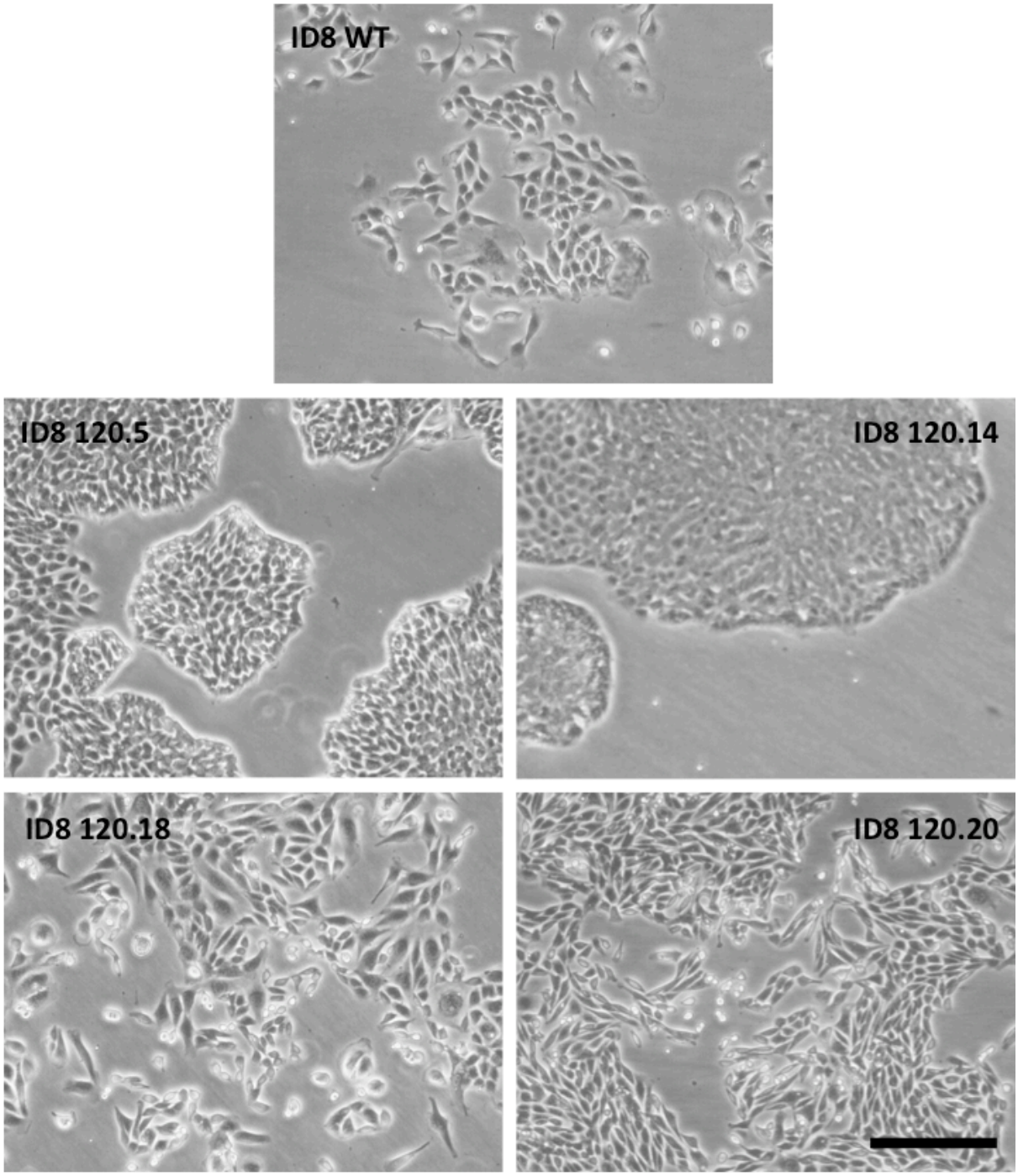

Figure 43. Cell morphology of ID8 WT and ID8 120 cells.

Phase contrast images of ID8 WT cells and ID8 120 clones at 37 °C, 21% O_2 and 5% CO_2 cell culture conditions. Microscopy was performed using the Nikon Eclipse TS100 system. Scale bar = 50 μm.

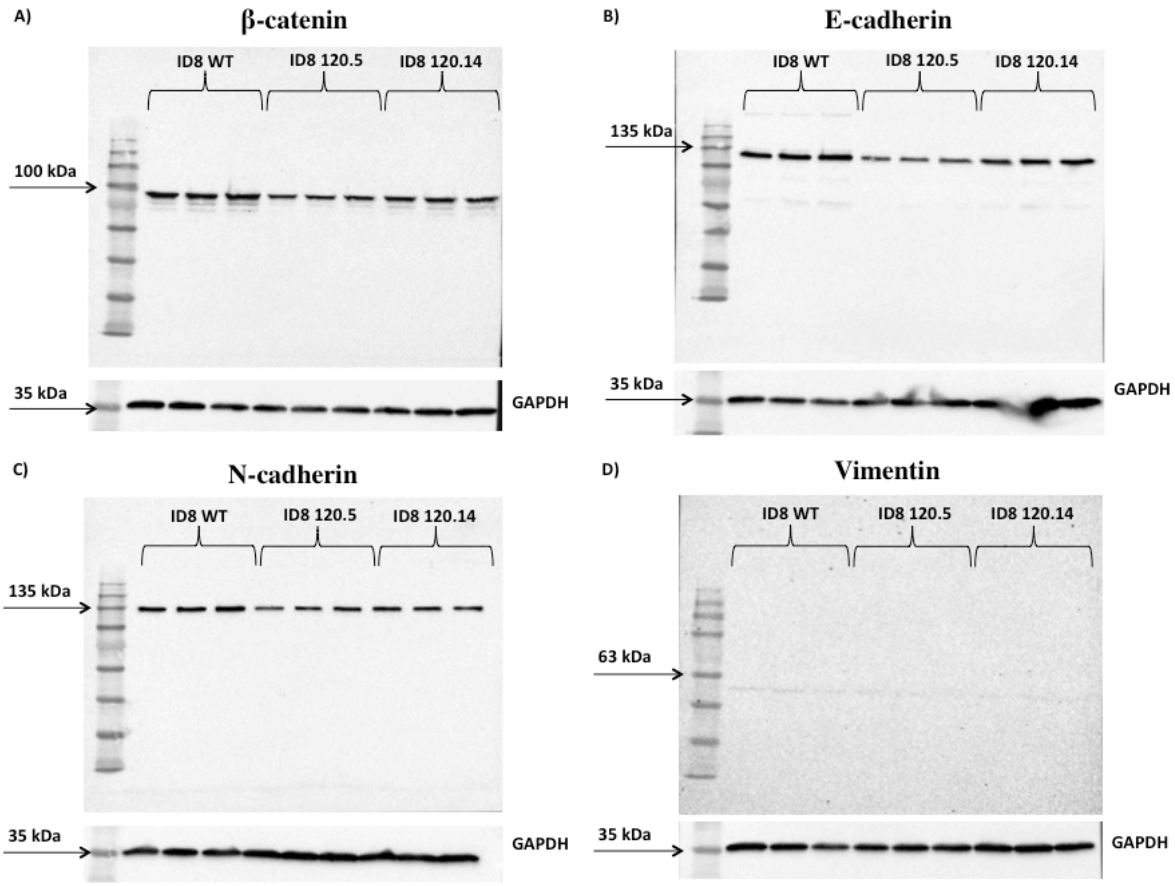

Figure 44. Western blot analysis of EMT markers in ID8 cells.

Example of Western blot images of **A)** β-catenin, **B)** E-cadherin, **C)** N-cadherin and **D)** Vimentin across ID8 WT and ID8 120 clones. GAPDH was used as a loading control. Western blots show that ID8 WT cells predominantly expressed β-catenin, E-cadherin, N-cadherin while a decrease in the expression of these proteins is observed in ID8 120.5 and 120.14 clones. No changes are observed for the expression vimentin between the different ID8 cells.

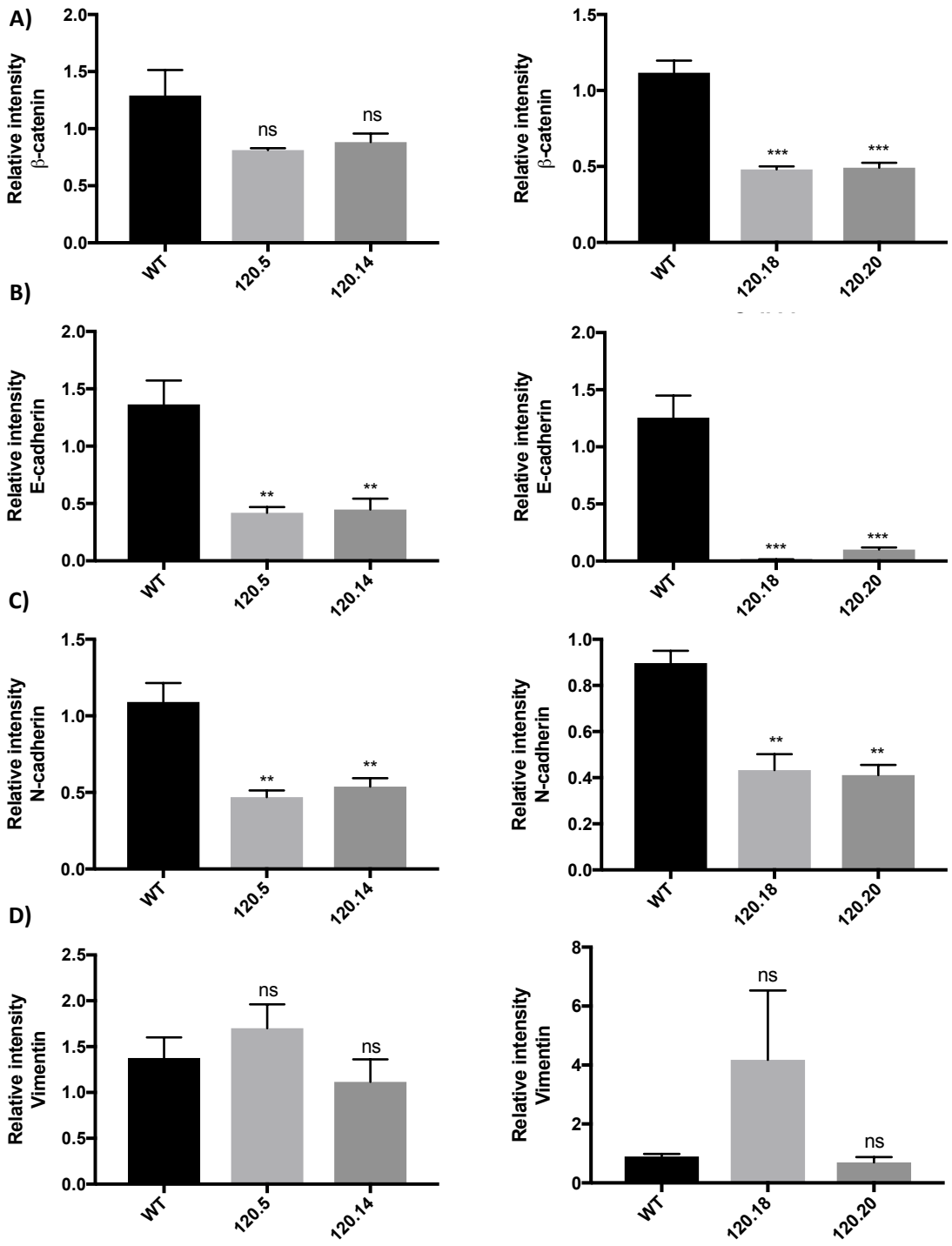

Figure 45. Western blot analysis of EMT markers in ID8 cells.

Relative intensity of **A)** β-catenin, **B)** E-cadherin, **C)** N-cadherin and **D)** Vimentin across ID8 WT and ID8 120 clones. All data values are expressed as mean ± standard error of three independent experiments. One-way ANOVA test was performed followed by multiple comparisons using the Dunnett's test. ns not significant, **p < 0.01, *** p<0.001.

4.3.4 The role of VEGFA120 expression in response to carboplatin

As EMT has been linked to chemoresistance in ovarian cancer, the sensitivity of our cell expressing increased VEGFA120 to carboplatin was investigated. MTT assays were used to measure cell viability and establish the best drug concentrations for further experiments. As time was limited, clone ID8 120.5 was selected for drug response experiments, as based on the AQRT-PCR assay it expressed the highest levels of VEGFA120 across the different cell lines with no significant change in expression of the other isoforms. The LD50 for carboplatin in ID8 WT and ID8 120.5 cells was 566.7 μM and 523.8 μM, respectively (Fig. 46). No significant difference was found for the cytotoxic activity of carboplatin between these cell lines (p-value > 0.05).

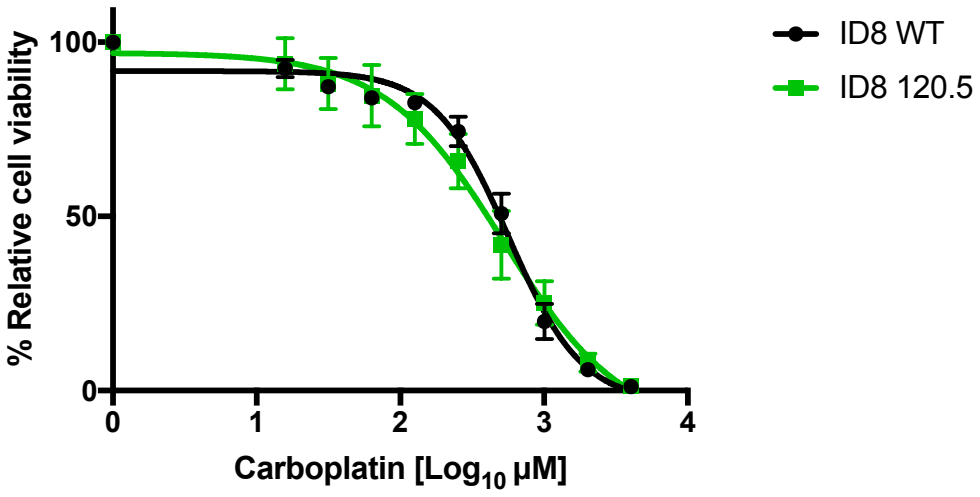

Figure 46. Response of ID8 WT and ID8 VEGFA120.5 cells to Carboplatin.

ID8 WT and ID8 120.5 cells were treated with carboplatin (0-4000 μM) for 48 hours at 21% O_2 and cell viability was measured using the MTT assay with absorbance read at 560 nm. Absorbance readings were normalised to non-treated samples. All data values are expressed as mean ± standard errors of three independent experiments.

4.4 Summary

Data obtained in this thesis chapter indicates that ZFN technology proved to be a challenging strategy for overexpression of VEGFA121 in human ovarian cancer cells mostly due to low gene editing efficiency and possibly high error rate. Due to time constraints and laboratory lock down due to the COVID pandemic, it was not possible to sequence the clones with inserted DNA to establish why no increased expression in VEGFA could be detected. However, as one clone expressed no VEGFA and was essentially a knockout line, it is possible the insertion led to frame shift errors. Additionally, COV362 cells showed a poor ability to grow at low density or as single cells for clone isolation, in addition to their low transfection efficiency using electroporation. It is possible other recently identified HGSOC cell lines may not have these characteristics making clonal growth studies from single cells conceivable in the future. On the other hand, the system using the [HRE]x5-minCMV element constructed as a promoter for VEGFA altogether with the pCLIIP transposon system proved to be a suitable tool for overexpressing VEGFA isoforms in human and mouse cells, although only the mouse system was evaluated further in this thesis. The development of an AQRT-PCR assay as a detection method to characterise isoform expression in mouse cell lines showed good efficiency and reproducibility. However, further optimisation is required in order to evaluate an AQRT-PCR assay for human samples. Initial studies have shown this performs well with isolated cell lines. Studies using sections from frozen and FFPE blocked from the same xenograft tumour also showed good correlation (Magon, 2018). However initial studies using mRNA from human FFPE tissue clinical samples indicate it needs further optimisation as RNA fragmentation was high and amplicons may need to be reduced to compensate.

Mouse ID8 ovarian cancer cell lines were developed overexpressing VEGFA120. Initial clone selection was made based on total VEGFA expression measured by ELISA. Two different clones were selected as representative for 3-4 fold expression (120.5 and 120.14) and a further two clones for 7-9 fold expression (120.18 and 120.20) when compared to the ID8 WT cells. However, total VEGFA expression across the different clones proved to be similar when measured in 1% O_2. Subsequent VEGFA isoform quantification using AQRT-PCR showed different levels of VEGFA120 across the clones, however VEGFA120 expression was higher in clone 120.5 and also increased in 1% O_2 when compared to the ID8 WT cells.

In vitro characterisation was performed to study proliferation and migration ability across the created cell lines. No effect on proliferation or migration was observed between ID8 WT cells and clones ID8 120.14 or 120.18, however a significant decrease in these processes was observed for clones ID8 120.5 and 120.20. These observations were not consistent with the expression levels of VEGFA120 in the cells. Also, morphology changes were observed between the cells lines and the VEGFA120 cell lines showed a decreased expression of EMT markers such as β-catenin, E-cadherin and N-cadherin, however these are not consistent with the VEGFA120 levels expressed within the cell lines. Further investigations are required to validate if these changes are due to VEGFA120 expression or as a result of clonal selection. This is particularly important as our results showed some clones had alterations in the expression of VEGFA164, demonstrating the importance of careful characterisation of expression of all VEGFA isoforms when generating cell lines designed only to have an increase in a single isoform. As inhibition of VEGFA or VEGFRs will not be isoform specific, alternative methods would need to be generated to validate that the effects are from overexpression of the VEGFA isoform of interest. This could be through the use of an inducible promoter e.g. Tet-on system, or through the use of isoform specific RNAi.

The clone ID8 120.5 was selected to continue with treatment response experiments as this cell line showed the highest VEGFA120 expression levels without changes in the other isoforms. Carboplatin kill curves showed no difference in treatment response between ID8 WT and ID8 120.5 cells. Unfortunately, due to COVID-19 pandemic leading to cessation of lab work, experiments to evaluate its response to anti-VEGFA therapy and carboplatin combination therapy were interrupted, in addition to signalling studies looking at alterations VEGFA-VEGFR signalling that might regulate changes in proliferation and EMT markers. Future studies will need to address this.

It is important to discuss that the methodology used in this work to overexpress VEGFA120 in mouse cells by transfection of a Piggy Bac transposon system had an impact on the expression of the other VEGFA isoforms, which consequently can have an effect in the interpretation of the experimental results. One of the limitations of this work is the lack of *in vitro* strategies for the inhibition of specific isoforms that would help to uncover the function of endogenous and modified variants, although VEGFA inhibitors such as B20 can be used in *in vitro* studies, this inhibition would be targeting all VEGFA species. Additional controls used to study the effect of proteins *in vitro* include the addition of exogenous components.

The addition of VEGFA120 can be used in future work in order to study the effect that this specific isoform has on cell proliferation, migration, treatment response and cell signalling.

Finally, previous works have described that ID8 cells express VEGFR1 and 2 and co-receptors such as NRP1 (Zhang, L. et al., 2003; Russell, 2015). Although the time within this project did not allow the characterisation of these receptors in the created cell lines, it is possible that changes in isoform expression can have an impact on VEGFRs and therefore modulate VEGFA-VEGFR signalling. It has been described that protein expression of VEGFR2 can be modulated by treatment with VEGFA165 in endothelial cells while no effect is observed with addition of VEGFA121 (Fearnley, G.W. et al., 2014). Future work should characterise VEGF receptors in ovarian cancer cells and evaluate if VEGFA isoform changes can modulate their expression and activation and consequently their biological function.

Chapter 5

5. The role of VEGFA120 expression in response to B20 in pre-clinical models of ovarian cancer

Pre-clinical models provide a valuable tool for the study of cancer biology and response to treatments. Different pre-clinical models have been widely studied with the objective of finding appropriate *in vivo* representations of the biology of human HGSOC and response to therapy. One vital pre-clinical approach is to characterise the growth and characteristics of ovarian cancer cell lines in mouse models to allow the translation of *in vitro* research to an *in vivo* mammalian model and ultimately into the clinic. However, it has been challenging to fully replicate the histopathological, molecular and genomic characteristics of human HGSOC in mouse models. An additional complexity is added to this challenge when considering the impact that the tumour microenvironment has on the progression of this disease and its poor representation in immune compromised models.

In order to study the role of VEGFA120 in ovarian cancer and response to anti-VEGFA therapy, a metastatic model was created using ID8 cells overexpressing VEGFA120 in immune competent mice. Subcutaneous and intraperitoneal syngeneic models were established to characterise the *in vivo* growth of different ID8 clones expressing VEGFA120 and subsequently response to anti-VEGFA therapy.

5.1 Introduction

Much work is being undertaken with the aim of creating mouse ovarian cancer models that better represent the biology of human HGSOC. There have been advances in the use of xenograft models that involve the inoculation of human ovarian cancer cell lines into immunodeficient mice through subcutaneous, intraperitoneal or orthotopic implantation (Lisio et al., 2019). Firstly, subcutaneous implantation is a practical tool to study tumour formation and drug response, however the anatomic site lacks appropriate microenvironment interactions that only partially represent human ovarian cancer (Arauchi et al., 2015). Secondly, intraperitoneal implantation is a suitable model for the study of advanced ovarian cancer that represents the metastatic spread of this disease through the peritoneum (Lisio et al., 2019). Thirdly, orthotopic implantation better replicates the early phase of cancer development and metastatic spread from the specific tissue of origin, however this requires more complex techniques to establish tumours within the ovaries or fallopian tubes in mouse models (Arauchi et al., 2015).

Unfortunately, most of the cell lines commonly used in xenograft models such as IGROV1 and SKOV3 poorly represent the genetic and molecular level of HGSOC (Domcke et al., 2013). Recently, more effort has been placed in trying to characterise *in vivo* growth of human cell lines that better represent the fundamental biology of HGSOC. Such an example is the cell line COV362, however these cell lines grow poorly as subcutaneous tumours and do not form intraperitoneal tumours in athymic (nude) mice (Mitra, A.K. et al., 2015). This is consistent with my preliminary data showing that COV362 cells grow poorly in severe immunocompromised mice such SCID and NSG. My results showed that COV362 cells occasionally formed intraperitoneal and subcutaneous tumours in NSG mice, however this showed poor reproducibility in larger experiments and intraperitoneal tumours remained very small (< 1 mm) (Fig. S17). Attempts to increase subcutaneous tumour formation from these cells in NSG mice were performed by increasing cell number and using a matrigel matrix, however no evidence of increased tumour formation was observed.

Genetically engineered mouse models have allowed researchers to replicate some of the genetic events that initially occur in the development of ovarian cancer. However most of these approaches have been mainly focused on the development of tumours from the ovarian surface epithelium, rather than the fallopian tubes, which have recently been defined as the site of origin for HGSOC (Lee, Y. et al., 2007). Tumours from these models do not therefore

match the characteristics of human disease histologically (Lisio et al., 2019). Recent attempts to address this issue have led to the creation of new genetically engineered mouse models that develop HGSOC from the fallopian tubes and better represent the histology and molecular features of human HGSOC, and offer the potential opportunity to understand early stages of HGSOC development (Walton, J.B. et al., 2017; Maniati et al., 2020; Kim et al., 2020).

Patient Derived Xenografts (PDXs) have also been used to implant human cells or tumour fragments from patients with HGSOC into immunodeficient mouse models. Orthotopic implantation of HGSOC PDXs in NSG mice has shown high efficiency of tumour implantation, close resemblance to the histological and molecular mechanisms of the human disease including progression from initial ovarian cancer development to metastatic spread into the peritoneum (George et al., 2017). However it has also been reported that there is still a high variation in the efficiency of tumour engrafting after transplantation depending on the tumour characteristics and specific mouse strain, with tumours taking up to six months to establish and grow after initial implantation (Tudrej et al., 2019).

The impact that the immune landscape plays in the tumour microenvironment of HGSOC is not fully reflected in these previous models. Syngeneic models use immunocompetent mice that are implanted with ovarian cancer cells derived from the same host. These models allow the study of tumour development and metastasis with the presence of the immune system (Tudrej et al., 2019). One example of this model includes ID8 cells, which were spontaneously transformed from normal ovarian surface epithelium from C57BL/6 mice. Briefly, ovarian epithelial cells were isolated from ovaries of female mice and cultured *in vitro* for more than 20 passages. However the genetic events driving this transformation are not well understood (Roby et al., 2000). The main disadvantages of this model is the lack of key genetic mutations that characterise HGSOC such as *TP53* and *BRCA*, however recent studies using genetic engineering have created new ID8 models with deletion of these genes (Walton, J. et al., 2016). Due to the early results shown in the bioinformatics analysis in this thesis, ID8 syngeneic models were used with the aim of studying the effect of VEGFA120 in immune interactions and anti-VEGFA treatment response.

Some of the previously described models have been used to study VEGFA isoforms or anti-angiogenic therapy. Intraperitoneal xenograft models with A2780 and Caov-3 cells have been previously used to study the effects of anti-VEGFA treatment in combination with cisplatin in ovarian cancer. Results showed that these treatments inhibit tumour growth and ascites

development while prolonging survival when used as a maintenance treatment (Mabuchi et al., 2008). Additionally, subcutaneous xenograft models using OVCAR-3 cells have evaluated the role of VEGFA165 in angiogenesis and macrophage infiltration in human ovarian cancer (Duyndam et al., 2002). In syngeneic models it has been reported that overexpression of VEGFA164 in ID8 cells increased tumour growth, ascites formation and angiogenesis in C57BL/6 mice (Zhang, L. et al., 2002b). Similar models using ID8 cells overexpressing VEGFA and Defb29 have been used to study the role of immune cells in antitumor immunity and immunotherapy response (Hartl et al., 2019).

In order to study the effect of anti-VEGFA therapy in pre-clinical models, Genentech created an anti-VEGFA antibody (B20-4.1.1) with similar binding affinity to the humanized version used clinically, bevacizumab (Avastin™), that can only bind human VEGFA. (Liang et al., 2006). This antibody was developed using the VEGFA antigen from human and murine species and synthetic antibody libraries. Subsequently, antibody affinity was determined using ELISAs and surface plasmon resonance assays and the interactions between antibody and VEGFA characterised by crystallography. Finally, initial *in vitro* VEGFA inhibition was characterised using HUVEC cells, while *in vivo* characterisation was performed in xenograft models using human colorectal, pancreatic and sarcoma cells in nude mice (Liang et al., 2006).

5.2 Characterisation of subcutaneous tumour growth of ID8 cells expressing VEGFA120

With the objective of evaluating the role of VEGFA120 in tumour progression and to assess suitable models for further study of anti-VEGFA treatment response, we attempted to establish subcutaneous tumours using ID8 WT and ID8 120 clones described in Chapter 4. It has previously been reported that ID8 WT cells can form small subcutaneous tumours in C57BL/6 mice (Hernandez et al., 2016; Janat-Amsbury et al., 2006b). However it has also been described that VEGFA164 overexpression in ID8 cells can increase subcutaneous tumour growth when compared to ID8 parental cells. (Janat-Amsbury et al., 2006a; Janat-Amsbury et al., 2006b; Zhang, L. et al., 2002b). ID8 WT and ID8 120 cells were inoculated subcutaneously in C57BL/6J mice for an initial pilot experiment and tumour volume was monitored. After one week from injection, ID8 WT cells showed slightly larger tumours than the rest of the ID8 120 cell lines, however after 30 days slower tumour growth was observed, resulting in extremely small tumours and no difference in tumour volume across the different cell lines was seen (Fig. 47).

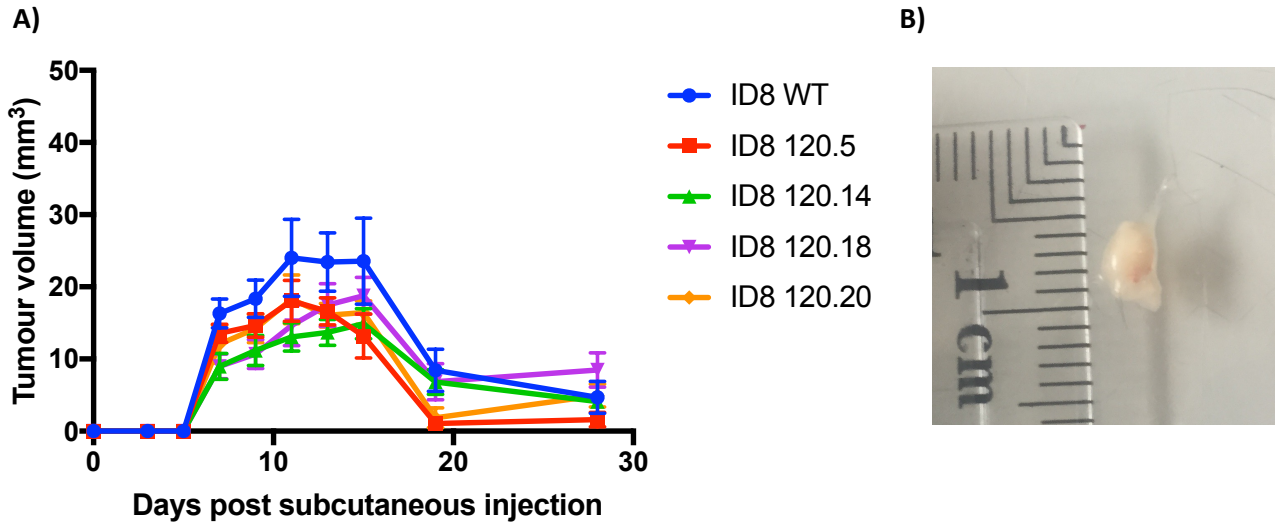

Figure 47. Tumour volumes of mice inoculated subcutaneously with ID8 cell lines expressing VEGFA120.

A) Six C57BL/6J mice per group were inoculated with 5 x 10^6 cells and tumour size was measured twice per week with calipers. Each line represents the tumour growth per group. All data values are expressed as mean ± standard error. **B)** Example image of an ID8 WT subcutaneous tumour on day 28.

5.3 Characterisation of intraperitoneal tumour growth as a model of metastatic ovarian cancer using ID8 cells expressing VEGFA120

A metastatic model in immune competent mice was created in order to study the role of VEGFA120 in tumour progression. ID8 WT and ID8 120 cells were transplanted intraperitoneally into C57BL/6J mice and monitored weekly by weight measurement or ultrasound. While bioluminescence imaging is traditionally used as a tool to monitor tumour growth in different *in vivo* cancer models, it has been reported that in advanced ovarian cancer models the development of ascites restrict bioluminescence signal due to a higher dilution of luciferin within the peritoneal fluid and therefore do not provide an appropriate quantification of tumour load (Baert et al., 2015). It was therefore decided that weight measurement or ultrasound would be a more accurate monitoring tool. A 30% weight increase has been previously described as the onset of ascites accumulation after 6-8 weeks when injecting 10 x 10^6 ID8-LUC cells in C57BL/6 J-Tyr^{c-2J}/J mice (Baert et al., 2015). This provides a good starting point for monitoring tumour and ascites formation in our models. Ultrasound was used in a limited number of mice in order to check intraperitoneal tumours were forming when 30% weight increase had been exceeded and to investigate the potential use of this technology for future monitoring of intraperitoneal tumour formation and ascites development.

The first experiment was performed using the ID8 WT and ID8 120 clones expressing different levels of total VEGFA and isoform expression as previously described in Chapter 4. This was used to characterise the growth of these different cell lines in the peritoneal cavity, with the aim of evaluating the best timeline for treatment and way to monitor tumour growth and ascites formation. Intraperitoneal growth of the newly developed ID8 cell lines was monitored by weight measurement and showed that after mice reached a 30% weight increase, they began to show abdominal distension and a further exponential increase in weight due to ascites formation (Fig. 48). This was observed in some of the mice implanted with ID8 120.18 cells, which reached 30% weight increase 60 days post injection and reached an endpoint 1-2 weeks after that, reaching a total weight increase of 50-60% (Fig. 49D-50). A 50-60% weight increase was decided as an appropriate endpoint to finish the protocol as from this point mice began to show signs of physical distress such as impaired movement due to increased abdominal distension, tremors and in some cases rapid weight loss. Most of the remaining ID8.120 clones and ID8 WT models did not reach 30% weight increase within 80

days of the protocol start (Fig. 49-50).

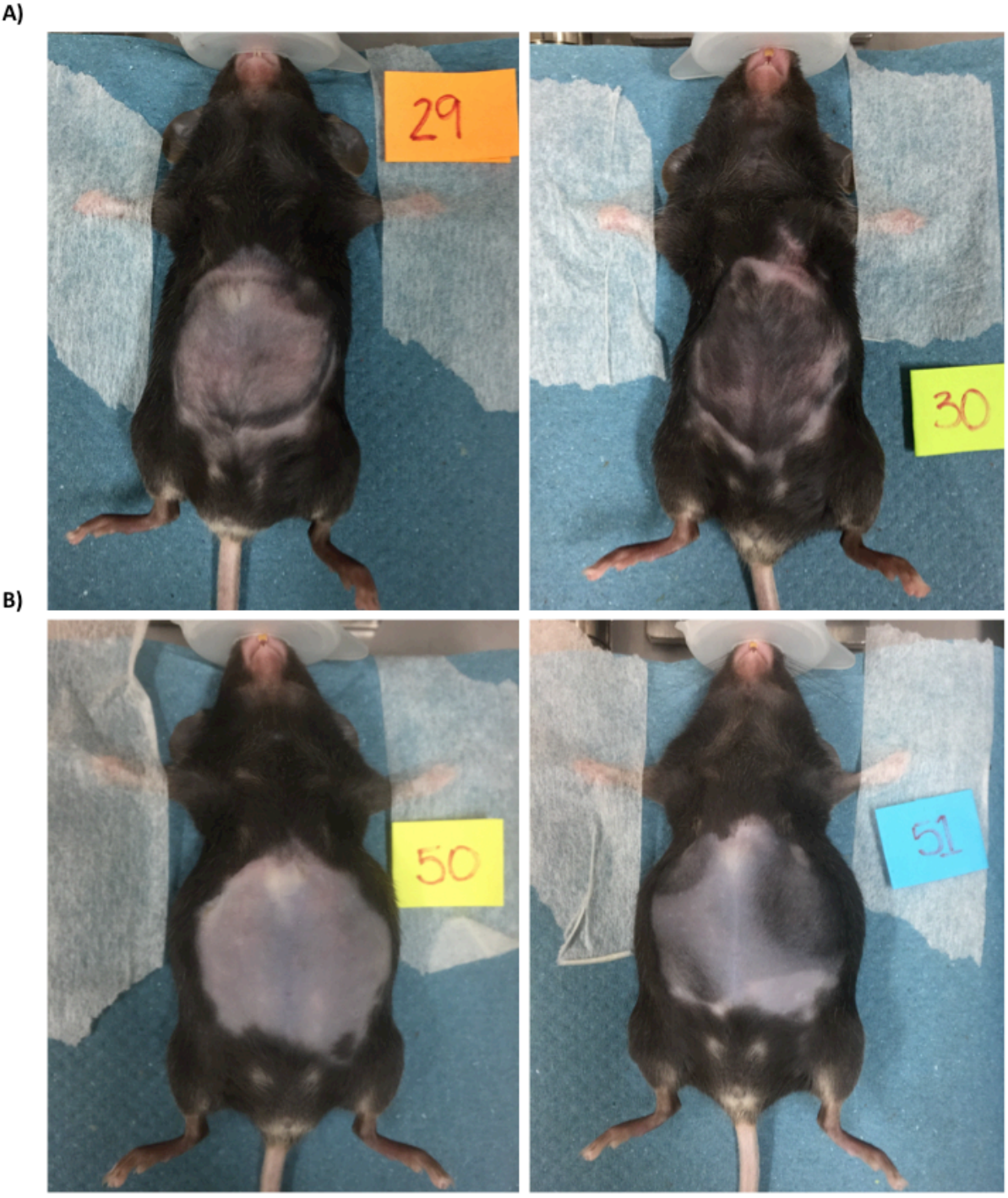

Figure 48. Comparison between C57BL/6J mice implanted with ID8 WT and ID8 120 cells with and without ascites.

A) Example images of ID8 WT mice without ascites at 77 days post inoculation showing ~ 24-28% weight increase. **B)** Example image of ID8 120.18 mice with noticeable ascites at 77 days post inoculation showing 48-54% weight increase.

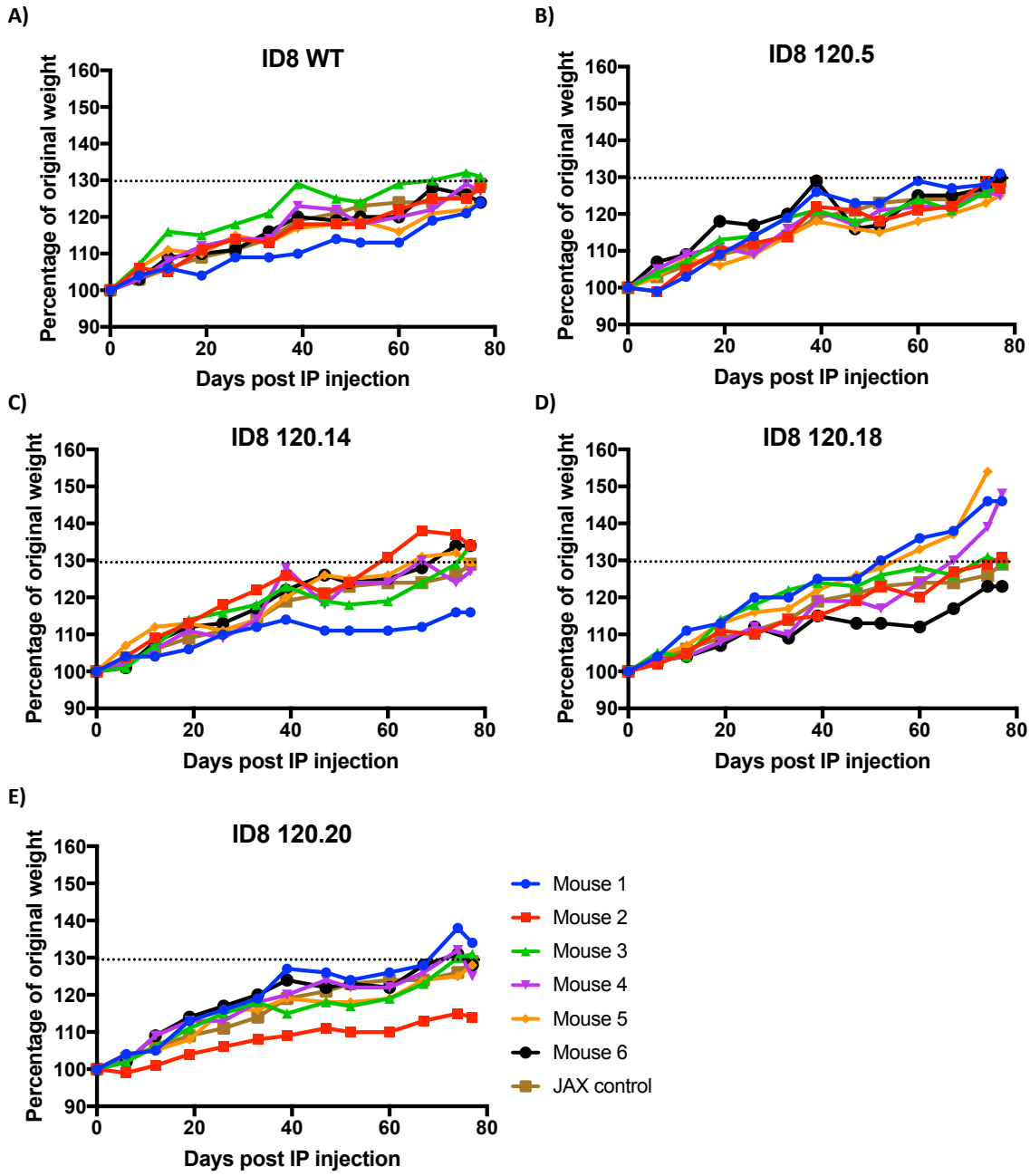

Figure 49. Weight measurements of mice inoculated intraperitoneally with ID8 cell lines.

A-E) Six C57BL/6J mice per group were inoculated with 5 x 10^6 ID8 WT or ID8 120 cells. Body weight was measured twice per week and percentage of original weight at inoculation point is shown. Each line represents a mouse for each group. Average weights from JAX were used as a reference measurement representing body weight information for healthy C57BL/6J mice at different weeks of age.

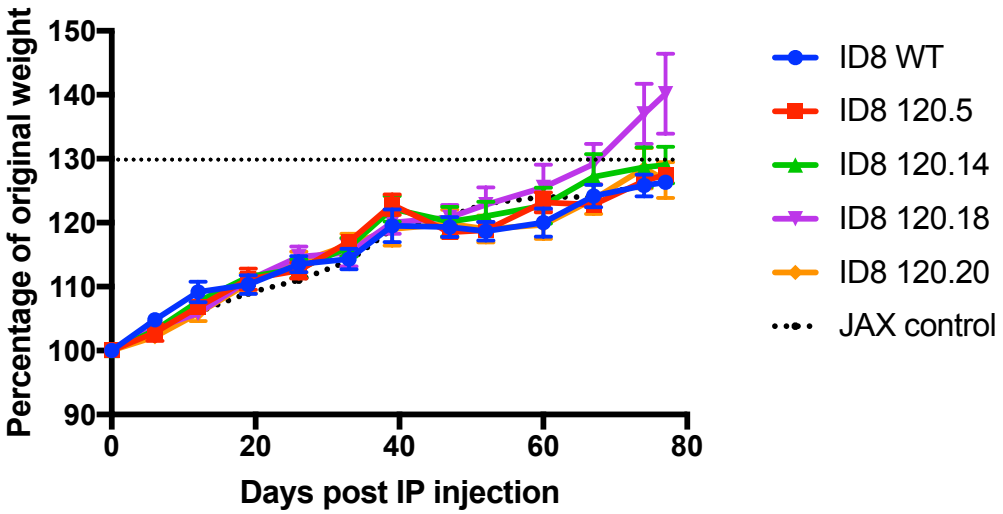

Figure 50. Average weight measurements of mice inoculated intraperitoneally with ID8 cell lines.

Six C57BL/6J mice per group were inoculated with 5 x 10^6 ID8 WT or ID8 120 cells. Body weight was measured twice per week and percentage of original weight at inoculation point is shown. Each line represents a specific group of mice. Average weights from JAX were used as a reference measurement representing body weight information for healthy C57BL/6J mice at different weeks of age. All data values are expressed as mean ± standard error.

Ultrasound has been described as an accurate and reliable tool to monitor ovarian tumours in pre-clinical models. In syngeneic orthotopic mouse models, ultrasound has allowed the detection and volume measurement of established ovarian tumours (Cho et al., 2013). More recently, this technology has been used to detect intraperitoneal tumours in xenograft models of epithelial ovarian cancer where it showed more sensitive results than bioluminescence *in vivo* imaging systems (e.g. IVIS by Perkin Elmer) by detecting smaller tumour sizes and ascites in a shorter period of time after cell implantation (Chambers et al., 2020).

Ultrasound imaging was used to confirm that tumours were present when mice showed weight increase in this pilot experiment and to be evaluated as a prospective tool for monitoring intraperitoneal tumour and ascites formation in our metastatic pre-clinical models. In the clinic, the presence of ascites can be detected by ultrasound by looking for free fluid collected around the different abdominal organs. The margin of the liver is usually easier to detect and ascitic fluid tends to surround and contour the borders of the liver, making this organ a suitable reference for detecting ascites. For each selected mouse, abdominal ultrasound was performed weekly using Vevo3100 system as described in methods section 2.2.1 (Fig. 51A). At the beginning of the experiment, ultrasound imaging was taken from a healthy mouse liver in order to have a baseline image to use a reference for future comparisons (Fig. 51B). Ascites surrounding the liver were detected in ID8 120.18 mice 74 days post IP injection (Fig. 51C) and also tumours between the spleen and the kidney were observed (Fig. 51D).

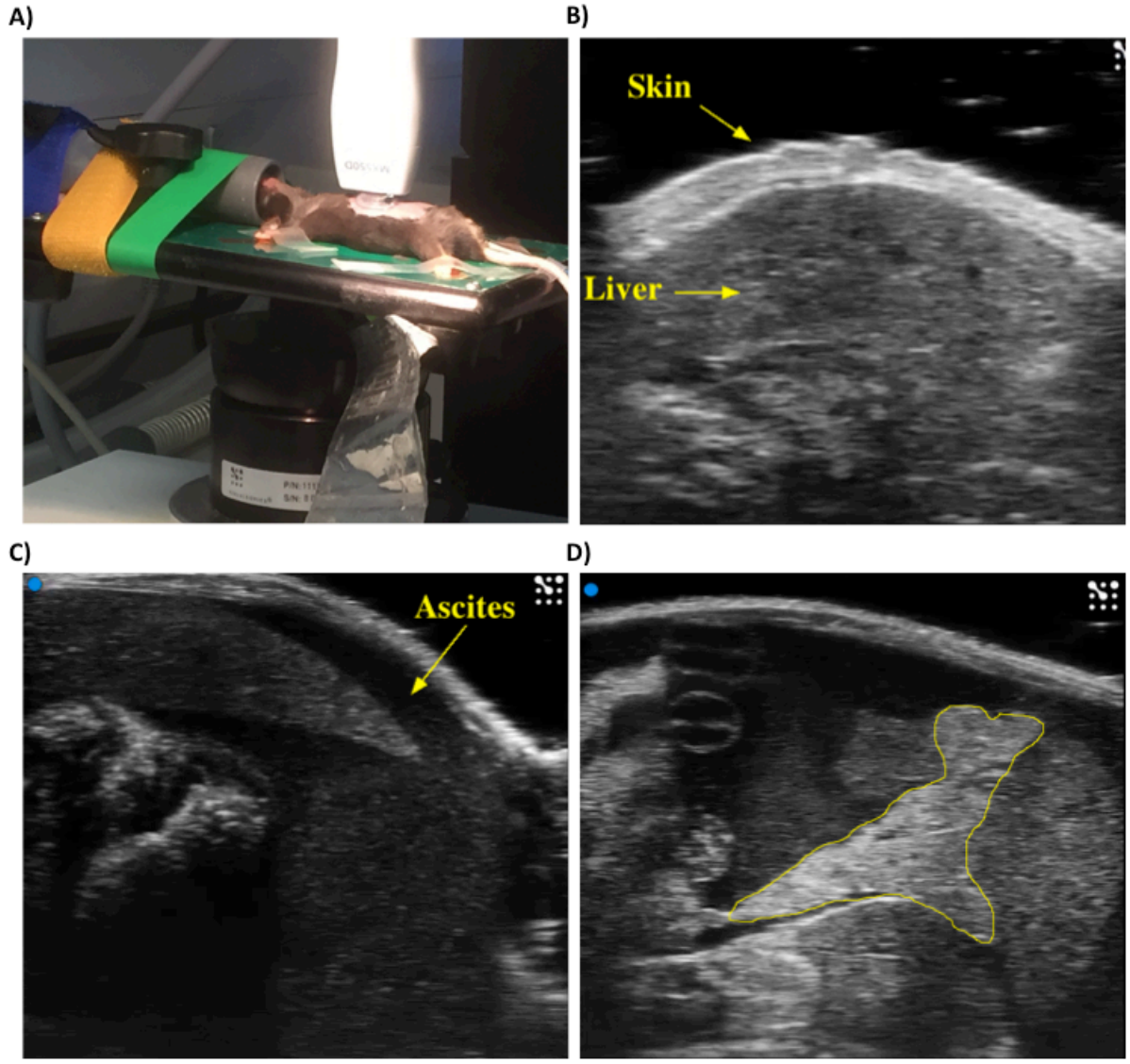

Figure 51. Ultrasound imaging for monitoring tumour formation and ascites in syngeneic ovarian cancer models.

A) Example image of transabdominal ultrasound setup using the Vevo3100 preclinical imaging system. **B)** Representative ultrasound image from a normal mouse liver. **C)** Ascites detection surrounding the liver area in an ID8 120.18 mouse at day 74 post intraperitoneal injection. **D)** Ultrasound image from a metastatic ovarian tumour (in yellow) detected between the kidney and the spleen in an ID8 120.18 mouse at day 74 post intraperitoneal injection.

For comparison in this pilot study, all mice were sacrificed after 80 days when the first mouse reached the established endpoint. Differences in ability to form tumours and ascites were observed between the different ID8 cell lines implanted intraperitoneally. For example ID8 120.5 and 120.18 cells formed tumours in approximately 80% of mice injected and showed development of ascites in some, however ID8 120.14 cells did not show tumour formation or ascites development within 80 days post-injection at all (Table 15).

Table 15. Intraperitoneal growth of ID8 WT and ID8 120 cell lines in C57BL/6J mice after 80 days of implantation.

5 x 10^6 ID8 WT and 120 cells were injected intraperitoneally. VEGFA expression within each cell line was quantified by ELISA and shown as ratio to its expression in WT cells. VEGFA isoform expression was measured by AQRT-PCR and shown as ratio to its expression in WT cells. Percentage of tumours and ascites is described as the number of mice showing visible abdominal tumour and presence of ascites at the end of the protocol (80 days after injection).

Cell line	VEGFA ratio to ID8 WT (ELISA)	Isoform ratio to ID8 WT (AQRT-PCR)	% Tumours	% Ascites
ID8 WT	-	-	50% (3/6)	0% (0/6)
ID8 120.5	3.5:1	120: 4:1 164: no change 188: no change	83.3% (5/6)	50% (3/6)
ID8 120.14	3:1	120: no change 164: no change 188: no change	0% (0/6)	0% (0/6)
ID8 120.18	9:1	120: 3:1 164: 3:1 188: no change	83.3% (5/6)	100% (6/6)
ID8 120.20	7:1	120: 2:1 164: 2:1 188: 2:1	33.3% (2/6)	16.6% (1/6)

5.4 The role of increased VEGFA120 expression in response to B20 in a metastatic model of ovarian cancer

A subsequent study was established to compare the response of ID8 WT and ID8 120.5 cells to anti-VEGFA therapy. ID8 120.5 cells were selected for this study, as this was the clone that showed increased levels of VEGFA120 without expression changes in the other isoforms. As before, 5 x 10^6 cells were implanted intraperitoneally and body weight was monitored. Mice were treated twice per week either with control IgG (antibody BE5) or anti-VEGFA antibody (B20-4.1.1) when each mouse showed a 30% weight increase (Fig. 52). Based on the pilot studies described earlier, the endpoint was established as either 50% weight increase or any other signs of distress such as rapid weight loss, hunched back, tremors or reduced movement. Unlike the previous pilot study, the endpoint was determined per individual animal rather that a final endpoint for the whole animal cohort.

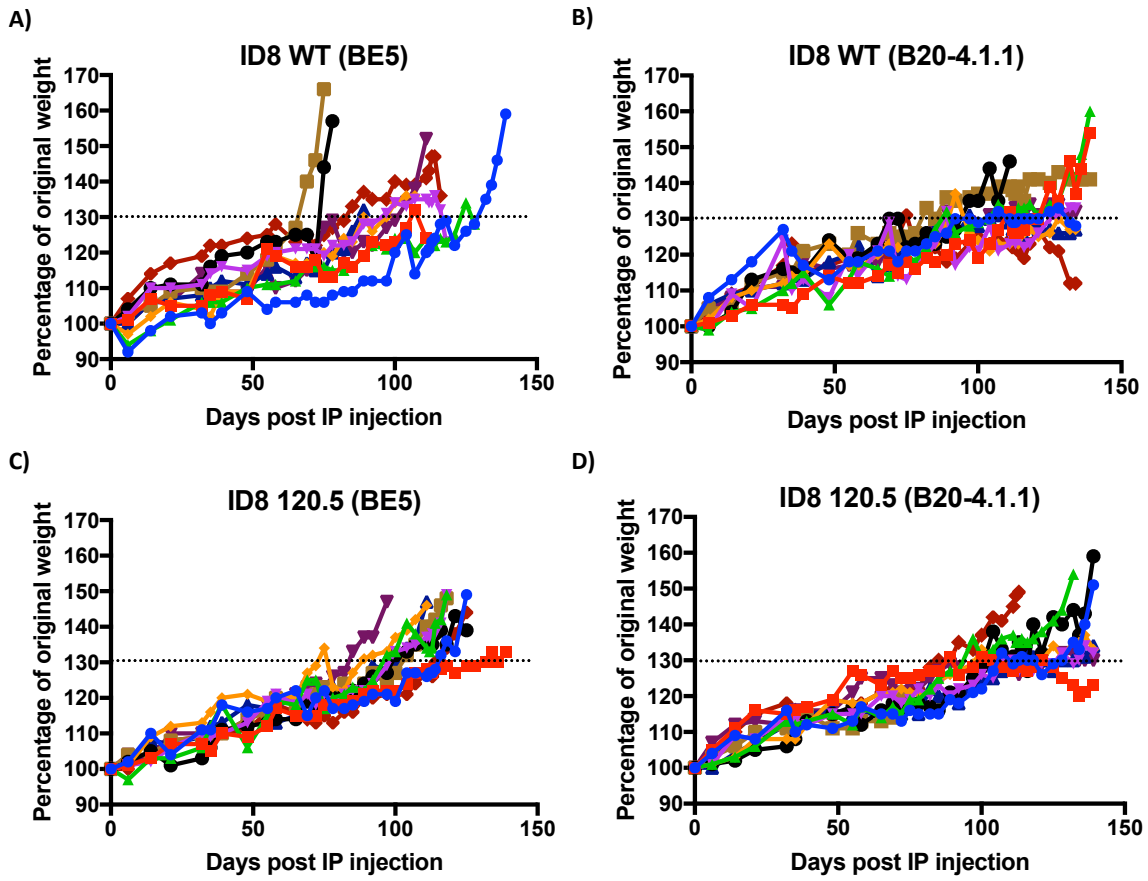

Figure 52. Weight measurements of mice inoculated intraperitoneally with ID8 cell lines treated with anti-VEGFA therapy.

10 mice per group were inoculated with 5x 10^6 cells. Body weight was measured twice per week and percentage of original weight at inoculation point is shown. Each line represents a mouse for each treatment group. **A-B)** Mice inoculated with ID8 WT cells were treated at 30% weight increase with either 5 mg/kg control IgG (BE5) or B20-4.1.1. **C-D)** Mice inoculated with ID8 120.5 cells were treated at 30% weight increase with either 5 mg/kg control IgG (BE5) or B20-4.1.1.

Survival analysis was performed to assess response to anti-VEGFA therapy in the metastatic ovarian cancer model. Treatment with the antibody B20-4.1.1 resulted in significantly extended survival when compared with mice treated with control IgG for both ID8 WT (p-value < 0.0001) and ID8 120.5 (p-value 0.0006). However, no significant difference was observed for survival between these ID8 cell lines, neither with control IgG treatment (p-value 0.1563) nor with B20-4.1.1 antibody (p-value 0.2245) (Fig. 53). Median survival were 5.5 days and 15 days for the control IgG ID8 and ID8 120.5 groups respectively, showing increased VEGFA120 expression delayed time to the protocol end point, although not statistically significant. While for the B20-4.1.1 treated groups, median survival was determined as 35 days for the ID8 120.5 mice, however median survival was undetermined for the ID8 WT group as more than 50% of the mice were still alive by the end of the protocol, which although statistical significance was not reached, suggests increased VEGFA120 expression may have reduced responsiveness to anti-VEGFA therapy.

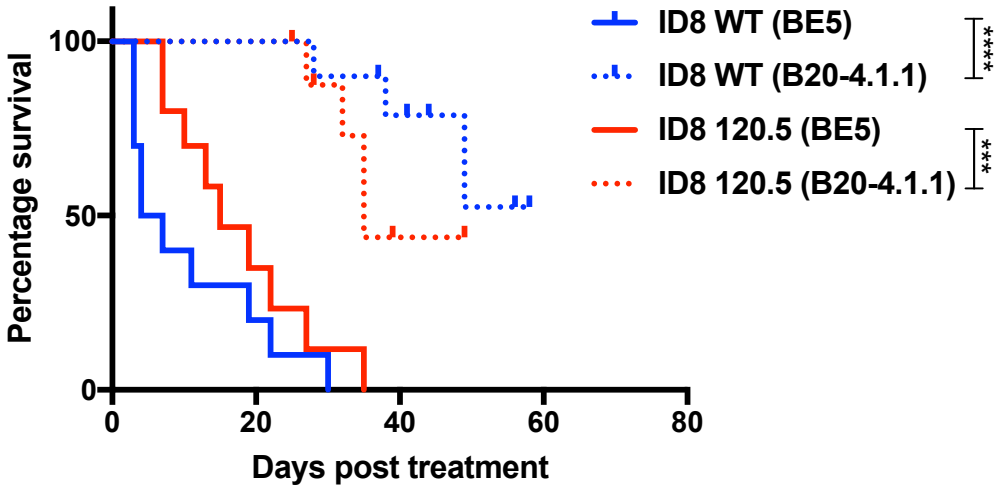

Figure 53. Survival in response to anti-VEGFA therapy in syngeneic ovarian cancer models expressing increased VEGFA120.

Kaplan-Meier plots in C57BL/6J inoculated with 5 x 10^6 ID8 WT or ID8 120 cells and treated with either control IgG (BE5) or B20-4.1.1, measured from treatment start (30% weight increase) to protocol endpoint as a surrogate for survival. 10 mice were used in each group. Long-rank test was performed using GraphPad Prism 7.0. *** p-value <0.001, **** p-value < 0.0001

In addition, tumour formation and ascites development was found to be similar between ID8 WT and ID8 120.5 injected mice when end point was reached (Table 16). In 90% of the cases for both cell lines, mice presented with intraperitoneal tumours surrounding the surface of different organs such as the liver and the stomach and extending to the intestines and the omentum. Tumours were also located on the abdominal wall and in some cases were found covering the diaphragm, consistent with spread of HGSOC (Fig. 54 and not shown). Although tumour formation in mice was not noticeably reduced by treatment with the B20-4.1.1 antibody (Table 16), there was a significant reduction in ascites volume collected from B20-4.1.1 treated mice when compared to the control IgG group and these results were observed for both ID8 WT and ID8 120.5 cell lines (Fig. 55). The mechanism by which anti-VEGF antibodies such as B20-4.1.1 reduce ascites is not completely understood. As described in section 1.1.1, VEGFA plays an important role in the development of ascites by increasing vascular permeability, which allows abnormal fluid accumulation within the peritoneal cavity. B20-4.1.1 can target ascites formation by neutralising secreted tumour VEGFA, blocking or restoring vascular permeability.

Table 16. Intraperitoneal growth of ID8 WT and ID8 120.5 cells in C57BL/6J mice when treated with anti-VEGFA (B20-4.1.1) antibody.

5 x 10^6 ID8 WT and 120.5 cells were injected intraperitoneally. Mice were treated twice per week either with 5 mg/kg control IgG (BE5) or B20-4.1.1 when each mouse showed a 30% weight increase. Percentage of tumours and ascites is described as the number of mice showing visible abdominal tumour and presence of ascites at the end of the protocol (<50% weight increase or any other signs of distress such as rapid weight loss, hunched back, tremors or reduced movement.).

Cell line	Treatment	% Tumours	% Ascites
ID8 WT	BE5	100% (10/10)	100% (10/10)
	B20-4.1.1	90% (9/10)	40% (4/10)
ID8 120.5	BE5	90% (9/10)	90% (9/10)
	B20-4.1.1	88.8% (8/9)	33.3% (3/9)

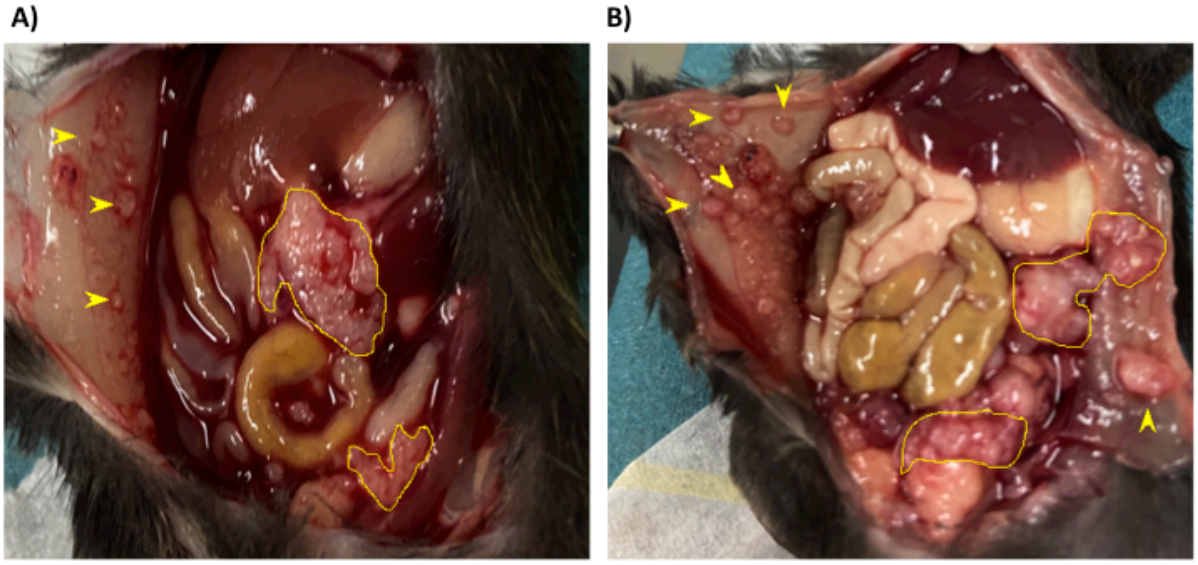

Figure 54. Intraperitoneal distribution of ID8 WT and ID8 120.5 tumours in C57Bl/6J.

A) Example images of ID8 WT tumours in the peritoneum and abdominal wall 116 days after inoculation. **B)** Example image of ID8 120.5 tumours in the peritoneum and abdominal wall 139 days after inoculation.

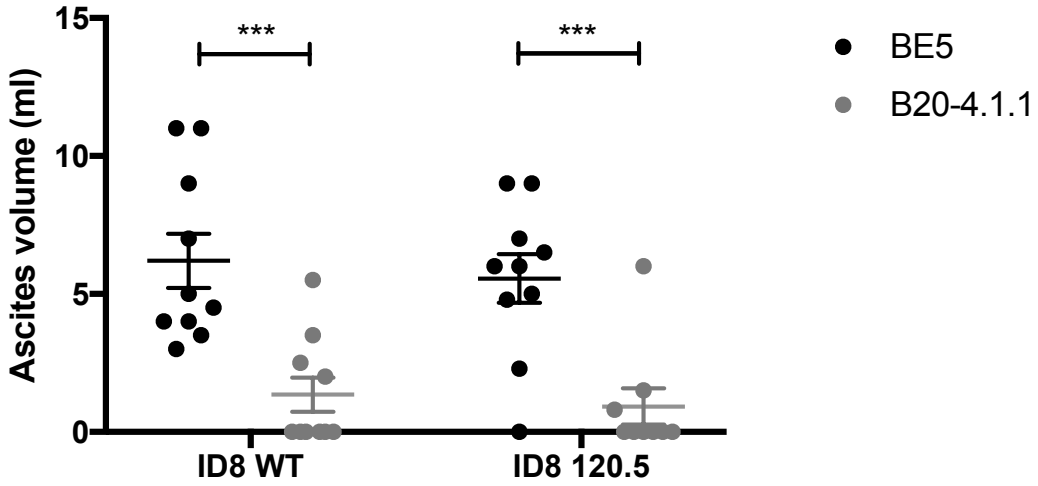

Figure 55. Ascites volumes in C57BL/6J mice implanted with ID8 WT and ID8 120.5 ovarian cancer cells.

Ascites volumes from mice at the end of the protocol for ID8 WT or ID8 120.5 cells treated with either control IgG (BE5) (n= 10 per group) or B20-4.1.1 antibody (n=10 for ID8 WT and n=9 for ID8 120.5). Ascitic fluid was removed with a needle through a small dermal incision to the side of the abdomen from mice under terminal anaesthesia (2-3% isofluorane in O_2) and volume was measured in millilitres. All data values are expressed as mean ± standard error per group. A one-way ANOVA test was performed followed by multiple comparisons using the Sidak's test. *** p-value < 0.001.

5.5 Summary

Based on the data obtained in this chapter, ID8 WT and ID8 120 cells overexpressing different levels of total VEGFA or VEGFA isoforms form extremely small subcutaneous tumours in C57BL/6J mice and no difference was observed in tumour size between the cell lines within 30 days of implantation. Additionally, pilot experiments for metastatic ovarian cancer using intraperitoneal implantation of ID8 WT and ID8 120 cells showed differences in their ability to form tumours and ascites. However these observations were not consistent with the total VEGFA expressed by ELISA or mRNA isoform expression levels within the ID8 cell lines. In this experiment all mice were sacrificed after 80 days when the first mice reached the established endpoint. From these results it was possible to determine that 30% weight increase was a good reference for initial tumour and ascites formation and to establish a 50-60% weight increase as endpoint for further experiments. Ultrasound imaging was evaluated as a prospective tool for monitoring tumour and ascites formation in our pre-clinical models. Although this proved to be a reliable tool, it was too time consuming for routine use, with mice under anaesthesia for prolonged periods, and not cost-effective. However it did confirm the 30% weight increase was a suitable point for start of treatment.

Finally, the metastatic model was used to evaluate the effect of anti-VEGFA treatment. Treatment with B20-4.1.1 antibody resulted in significantly extended survival when compared with mice treated with control IgG for both ID8 WT and ID8 120.5. Although no significant difference was observed for survival between these ID8 cell lines, neither with control IgG treatment nor with the B20-4.1.1 antibody, increased VEGFA120 expression delayed the time to the protocol end point and suggested reduced responsiveness to anti-VEGFA therapy. Additionally, tumour formation and ascites development was found to be similar between ID8 WT and ID8 120.5 models. Due to the COVID-19 pandemic resulting in laboratory lockdown, it was not possible to quantify VEGFA using ELISA and AQRT-PCR in the tumours and ascites. Equally, further characterisation of the tumours in terms of cancer cell proliferation, apoptosis or characterisation of the tumour microenvironment including vascular biology and immune content could not be performed.

6. Discussion and future directions

6.1 Potential impact of VEGFA isoform switching on HGSOC prognosis

The potential value of VEGFA as a prognostic and predictive biomarker has been commonly studied in different cancers. In ovarian cancer, most of the studies looking at associations between VEGFA levels and clinical outcome have mainly been focused on epithelial ovarian cancer rather than the HGSOC subtype (Li, L. et al., 2004) (Dalal et al., 2018) (Guo, B.Q. and Lu, 2018), however they do help highlight the potential value of this growth factor as a prognostic tool. High levels of VEGFA, measured by IHC specifically in HGSOC tissues, have been associated with poor overall survival and resistance to chemotherapy but no association with progression-free survival has been found (Williams et al., 2012). Our results from the TCGA ovarian cancer cohort did not show an association between total levels of VEGFA mRNA and overall or progression-free survival. The main difference between the Williams et al. study and our own relates to the detection methods used and the disease stage characteristics included in the analyses. While studies by Williams et al. used IHC in tissue samples from FIGO stage I-IV, our analysis is focused in RNAseq measurements from stage IIIC tumours. It is not currently clear if an IHC based approach can detect all VEGFA variants within the tissue. Experience of the English lab with commercially available antibodies for ELISA or Western blot analysis suggests detection is weaker for VEGFA188/189 than VEGFA120/121 and VEGFA164/VEGFA165. It is possible the IHC results reflect a bias towards detection of the shorter isoforms. Further studies are needed to correlate protein level detection and mRNA of VEGFA to determine if this is the case.

Analysis of TCGA and GTEx data from our work showed changes in VEGFA isoform expression between normal and tumour ovarian tissue. It is important to mention than transcript quantification in normal tissue within the GTEx data refers exclusively to ovarian tissue and that there is no information regarding transcript expression in normal fallopian tissue, thought to be a site of origin for HGSOC. It is unclear whether a difference in VEGFA mRNA isoform expression exists between these anatomic sites. Recently, Ahmed et al. profiled the molecular signatures of normal fallopian tube epithelium cells by single-cell RNA sequencing in order to predict future HGSOC development. In this study, fallopian tube samples were collected from patients both with HGSOC and without cancer conditions during diagnostic biopsies (Hu et al., 2020). Although sequencing data from this study is not

publically available, VEGFA transcript analysis from this type of studies could be used to further study the VEGFA isoform expression changes between HGSOC and normal fallopian tube tissue. Transcript level changes in VEGFA isoforms have been previously described between normal and malignant tissue in oral, head and neck, lung and colon cancer patients, which supports data presented in Chapter 3 showing an isoform expression switch may occur between normal ovarian tissue and HGSOC (Patel et al., 2015; O-charoenrat et al., 2001; Cheung et al., 1998). In light of these results, a potential avenue of future work could be to evaluate if changes in circulating mRNA levels of diffusible VEGFA isoforms such as VEGFA121 or VEGFA165 could be used as a diagnostic strategy to detect ovarian cancer at earlier stages of the disease. For example, measurements of circulating mRNA in plasma have been previously suggested as potential markers for prognosis and treatment response in breast cancer patients (Garcia et al., 2008; Silva et al., 2007).

VEGFA mRNA isoform expression has been correlated with tumour progression and survival in different cancers. High levels of VEGFA121 have been associated with increased overall survival in patients with lymphoma (DLBCL) (Broseus et al., 2017). Increased levels of VEGFA189 have been associated with worse survival and tumour angiogenesis in lung cancer (Yuan et al., 2001). In ovarian cancer, increased protein levels of VEGFA165 measured in serum has been associated with poor overall and progression-free survival and its levels have shown significant variation before and after surgery or chemotherapy (Mahner et al., 2010). Our individual segregation model showed that low levels of VEGFA121, 165 and 189 are independently associated with worse overall survival in HGSOC patients when compared with their high expression groups. This method, in accordance with the previously mentioned VEGFA isoform studies, measures the expression of each VEGFA isoform in isolation while omitting the rest. However it is known that multiple VEGFA isoforms are simultaneously expressed in healthy and disease conditions and downstream signalling is dependent on the ratio of these, therefore measuring individual isoform expression does not fully represent the whole VEGFA isoform landscape and will not aid in understanding the mechanisms by which VEGFA influences disease progression.

Recently, the relevance of alternative mRNA splicing has been increasingly studied in cancer. It has been described that changes in isoform patterns can be observed between healthy and disease conditions (Vitting-Seerup and Sandelin, 2017). These findings suggest that targeting splicing mechanisms that are altered in cancer could be a potential treatment strategy.

Different VEGFA isoform patterns have been described in colorectal (Tokunaga et al., 1998) and hepatocellular cancer (Chesnokov et al., 2018). In the former study, a VEGFA pattern including high VEGFA121 + VEGFA165 + VEGFA189 (type 3) detected by RT-PCR, is associated with increased metastasis and poor prognosis (Tokunaga et al., 1998). Our clustered segregation model has more specifically shown that higher levels of VEGFA121 when compared to levels of VEGFA165 and VEGFA189 are associated with worse overall survival in HGSOC.

Comparisons between our two segregation models allowed us to explore associations between VEGFA isoform expression and survival. Our observations suggest that regardless of the method used to segregate patients, there is a notable trend for groups with levels of VEGFA121 higher than the other isoforms to show poor overall survival. However, the opposite association is observed when patients were segregated based on the individual expression of VEGFA121. There is not a clear explanation for this discrepancy between the models studied, however future studies of differential gene expression in each of the comparisons proposed might explain if there are other biological elements that could clarify these observations. These could include expression of VEGFRs, co-receptors, ECM components, other proteins within the VEGFA isoform signalling or genomic alterations. Additionally, increasing the sample size, optimising cut-off values for mRNA VEGFA isoform expression (e.g. middle 50% or tertiles) and performing analysis in an independent patient cohort could help to understand differences in results between these models. Survival outcomes were consistent when patient groups were segregated using mRNA expression of the ECM-binding isoforms (VEGFA165 and 189), this suggests that the abundance of the longer isoforms might have a stronger biological impact within the TME and therefore increased clinical relevance than looking at the short, diffusible isoforms such as VEGFA121.

Measurement of VEGFA165 alone was selected as the segregation model to study survival in more detail. Multivariate analysis showed that low VEGFA165 expression (and also high VEGFA121) is associated with decreased overall survival when compared with the high VEGFA165 (and low VEGFA121) expression group independent of other clinical variables such as age, grade and molecular subtype. The effects of treatments were not included due to a lack of specific treatment information per patient within the TCGA data, however early TCGA reports described that ovarian cancer clinical samples were collected before systemic treatment which later included a platinum agent for all patients and a taxane compound in

94% of the cases (Cancer Genome Atlas Research, 2011). It was therefore assumed that treatment strategies were similar across all patients. Access to treatment strategies might explain why a significant difference can be observed for overall survival but not for progression-free survival between the studied groups.

Following VEGFA165 quartile segregation, GSEA analysis showed that enriched gene signatures associated with the high VEGFA165 expression group included hypoxia, angiogenesis and EMT processes. The PPI network of up-regulated genes in the high VEGFA165 group showed *CA9* and *MTOR* genes to be associated with a response to hypoxia. CA9 expression has previously been suggested as being involved with an increased hypoxic profile in HGSOC tissues (Williams et al., 2012), which is consistent with our observation of a high hypoxic score in our high VEGFA165 group. In addition, VEGFA expression in HGSOC patients has been directly linked with the MTOR pathways and has been suggested as a potential biomarker for patient stratification for MTOR targeted therapies (Andorfer et al., 2016). Based on this, our results suggest that VEGFA165 expression could be selectively regulated under hypoxic conditions together with CA9 and MTOR. As previously described, the VEGFA165 transcript has an extended 5' UTR encoding a longer signal peptide which is not present in the other two isoforms, which potentially indicates the presence of a specific regulation mechanism that allows an unique adaptation during hypoxia (Rosenbaum-Dekel et al., 2005).

The DNA repair gene signature is enriched in patients with low levels of VEGFA165, the group with decreased OS (Fig. 21). DNA repair mechanisms have been considered important processes for preventing the cytotoxic effect of platinum compounds after formation of DNA adducts (Ohmichi et al., 2005). DNA adducts caused by platinum compounds can be removed through the nucleotide excision repair mechanism (Furuta et al., 2002) or though DNA mismatch repair, which mediate the activation of cell cycle check points, allowing the recovery of DNA repair mechanisms (Galluzzi et al., 2011). Increases in DNA repair mechanisms have recently been associated with the development of chemoresistance in cancer cells due to their ability to repair lesions induced by cytotoxic therapy (Kiwerska and Szyfter, 2019). Taking into account these observations, the group of patients with low levels of VEGFA165 could potentially present a greater risk of chemoresistance and in consequence a reduced survival. Additionally, it has been suggested that PARP inhibitors such as Olaparib might work in combination with VEGF-VEGFR targeting such as cediranib in BRCA

mutated ovarian cancer (Liu, J.F. et al., 2020). Our results indicate that the group of patients with high levels of VEGFA165 showed slightly increased HRD scores. Going forward it will be important to evaluate if this group of patients can respond better to this combination therapy.

Our cell population analysis suggests that tumours with low expression of VEGFA165 (and high VEGFA121) have lower pericyte abundance when compared with tumours with high VEGFA165 (and low VEGFA121). These results are in line with previous studies that indicate that *in vivo* model fibrosarcoma tumours expressing VEGFA120 had reduced pericyte coverage than the corresponding tumours expressing VEGFA188 (Tozer et al., 2008; English et al., 2017). These tumours also had a tendency towards increased hypoxia, although this was not statistically significant (Akerman et al., 2013).

Our study measured VEGFA isoform mRNA expression within the tumour using RNAseq and interestingly our results contradicted our starting hypothesis. Based upon the literature it was hypothesised that patients with high levels of VEGFA121 would be more responsive to bevacizumab treatment. A limitation of our investigations is that we did not have access to tumour samples from patients treated with bevacizumab. In my studies, a gene signature that indicates responsiveness to bevacizumab developed previously by Yin et al was used. Based on this my results indicate that patients with high VEGFA165 expression (and also low VEGFA121) have an enrichment in genes that correlate with an improved bevacizumab response. Our analysis did not show any differential expression of previously described markers for response to bevacizumab in ovarian cancer, such as CD31 or IL6, however these markers were originally measured on tumour tissue and plasma respectively and this might be the reason why we did not observe changes in the mRNA expression of these genes (Bais et al., 2017; Alvarez Secord et al., 2020). Data obtained in the English lab shows MVD determined through CD31 staining does not correlate with CD31 mRNA levels in fibrosarcomas expressing VEGFA120 or VEGFA188 (W English, unpublished). In order for accurate conclusions to be drawn, further work is needed to validate these results. This could be achieved using additional RNAseq databases or clinical samples, particularly from patients treated with bevacizumab, to correlate with additional biomarkers for bevacizumab with VEGFA isoform expression, for example mean vascular density as identified by Bais et al. (2014) from the GOG-0218 study, or changes in circulating cytokines and growth factors as characterised by Alvarez Secord et al. (2020).

6.2 Challenges in developing *in vitro* and *in vivo* models of HGSOC expressing different VEGFA isoforms

Cancer cell lines express variable percentages of VEGFA isoforms. For example, ovarian SKOV3 cancer cells express higher levels of VEGFA121 (70.5%) than VEGFA165 and VEGFA189 (24.5% and 5%, respectively) (Stimpfl et al., 2002). OVCAR-3 cells express simultaneously higher levels of VEGFA121 and VEGFA165 (47% and 42.1%) than VEGFA189 (6.1%) (Stimpfl et al., 2002). IGROV-1 cells show VEGFA189 levels higher than VEGFA121 and VEGFA165 (Valluru M and English WR unpublished). ID8 cells used in this study showed higher expression of VEGFA121 compared to VEGFA165 and VEGFA189 and these observations are consistent with previous VEGFA isoform characterisation using Taqman RT-PCR (Zhang, L. et al., 2002a). The common approach to study the effect of individual VEGFA isoforms is to increase or inhibit its expression in cancer cells, however this method does not take into consideration the functional background that the other isoforms provide. It is therefore important to extensively characterise cell lines for future studies looking at VEGFA isoforms not only in ovarian cancer but also in different cancer types.

VEGFA is up-regulated by hypoxia (Ramakrishnan et al., 2014). In a similar way expression of VEGFA variants is increased under hypoxic conditions in different types of cells such as in astrocytes, retinal, endothelial and cancer cells (Watkins et al., 2013; Kazemi et al., 2016). Data from this work showed that ID8 cells express increased levels of VEGFA120, VEGFA164 and VEGFA188 under hypoxic conditions when compared to normal oxygen levels, however across these isoforms VEGFA120 showed the highest expression in both 1% and 21% O2 conditions in WT cells. This differs from observations in other cancer cell types and endothelial cells where hypoxia induces higher changes in the expression of VEGFA165 (Kazemi et al., 2016).

Overexpression of the different VEGFA isoforms in MCF-7 breast cancer clones did not show an effect on cell proliferation (Zhang, H et al., 2000). Additionally, fibrosarcoma cells expressing VEGFA120 or VEGFA164 proliferate faster but migrate more slowly than those expressing VEGFA188 (Tozer et al., 2008; Kanthou et al., 2014). Overexpression of VEGFA165 does not have an effect on *in vitro* proliferation of OVCAR-3 cells when compared with the WT cells (Duyndam et al., 2002). We observed a decrease in cell proliferation and migration in clones ID8 120.5 and 120.20, where both clones showed

increased expression ratio of VEGFA120 when compared with the WT cells. ID8 120.20 also showed increased levels of VEGFA164 and VEGFA188. It is not clear if the observed changes in these biological processes are a consequence of VEGFA isoform expression. In order to investigate this further, studies inhibiting VEGFA isoform expression are required to evaluate its effect in cell proliferation and migration. Selective inhibition of VEGFA isoforms could be achieved using RNAi targeting specific exon-exon regions that characterise each isoform.

Morphological changes were detected across the ID8 120 clones created. Clones with lower VEGFA expression showed a more epithelial phenotype while those with the highest levels of VEGFA were associated with a mesenchymal like phenotype. This observation was not consistent with a specific VEGFA isoform expression level. Kanthou et al. described changes in the morphology of fibrosarcoma cells expressing a single VEGFA isoform. Specifically, a mesenchymal phenotype was observed in Fs188 cells but not in Fs164 or Fs120 cells and this characteristic was more notable when cells were grown on surfaces coated with fibrillar collagen (Kanthou et al., 2014). From our results it is clear that ID8 WT cells express both epithelial and mesenchymal markers such as β-catenin, E-cadherin, N-cadherin and vimentin. This is consistent with what has been found in previous studies describing that ovarian cancer cells can show high plasticity and present both epithelial and mesenchymal characteristics (Loret et al., 2019). Additionally, changes in E-cadherin and N-cadherin expression were observed between ID8 WT and ID8 120 clones. Decreased expression of E-cadherin has been associated with metastasis of ovarian cancer by increasing cell adhesion and invasion via α_5-integrin (Sawada et al., 2008). Loss of E-cadherin and N-cadherin do not follow the typical changes observed during EMT, however it has been described that ovarian cancer cells can be classified in intermediate epithelial or mesenchymal phenotypes based on the expression levels of these cadherins (Rosso et al., 2017).

In vivo models designed to study the role of VEGFA isoforms have been previously described in different cancers. Zhang et al. demonstrated that overexpression of VEGFA121 in MCF-7 cells induced faster subcutaneous tumour growth compared to WT cells or those overexpressing the VEGFA 165 or 189 isoform in xenograft models using BALBc mice (Zhang, H et al., 2000). Kazemi et al. using colorectal cancer and melanoma cells made similar observations, where overexpression of VEGFA121 using recombinant vectors stimulates increased subcutaneous tumour growth in *in vivo* models (Kazemi et al., 2016). In

several ovarian cancer studies, increased subcutaneous growth has been described for ID8 cells overexpressing VEGFA164 when compared with the WT cells implanted in C57BL/6 mice (Janat-Amsbury et al., 2006a; Janat-Amsbury et al., 2006b; Zhang, L. et al., 2002b). These previous ovarian cancer studies with ID8 cells used retroviral systems to increase VEGFA164 expression, however in most of the cases the characterisation of all VEGFA isoforms within the cells or tumours was not considered. Our results did not show an effect of VEGFA120 expression levels in subcutaneous growth using ID8 cells in C57BL/6J mice.

Intraperitoneal tumour growth in our metastatic model of ovarian cancer indicates that ID8 cells form tumours surrounding the surface of different organs such as the liver and the stomach and extending to the intestines and the omentum. Tumours were also located on the abdominal wall and in some cases were found covering the diaphragm. These results are consistent with initial characterisation studies for the *in vivo* growth of ID8 cells performed by Roby et al. (Roby et al., 2000). Additionally, our results from these models using either ID8 WT or ID8 120 cells show similar tumour formation and ascites development between these cell lines. A previous study reported that overexpression of VEGFA164 in ID8 cells induces high volumes of ascites formation when compared with the WT in syngeneic mice models (Zhang, L. et al., 2002b). In line with this study, we observed higher ascites development in some mice implanted with clone ID8 120.18 in our initial intraperitoneal characterisation when compared with the WT cells and the rest of the ID8 120 clones. It is important to highlight the fact that the ID8 120.18 clone showed not only an increased expression of VEGFA120 but also of VEGFA164, which might indicate that VEGFA164 could be accelerating ascites formation. Unfortunately, our experimental timeline did not allow further conclusions to be drawn.

Survival analysis in our *in vivo* models showed that mice implanted with the ID8 120.5 clone, that only had increased expression of VEGFA120, took more time to reach the protocol end point when compared with the WT group. These results were obtained when increased weight due to ascites was used as main endpoint together with other criteria such as physical discomfort, abnormal behaviour or significant weight loss. Baert et al. have suggested that ascites might not be a good reference point to determine survival outcome in ovarian cancer *in vivo* models. This is mainly due to the fact that drainage of ascites can significantly improve survival in mouse models in a similar way to the clinical setting (Baert et al., 2015). Although the suggested strategy implies more complex experimental work, it is important for

future work to consider the impact of draining ascitic fluid in mouse models for estimates of survival with the objective to avoid the underestimation of this outcome.

Additional results from survival in *in vivo* models showed that the B20-4.1.1 antibody significantly improved survival in treated mice when compared with the control IgG (BE5) group. These findings are in accordance with previous studies in xenograft ovarian cancer models showing that bevacizumab improved animal survival either alone or in combination with cytotoxic therapy such as cisplatin and paclitaxel (Shah et al., 2011; Oliva et al., 2012; Mabuchi et al., 2008). Our observations also indicate that treatment with B20-4.1.1 decreased ascites volume but not tumour formation in our metastatic ovarian mouse models. Oliva et al. who described that bevacizumab as single agent reduces ascites but not tumour burden in xenograft models, reached a similar conclusion. Their results however also showed that reduced ascites and metastasis was achieved when bevacizumab treatment was administrated with cisplatin and paclitaxel (Oliva et al., 2012). Increased survival and tumour growth inhibition has also been observed in ovarian xenograft models when bevacizumab is used as maintenance therapy after initial treatment with bevacizumab alongside cisplatin (Mabuchi et al., 2008). Future work looking at the effect of VEGFA isoform expression and response to anti-angiogenic therapy in ovarian cancer models should include treatment combinations with chemotherapy commonly used in the clinical setting.

Although no significant difference was observed for the effect of B20-4.1.1 treatment between ID8 WT and ID8 120.5 mouse models, survival analysis suggests that increased VEGFA120 expression may reduce responsiveness to anti-VEGFA treatment. These results contradict previous findings within the English' lab, which suggested that tumours derived from human ovarian cells with increased VEGFA121 expression showed a benefit response from anti-VEGFA therapy as well as increased cachexia. It is important to mention that subsequent characterisation of COV362-121 clone used for these experiments showed that these cells were not only expressing increased levels of VEGFA121 but also higher levels of VEGFA165 than the parental cell lines. This might be the reason why we did not observe an increased response to B20-4.1.1 in our *in vivo* model using ID8 120.5. Time did not allow investigations into the response of ID8 120.18 that also had increased expression of VEGFA164. It remains unclear whether the bevacizumab response in the previous COV362 model was an effect of VEGFA121 overexpression or increased VEGFA165, or whether it is due to the balance between the two. It is worth noting that in the majority of cases where cell

lines were developed by other investigators to overexpress VEGFA isoforms, studies were not conducted to see if the expression of endogenous isoforms also changed in their modified cell lines. Considering our findings, this is clearly critical in interpreting results obtained *in vitro* and *in vivo*. In the future, it will also be essential to characterise VEGFA isoform expression not only in the cancer cells but also in tumours and ascites as it is not clear if VEGFA isoform abundance remains similar *in vitro* and *in vivo*.

Two main limitations can be identified regarding the *in vitro* and *in vivo* models developed for this study. The first one is associated with the use of ID8 cells to study HGSOC. These cells lack the main genomic alterations that characterise this disease such as *TP53* and *BRCA* mutations. Future work should consider the use of genetically modified cells with *TP53* or *BRCA* depletion as a model to better represent HGSOC (Walton, J. et al., 2016). The second limitation is related to the VEGFA isoform pattern observed within our bioinformatics analysis. Unfortunately, *in vitro* and *in vivo* models in this work do not fully represent VEGFA isoform changes observed in HGSOC patients within the TCGA. Although overexpression of VEGFA120 was induced in ID8 cells, the WT cells already expressed high levels of this isoform. Therefore new models should be developed not to increase a single VEGFA isoform but to replicate the isoform switch present in cancer patients. As this will require complex gene editing, probably including a combination of gene deletion and overexpression of more than one VEGFA isoform within a cell line. It will be important that future research investigates the use of models such as PDX that can retain the characteristics of original tumours to study the role of VEGFA isoforms.

In conclusion, this work has shown that the predominant VEGFA isoforms in HGSOC are VEGFA121, VEGFA165 and VEGFA189 and that expression of these are increased in HGSOC when compare with normal ovary tissue. Additionally, different isoform expression patterns can be found in HGSOC patients. Results from our bioinformatic analyses suggest that patient segregation can be achieved using different methods either using individual or clustered isoform expression, however, regardless of the method used, the impact of all VEGFA isoforms expressed should be considered. TCGA data has allowed us to explore the associations between VEGFA mRNA isoform and clinical outcomes. Low VEGFA165 (and high VEGFA121) expression showed decreased progression-free survival when compared with high VEGFA165 (and low VEGFA121) levels. Additionally, GSEA analysis suggested that high VEGFA165 levels might be associated with increased benefit from bevacizumab

therapy. Further studies should be done in order to explore these observations. Initial experiments were performed using FFPE clinical samples from HGSOC patients in order to validate the prognostic value of VEGFA isoforms and associations between potential predictive biomarkers like MVD, however the time limit did not allow this work to be completed.

Additionally, *in vitro* and *in vivo* models were created using a mouse ovarian cancer cell line overexpressing VEGFA120. In order to characterise VEGFA isoform expression, an AQRT-PCR assay was developed and VEGFA isoform were quantified in 1% and 21% O_2. Although some changes in proliferation, migration, morphology and EMT markers were observed *in vitro* between some of the ID8 120 clones and the WT cells, it was not clear if these changes were a consequence of VEGFA isoforms expression levels within the cells. Unfortunately, due to the COVID-19 pandemic restricting lab access, experiments to evaluate the cell lines response to anti-VEGFA therapy and VEGFA-VEGFR signalling were not completed. *In vivo* characterisation using ID8 120 cells did not show tumour growth in subcutaneous models, however intraperitoneal implantation showed differences in tumour formation and ascites. Additionally, treatment with B20-4.1.1 antibody resulted in significant extended survival and reduced ascites when compared with the control IgG group. Although no significant difference was observed, increase VEGFA120 delayed time to protocol end point and suggest reduced responsiveness to anti-VEGFA therapy. Unfortunately, further tumour characterisation and VEGFA quantification from the *in vivo* models was also not possible due to the COVID-19 pandemic.

7. Supplementary data

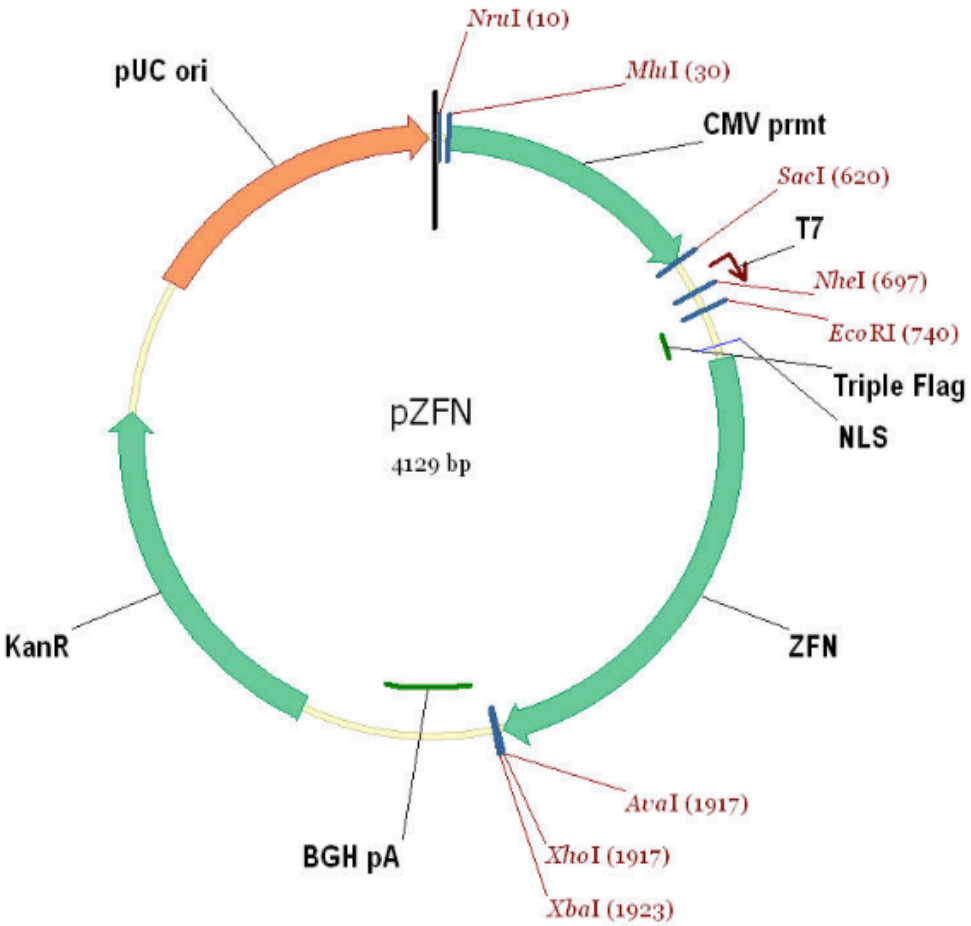

Figure S1. Map of the ZFN plasmids.

ZFN elements consist of two main functional domains: a chain of zinc finger proteins for DNA binding and a nuclease domain (*FokI*) for DNA cleavage. The designed ZFN system recognises a 15-18 base pair sequence within the exon 4 of the *VEGFA* gene. Additionally, the endonuclease domain cleaves within this recognition site at a specific DNA sequence (5' TGCGAT 3').

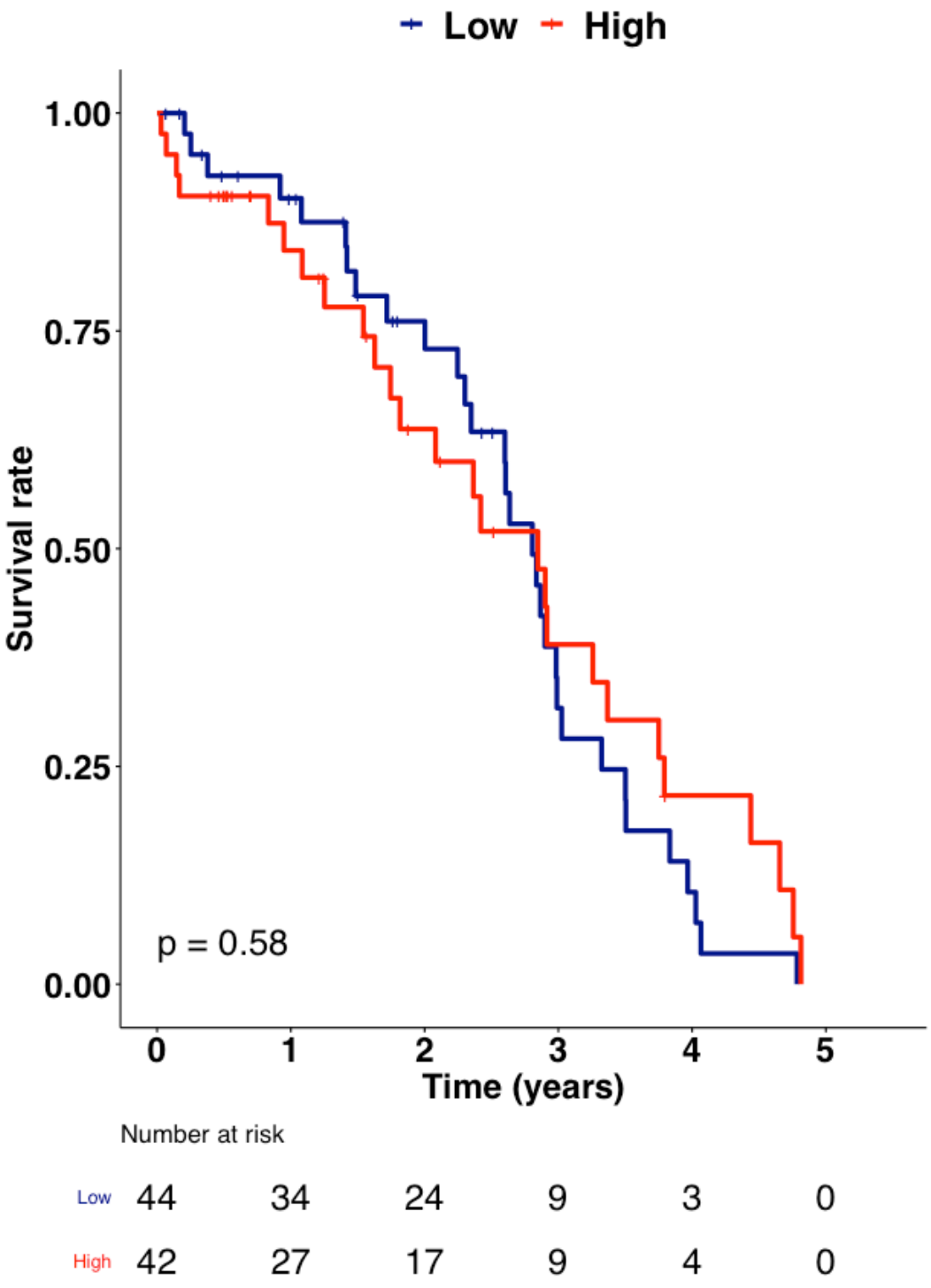

Figure S2. Overall survival for total VEGFA segregation groups.

Kaplan-Meier analysis for overall survival in patients with low and high total VEGFA expression based on quartile segregation. Differences between groups were assessed using a long rank test and P-values below 0.05 were considered statistically significant.

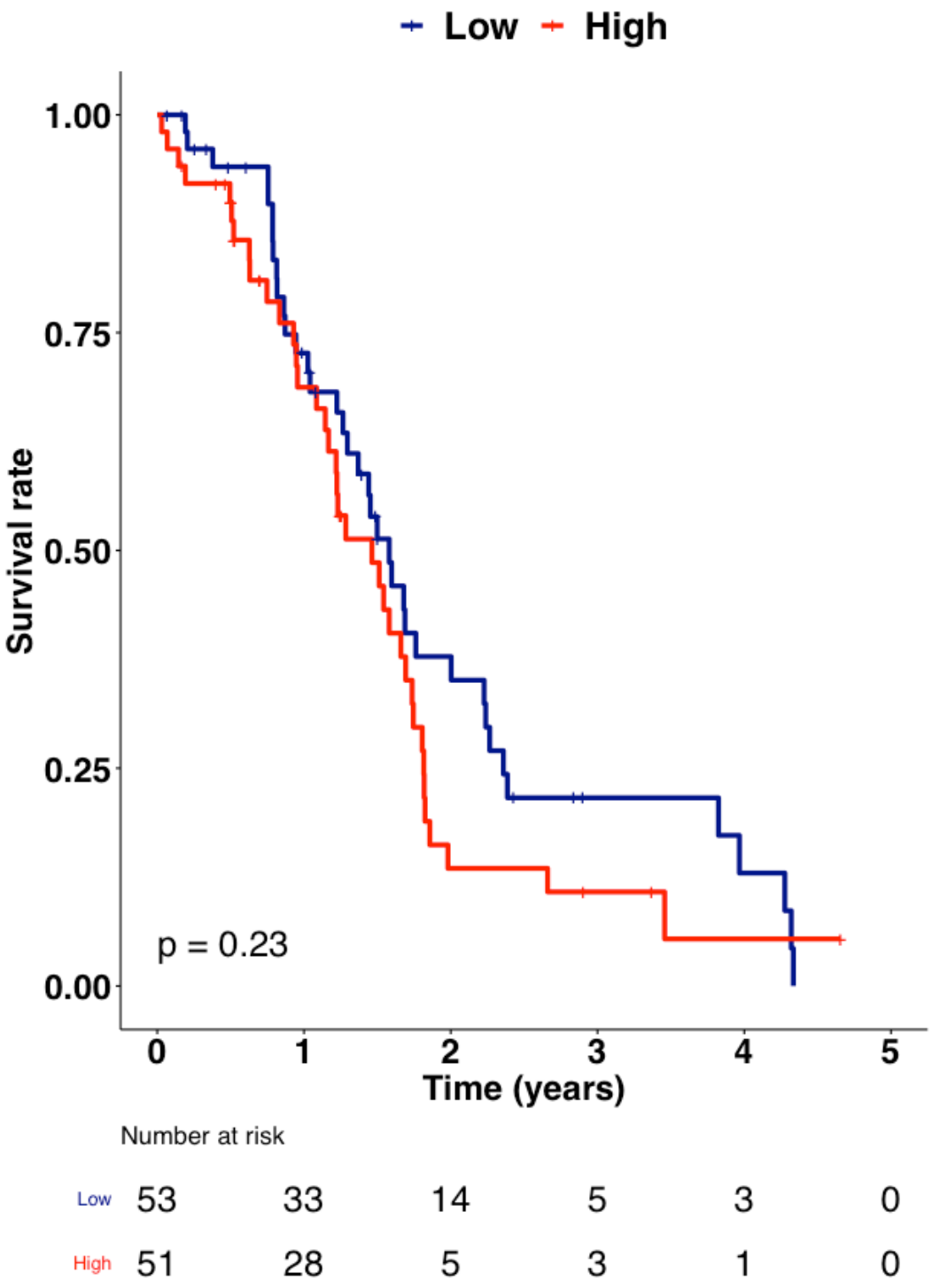

Figure S3. Progression-free survival for total VEGFA segregation groups.

Kaplan-Meier analysis for progression-free survival in patients with low and high total VEGFA expression based on quartile segregation. Differences between groups were assessed using a long rank test and P-values below 0.05 were considered statistically significant.

Table S1. GSEA results. The hallmark gene sets (h.all.V7.1 MSigDB).

	Name	Size	ES	NES	p-value	FDR q-value
LOW VEGFA165	OXIDATIVE_PHOSPHORYLATION	182	-0.6317771	-2.6123374	0	0
	MYC_TARGETS_V1	188	-0.51903516	-2.1489573	0	0
	MYC_TARGETS_V2	58	-0.46150544	-1.6031888	0.007481297	0.016318107
	ALLOGRAFT_REJECTION	179	-0.3793617	-1.5564154	0	0.021446683
	FATTY_ACID_METABOLISM	141	-0.38055494	-1.5257115	0	0.02284943
	PEROXISOME	95	-0.3975846	-1.5254663	0.00273224	0.01904119
	DNA_REPAIR	140	-0.37550208	-1.4863824	0	0.024099575
	ADIPOGENESIS	182	-0.34566697	-1.4419718	0	0.031806026
	BILE_ACID_METABOLISM	97	-0.36971352	-1.4066579	0.015625	0.040476985
	PANCREAS_BETA_CELLS	25	-0.44706714	-1.2912692	0.12785389	0.11151953
	ANDROGEN_RESPONSE	94	-0.31727812	-1.1900805	0.13002364	0.23157854
	REACTIVE_OXYGEN_SPECIES_PATHWAY	44	-0.36282647	-1.1823199	0.21212122	0.22552656
	PROTEIN_SECRETION	95	-0.29279822	-1.1026067	0.21798365	0.37230617
	INTERFERON_GAMMA_RESPONSE	196	-0.24318652	-1.0051588	0.42296073	0.65203637
	NOTCH_SIGNALING	32	-0.31299964	-0.95326704	0.52863437	0.8100687
	APOPTOSIS	155	-0.23506176	-0.95105946	0.6045198	0.7693902
	XENOBIOTIC_METABOLISM	166	-0.23061712	-0.942889	0.6114458	0.75522876
	INTERFERON_ALPHA_RESPONSE	92	-0.2263158	-0.85332566	0.84010154	0.9764386
	PI3K_AKT_MTOR_SIGNALING	100	-0.19977458	-0.752415	0.9701087	1
	HEME_METABOLISM	168	-0.17921539	-0.7409682	0.9915254	1
	COAGULATION	109	-0.17681946	-0.6876789	0.9951338	0.9862475
HIGH VEGFA165	HYPOXIA	181	0.62167484	2.3726995	0	0
	HEDGEHOG_SIGNALING	33	0.7641555	2.2676477	0	0
	G2M_CHECKPOINT	183	0.56765145	2.1731038	0	0
	ANGIOGENESIS	33	0.7115643	2.0923653	0	0
	MITOTIC_SPINDLE	196	0.5336036	2.07577	0	0
	TNFA_SIGNALING_VIA_NFKB	195	0.5127622	1.9908674	0	0.001034598
	E2F_TARGETS	187	0.4983723	1.9023609	0	0.001664309
	EPITHELIAL_MESENCHYMAL_TRANSITION	191	0.45673972	1.7574736	0	0.005942552
	GLYCOLYSIS	189	0.45741388	1.7475789	0	0.006138033
	WNT_BETA_CATENIN_SIGNALING	39	0.43173003	1.309092	0.10375671	0.1694471
	MYOGENESIS	172	0.34082133	1.3078643	0.048543688	0.15543717
	UNFOLDED_PROTEIN_RESPONSE	105	0.35914072	1.2802411	0.08866995	0.17591524
	SPERMATOGENESIS	94	0.34976658	1.2344395	0.10517799	0.2308027
	UV_RESPONSE_DN	137	0.33390075	1.2185576	0.10856269	0.24084991
	APICAL_JUNCTION	181	0.29788268	1.1310405	0.19359756	0.41116983
	IL2_STAT5_SIGNALING	188	0.29319438	1.1271068	0.20182094	0.39453956
	ESTROGEN_RESPONSE_EARLY	188	0.29324636	1.1201351	0.2234957	0.38908747
	KRAS_SIGNALING_DN	132	0.29865733	1.1079838	0.2388535	0.39461392
	CHOLESTEROL_HOMEOSTASIS	71	0.31803963	1.0749828	0.29180887	0.45540604
	MTORC1_SIGNALING	192	0.2671858	1.0276651	0.38694993	0.55853486
	TGF_BETA_SIGNALING	54	0.2915448	0.93823224	0.55791193	0.8128178
	IL6_JAK_STAT3_SIGNALING	82	0.27230632	0.928485	0.5870647	0.8076632
	APICAL_SURFACE	40	0.3033882	0.90935546	0.59717315	0.8325199
	INFLAMMATORY_RESPONSE	186	0.2112523	0.805062	0.9036697	1
	P53_PATHWAY	188	0.20344523	0.7692833	0.9596899	1
	KRAS_SIGNALING_UP	181	0.18222696	0.69240016	1	1
	COMPLEMENT	179	0.16972785	0.65234965	1	1
	ESTROGEN_RESPONSE_LATE	190	0.15994492	0.61282444	1	1
	UV_RESPONSE_UP	147	0.16380624	0.60822403	1	0.9960304

Table S2. Up-regulated angiogenesis specific genes

Significantly up-regulated angiogenesis genes in patients with high VEGFA165 expression when compared with the low VEGFA165 expression group within the individual VEGFA165 expression model.

Gene Symbol	logFC*	p-value	FDR*
ANGPT2	0.866361664	9.57E-08	0.000166929
ANGPTL4	1.283107967	5.00E-06	0.002377187
COL4A1	0.671547229	0.000135568	0.01371301
COL4A2	0.581363419	0.000540155	0.025940647
DLL4	0.485706414	0.000191141	0.016492744
EPAS1	0.501913167	0.001222211	0.038464132
ESM1	1.197600474	1.48E-10	7.76E-07
EXOC3L2	0.543639754	0.000149154	0.01428238
FLT1	0.915818916	2.89E-11	2.27E-07
KDR	0.642691188	9.47E-06	0.003379643
MCAM	0.476941984	0.000510544	0.025133512
NFIB	0.566239296	0.000426988	0.023963516
NOTCH4	0.667022548	2.33E-08	5.23E-05
* FC = Fold Change, FDR = False Discovery Rate			

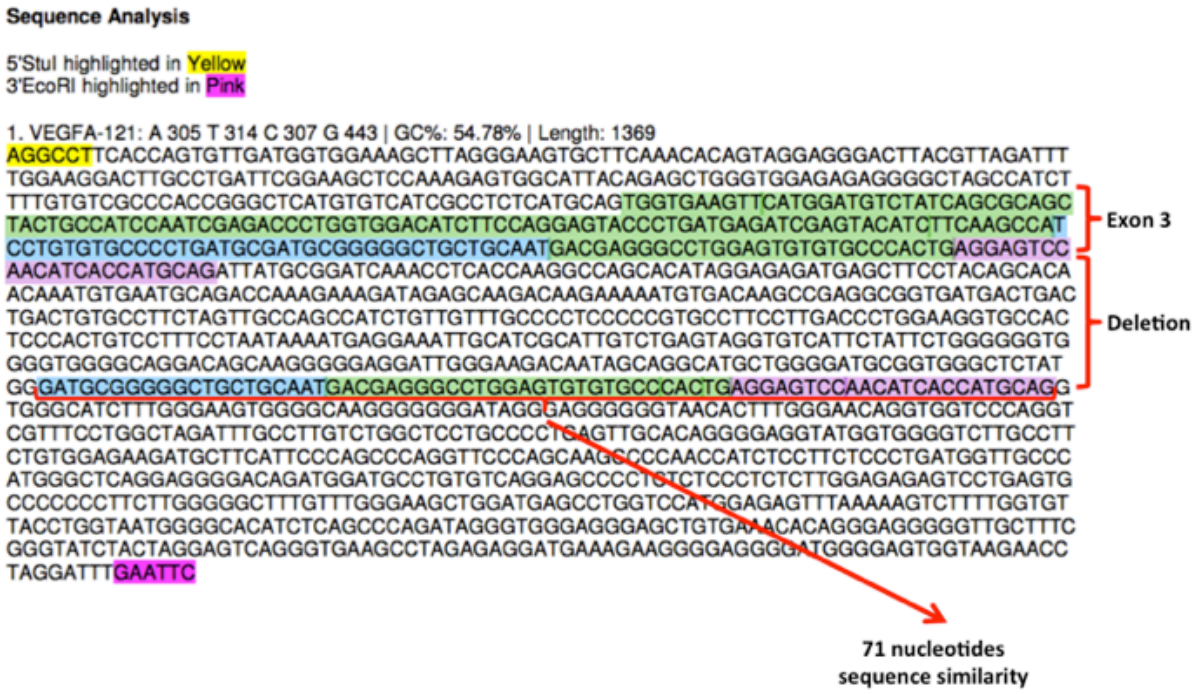

Figure S4. Donor pVEGFA121 sequence analysis.

Sequence analysis showing the 71 nucleotide sequence similarity within the pVEGFA121 vector and the deleted sequence after mutation. Exon 3 is indicated in green and mutation region is indicated in blue.

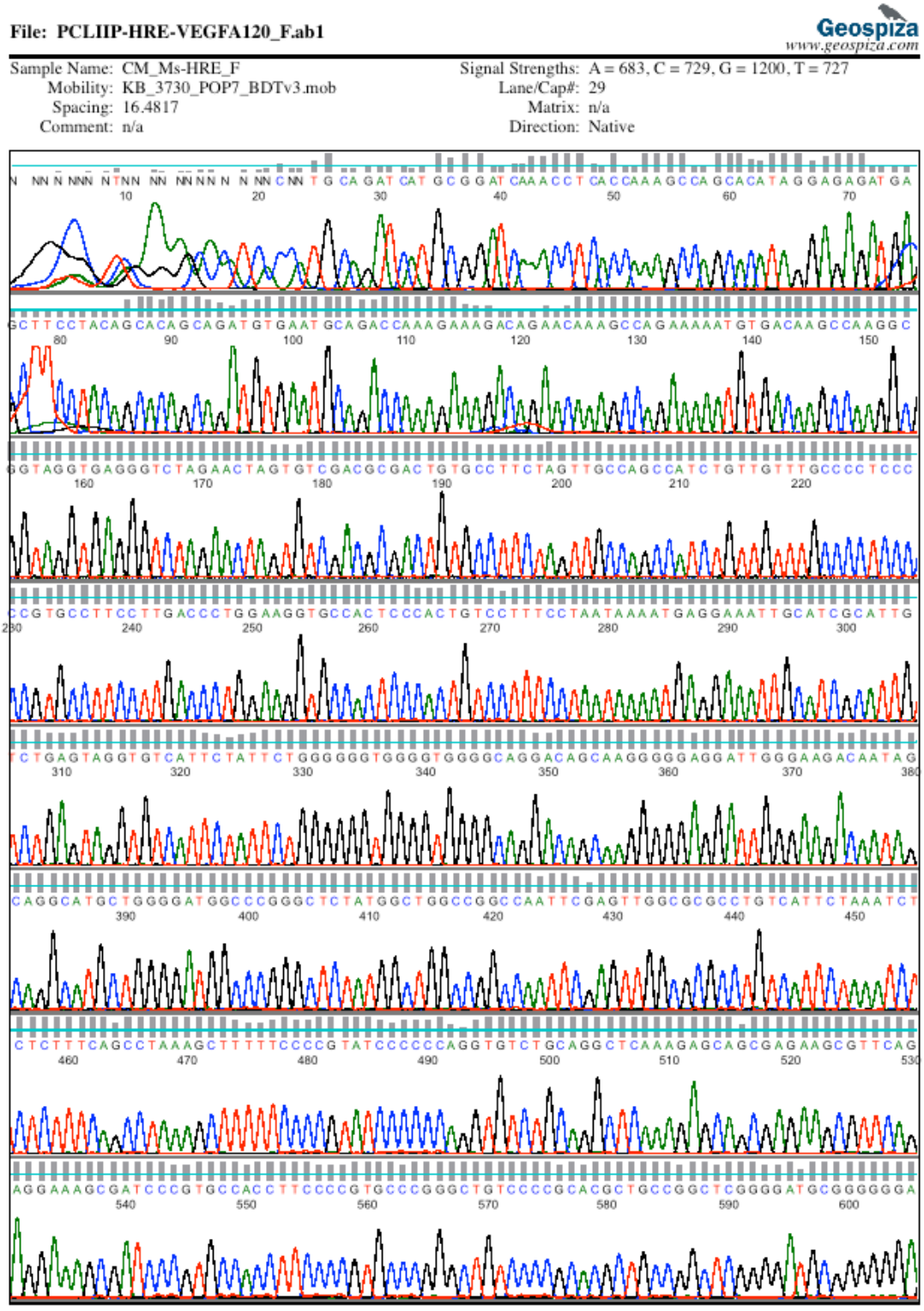

Figure S5. PCLIIP-[HRE]x5-minCMV-VEGFA120 Forward Sequencing.

Chromatogram of forward sequencing of cloned PCLIIP-[HRE]x5-minCMV-VEGFA120 vector.

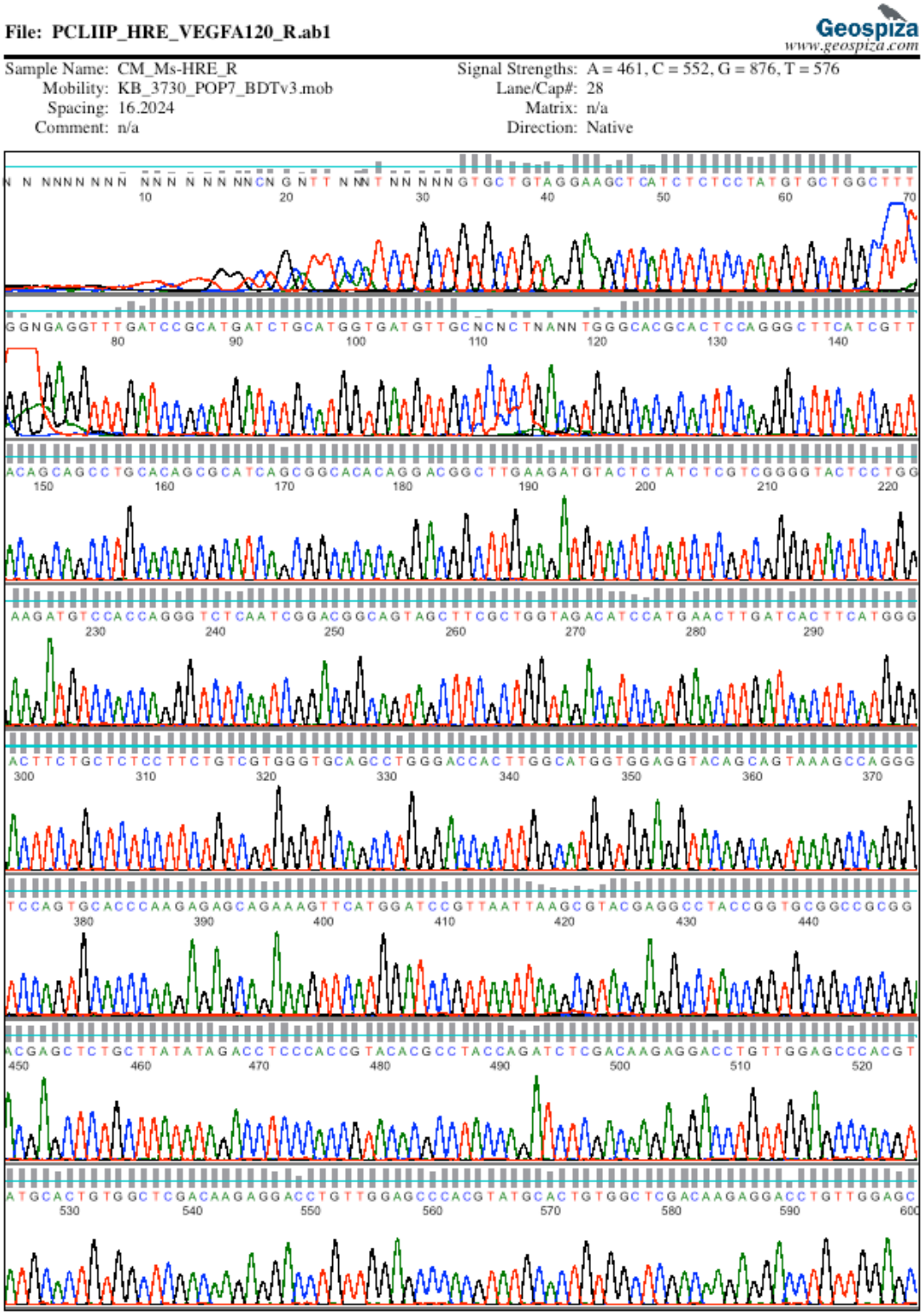

Figure S6. PCLIIP-[HRE]x5-minCMV-VEGFA120 Reverse Sequencing.

Chromatogram of reverse sequencing of cloned PCLIIP-[HRE]x5-minCMV-VEGFA120 vector.

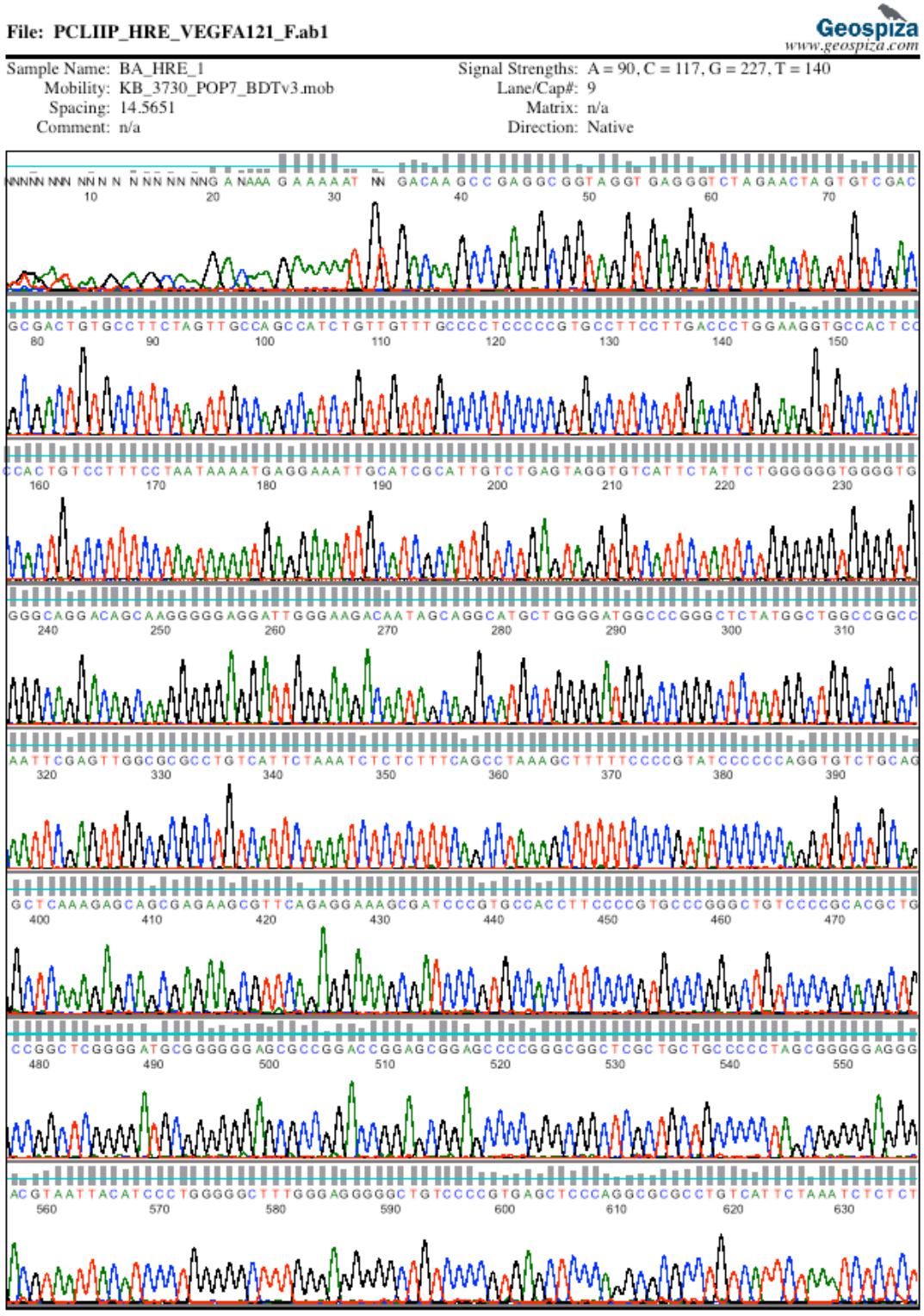

Figure S7. PCLIIP-[HRE]x5-minCMV-VEGFA121 Forward Sequencing.

Chromatogram of forward sequencing of cloned PCLIIP-[HRE]x5-minCMV-VEGFA121 vector.

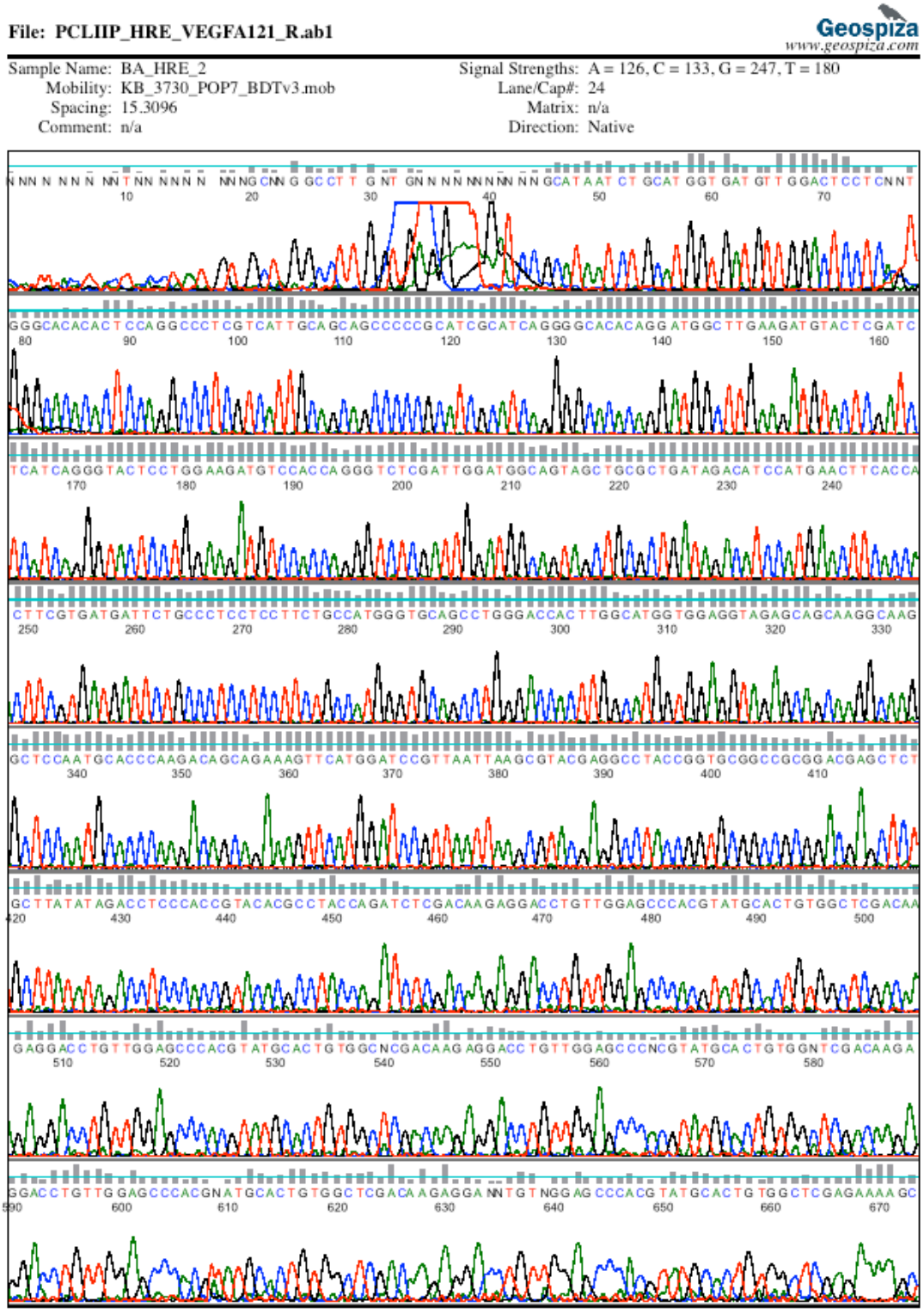

Figure S8. PCLIIP-[HRE]x5-minCMV-VEGFA121 Reverse Sequencing.

Chromatogram of reverse sequencing of cloned PCLIIP-[HRE]x5-minCMV-VEGFA121 vector.

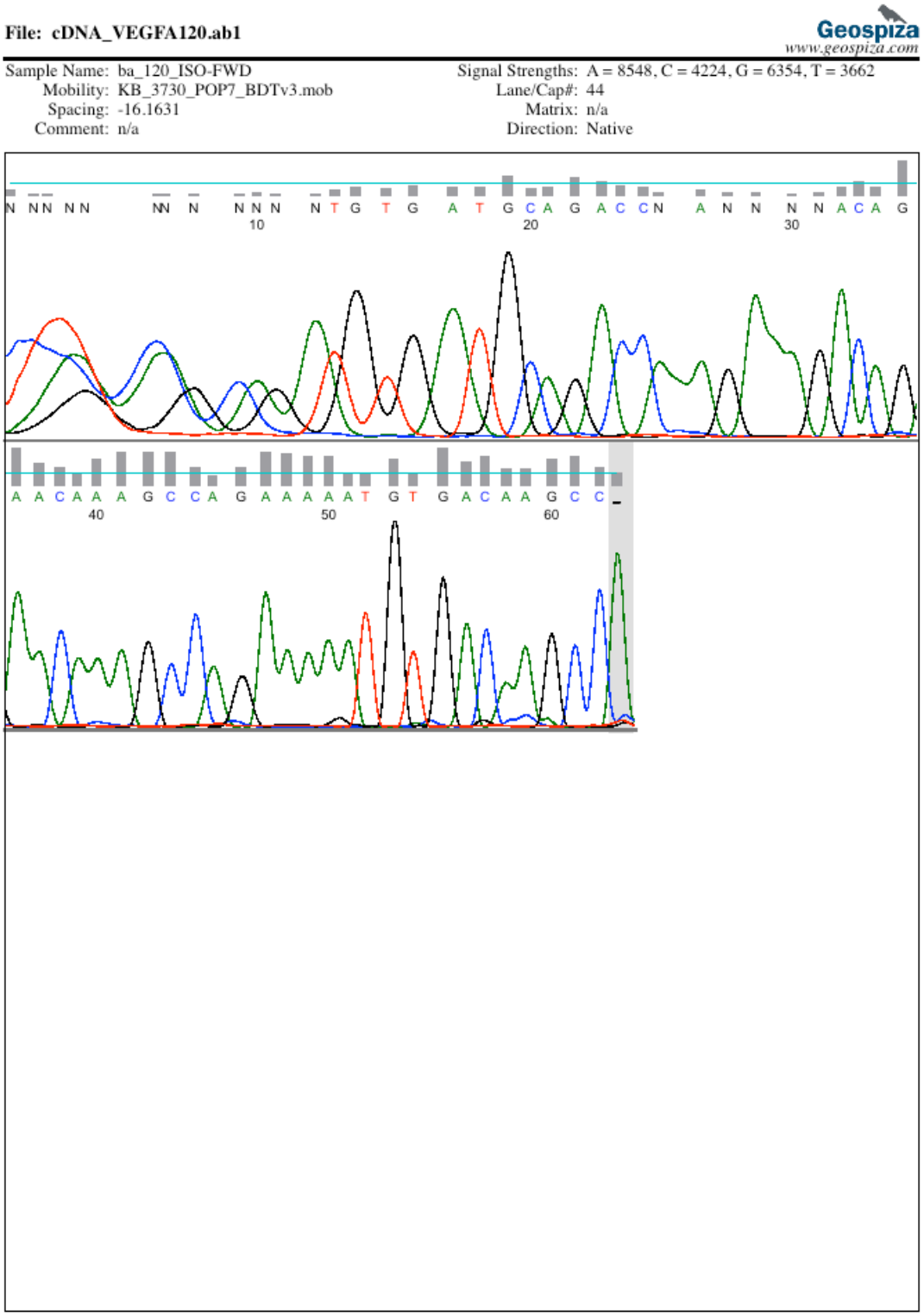

Figure S9. Mouse cDNA VEGFA120 sequencing.

AQRT-PCR primer specificity was validated for mouse VEGFA120 by sequencing the resulting cDNA products from the specific isoform primer pair after reverse transcription using RNA samples from ID8 WT cells.

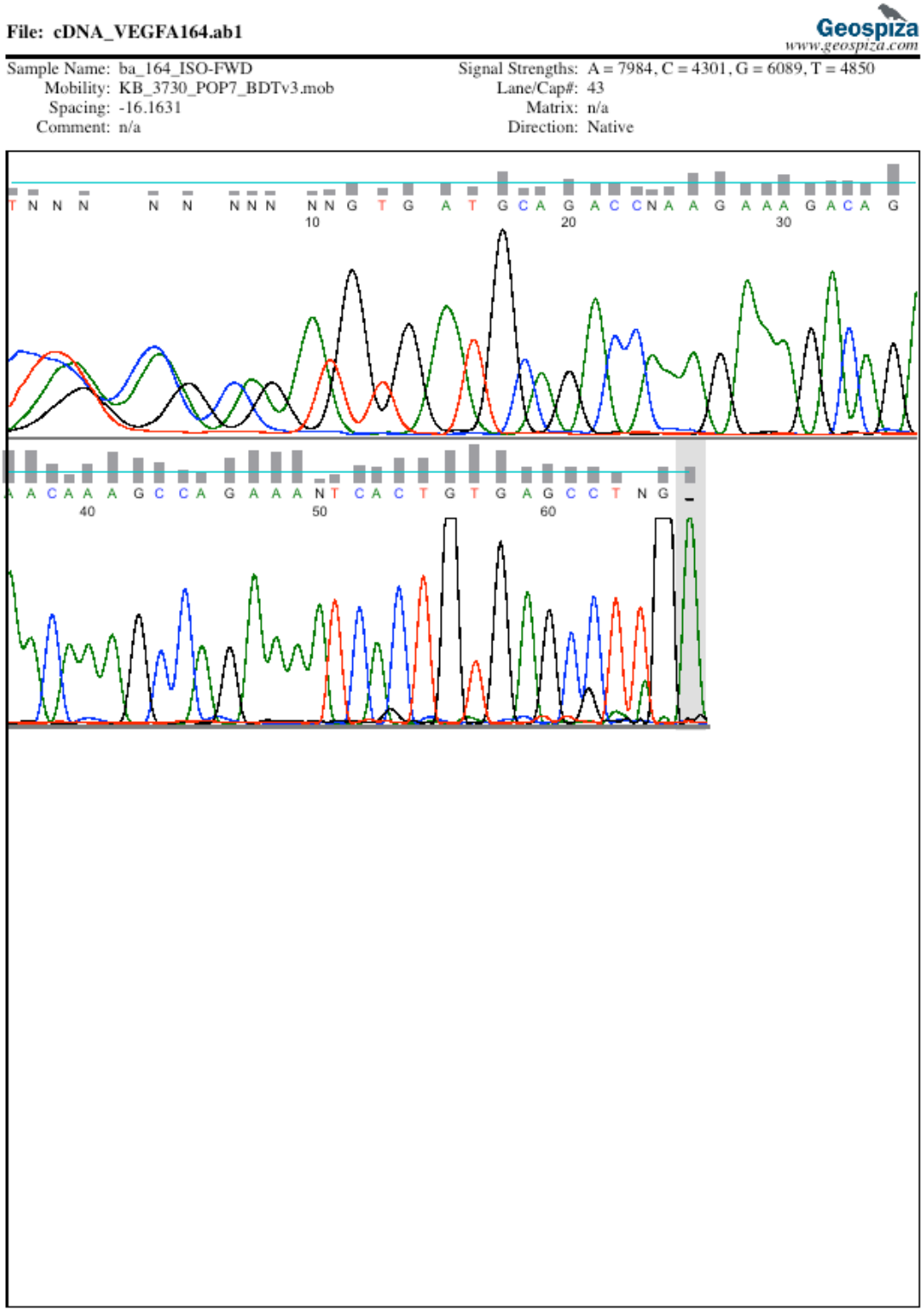

Figure S10. Mouse cDNA VEGFA164 sequencing.

AQRT-PCR primer specificity was validated for mouse VEGFA164 by sequencing the resulting cDNA products from the specific isoform primer pair after reverse transcription using RNA samples from ID8 WT cells.

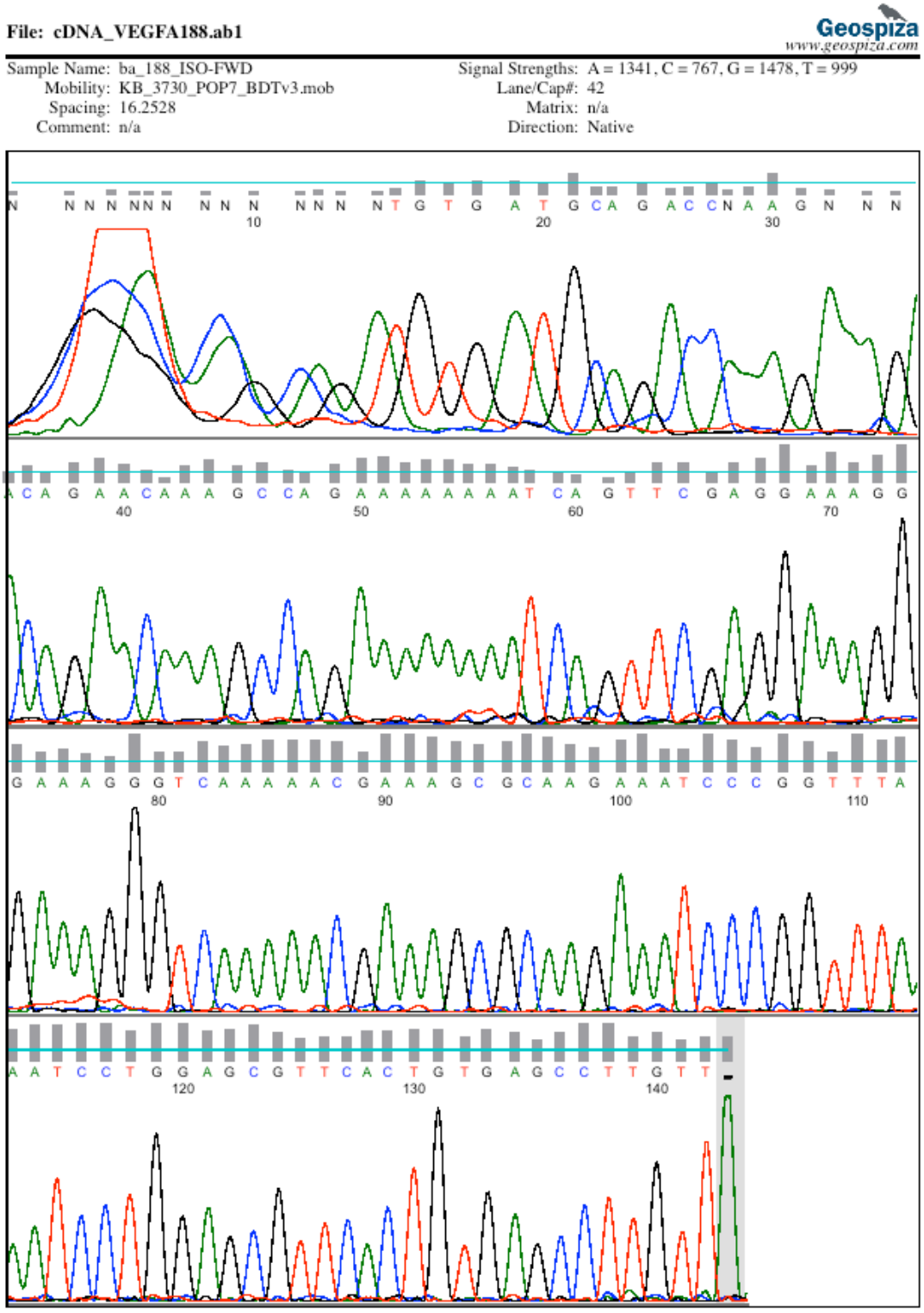

Figure S11. Mouse cDNA VEGFA188 sequencing.

AQRT-PCR primer specificity was validated for mouse VEGFA188 by sequencing the resulting cDNA products from the specific isoform primer pair after reverse transcription using RNA samples from ID8 WT cells.

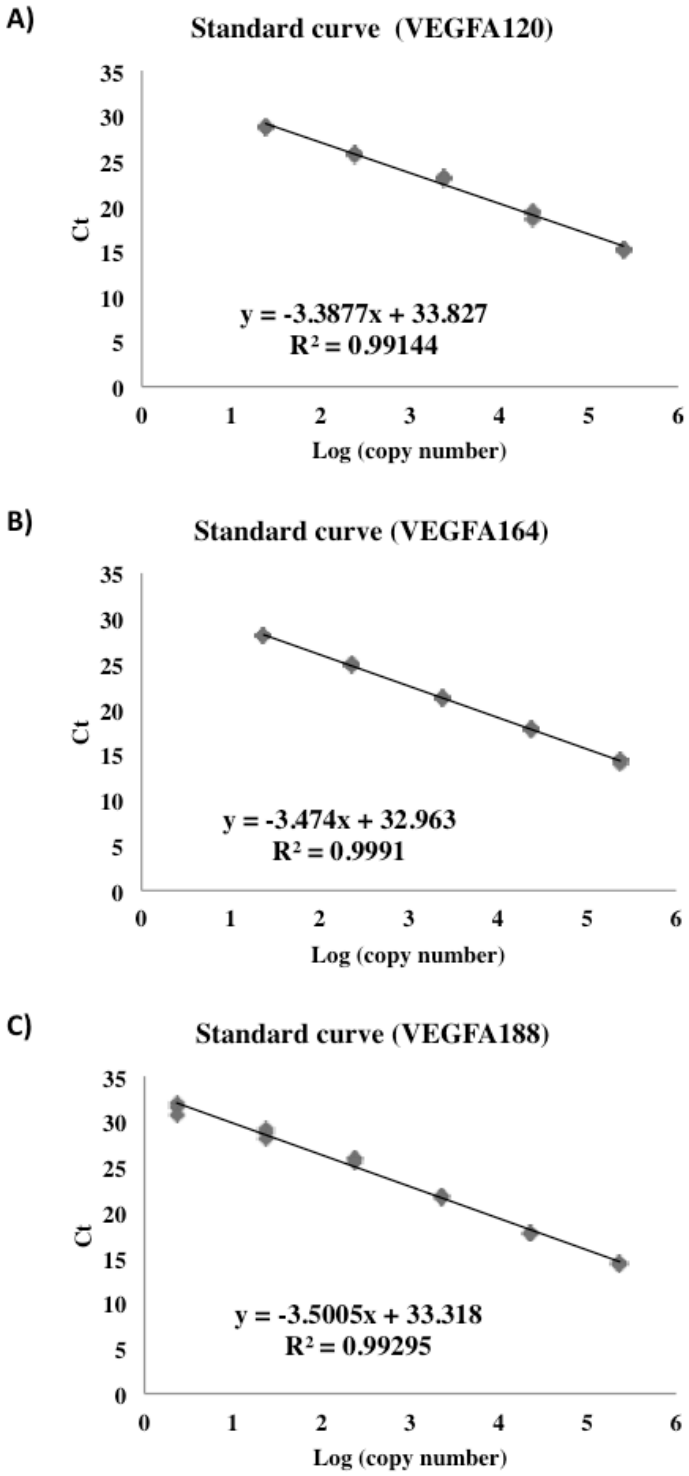

Figure S12. Example of AQRT-PCR standard curves using plasmids.

A) VEGFA120 standard curve using linearised [HRE]x5-minCMV-VEGFA120 plasmid. **B)** VEGFA164 standard curve using linearised [HRE]x5-minCMV-VEGFA164 plasmid. **C)** VEGFA188 standard curve using linearised [HRE]x5-minCMV-VEGFA188 plasmid. 10-fold serial dilutions of each linearised standard were used from of 2.5 copies to 250,000 copies.

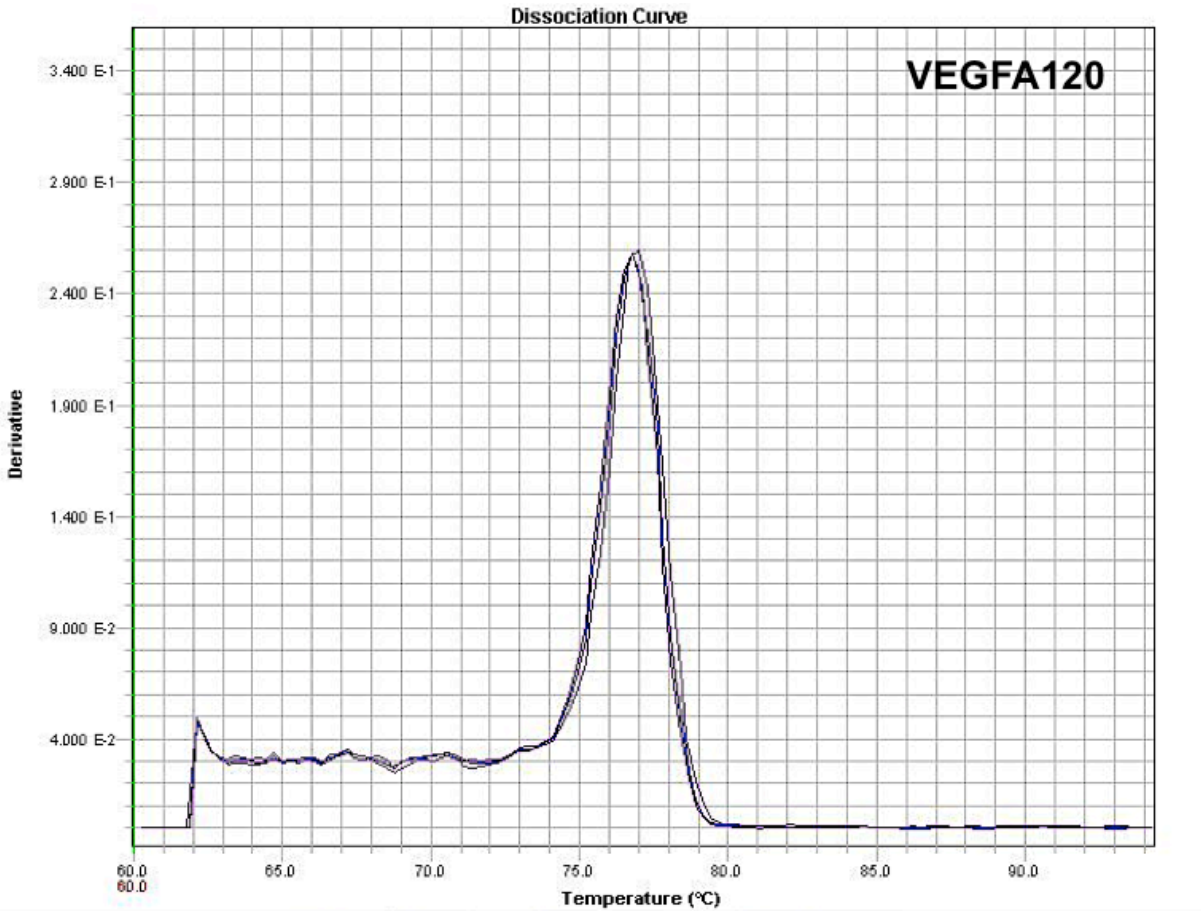

Figure S13. Example of VEGFA120 melt curves.

AQRT-PCR specificity was evaluated using a melt curve analysis in order to identify a single PCR product within each analysed sample. This example is using RNA samples from ID8 WT cells.

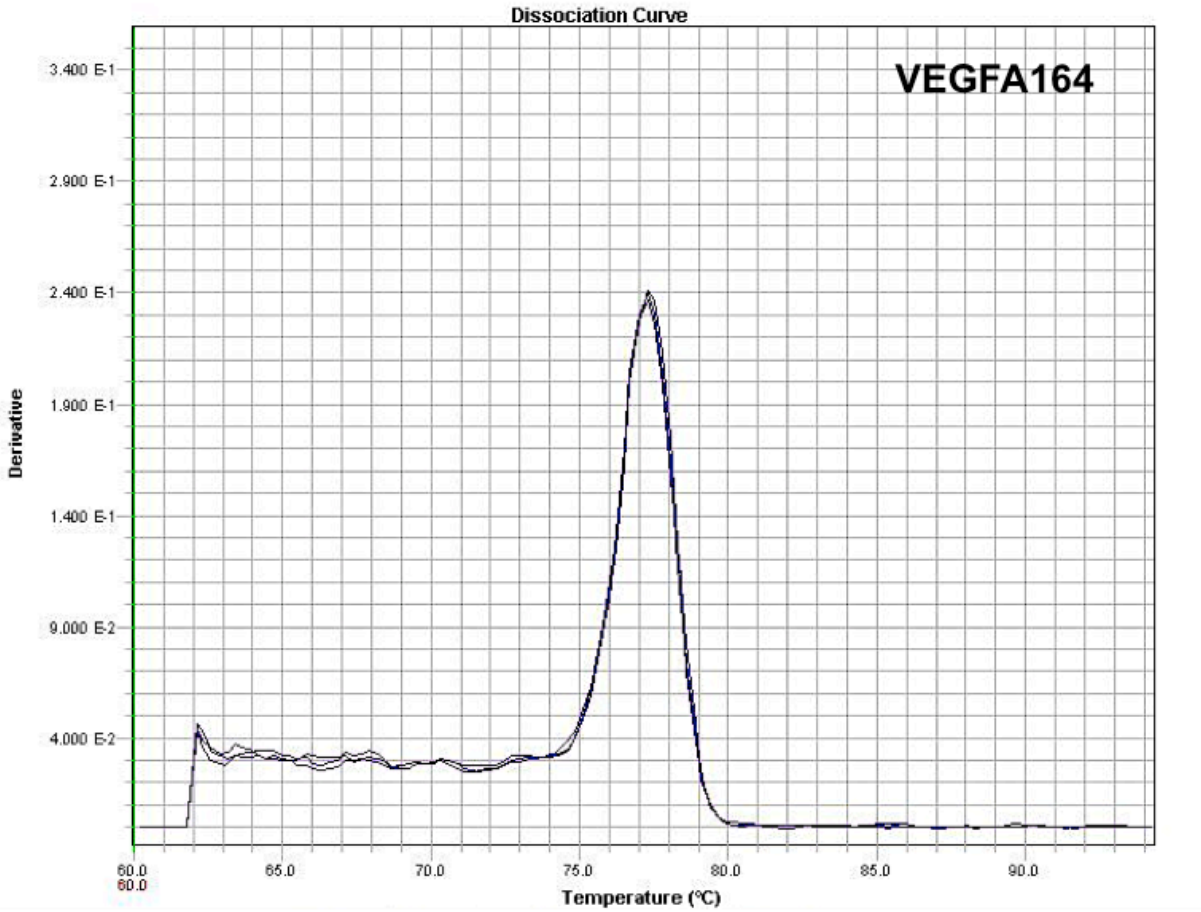

Figure S14. Example of VEGFA164 melt curves.

AQRT-PCR specificity was evaluated using a melt curve analysis in order to identify a single PCR product within each analysed sample. This example is using RNA samples from ID8 WT cells.

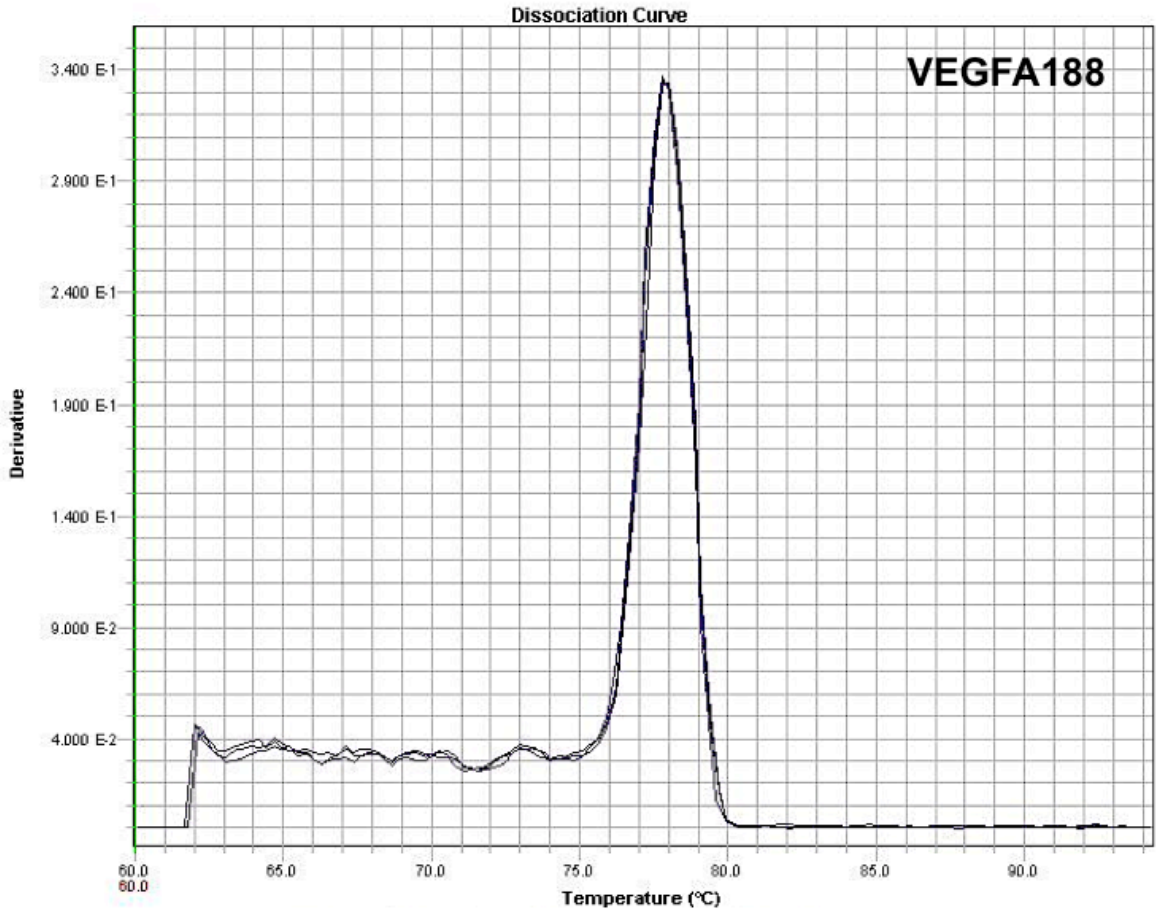

Figure S15. Example of VEGFA188 melt curves.

AQRT-PCR specificity was evaluated using a melt curve analysis in order to identify a single PCR product within each analysed sample. This example is using RNA samples from ID8 WT cells.

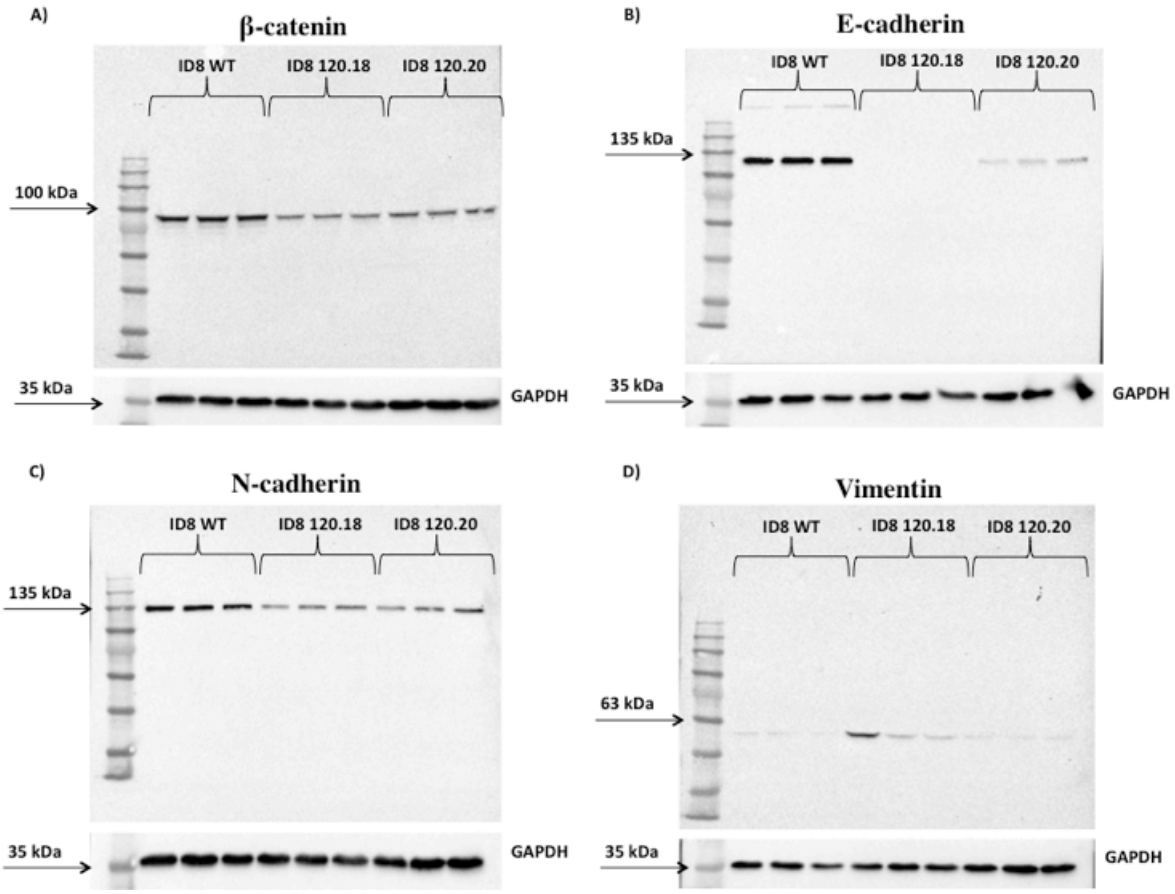

Figure S16. Western blot analysis of EMT markers in ID8 cells.

Example of Western blot images of **A)** β-catenin, **B)** E-cadherin, **C)** N-cadherin and **D)** Vimentin across ID8 WT and ID8 120 clones. GAPDH was used as a loading control

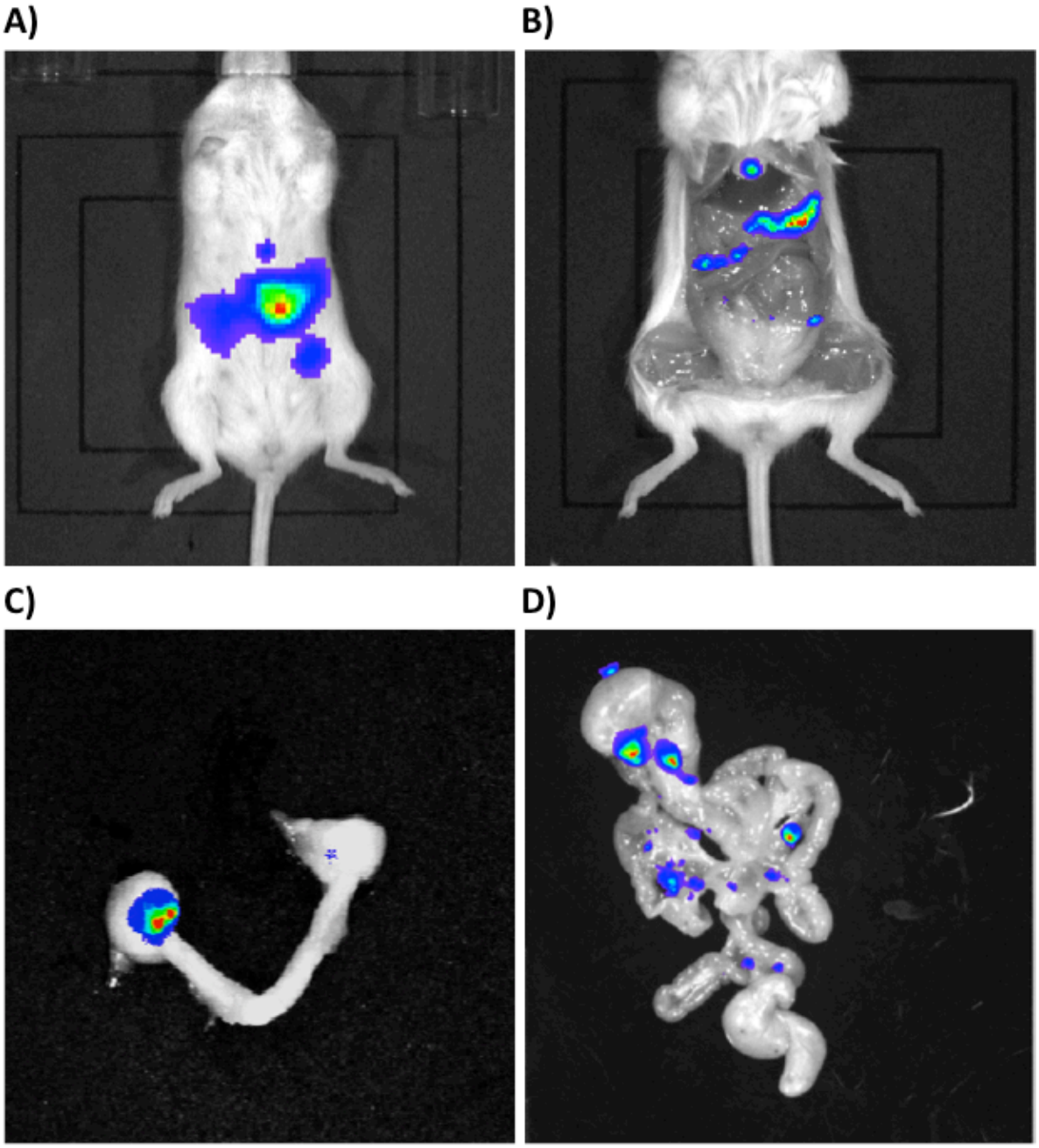

Figure S17. Intraperitoneal distribution of COV362 cells in NSG mice.

Example images of COV362 tumours in the peritoneum and abdominal organs 60 days after inoculation. **A)** Image of the whole body of the live animal, **B)** Image of abdomen in necropsy, **C)** Image of isolated ovaries, **D)** Image of intestines with mesentery. 6-8 weeks old NSG mice (n=4) were injected with 1 x 10^6 COV362 cells expressing luciferase in 100μl PBS intraperitoneally. Tumour growth was monitored weekly using non-invasive bioluminescent imaging on the Xenogen IVIS II.

8. References

Adamcic, U., Skowronski, K., Peters, C., Morrison, J. and Coomber, B. 2012. The effect of bevacizumab on human malignant melanoma cells with functional VEGF/VEGFR2 autocrine and intracrine signaling loops. *Neoplasia*. **14**(7), p612.

Aghajanian, C., Blank, S., Goff, B., Judson, P., Teneriello, M., Husain, A., Sovak, M., Yi, J. and Nycum, L. 2012. OCEANS: a randomized, double-blind, placebo-controlled phase III trial of chemotherapy with or without bevacizumab in patients with platinum-sensitive recurrent epithelial ovarian, primary peritoneal, or fallopian tube cancer. *Journal of clinical oncology : official journal of the American Society of Clinical Oncology*. **30**(17), p2039.

Ahmed, N. and Stenvers, K. 2013. Getting to know ovarian cancer ascites: opportunities for targeted therapy-based translational research. *Frontiers in Oncology*. **3**, p256.

Akerman, S., Fisher, M., Daniel, R.A., Lefley, D., Reyes-Aldasoro, C.C., Lunt, S.J., Harris, S., Bjorndahl, M., Williams, L.J., Evans, H., Barber, P.R., Prise, V.E., Vojnovic, B., Kanthou, C. and Tozer, G.M. 2013. Influence of soluble or matrix-bound isoforms of vascular endothelial growth factor-A on tumor response to vascular-targeted strategies. *Int J Cancer*. **133**(11), pp.2563-2576.

Alvarez Secord, A., Bell Burdett, K., Owzar, K., Tritchler, D., Sibley, A.B., Liu, Y., Starr, M.D., Brady, J.C., Lankes, H.A., Hurwitz, H.I., Mannel, R.S., Tewari, K.S., O'Malley, D.M., Gray, H., Bakkum-Gamez, J.N., Fujiwara, K., Boente, M., Deng, W., Burger, R.A., Birrer, M.J. and Nixon, A.B. 2020. Predictive Blood-Based Biomarkers in Patients with Epithelial Ovarian Cancer Treated with Carboplatin and Paclitaxel with or without Bevacizumab: Results from GOG-0218. *Clin Cancer Res*. **26**(6), pp.1288-1296.

Andorfer, P., Heuwieser, A., Heinzel, A., Lukas, A., Mayer, B. and Perco, P. 2016. Vascular endothelial growth factor A as predictive marker for mTOR inhibition in relapsing high-grade serous ovarian cancer. *BMC Syst Biol*. **10**, p33.

Aran, D., Hu, Z. and Butte, A.J. 2017. xCell: digitally portraying the tissue cellular heterogeneity landscape. *Genome Biol*. **18**(1), p220.

Arauchi, A., Yang, C.H., Cho, S., Jarboe, E.A., Peterson, C.M., Bae, Y.H., Okano, T. and Janat-Amsbury, M.M. 2015. An immunocompetent, orthotopic mouse model of epithelial ovarian cancer utilizing tissue engineered tumor cell sheets. *Tissue Eng Part C Methods*. **21**(1), pp.23-34.

Arcondeguy, T., Lacazette, E., Millevoi, S., Prats, H. and Touriol, C. 2013. VEGF-A mRNA processing, stability and translation: a paradigm for intricate regulation of gene expression at the post-transcriptional level. *Nucleic Acids Res*. **41**(17), pp.7997-8010.

Aust, S., Knogler, T., Pils, D., Obermayr, E., Reinthaller, A., Zahn, L., Radlgruber, I., Mayerhoefer, M., Grimm, C. and Polterauer, S. 2015. Skeletal muscle depletion and markers for cancer cachexia are strong prognostic factors in epithelial ovarian cancer. *PLoS ONE*. **10**(10).

Backen, A., Renehan, A.G., Clamp, A.R., Berzuini, C., Zhou, C., Oza, A., Bannoo, S., Scherer, S.J., Banks, R.E., Dive, C. and Jayson, G.C. 2014. The combination of circulating Ang1 and Tie2 levels predicts progression-free survival advantage in bevacizumab-treated patients with ovarian cancer. *Clin Cancer Res*. **20**(17), pp.4549-4558.

Baert, T., Verschuere, T., Van Hoylandt, A., Gijsbers, R., Vergote, I. and Coosemans, A. 2015. The dark side of ID8-Luc2: pitfalls for luciferase tagged murine models for ovarian cancer. *J Immunother Cancer*. **3**, p57.

Bais, C., Mueller, B., Brady, M.F., Mannel, R.S., Burger, R.A., Wei, W., Marien, K.M., Kockx, M.M., Husain, A., Birrer, M.J. and Group, N.R.G.O.G.O. 2017. Tumor Microvessel Density as a Potential Predictive Marker for Bevacizumab Benefit: GOG-0218 Biomarker Analyses. *J Natl Cancer Inst*. **109**(11).

Bais, C., Rabe, C., Wild, N., Swiatek-De Lange, M., Chen, D., Hong, K., Amier, L., Moore, N. and Hegde, P.S. 2014. Comprehensive reassessment of plasma VEGFA(pVEGFA) as a candidate predictive biomarker for bevacizumab (Bv) in 13 pivotal trials (seven indications). *J. Clin. Oncol*. **32**(15).

Banerjee, S. and Kaye, S.B. 2013. New strategies in the treatment of ovarian cancer: Current clinical perspectives and future potential. *Clinical Cancer Research*. **19**(5), pp.961-968.

Bates, D.O., Cui, T.G., Doughty, J.M., Winkler, M., Sugiono, M., Shields, J.D., Peat, D., Gillatt, D. and Harper, S.J. 2002. VEGF165b, an inhibitory splice variant of vascular endothelial growth factor, is down-regulated in renal cell carcinoma. *Cancer Res*. **62**(14), pp.4123-4131.

Bayko, L., Rak, J., Man, S., Bicknell, R., Ferrara, N. and Kerbel, R.S. 1998. The dormant in vivo phenotype of early stage primary human melanoma: termination by overexpression of vascular endothelial growth factor. *Angiogenesis*. **2**(3), pp.203-217.

Beaufort, C., Helmijr, J., Piskorz, A., Hoogstraat, M., Ruigrok-Ritstier, K., Besselink, N., Murtaza, M., van Ijcken, W., Heine, A., Smid, M., Koudijs, M., Brenton, J., Berns, E., Helleman, J. and Pearson, R. 2014. Ovarian Cancer Cell Line Panel (OCCP): Clinical Importance of In Vitro Morphological Subtypes. *PLoS ONE*. **9**(9).

Berridge, M.V., Tan, A.S., McCoy, K.D. and Wang, R. 1996. The biochemical and cellular basis of cell proliferation assays that use tetrazolium salts. *Biochemica*. **4**(1), pp.14-19.

Bhattacharya, R., Ye, X., Wang, R., Ling, X., McManus, M., Fan, F., Boulbes, D. and Ellis, L. 2016. Intracrine VEGF Signaling Mediates the Activity of Prosurvival Pathways in Human Colorectal Cancer Cells. *Cancer research*. **76**(10), p3014.

Biselli-Chicote, P., Oliveira, A., Pavarino, E. and Goloni-Bertollo, E. 2012. VEGF gene alternative splicing: pro- and anti-angiogenic isoforms in cancer. *Journal of Cancer Research and Clinical Oncology*. **138**(3), pp.363-370.

Bowtell, D.D., Bohm, S., Ahmed, A.A., Aspuria, P., Bast, R.C., Beral, V., Berek, J., Birrer, M., Blagden, S., Bookman, M.A., Brenton, J.D., Chiappinelli, K., Martins, F., Coukos, G., Drapkin, R., Edmondson, R., Fotopoulou, C., Gabra, H., Galon, J., Gourley, C., Heong, V., Huntsman, D.G., Iwanicki, M., Karlan, B., Kaye, A., Lengyel, E., Levine, D., Lu, K., McNeish, I., Menon, U., Narod, S.A., Nelson, B., Nephew, K., Pharoah, P., Powell, D., Ramos, P., Romero, I., Scott, C., Sood, A., Stronach, E. and Balkwill, F. 2015. *Rethinking ovarian cancer II: reducing mortality from high-grade serous ovarian cancer*. Nat. Rev. Cancer. 15. pp.668-679.

Brennan, S.E., Kuwano, Y., Alkharouf, N., Blackshear, P.J., Gorospe, M. and Wilson, G.M. 2009. The mRNA-destabilizing protein tristetraprolin is suppressed in many cancers, altering tumorigenic phenotypes and patient prognosis. *Cancer Res*. **69**(12), pp.5168-5176.

Broseus, J., Mourah, S., Ramstein, G., Bernard, S., Mounier, N., Cuccuini, W., Gaulard, P., Gisselbrecht, C., Briere, J., Houlgatte, R. and Thieblemont, C. 2017. VEGF121, is predictor for survival in activated B-cell-like diffuse large B-cell lymphoma and is related to an immune response gene signature conserved in cancers. *Oncotarget*. **8**(53), pp.90808-90824.

Buffa, F.M., Harris, A.L., West, C.M. and Miller, C.J. 2010. Large meta-analysis of multiple cancers reveals a common, compact and highly prognostic hypoxia metagene. *Br J Cancer*. **102**(2), pp.428-435.

Burger, R. 2011. Overview of anti-angiogenic agents in development for ovarian cancer. *Gynecologic Oncology*. **121**(1), pp.230-238.

Burger, R.A., Brady, M.F., Bookman, M.A., Fleming, G.F., Monk, B.J., Huang, H., Mannel, R.S., Homesley, H.D., Fowler, J., Greer, B.E., Boente, M., Birrer, M.J., Liang, S.X. and Gynecologic Oncology, G. 2011. Incorporation of bevacizumab in the primary treatment of ovarian cancer. *N Engl J Med*. **365**(26), pp.2473-2483.

Buroker, N. 2015. VEGFA SNPs (rs34357231 & rs35569394), Transcriptional Factor Binding Sites and Human Disease. *Journal of Advances in Medicine and Medical Research*. **10**(12), pp.1-11.

Cancer Genome Atlas Research, N. 2011. Integrated genomic analyses of ovarian carcinoma. *Nature*. **474**(7353), pp.609-615.

Chambers, L.M., Esakov, E., Braley, C., AlHilli, M., Michener, C. and Reizes, O. 2020. Use of Transabdominal Ultrasound for the detection of intra-peritoneal tumor engraftment and growth in mouse xenografts of epithelial ovarian cancer. *PLoS One*. **15**(4), pe0228511.

Chen, G.M., Kannan, L., Geistlinger, L., Kofia, V., Safikhani, Z., Gendoo, D.M.A., Parmigiani, G., Birrer, M., Haibe-Kains, B. and Waldron, L. 2018. Consensus on Molecular Subtypes of High-Grade Serous Ovarian Carcinoma. *Clin Cancer Res*. **24**(20), pp.5037-5047.

Chen, V.W., Ruiz, B., Killeen, J.L., Cote, T.R., Wu, X.C. and Correa, C.N. 2003. Pathology and classification of ovarian tumors. *Cancer*. **97**(10 Suppl), pp.2631-2642.

Chesnokov, M.S., Khesina, P.A., Shavochkina, D.A., Kustova, I.F., Dyakov, L.M., Morozova, O.V., Mugue, N.S., Kudashkin, N.E., Moroz, E.A., Patyutko, Y.I. and Lazarevich, N.L. 2018. Shift in VEGFA isoform balance towards more angiogenic variants is associated with tumor stage and differentiation of human hepatocellular carcinoma. *PeerJ*. **6**, pe4915.

Cheung, N., Wong, M.P., Yuen, S.T., Leung, S.Y. and Chung, L.P. 1998. Tissue-specific expression pattern of vascular endothelial growth factor isoforms in the malignant transformation of lung and colon. *Hum Pathol*. **29**(9), pp.910-914.

Cho, S., Sun, Y., Soisson, A.P., Dodson, M.K., Peterson, C.M., Jarboe, E.A., Kennedy, A.M. and Janat-Amsbury, M.M. 2013. Characterization and evaluation of pre-clinical suitability of a syngeneic orthotopic mouse ovarian cancer model. *Anticancer Res*. **33**(4), pp.1317-1324.

Ciciola, P., Cascetta, P., Bianco, C., Formisano, L. and Bianco, R. 2020. Combining Immune Checkpoint Inhibitors with Anti-Angiogenic Agents. *J Clin Med*. **9**(3).

Claesson-Welsh, L. and Welsh, M. 2013. VEGFA and tumour angiogenesis. *J Intern Med*. **273**(2), pp.114-127.

Clarke, J.M. and Hurwitz, H.I. 2013. Understanding and targeting resistance to anti-angiogenic therapies. *J Gastrointest Oncol*. **4**(3), pp.253-263.

Coleman, R., Monk, B., Sood, A. and Herzog, T. 2013. Latest research and treatment of advanced-stage epithelial ovarian cancer. *Nature Reviews Clinical Oncology*. **10**(4), p211.

Coleman, R.L., Brady, M.F., Herzog, T.J., Sabbatini, P., Armstrong, D.K., Walker, J.L., Kim, B.G., Fujiwara, K., Tewari, K.S., O'Malley, D.M., Davidson, S.A., Rubin, S.C., DiSilvestro, P., Basen-Engquist, K., Huang, H., Chan, J.K., Spirtos, N.M., Ashfaq, R. and Mannel, R.S. 2017. Bevacizumab and paclitaxel-carboplatin chemotherapy and secondary cytoreduction in recurrent, platinum-sensitive ovarian cancer (NRG Oncology/Gynecologic Oncology Group study GOG-0213): a multicentre, open-label, randomised, phase 3 trial. *Lancet Oncol*. **18**(6), pp.779-791.

Collinson, F., Hutchinson, M., Craven, R.A., Cairns, D.A., Zougman, A., Wind, T.C., Gahir, N., Messenger, M.P., Jackson, S., Thompson, D., Adusei, C., Ledermann, J.A., Hall, G., Jayson, G.C., Selby, P.J. and Banks, R.E. 2013. Predicting response to bevacizumab in ovarian cancer: a panel of potential biomarkers informing treatment selection. *Clin Cancer Res*. **19**(18), pp.5227-5239.

Dalal, V., Kumar, R., Kumar, S., Sharma, A., Kumar, L., Sharma, J.B., Roy, K.K., Singh, N. and Vanamail, P. 2018. Biomarker potential of IL-6 and VEGF-A in ascitic fluid of epithelial ovarian cancer patients. *Clin Chim Acta*. **482**, pp.27-32.

Dardente, H., English, W.R., Valluru, M.K., Kanthou, C. and Simpson, D. 2020. Debunking the Myth of the Endogenous Antiangiogenic Vegfaxxxb Transcripts. *Trends Endocrinol Metab*. **31**(6), pp.398-409.

Darland, D.C., Cain, J.T., Berosik, M.A., Saint-Geniez, M., Odens, P.W., Schaubhut, G.J., Frisch, S., Stemmer-Rachamimov, A., Darland, T. and D'Amore, P.A. 2011. Vascular endothelial growth factor (VEGF) isoform regulation of early forebrain development. *Dev Biol*. **358**(1), pp.9-22.

Decio, A., Taraboletti, G., Patton, V., Alzani, R., Perego, P., Fruscio, R., Jürgensmeier, J.M., Giavazzi, R. and Belotti, D. 2014. Vascular Endothelial Growth Factor C Promotes Ovarian Carcinoma Progression through Paracrine and Autocrine Mechanisms. *The American Journal of Pathology*. **184**(4), pp.1050-1061.

Di Benedetto, M., Toullec, A., Buteau-Lozano, H., Abdelkarim, M., Vacher, S., Velasco, G., Christofari, M., Pocard, M., Bieche, I. and Perrot-Applanat, M. 2015. MDA-MB-231 breast cancer cells overexpressing single VEGF isoforms display distinct colonisation characteristics. *Br J Cancer*. **113**(5), pp.773-785.

Domcke, S., Sinha, R., Levine, D., Sander, C. and Schultz, N. 2013. Evaluating cell lines as tumour models by comparison of genomic profiles. *Nature Communications*. **4**, p2126.

Domigan, K.C., Ziyad, L.S. and Iruela-Arispe, L.M. 2015. Canonical and Noncanonical Vascular Endothelial Growth Factor Pathways: New Developments in Biology and Signal Transduction. *Arteriosclerosis, Thrombosis, and Vascular Biology*. **35**(1), pp.30-39.

Duyndam, M.C., Hilhorst, M.C., Schluper, H.M., Verheul, H.M., van Diest, P.J., Kraal, G., Pinedo, H.M. and Boven, E. 2002. Vascular endothelial growth factor-165 overexpression stimulates angiogenesis and induces cyst formation and macrophage infiltration in human ovarian cancer xenografts. *Am J Pathol*. **160**(2), pp.537-548.

English, W.R., Lunt, S.J., Fisher, M., Lefley, D.V., Dhingra, M., Lee, Y.C., Bingham, K., Hurrell, J.E., Lyons, S.K., Kanthou, C. and Tozer, G.M. 2017. Differential Expression of VEGFA Isoforms Regulates Metastasis and Response to Anti-VEGFA Therapy in Sarcoma. *Cancer Res*. **77**(10), pp.2633-2646.

Farolfi, A., Petrone, M., Scarpi, E., Galla, V., Greco, F., Casanova, C., Longo, L., Cormio, G., Orditura, M., Bologna, A., Zavallone, L., Ventriglia, J., Franzese, E., Loizzi, V., Giardina, D., Pigozzi, E., Cioffi, R., Pignata, S., Giorda, G. and De Giorgi, U. 2018. Inflammatory Indexes as Prognostic and Predictive Factors in Ovarian Cancer Treated with Chemotherapy Alone or Together with Bevacizumab. A Multicenter, Retrospective Analysis by the MITO Group (MITO 24). *Target Oncol*. **13**(4), pp.469-479.

Fearnley, G., Smith, G., Abdul-Zani, I., Yuldasheva, N., Mughal, N., Homer-Vanniasinkam, S., Kearney, M., Zachary, I., Tomlinson, D.C., Harrison, M.A., Wheatcroft, S.B. and Ponnambalam, S. 2016. VEGF-A isoforms program differential VEGFR2 signal transduction, trafficking and proteolysis. *Biol. Open*. **5**(5), pp.571-583.

Fearnley, G.W., Bruns, A.F., Wheatcroft, S.B. and Ponnambalam, S. 2015. VEGF-A isoform-specific regulation of calcium ion flux, transcriptional activation and endothelial cell migration. *Biol Open*. **4**(6), pp.731-742.

Fearnley, G.W., Odell, A.F., Latham, A.M., Mughal, N.A., Bruns, A.F., Burgoyne, N.J., Homer-Vanniasinkam, S., Zachary, I.C., Hollstein, M.C., Wheatcroft, S.B. and Ponnambalam, S. 2014. VEGF-A isoforms differentially regulate ATF-2-dependent VCAM-1 gene expression and endothelial-leukocyte interactions. *Mol Biol Cell*. **25**(16), pp.2509-2521.

Fenton, B.M., Paoni, S.F., Liu, W., Cheng, S.Y., Hu, B. and Ding, I. 2004. Overexpression of VEGF121, but not VEGF165 or FGF-1, improves oxygenation in MCF-7 breast tumours. *Br J Cancer*. **90**(2), pp.430-435.

Furuta, T., Ueda, T., Aune, G., Sarasin, A., Kraemer, K. and Pommier, Y. 2002. Transcription-coupled nucleotide excision repair as a determinant of cisplatin sensitivity of human cells. *Cancer Research*. **62**(17), p4899.

Galluzzi, L., Senovilla, L., Vitale, I., Michels, J., Martins, I., Kepp, O., Castedo, M. and Kroemer, G. 2011. Molecular mechanisms of cisplatin resistance. *Oncogene*. **31**(15), p1869.

Gao, J., Aksoy, B.A., Dogrusoz, U., Dresdner, G., Gross, B., Sumer, S.O., Sun, Y., Jacobsen, A., Sinha, R., Larsson, E., Cerami, E., Sander, C. and Schultz, N. 2013. Integrative analysis of complex cancer genomics and clinical profiles using the cBioPortal. *Sci Signal*. **6**(269), ppl1.

Garcia, V., Garcia, J.M., Pena, C., Silva, J., Dominguez, G., Lorenzo, Y., Diaz, R., Espinosa, P., de Sola, J.G., Cantos, B. and Bonilla, F. 2008. Free circulating mRNA in plasma from breast cancer patients and clinical outcome. *Cancer Lett*. **263**(2), pp.312-320.

Gavalas, N., Tsiatas, M., Tsitsilonis, O., Politi, E., Ioannou, K., Ziogas, A., Rodolakis, A., Vlahos, G., Thomakos, N., Haidopoulos, D., Terpos, E., Antsaklis, A., Dimopoulos, M. and Bamias, A. 2012. VEGF directly suppresses activation of T cells from ascites secondary to ovarian cancer via VEGF receptor type 2. *British Journal of Cancer*. **107**(11), p1869.

George, E., Kim, H., Krepler, C., Wenz, B., Makvandi, M., Tanyi, J.L., Brown, E., Zhang, R., Brafford, P., Jean, S., Mach, R.H., Lu, Y., Mills, G.B., Herlyn, M., Morgan, M., Zhang, X., Soslow, R., Drapkin, R., Johnson, N., Zheng, Y., Cotsarelis, G., Nathanson, K.L. and Simpkins, F. 2017. A patient-derived-xenograft platform to study BRCA-deficient ovarian cancers. *JCI Insight*. **2**(1), pe89760.

Goel, H. and Mercurio, A. 2013. VEGF targets the tumour cell. *Nature Reviews Cancer*. **13**(12), p871.

Goel, S., Wong, A. and Jain, R. 2012. Vascular normalization as a therapeutic strategy for malignant and nonmalignant disease. *Cold Spring Harbor perspectives in medicine*. **2**(3), pa006486.

Goldman, M.J., Craft, B., Hastie, M., Repecka, K., McDade, F., Kamath, A., Banerjee, A., Luo, Y., Rogers, D., Brooks, A.N., Zhu, J. and Haussler, D. 2020. Visualizing and interpreting cancer genomics data via the Xena platform. *Nat Biotechnol*. **38**(6), pp.675-678.

GTEx Consortium. 2013. The Genotype-Tissue Expression (GTEx) project. *Nat Genet*. **45**(6), pp.580-585.

Guo, B.Q. and Lu, W.Q. 2018. The prognostic significance of high/positive expression of tissue VEGF in ovarian cancer. *Oncotarget*. **9**(55), pp.30552-30560.

Guo, P., Fang, Q., Tao, H.Q., Schafer, C.A., Fenton, B.M., Ding, I., Hu, B. and Cheng, S.Y. 2003. Overexpression of vascular endothelial growth factor by MCF-7 breast cancer cells promotes estrogen-independent tumor growth in vivo. *Cancer Res*. **63**(15), pp.4684-4691.

Halvorsen, A.R., Kristensen, G., Embleton, A., Adusei, C., Barretina-Ginesta, M.P., Beale, P. and Helland, A. 2017. Evaluation of Prognostic and Predictive Significance of Circulating MicroRNAs in Ovarian Cancer Patients. *Dis Markers*. **2017**, p3098542.

Hanahan, D. and Weinberg, R.A. 2011. Hallmarks of cancer: the next generation. *Cell*. **144**(5), pp.646-674.

Hansen, K., Coussens, M.J., Sago, J., Subramanian, S., Gjoka, M. and Briner, D. 2012. Genome editing with CompoZr custom zinc finger nucleases (ZFNs). *J Vis Exp*. (64), pe3304.

Harris, S., Craze, M., Newton, J., Fisher, M., Shima, D.T., Tozer, G.M. and Kanthou, C. 2012. Do anti-angiogenic VEGF (VEGFxxxb) isoforms exist? A cautionary tale. *PLoS One*. **7**(5), pe35231.

Hartl, C.A., Bertschi, A., Puerto, R.B., Andresen, C., Cheney, E.M., Mittendorf, E.A., Guerriero, J.L. and Goldberg, M.S. 2019. Combination therapy targeting both innate and adaptive immunity improves survival in a pre-clinical model of ovarian cancer. *J Immunother Cancer*. **7**(1), p199.

Hernandez, L., Kim, M.K., Lyle, L.T., Bunch, K.P., House, C.D., Ning, F., Noonan, A.M. and Annunziata, C.M. 2016. Characterization of ovarian cancer cell lines as in vivo models for preclinical studies. *Gynecol Oncol*. **142**(2), pp.332-340.

Herve, M.A., Buteau-Lozano, H., Vassy, R., Bieche, I., Velasco, G., Pla, M., Perret, G., Mourah, S. and Perrot-Applanat, M. 2008. Overexpression of vascular endothelial growth factor 189 in breast cancer cells leads to delayed tumor uptake with dilated intratumoral vessels. *Am J Pathol*. **172**(1), pp.167-178.

Honami, N. and Denise, J.M. 2005. Ovarian Cancer Metastasis: Integrating insights from disparate model organisms. *Nature Reviews Cancer*. **5**(5), p355.

Horikawa, N., Abiko, K., Matsumura, N., Hamanishi, J., Baba, T., Yamaguchi, K., Yoshioka, Y., Koshiyama, M. and Konishi, I. 2017. Expression of Vascular Endothelial Growth Factor in Ovarian Cancer Inhibits Tumor Immunity through the Accumulation of Myeloid-Derived Suppressor Cells. *Clin Cancer Res*. **23**(2), pp.587-599.

Hou, Y., Zhang, H., Miranda, L. and Lin, S. 2010. Serious overestimation in quantitative PCR by circular (supercoiled) plasmid standard: microalgal pcna as the model gene. *PLoS One*. **5**(3), pe9545.

Hu, Z., Artibani, M., Alsaadi, A., Wietek, N., Morotti, M., Shi, T., Zhong, Z., Santana Gonzalez, L., El-Sahhar, S., KaramiNejadRanjbar, M., Mallett, G., Feng, Y., Masuda, K., Zheng, Y., Chong, K., Damato, S., Dhar, S., Campo, L., Garruto Campanile, R., Soleymani majd, H., Rai, V., Maldonado-Perez, D., Jones, S., Cerundolo, V., Sauka-Spengler, T., Yau, C. and Ahmed, A.A. 2020. The Repertoire of Serous Ovarian Cancer Non-genetic Heterogeneity Revealed by Single-Cell Sequencing of Normal Fallopian Tube Epithelial Cells. *Cancer Cell*. **37**(2), pp.226-242.e227.

Huez, I., Bornes, S., Bresson, D., Creancier, L. and Prats, H. 2001. New vascular endothelial growth factor isoform generated by internal ribosome entry site-driven CUG translation initiation. *Mol Endocrinol*. **15**(12), pp.2197-2210.

Janardhan, B., Vaderhobli, S., Bhagat, R., Chennagiri Srinivasamurthy, P., Venketeshiah Reddihalli, P., Gawari, R. and Krishnamoorthy, L. 2015. Investigating impact of Vascular Endothelial Growth Factor Polymorphisms in Epithelial Ovarian Cancers: A Study in the Indian Population. *PLoS One*. **10**(7), pe0131190.

Janat-Amsbury, M.M., Yockman, J.W., Anderson, M.L., Kieback, D.G. and Kim, S.W. 2006a. Combination of local, non-viral IL12 gene therapy and systemic paclitaxel chemotherapy in a syngeneic ID8 mouse model for human ovarian cancer. *Anticancer Res*. **26**(5A), pp.3223-3228.

Janat-Amsbury, M.M., Yockman, J.W., Anderson, M.L., Kieback, D.G. and Kim, S.W. 2006b. Comparison of ID8 MOSE and VEGF-modified ID8 cell lines in an immunocompetent animal model for human ovarian cancer. *Anticancer Res*. **26**(4B), pp.2785-2789.

Jayson, G.C., Kohn, E.C., Kitchener, H.C. and Ledermann, J.A. 2014. Ovarian cancer. *The Lancet*. **384**(9951), pp.1376-1388.

Kanthou, C., Dachs, G.U., Lefley, D.V., Steele, A.J., Coralli-Foxon, C., Harris, S., Greco, O., Dos Santos, S.A., Reyes-Aldasoro, C.C., English, W.R. and Tozer, G.M. 2014. Tumour cells expressing single VEGF isoforms display distinct growth, survival and migration characteristics. *PLoS One*. **9**(8), pe104015.

Karaa, Z.S., Iacovoni, J.S., Bastide, A., Lacazette, E., Touriol, C. and Prats, H. 2009. The VEGF IRESes are differentially susceptible to translation inhibition by miR-16. *RNA*. **15**(2), pp.249-254.

Kazemi, M., Carrer, A., Moimas, S., Zandona, L., Bussani, R., Casagranda, B., Palmisano, S., Prelazzi, P., Giacca, M., Zentilin, L., De Manzini, N., Giacca, M. and Zacchigna, S. 2016. VEGF121 and VEGF165 differentially promote vessel maturation and tumor growth in mice and humans. *Cancer Gene Ther*. **23**(5), pp.125-132.

Kim, O., Park, E.Y., Klinkebiel, D.L., Pack, S.D., Shin, Y.H., Abdullaev, Z., Emerson, R.E., Coffey, D.M., Kwon, S.Y., Creighton, C.J., Kwon, S., Chang, E.C., Chiang, T., Yatsenko, A.N., Chien, J., Cheon, D.J., Yang-Hartwich, Y., Nakshatri, H., Nephew, K.P., Behringer, R.R., Fernandez, F.M., Cho, C.H., Vanderhyden, B., Drapkin, R., Bast, R.C., Jr., Miller, K.D., Karpf, A.R. and Kim, J. 2020. In vivo modeling of metastatic human high-grade serous ovarian cancer in mice. *PLoS Genet*. **16**(6), pe1008808.

Kiwerska, K. and Szyfter, K. 2019. DNA repair in cancer initiation, progression, and therapy-a double-edged sword. *J Appl Genet*. **60**(3-4), pp.329-334.

Koch, S., Tugues, S., Li, X., Gualandi, L. and Claesson-Welsh, L. 2011. *Signal transduction by vascular endothelial growth factor receptors*. Biochem. J. 437. pp.169-183.

Kommoss, S., Winterhoff, B., Oberg, A.L., Konecny, G.E., Wang, C., Riska, S.M., Fan, J.B., Maurer, M.J., April, C., Shridhar, V., Kommoss, F., du Bois, A., Hilpert, F., Mahner, S., Baumann, K., Schroeder, W., Burges, A., Canzler, U., Chien, J., Embleton, A.C., Parmar, M., Kaplan, R., Perren, T., Hartmann, L.C., Goode, E.L., Dowdy, S.C. and Pfisterer, J. 2017. Bevacizumab May Differentially Improve Ovarian Cancer Outcome in Patients with Proliferative and Mesenchymal Molecular Subtypes. *Clin Cancer Res*. **23**(14), pp.3794-3801.

Konecny, G.E., Wang, C., Hamidi, H., Winterhoff, B., Kalli, K.R., Dering, J., Ginther, C., Chen, H.W., Dowdy, S., Cliby, W., Gostout, B., Podratz, K.C., Keeney, G., Wang, H.J., Hartmann, L.C., Slamon, D.J. and Goode, E.L. 2014. Prognostic and therapeutic relevance of molecular subtypes in high-grade serous ovarian cancer. *J Natl Cancer Inst*. **106**(10).

Kumaran, G., Jayson, G. and Clamp, A. 2008. Antiangiogenic drugs in ovarian cancer. *British Journal of Cancer*. **100**(1), p1.

Küsters, B., De Waal, R.M.W., Wesseling, P., Verrijp, K., Maass, C., Ruiter, D.J., Leenders, W.P.J., Heerschap, A., Barentsz, J.O. and Sweep, F. 2003. Differential effects of vascular endothelial growth factor A isoforms in a mouse brain metastasis model of human melanoma. *Cancer Research*. **63**(17), pp.5408-5413.

Ladomery, M.R., Harper, S.J. and Bates, D.O. 2007. Alternative splicing in angiogenesis: the vascular endothelial growth factor paradigm. *Cancer Lett*. **249**(2), pp.133-142.

LaTulippe, E., Satagopan, J., Smith, A., Scher, H., Scardino, P., Reuter, V. and Gerald, W.L. 2002. Comprehensive gene expression analysis of prostate cancer reveals distinct transcriptional programs associated with metastatic disease. *Cancer Res*. **62**(15), pp.4499-4506.

Lee, S., Jilani, S.M., Nikolova, G.V., Carpizo, D. and Iruela-Arispe, M.L. 2005. Processing of VEGF-A by matrix metalloproteinases regulates bioavailability and vascular patterning in tumors. *J Cell Biol*. **169**(4), pp.681-691.

Lee, T., Seng, S., Sekine, M., Hinton, C., Fu, Y., Avraham, H. and Avraham, S. 2007. Vascular Endothelial Growth Factor Mediates Intracrine Survival in Human Breast Carcinoma Cells through Internally Expressed VEGFR1/ FLT1 (Survival of VEGF through VGFR1). *PLoS Medicine*. **4**(6), pe186.

Lee, Y., Miron, A., Drapkin, R., Nucci, M., Medeiros, F., Saleemuddin, A., Garber, J., Birch, C., Mou, H., Gordon, R., Cramer, D., McKeon, F. and Crum, C. 2007. A candidate precursor to serous carcinoma that originates in the distal fallopian tube. *Journal of Pathology*. **211**(1), pp.26-35.

Leenders, W.P., Kusters B Fau - de Waal, R.M.W. and de Waal, R.M. 2002. Vessel co-option: how tumors obtain blood supply in the absence of sprouting angiogenesis. *Endothelium*. (1062-3329 (Print)).

Lengyel, E. 2010. Ovarian cancer development and metastasis. *Am J Pathol*. **177**(3), pp.1053-1064.

Li, L., Wang, L., Zhang, W., Tang, B., Zhang, J., Song, H., Yao, D., Tang, Y., Chen, X., Yang, Z., Wang, G., Li, X., Zhao, J., Ding, H., Reed, E. and Li, Q.Q. 2004. Correlation of serum VEGF levels with clinical stage, therapy efficacy, tumor metastasis and patient survival in ovarian cancer. *Anticancer Res*. **24**(3b), pp.1973-1979.

Li, Y.L., Zhao, H. and Ren, X.B. 2016. Relationship of VEGF/VEGFR with immune and cancer cells: staggering or forward? *Cancer Biol Med*. **13**(2), pp.206-214.

Liang, W.C., Wu, X., Peale, F.V., Lee, C.V., Meng, Y.G., Gutierrez, J., Fu, L., Malik, A.K., Gerber, H.P., Ferrara, N. and Fuh, G. 2006. Cross-species vascular endothelial growth factor (VEGF)-blocking antibodies completely inhibit the growth of human tumor xenografts and measure the contribution of stromal VEGF. *J Biol Chem*. **281**(2), pp.951-961.

Lim, J., Yang, K., Taylor-Harding, B., Wiedemeyer, W.R. and Buckanovich, R.J. 2014. VEGFR3 Inhibition Chemosensitizes Ovarian Cancer Stemlike Cells through Down- Regulation of BRCA1 and BRCA2. *Neoplasia*. **16**(4), pp.343-353.e342.

Lisio, M.A., Fu, L., Goyeneche, A., Gao, Z.H. and Telleria, C. 2019. High-Grade Serous Ovarian Cancer: Basic Sciences, Clinical and Therapeutic Standpoints. *Int J Mol Sci*. **20**(4).

Liu, D., Song, J., Ji, X., Liu, Z., Cong, M. and Hu, B. 2016. Association of Genetic Polymorphisms on VEGFA and VEGFR2 With Risk of Coronary Heart Disease. *Medicine (Baltimore)*. **95**(19), pe3413.

Liu, J.F., Brady, M.F., Matulonis, U.A., Miller, A., Kohn, E.C., Swisher, E.M., Tew, W.P., Cloven, N.G., Muller, C., Bender, D., Moore, R.G., Michelin, D.P., Waggoner, S.E., Geller, M.A., Fujiwara, K., D'Andre, S.D., Carney, M., Secord, A.A., Moxley, K.M. and Bookman, M.A. 2020. A phase III study comparing single-agent olaparib or the combination of cediranib and olaparib to standard platinum-based chemotherapy in recurrent platinum-sensitive ovarian cancer. *Journal of Clinical Oncology*. **38**(15_suppl), pp.6003-6003.

Loret, N., Denys, H., Tummers, P. and Berx, G. 2019. The Role of Epithelial-to-Mesenchymal Plasticity in Ovarian Cancer Progression and Therapy Resistance. *Cancers (Basel)*. **11**(6).

Mabuchi, S., Morishige, K., Sakata, M., Kimura, T., Terai, Y., Tanabe-Kimura, A., Sasaki, H., Kanemura, M., Tsunetoh, S., Tanaka, Y., Ohmichi, M. and Burger, R. 2008. Maintenance treatment with bevacizumab prolongs survival in an in vivo ovarian cancer model. *Clinical Cancer Research*. **14**(23), pp.7781-7789.

Magon, K. 2018. Development of Novel Biomarker Assays for Quantification of VEGFA mRNA Isoforms. Master of Science thesis, The University of Sheffield.

Mahner, S., Woelber, L., Eulenburg, C., Schwartz, J., Carney, W., Jaenicke, F., Milde-Langosch, K. and Mueller, V. 2010. TIMP-1 and VEGF-165 serum concentration during first-line therapy of ovarian cancer patients. *BMC Cancer*. **10**(139).

Maniati, E., Berlato, C., Gopinathan, G., Heath, O., Kotantaki, P., Lakhani, A., McDermott, J., Pegrum, C., Delaine-Smith, R.M., Pearce, O.M.T., Hirani, P., Joy, J.D., Szabova, L., Perets, R., Sansom, O.J., Drapkin, R., Bailey, P. and Balkwill, F.R. 2020. Mouse Ovarian Cancer Models Recapitulate the Human Tumor Microenvironment and Patient Response to Treatment. *Cell Rep*. **30**(2), pp.525-540 e527.

Medina, M.A., Munoz-Chapuli, R. and Quesada, A.R. 2007. Challenges of antiangiogenic cancer therapy: trials and errors, and renewed hope. *J Cell Mol Med*. **11**(3), pp.374-382.

Miles, D., Cameron, D., Bondarenko, I., Manzyuk, L., Alcedo, J.C., Lopez, R.I., Im, S.-A., Canon, J.-L., Shparyk, Y., Yardley, D.A., Masuda, N., Ro, J., Denduluri, N., Hubeaux, S., Quah, C., Bais, C., amp, Apos and Shaughnessy, J. 2017. Bevacizumab plus paclitaxel versus placebo plus paclitaxel as first- line therapy for HER2- negative metastatic breast cancer (MERiDiAN): A double-blind placebo-controlled randomised phase III trial with prospective biomarker evaluation. *European Journal of Cancer*. **70**, pp.146-155.

Miles, D., De Haas, S., Dirix, L., Romieu, G., Chan, A., Pivot, X., Tomczak, P., Provencher, L., Cortés, J., Delmar, P.R. and Scherer, S.J. 2013. Biomarker results from the AVADO phase 3 trial of first- line bevacizumab plus docetaxel for HER2- negative metastatic breast cancer. *British Journal of Cancer*. **108**(5), p1052.

Miow, Q., Tan, T., Ye, J., Lau, J., Yokomizo, T., Thiery, J. and Mori, S. 2014. Epithelial–mesenchymal status renders differential responses to cisplatin in ovarian cancer. *Oncogene*.

Mitra, A. 2016. Ovarian Cancer Metastasis: A Unique Mechanism of Dissemination. In: Xu, K. ed. *Tumor Metastasis*. InTech, pp.43-58.

Mitra, A.K., Davis, D.A., Tomar, S., Roy, L., Gurler, H., Xie, J., Lantvit, D.D., Cardenas, H., Fang, F., Liu, Y., Loughran, E., Yang, J., Sharon Stack, M., Emerson, R.E., Cowden Dahl, K.D., M, V.B., Nephew, K.P., Matei, D. and Burdette, J.E. 2015. In vivo tumor growth of high-grade serous ovarian cancer cell lines. *Gynecol Oncol*. **138**(2), pp.372-377.

Monk, B., Pujade-Lauraine, E. and Burger, R. 2013. Integrating bevacizumab into the management of epithelial ovarian cancer: the controversy of front-line versus recurrent disease. *Annals of Oncology*. **24**(suppl10), pp.x53-x58.

Morelli, M.P., Brown, A.M., Pitts, T.M., Tentler, J.J., Eckhardt, S.G., Ciardiello, F., Ryan, A. and Jürgensmeier, J.M. 2009. Targeting vascular endothelial growth factor receptor- 1 and -3 with cediranib (AZD2171): Effects on migration and invasion of gastrointestinal cancer cell lines. *Molecular Cancer Therapeutics*. **8**(9), pp.2546-2558.

Ning, Q., Hou, L., Meng, M., Zhang, X., Luo, M., Shao, S., Zuo, X., Zhao, X. and Liu, C. 2013. Vascular Endothelial Growth Factor Receptor-1 Activation Promotes Migration and Invasion of Breast Cancer Cells through Epithelial-Mesenchymal Transition. *PLoS ONE*. **8**(6).

Nishida, T., Kondo, S., Maeda, A., Kubota, S., Lyons, K.M. and Takigawa, M. 2009. CCN family 2/connective tissue growth factor (CCN2/CTGF) regulates the expression of Vegf through Hif-1alpha expression in a chondrocytic cell line, HCS-2/8, under hypoxic condition. *Bone*. **44**(1), pp.24-31.

O-charoenrat, P., Rhys-Evans, P. and Eccles, S. 2001. Expression of vascular endothelial growth factor family members in head and neck squamous cell carcinoma correlates with lymph node metastasis. *Cancer*. **92**(3), pp.556-568.

Ohba, T., Cates, J.M.M., Cole, H.A., Slosky, D.A., Haro, H., Ando, T., Schwartz, H.S. and Schoenecker, J.G. 2014. Autocrine VEGF/VEGFR1 signaling in a subpopulation of cells associates with aggressive osteosarcoma. *Molecular cancer research : MCR*. **12**(8), p1100.

Ohmichi, M., Hayakawa, J., Tasaka, K., Kurachi, H. and Murata, Y. 2005. Mechanisms of platinum drug resistance. *Trends in Pharmacological Sciences*. **26**(3), pp.113-116.

Oliva, P., Decio, A., Castiglioni, V., Bassi, A., Pesenti, E., Cesca, M., Scanziani, E., Belotti, D. and Giavazzi, R. 2012. Cisplatin plus paclitaxel and maintenance of bevacizumab on tumour progression, dissemination, and survival of ovarian carcinoma xenograft models. *Br J Cancer*. **107**(2), pp.360-369.

Papa, A., Caruso, D., Strudel, M., Tomao, S. and Tomao, F. 2016. Update on Poly-ADP-ribose polymerase inhibition for ovarian cancer treatment. *J Transl Med*. **14**, p267.

Patel, K.R., Vajaria, B.N., Begum, R., Patel, J.B., Shah, F.D., Joshi, G.M. and Patel, P.S. 2015. VEGFA isoforms play a vital role in oral cancer progression. *Tumour Biol*. **36**(8), pp.6321-6332.

Perets, R., Wyant, G.A., Muto, K.W., Bijron, J.G., Poole, B.B., Chin, K.T., Chen, J.Y., Ohman, A.W., Stepule, C.D., Kwak, S., Karst, A.M., Hirsch, M.S., Setlur, S.R., Crum, C.P., Dinulescu, D.M. and Drapkin, R. 2013. Transformation of the fallopian tube secretory epithelium leads to high-grade serous ovarian cancer in Brca;Tp53;Pten models. *Cancer Cell*. **24**(6), pp.751-765.

Perren, T.J., Swart, A.M., Pfisterer, J., Ledermann, J.A., Pujade-Lauraine, E., Kristensen, G., Carey, M.S., Beale, P., Cervantes, A., Kurzeder, C., du Bois, A., Sehouli, J., Kimmig, R., Stahle, A., Collinson, F., Essapen, S., Gourley, C., Lortholary, A., Selle, F., Mirza, M.R., Leminen, A., Plante, M., Stark, D., Qian, W., Parmar, M.K., Oza, A.M. and Investigators, I. 2011. A phase 3 trial of bevacizumab in ovarian cancer. *N Engl J Med*. **365**(26), pp.2484-2496.

Pinto, M.P., Balmaceda, C., Bravo, M.L., Kato, S., Villarroel, A., Owen, G.I., Roa, J.C., Cuello, M.A. and Ibanez, C. 2018. Patient inflammatory status and CD4+/CD8+ intraepithelial tumor lymphocyte infiltration are predictors of outcomes in high-grade serous ovarian cancer. *Gynecol Oncol*. **151**(1), pp.10-17.

Pujade-Lauraine, E., Hilpert, F., Weber, B., Reuss, A., Poveda, A., Kristensen, G., Sorio, R., Vergote, I., Witteveen, P., Bamias, A., Pereira, D., Wimberger, P., Oaknin, A., Mirza, M.R., Follana, P., Bollag, D. and Ray-Coquard, I. 2014. Bevacizumab combined with chemotherapy for platinum-resistant recurrent ovarian cancer: The AURELIA open-label randomized phase III trial. *J Clin Oncol*. **32**(13), pp.1302-1308.

Ramakrishnan, S., Anand, V. and Roy, S. 2014. Vascular endothelial growth factor signaling in hypoxia and inflammation. *J Neuroimmune Pharmacol*. **9**(2), pp.142-160.

Rana, P., Pritchard, K.I. and Kerbel, R. 2017. Plasma vascular endothelial growth factor as a predictive biomarker: Door closed? *European Journal of Cancer*. **70**, pp.143-145.

Ribatti, D. 2007. The contribution of Harold F. Dvorak to the study of tumor angiogenesis and stroma generation mechanisms. *Endothelium*. (1062-3329 (Print)).

Ribatti, D. 2008a. Judah Folkman, a pioneer in the study of angiogenesis. *Angiogenesis*. **11**(1), pp.3-10.

Ribatti, D. 2008b. Napoleone Ferrara and the saga of vascular endothelial growth factor. *Endothelium*. **1**(1029-2373 (Electronic)), pp.1-8.

Roby, K.F., Taylor, C.C., Sweetwood, J.P., Cheng, Y., Pace, J.L., Tawfik, O., Persons, D.L., Smith, P.G. and Terranova, P.F. 2000. Development of a syngeneic mouse model for events related to ovarian cancer. *Carcinogenesis*. **21**(4), pp.585-591.

Rosenbaum-Dekel, Y., Fuchs, A., Yakirevich, E., Azriel, A., Mazareb, S., Resnick, M.B. and Levi, B.Z. 2005. Nuclear localization of long-VEGF is associated with hypoxia and tumor angiogenesis. *Biochem Biophys Res Commun*. **332**(1), pp.271-278.

Rosso, M., Majem, B., Devis, L., Lapyckyj, L., Besso, M.J., Llaurado, M., Abascal, M.F., Matos, M.L., Lanau, L., Castellvi, J., Sanchez, J.L., Perez Benavente, A., Gil-Moreno, A., Reventos, J., Santamaria Margalef, A., Rigau, M. and Vazquez-Levin, M.H. 2017. E-cadherin: A determinant molecule associated with ovarian cancer progression, dissemination and aggressiveness. *PLoS One*. **12**(9), pe0184439.

Roth, D., Piekarek, M., Paulsson, M., Christ, H., Bloch, W., Krieg, T., Davidson, J.M. and Eming, S.A. 2006. Plasmin modulates vascular endothelial growth factor-A-mediated angiogenesis during wound repair. *Am J Pathol*. **168**(2), pp.670-684.

Russell, S., Duquette, M., Liu, J., Drapkin, R., Lawler, J. and Petrik, J. 2015. Combined therapy with thrombospondin-1 type I repeats (3TSR) and chemotherapy induces regression and significandy improves survival in a preclinical model of advanced stage epithelial ovarian cancer. . *The FASEB journal : official publication of the Federation of American Societies for Experimental Biology*. **29**, pp.576-588.

Samuel, S., Fan, F., Dang, L., Xia, L., Gaur, P. and Ellis, L. 2010. Intracrine vascular endothelial growth factor signaling in survival and chemoresistance of human colorectal cancer cells. *Oncogene*. **30**(10), p1205.

Sawada, K., Mitra, A.K., Radjabi, A.R., Bhaskar, V., Kistner, E.O., Tretiakova, M., Jagadeeswaran, S., Montag, A., Becker, A., Kenny, H.A., Peter, M.E., Ramakrishnan, V., Yamada, S.D. and Lengyel, E. 2008. Loss of E-cadherin promotes ovarian cancer metastasis via alpha 5-integrin, which is a therapeutic target. *Cancer Res*. **68**(7), pp.2329-2339.

Schlessinger, J. 2000. Cell Signaling by Receptor Tyrosine Kinases. *Cell*. **103**(2), pp.211-225.

Schmid, B. and Oehler, M. 2014. New perspectives in ovarian cancer treatment. *Maturitas*. **77**(2), pp.128-136.

Shah, D.K., Veith, J., Bernacki, R.J. and Balthasar, J.P. 2011. Evaluation of combined bevacizumab and intraperitoneal carboplatin or paclitaxel therapy in a mouse model of ovarian cancer. *Cancer Chemother Pharmacol*. **68**(4), pp.951-958.

Shibata, T., Akiyama, N., Noda, M., Sasai, K. and Hiraoka, M. 1998. Enhancement of gene expression under hypoxic conditions using fragments of the human vascular endothelial growth factor and the erythropoietin genes. *Int J Radiat Oncol Biol Phys*. **42**(4), pp.913-916.

Shibata, T., Giaccia, A.J. and Brown, J.M. 2000. Development of a hypoxia-responsive vector for tumor-specific gene therapy. *Gene Ther*. **7**(6), pp.493-498.

Shibuya, M. 2011. Vascular endothelial growth factor (VEGF) and its receptor (VEGFR) Signaling in Angiogenesis. *Genes Cancer*. **2**(12), pp.1097–1105.

Silva, J., Garcia, V., Garcia, J.M., Pena, C., Dominguez, G., Diaz, R., Lorenzo, Y., Hurtado, A., Sanchez, A. and Bonilla, F. 2007. Circulating Bmi-1 mRNA as a possible prognostic factor for advanced breast cancer patients. *Breast Cancer Res*. **9**(4), pR55.

Simon, T., Gagliano, T. and Giamas, G. 2017. Direct Effects of Anti- Angiogenic Therapies on Tumor Cells: VEGF Signaling. *Trends in Molecular Medicine*. **23**(3), pp.282-292.

Slaughter, K.N., Thai, T., Penaroza, S., Benbrook, D.M., Thavathiru, E., Ding, K., Nelson, T., McMeekin, D.S. and Moore, K.N. 2014. Measurements of adiposity as clinical biomarkers for first-line bevacizumab-based chemotherapy in epithelial ovarian cancer. *Gynecol Oncol*. **133**(1), pp.11-15.

Sonoda, Y., Kanamori, M., Deen, D.F., Cheng, S.Y., Berger, M.S. and Pieper, R.O. 2003. Overexpression of vascular endothelial growth factor isoforms drives oxygenation and growth but not progression to glioblastoma multiforme in a human model of gliomagenesis. *Cancer Res*. **63**(8), pp.1962-1968.

Steffensen, K.D., Waldstrom, M., Brandslund, I. and Jakobsen, A. 2010. The relationship of VEGF polymorphisms with serum VEGF levels and progression-free survival in patients with epithelial ovarian cancer. *Gynecol Oncol*. **117**(1), pp.109-116.

Stephen, B., Margaret, D. and David, A.S. 2017. RNA- Sequencing data supports the existence of novel VEGFA splicing events but not of VEGFAxxxb isoforms. *Scientific Reports*. **7**(1), p1.

Stimpfl, M., Tong, D., Fasching, B., Schuster, E., Obermair, A., Leodolter, S. and Zeillinger, R. 2002. Vascular endothelial growth factor splice variants and their prognostic value in breast and ovarian cancer. *Clinical Cancer Research*. **8**(7), pp.2253-2259.

Sun, X.Z., Liu, G.H., Wang, Z.Q., Zheng, F.F., Bian, J., Huang, Y.P., Gao, Y., Zhang, Y.D. and Deng, C.H. 2011. Over-expression of VEGF165 in the adipose tissue-derived stem cells via the lentiviral vector. *Chin Med J (Engl)*. **124**(19), pp.3093-3097.

Takaya, H., Nakai, H., Takamatsu, S., Mandai, M. and Matsumura, N. 2020. Homologous recombination deficiency status-based classification of high-grade serous ovarian carcinoma. *Sci Rep*. **10**(1), p2757.

Tee, M.K. and Jaffe, R.B. 2001. A precursor form of vascular endothelial growth factor arises by initiation from an upstream in-frame CUG codon. *Biochem J*. **359**(Pt 1), pp.219-226.

Thorsson, V., Gibbs, D.L., Brown, S.D., Wolf, D., Bortone, D.S., Ou Yang, T.H., Porta-Pardo, E., Gao, G.F., Plaisier, C.L., Eddy, J.A., Ziv, E., Culhane, A.C., Paull, E.O., Sivakumar, I.K.A., Gentles, A.J., Malhotra, R., Farshidfar, F., Colaprico, A., Parker, J.S., Mose, L.E., Vo, N.S., Liu, J., Liu, Y., Rader, J., Dhankani, V., Reynolds, S.M., Bowlby, R., Califano, A., Cherniack, A.D., Anastassiou, D., Bedognetti, D., Mokrab, Y., Newman, A.M., Rao, A., Chen, K., Krasnitz, A., Hu, H., Malta, T.M., Noushmehr, H., Pedamallu, C.S., Bullman, S., Ojesina, A.I., Lamb, A., Zhou, W., Shen, H., Choueiri, T.K., Weinstein, J.N., Guinney, J., Saltz, J., Holt, R.A., Rabkin, C.S., Cancer Genome Atlas Research, N., Lazar, A.J., Serody,

J.S., Demicco, E.G., Disis, M.L., Vincent, B.G. and Shmulevich, I. 2018. The Immune Landscape of Cancer. *Immunity*. **48**(4), pp.812-830 e814.

Tokunaga, T., Oshika, Y., Abe, Y., Ozeki, Y., Sadahiro, S., Kijima, H., Tsuchida, T., Yamazaki, H., Ueyama, Y., Tamaoki, N. and Nakamura, M. 1998. Vascular endothelial growth factor (VEGF) mRNA isoform expression pattern is correlated with liver metastasis and poor prognosis in colon cancer. *British Journal of Cancer*. **77**(6), p998.

Townsend, K.N., Spowart, J.E., Huwait, H., Eshragh, S., West, N.R., Elrick, M.A., Kalloger, S.E., Anglesio, M., Watson, P.H., Huntsman, D.G. and Lum, J.J. 2013. Markers of T cell infiltration and function associate with favorable outcome in vascularized high-grade serous ovarian carcinoma. *PLoS One*. **8**(12), pe82406.

Tozer, G.M., Akerman, S., Cross, N.A., Barber, P.R., Bjorndahl, M.A., Greco, O., Harris, S., Hill, S.A., Honess, D.J., Ireson, C.R., Pettyjohn, K.L., Prise, V.E., Reyes-Aldasoro, C.C., Ruhrberg, C., Shima, D.T. and Kanthou, C. 2008. Blood vessel maturation and response to vascular-disrupting therapy in single vascular endothelial growth factor-A isoform-producing tumors. *Cancer Res*. **68**(7), pp.2301-2311.

Tudrej, P., Kujawa, K.A., Cortez, A.J. and Lisowska, K.M. 2019. Characteristics of in Vivo Model Systems for Ovarian Cancer Studies. *Diagnostics (Basel)*. **9**(3).

UniProt, C. 2019. UniProt: a worldwide hub of protein knowledge. *Nucleic Acids Res*. **47**(D1), pp.D506-D515.

Van Cutsem, E., de Haas, S., Kang, Y.-K., Ohtsu, A., Tebbutt, N.C., Ming Xu, J., Peng Yong, W., Langer, B., Delmar, P., Scherer, S.J. and Shah, M.A. 2012. Bevacizumab in combination with chemotherapy as first- line therapy in advanced gastric cancer: a biomarker evaluation from the AVAGAST randomized phase III trial. *Journal of clinical oncology : official journal of the American Society of Clinical Oncology*. **30**(17), p2119.

Van Cutsem, E., Jayson, G., Dive, C., Dilba, P., de Haas, S., Wild, N., Delmar, P. and Scherer, S.J. 2011. 803 ORAL Analysis of Blood Plasma Factors in the AVITA Phase III Randomized Study of Bevacizumab (bev) With Gemcitabine-Erlotinib (GE) in Patients (pts) With Metastatic Pancreatic Cancer (mPC). *European Journal of Cancer*. **47**, pp.S95-S96.

Vaughan, S., Coward, J., Bast, R., Berchuck, A., Berek, J., Brenton, J., Coukos, G., Crum, C., Drapkin, R., Etemadmoghadam, D., Friedlander, M., Gabra, H., Kaye, S., Lord, C., Lengyel, E., Levine, D., Mcneish, I., Menon, U., Mills, G., Nephew, K., Oza, A., Sood, A., Stronach, E., Walczak, H., Bowtell, D. and Balkwill, F. 2011. Rethinking ovarian cancer: recommendations for improving outcomes. *Nature Reviews Cancer*. **11**(10), p719.

Vempati, P., Popel, A. and Mac, F. 2014. Extracellular regulation of VEGF: Isoforms, proteolysis, and vascular patterning. *Cytokine and Growth Factor Reviews*. **25**(1), pp.1-19.

Verheul, H. and Pinedo, H. 2000. The role of vascular endothelial growth factor (VEGF) in tumor angiogenesis and early clinical development of VEGF-receptor kinase inhibitors. *Clinical Breast Cancer*. **1**, pp.S80-84.

Vieira, J.M., Schwarz, Q. and Ruhrberg, C. 2007. Selective requirements for NRP1 ligands during neurovascular patterning. *Development*. **134**(10), pp.1833-1843.

Vitting-Seerup, K. and Sandelin, A. 2017. The Landscape of Isoform Switches in Human Cancers. *Mol Cancer Res*. **15**(9), pp.1206-1220.

Voron, T., Colussi, O., Marcheteau, E., Pernot, S., Nizard, M., Pointet, A.L., Latreche, S., Bergaya, S., Benhamouda, N., Tanchot, C., Stockmann, C., Combe, P., Berger, A., Zinzindohoue, F., Yagita, H., Tartour, E., Taieb, J. and Terme, M. 2015. VEGF-A modulates expression of inhibitory checkpoints on CD8+ T cells in tumors. *J Exp Med*. **212**(2), pp.139-148.

Walton, J., Blagih, J., Ennis, D., Leung, E., Dowson, S., Farquharson, M., Tookman, L.A., Orange, C., Athineos, D., Mason, S., Stevenson, D., Blyth, K., Strathdee, D., Balkwill, F.R., Vousden, K., Lockley, M. and McNeish, I.A. 2016. CRISPR/Cas9-Mediated Trp53 and Brca2 Knockout to Generate Improved Murine Models of Ovarian High-Grade Serous Carcinoma. *Cancer Res*. **76**(20), pp.6118-6129.

Walton, J.B., Farquharson, M., Mason, S., Port, J., Kruspig, B., Dowson, S., Stevenson, D., Murphy, D., Matzuk, M., Kim, J., Coffelt, S., Blyth, K. and McNeish, I.A. 2017. CRISPR/Cas9-

derived models of ovarian high grade serous carcinoma targeting Brca1, Pten and Nf1, and correlation with platinum sensitivity. *Sci Rep*. **7**(1), p16827.

Wang, Q., Armenia, J., Zhang, C., Penson, A.V., Reznik, E., Zhang, L., Minet, T., Ochoa, A., Gross, B.E., Iacobuzio-Donahue, C.A., Betel, D., Taylor, B.S., Gao, J. and Schultz, N. 2018. Unifying cancer and normal RNA sequencing data from different sources. *Sci Data*. **5**, p180061.

Wang, Z., Gerstein, M. and Snyder, M. 2009. RNA-Seq: a revolutionary tool for transcriptomics. *Nat Rev Genet*. **10**(1), pp.57-63.

Watkins, W.M., McCollum, G.W., Savage, S.R., Capozzi, M.E., Penn, J.S. and Morrison, D.G. 2013. Hypoxia-induced expression of VEGF splice variants and protein in four retinal cell types. *Exp Eye Res*. **116**, pp.240-246.

Webb, J.R., Milne, K., Kroeger, D.R. and Nelson, B.H. 2016. PD-L1 expression is associated with tumor-infiltrating T cells and favorable prognosis in high-grade serous ovarian cancer. *Gynecol Oncol*. **141**(2), pp.293-302.

Williams, E., Martin, S., Moss, R., Durrant, L. and Deen, S. 2012. Co-expression of VEGF and CA9 in ovarian high-grade serous carcinoma and relationship to survival. *Virchows Arch*. **461**(1), pp.33-39.

Wu, B., Zhang, L., Yu, Y., Lu, T., Zhang, Y., Zhu, W., Song, Q., Lv, C., Guo, J., Tian, Y. and Deng, N. 2020. miR-6086 inhibits ovarian cancer angiogenesis by downregulating the OC2/VEGFA/EGFL6 axis. *Cell Death Dis*. **11**(5), p345.

Yang, A., Camp, E., Fan, F., Shen, L., Gray, M., Liu, W., Somcio, R., Bauer, T., Wu, Y., Hicklin, D. and Ellis, L. 2006. Vascular endothelial growth factor receptor-1 activation mediates epithelial to mesenchymal transition in human pancreatic carcinoma cells. *Cancer research*. **66**(1), p46.

Yin, X., Wang, X., Shen, B., Jing, Y., Li, Q., Cai, M.C., Gu, Z., Yang, Q., Zhang, Z., Liu, J., Li, H., Di, W. and Zhuang, G. 2016. A VEGF-dependent gene signature enriched in mesenchymal ovarian cancer predicts patient prognosis. *Sci Rep*. **6**, p31079.

Yuan, A., Lin, C.Y., Chou, C.H., Shih, C.M., Chen, C.Y., Cheng, H.W., Chen, Y.F., Chen, J.J., Chen, J.H., Yang, P.C. and Chang, C. 2011. Functional and structural characteristics of tumor angiogenesis in lung cancers overexpressing different VEGF isoforms assessed by DCE- and SSCE-MRI. *PLoS One*. **6**(1), pe16062.

Yuan, A., Yu, C.J., Kuo, S.H., Chen, W.J., Lin, F.Y., Luh, K.T., Yang, P.C. and Lee, Y.C. 2001. Vascular endothelial growth factor 189 mRNA isoform expression specifically correlates with tumor angiogenesis, patient survival, and postoperative relapse in non-small-cell lung cancer. *J Clin Oncol*. **19**(2), pp.432-441.

Zhang, H., Chen, Y., Fan, B., Wang, W. and Zhu, W. 2015. Overexpression of VEGF183 promotes murine breast cancer cell proliferation in vitro and induces dilated intratumoral microvessels. *Tumour Biol*. **36**(5), pp.3871-3880.

Zhang, H., Scott, P., Morbidelli, L., Peak, S., Moore, J., Turley, H., Harris, A., Ziche, M. and Bicknell, R. 2000. The 121 amino acid isoform of vascular endothelial growth factor is more strongly tumorigenic than other splice variants in vivo. *British Journal of Cancer*. **83**(1), p63.

Zhang, L., Conejo-Garcia, J.R., Yang, N., Huang, W., Mohamed-Hadley, A., Yao, W., Benencia, F. and Coukos, G. 2002a. Different effects of glucose starvation on expression and stability of VEGF mRNA isoforms in murine ovarian cancer cells. *Biochem Biophys Res Commun*. **292**(4), pp.860-868.

Zhang, L., Yang, N., Garcia, J.R., Mohamed, A., Benencia, F., Rubin, S.C., Allman, D. and Coukos, G. 2002b. Generation of a syngeneic mouse model to study the effects of vascular endothelial growth factor in ovarian carcinoma. *Am J Pathol*. **161**(6), pp.2295-2309.

Zhang, L., Yang, N., Park, J.W., Katsaros, D., Fracchioli, S., Cao, G., O'Brien-Jenkins, A., Randall, T.C., Rubin, S.C. and Coukos, G. 2003. Tumor-derived vascular endothelial growth factor up-regulates angiopoietin-2 in host endothelium and destabilizes host vasculature, supporting angiogenesis in ovarian cancer. *Cancer Res*. **63**(12), pp.3403-3412.

Zhang, Y., Furumura, M. and Morita, E. 2008. Distinct signaling pathways confer different vascular responses to VEGF 121 and VEGF 165. *Growth Factors*. **26**(3), pp.125-131.

Zhao, S., Jiang, E., Chen, S., Gu, Y., Shangguan, A.J., Lv, T., Luo, L. and Yu, Z. 2016. PiggyBac transposon vectors: the tools of the human gene encoding. *Transl Lung Cancer Res*. **5**(1), pp.120-125.

Zhou, C., Clamp, A., Backen, A., Berzuini, C., Renehan, A., Banks, R.E., Kaplan, R., Scherer, S.J., Kristensen, G.B., Pujade-Lauraine, E., Dive, C. and Jayson, G.C. 2016. Systematic analysis of circulating soluble angiogenesis-associated proteins in ICON7 identifies Tie2 as a biomarker of vascular progression on bevacizumab. *Br J Cancer*. **115**(2), pp.228-235.